Sediment transport modelling

Determination of the main areas contributing to the suspended sediment load in the Mara River, Kenya

MSc Thesis

By Petra Hulsman

April 2015

Sediment transport modelling

Determination of the main areas contributing to the suspended sediment load in the Mara River, Kenya

By

Petra Hulsman

In partial fulfilment of the requirements for the degree of Master of Science in Hydraulic Engineering and Water Resources Management at the Delft University of Technology and National University of Singapore.

30th April 2015

Graduation committee

Prof. Dr. Ir. H.H.G. Savenije	(Chairman, TU Delft)
Dr. T.A. Bogaard	(Supervisor, TU Delft)
Dr. Ir. E. Mosselman	(Supervisor, TU Delft)
Dr. J.-F. Yeh	(Co-supervisor, NUS)
Dr. J. Yuan	(Examiner, NUS)

TU Delft Delft University of Technology

UNESCO-IHE Institute for Water Education

NUS National University of Singapore

Preface

This graduation thesis is the final part of a double degree master 'Hydraulic Engineering and Water Resources Management' at Delft University of Technology and National University of Singapore. This research is part of the MaMaSe project (Mau Mara Serengeti) which is a four-year project that started in January 2014 and is led by UNESCO-IHE. The goal of this project is to improve the water safety to support poverty reduction, sustainable economic growth and to conserve the ecosystem. Within this MaMaSe project, this thesis focuses on assessing the hydrological system and locating the main sources of sediments in the Mara River.

In this document, background information is given on the current situation (section *3 The study area*) before going into the hydrology (section *4 Hydrology*) and sedimentology (section *5 Sedimentology*) of the area. For those who are interested in more details, additional information on these topics is provided in the appendices.

I am thankful to many people who have helped me during this research. Special thanks to:

- My supervisors at TU Delft: Prof. Dr. Ir. H.H.G. Savenije, Dr. T.A. Bogaard and Dr. Ir. E. Mosselman
- My supervisors at NUS: Dr. J.-F. Yeh
- The people involved in the MaMaSe project: Ingrid De Loof (project coordinator), Prof. M. McClain (project manager), John Conallin and Chris Dutton

All wisdom comes from the Lord,
and so do common sense and understanding.
(Proverbs 2:6)

Summary

The Serengeti is a vast ecosystem of about 30,000 km^2 located in southwest Kenya and northern Tanzania. This region encompasses, among other areas, the Serengeti National Park in Tanzania and the Masai Mara National Reserve in Kenya. Through both reserves flows the Mara River that originates in Kenya in the Mau Escarpment and flows into Lake Victoria in Tanzania. In its catchment, human interventions have led to deforestation and the increase of agricultural areas. This conversion to cultivation, combined with the application of non-optimal agricultural practices, has resulted in increased soil compaction. As a result, less rainwater infiltrates the soil and more water flows as rapid surface runoff towards the river. With the increased fast runoff, more topsoil is expected to erode and to be transported to the river, thus polluting it. This research focuses on the modelling of the hydrology and soil loss from the catchment to locate the main sources of transported suspended sediment in the Mara River Basin.

The suspended load in the Mara River consists of coarse sediments in the river bed and fine sediments in the wash load originating from the top soil in the entire catchment. The main sources of the coarse sediments are assessed hydraulically whereas for the fine sediments a hydrological model is combined with an empirical sediment yield model.

The coarse sediments in the Mara River are mainly found in the bed and can originate from gullies or the river itself as high flow velocities are needed for their transport. To determine the main source, the sediment transport capacity of the river was compared with the one of a typical gully observed locally and the occurrence of river meandering was analysed.

The fine sediments in the Mara River are mainly found in the wash load and are assumed to originate from eroded topsoil. To assess the main sources, a semi-distributed hydrological model based on the concept of FLEX-Topo was created and combined with the empirical model MUSLE (Modified Universal Soil Loss Equation). With this hydrological and sediment transport model, the soil loss was calculated on daily time-scale. It is assumed that this soil loss is equal to wash load in the river. In the hydrological model five sub-catchments and four hydrological response units (HRUs) were defined; the sub-catchments are: North, Middle, Talek, Sand, Lower and the HRUs are: forested hill slopes, shrubs on hill slopes, agriculture and grasslands. Only for croplands and grasslands, the MUSLE model were applied to calculate the soil loss as no significant erosion was observed in forests and shrub lands.

This model simulated the hydrology well and also captured the order of magnitude of the soil loss; however not the exact patterns. The largest soil losses were found in the Sand and Lower sub-catchment: the soil loss is 0.30 mm/yr in the grasslands in the Sand and 0.2 mm/yr in the cultivated areas in the Lower sub-catchment. It is recommended to increase the model accuracy by using additional field measurements at multiple locations in the catchment, for example precipitation, temperature and discharge to improve the hydrological part and turbidity data to improve the sediment part of the model.

This means that the main sources for the fine suspended sediments are the grasslands in the Sand and the crop lands in the Lower sub-catchment. It is recommended to focus on these areas for decreasing the fine suspended sediment load most efficiently. However, currently most studies seem to focus on the cultivated areas in the North where local people have observed decreased crop yields in the past 20 years and suspect it is a result of eroded fertile top soil. The coarse sediments are found to originate from the river itself which has caused and still causes meandering.

Abbreviations

DEM	Digital Elevation Map
E	Evaporation [mm/d]
EFA	Environmental Flow Assessment
FAO	Food and Agriculture Organization of the United Nations
FDC	Flow duration curve
HAND	Height Above Nearest Drain
HOF	Hortonian Overland Flow
HRU	Hydrological Response Unit
ILRI	International Livestock Research
ITCZ	Inter –tropical Convergence Zone
KENSOTER	Kenya Soil and Terrain database
MaMaSe	Mau Mara Serengeti
S.L.	Sea Level
MRB	Mara River Basin
MUSLE	Modified Universal Soil Loss Equation
NDVI	Normalized Difference Vegetation Index
NS	Nash-Sutcliffe objective function [-]
P	Precipitation [mm/d]
S	Soil loss [t/d]
SCMP	Sub-catchment Management Plan
S_i	Storage component i; for example unsaturated zone, fast runoff etc. [mm]
SOTER	Soil and Terrain database
SOTWIS	Combination of SOTER and WISE
SSF	Shallow Subsurface Flow
TSS	Total suspended solids [mg/l]
USGS	U.S. Geological Survey
WISE	World Inventory of Soil Emmission Potentials
WRUA	Water Resources Users Associations

Table of Contents

1. Introduction

1.1. Site description

The Serengeti is a vast ecosystem of about 30,000 km^2 located in northern Tanzania and southwest Kenya. This region encompasses the Serengeti National Park, the Ngorongoro Conservation Area, Maswa Game Reserve, Grumeti Game Reserve and Ikorongo Controlled Areas in Tanzania and the Masai Mara National Reserve in Kenya (see Figure 1-1). The Serengeti National Park is a 14,763 km^2 large park that is famous for the annual migration of over a million wildebeest and nearly 200,000 zebras searching for pastures and water. Every year, nearly 90,000 tourists visit this park as it is a popular destination for safaris in Africa (SerengetiPark, 2000).

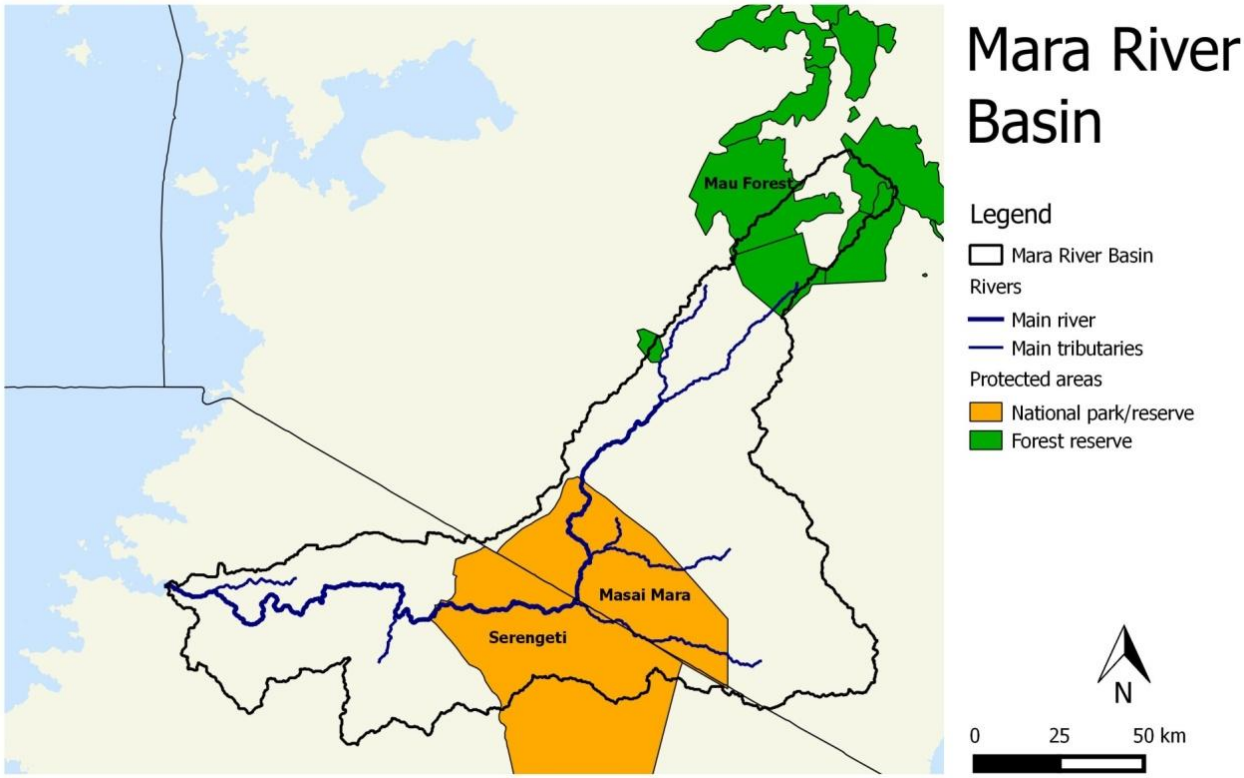

Figure 1-1: Location of the nature reserves in the Mara River Basin

Through the Serengeti National Park flows the Mara River that originates in Kenya in the Mau Escarpment and flows into Lake Victoria in Tanzania. The main tributaries are the Nyangores and Amala Rivers in the upper reach and the Engare Ngobit, Talak and Sand in the middle reache (see Figure 1-2). The first two tributaries are perennial rivers while the remaining tributaries are ephemeral rivers, thus they often dry up in rainless periods. In total, the river is 395 km long (Dessu et al., 2014) and its catchment covers an area of about 11,500 km^2 (McClain et al., 2013) of which about 65% is located in Kenya (Mati et al., 2008).

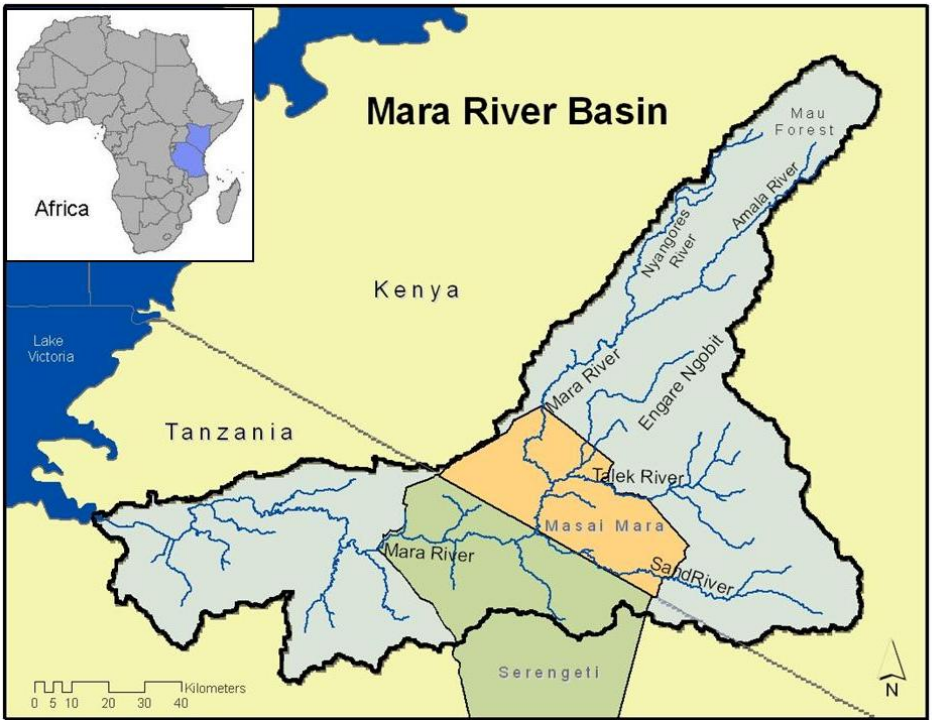

Figure 1-2: Map of the Mara River Basin with its tributaries (GLOWS, 2014)

1.2.Problem description

In the Mara River Basin (MRB), human interventions have led to deforestation and the increase of agricultural areas (Melesse et al., 2008). This conversion to cultivation, combined with the application of sub-optimal agricultural practices, would result in increased soil compaction. As a result, less rainwater would infiltrate into the soil and more water would flow as rapid surface runoff towards the river. This development could have significant impacts on the hydrology and ecology of the catchment.

One of the expected impacts is more extreme floods and dry periods (Mango et al., 2011). Through decreased infiltration, less water can be stored. In the worst case, the water is insufficient to cover the total water demand. Another consequence of the decreased infiltration is increased runoff. Most of the rainwater will directly flow into the river, causing a more rapid increase in water level and in more extreme peaks. In the worst case, this might result in flooding.

Another possible impact is decreasing water quality. With the increased fast runoff, more topsoil is expected to erode and to be transported to the river, polluting it (Defersha et al., 2012). An increase in sediment load results in a larger turbidity (see for example Figure 1-3) and therefore harm the ecology significantly: Through the increased turbidity, sunlight penetration decreases resulting in restricted photosynthesis and consequenctly the plant survival and dissolved oxygen content could decrease (Ven, 2011). However, the sediments could also encapsulate particles; for example, nutrients, phosphorus, heavy metals and pesticides that originate from agricultural fields and pollute the water.

In the Mara Basin, the loss of fertile soil is mostly addressed in the north where most of the cultivated areas are located. Currently, local people in the north are working on improving agricultural practices to reduce this erosion. A study by Kiragu (2009) has showed that the average daily sediment concentration is around 95 mg/l in the Nyangores River and Amala River, which is above the recommended standard of 30 mg/l in Kenya. This sediment concentration is measured between February 2007 and July 2007.

Figure 1-3: Example of turbid water in the Mara River

1.3.Stakeholders

To cope with these expected problems, UNESCO-IHE has started a project called MaMaSe (Mau Mara Serengeti). The goal of this project is improvement of water safety and security in this basin to support poverty reduction, a sustainable economic growth and conservation of the forest and rangeland ecosystems. Hence, the aim is to prevent deteriorating trends in this basin, while promoting an economic development that is water-wise to help people out of poverty and to help them improve their well-being independently.

In this project, several partners, both international and national, consisting of governmental, civil society, private sector, NGO and knowledge institutions, are working together (see Table 1-1).

Table 1-1: Overview of stakeholders and their stakes

Partner name	Country	Type	Involvement
UNESCO-IHE	Netherlands	Knowledge institute & project leader	Projectleader with WWF Kenya
WWF Kenya Country Office	Kenya	Knowledge institute & project leader	Close cooperation with UNESCO-IHE in leading the project
Egerton University	Kenya	Knowledge institute	Knowledge provision
Kenya Water Resource Management Authority	Kenya	Kenya public sector	Knowledge provision
Mara Farming	Kenya	International private sector	Located in the Mara River Basin
Netherlands Embassy Nairobi	Kenya	Kenya public sector	Financial support
GIZ (Gesellschaft für Internationale Zusammenarbeit)	Germany	NGO	Knowledge provision, promotes food security and drought resilience in Kenya
HSBC Bank	International	International private sector	Financial support
Regional Water Authority Brabantse Delta	Netherlands	Duth public sector	Knowledge provision
SNV (Netherlands Development Organisation)	Netherlands	NGO	Promotes clean water in Kenya
Wageningen UR	Netherlands	Knowledge institute	Knowledge provision
ITC-Twente	Netherlands	Knowledge institute	Knowledge provision
Deltares	Netherlands	Knowledge institute	Knowledge provision
Nile Basin Initiative - NELSAP	International	International private sector	The Mara River Basin is part of the Nile Basin
East African Community Lake Victoria Basin Commision	Inter-governmental	International public sector	The Mara River flows into Lake Victoria

1.4.Project details

With the increased runoff, more erosion of the topsoil is expected, which could result in decreased water quality, loss of fertile soil, siltation and morphological river changes. Within this study, the hydrology and sediment flow is modelled to evaluate this hypothesis and to locate the major sources of the sediments. Focusing on river catchment in Kenya and the detected erosion in the upper catchments, the main research question is:

What are the main sources of the suspended sediments in the Mara River in Kenya?

This question is solved with the following methodological steps:

1. Create a semi-distributed hydrological model applying the concept of FLEX-Topo.
2. Combine this hydrological model with the empirical model MUSLE (Modified Universal Soil Loss Equation) to assess the soil loss from the catchment.
3. Use this model to assess the main areas contributing to the suspended sediment load in the Mara River.

With this model, the hydrological system and the main sediment sources are assessed. In future, this model can be used to study the influence of expected land use changes or of proposed measures.

2. Methodology

In this section, the methodododology to determine the major sediment sources is explained.

At first, an impression of the current situation was obtained through desk study. This included: climate, topography, land use, soil type and current challenges in the catchment such as water scarcity and decreasing water quality. See section 3.1 *Site description* for the results of this study.

Then, data series and maps were collected and analysed to determine their quality and availability. An overview of the required data and type of analysis is given in Table 2-1. See section *3.2 Data* for more details on the analyses and their results.

These data were then used in the modelling step: first, a hydrological model was created and then combined with the empirical sediment yield model MUSLE to determine the soil loss from the catchment. In Overview 2-1, a summary is given of the steps required for the set-up of the model. In sections *4 Hydrology* and *5 Sedimentology* the details are given on the modelling methodology.

Table 2-1: Overview of the required data and the type of data analysis

Data	Type of analysis
Precipitation	Check the data quality at each station using double-mass curves
Temperature	Check the data quality by comparing the temperature variability in the MRB with satellite data
Discharge, water level	Check the data quality of the discharge and water level data by looking at the rating curves
Cross-section profile	Check the data quality by looking for possible inconsistencies
Sediment concentration	Check the data quality by looking at the accuracy of the measuring device, and Check which grain sizes are included in these data based on the measuring method
Turbidity	Check the data quality by verifying the data does not exceed the devices maximum and by looking at the device accuracy
Digital Elevation Map (DEM)	Check the data quality looking at the resolution and possible inconsistencies
Land cover map	Check the data quality looking at the resolution and possible inconsistencies
Soil map	Check the data quality looking at the resolution and possible inconsistencies
NDVI map	Check the data quality looking at the resolution and possible inconsistencies
Field observations	Identify the hydrological response units, erosion features and currently applied mitigating measures

Overview 2-1: Required steps to set-up a hydrological model and combine it with a suspended sediment transport model

1. Hydrological modelling
    a. Classification into hydrological response units (HRUs) based on the landscapes and land cover. These are areas that are expected to respond similarly.
    b. Set up the hydrological model. Define a model structure for each HRU and limit the number of calibration parameters by estimating or constraining them. Also apply process constraints where possible.
    c. Run, evaluate and improve the model
2. Suspended sediment transport modelling
    a. Split the suspended sediments into coarse sediments, mainly found in the bed and fine sediments, mainly found in the wash load.
    b. Assess the origin and order of magnitude of the suspended sediments for the coarse sediments assuming the transport is capacity limited
    c. Assess the origin and order of magnitude of the suspended sediments for the fine sediments using the empirical formula MUSLE

3. The study area

3.1.Site description

Climate

Within the Mara River Basin, there are two wet seasons linked to the annual oscillations of the ITCZ (Inter-tropical Convergence Zone). The first wet season is approximately from March to May and the second from October to December (McClain et al., 2013). The precipitation varies spatially over the catchment following the local topography. The largest annual rainfall can be found in the upstream area of the catchment; there it is between 1000 and 1750 mm. In the middle and downstream areas, the annual rainfall is between 900 and 1000 mm and between 300 and 850 mm, respectively (Dessu et al., 2014). See Appendix A: Site description for a map of the precipitation.

Topography

The elevation varies in the river basin between 3000 m + S.L. (Sea Level) at the Mau Escarpment, 1480 masl at the border to Tanzania and 1130 m + S.L. at Lake Victoria (McClain et al., 2013). For the modelling a digital elevation map (SRTM) as shown in Figure 3-1 is used with a resolution of 90 m and vertical accuracy of 16 m (U.S. Geological Survey, 2014).

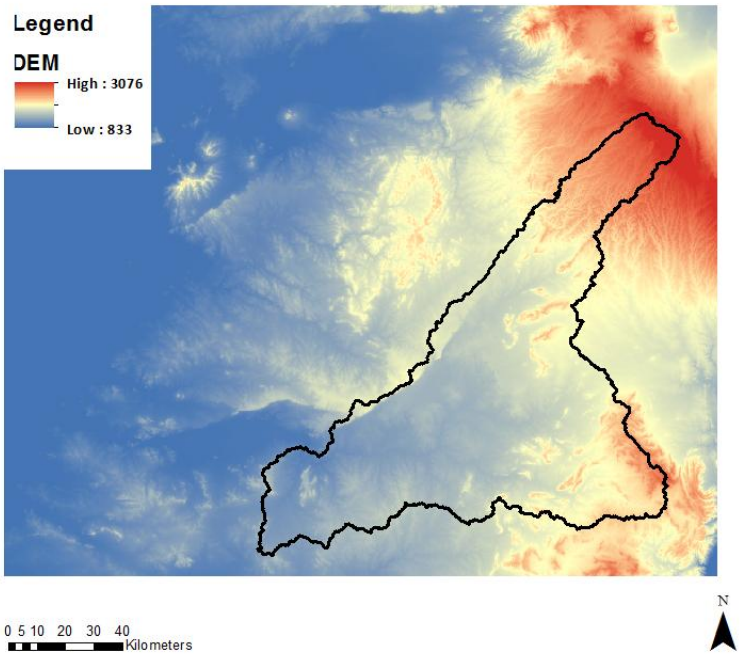

Figure 3-1: Digital elevation map (DEM) of the Mara River Basin (U.S. Geological Survey, 2014)

Land cover

For the assessment of the main land covers, groundtruth and satellite images are used in Africover. In the Mara River Basin, the main land cover types are agriculture, grass, shrubs and forests (see Figure 3-2). The main forest in the catchment is the Mau Forest, which is located in the north. Also, croplands are mainly found in the north and in the south, whereas the middle part is dominated by grasslands.

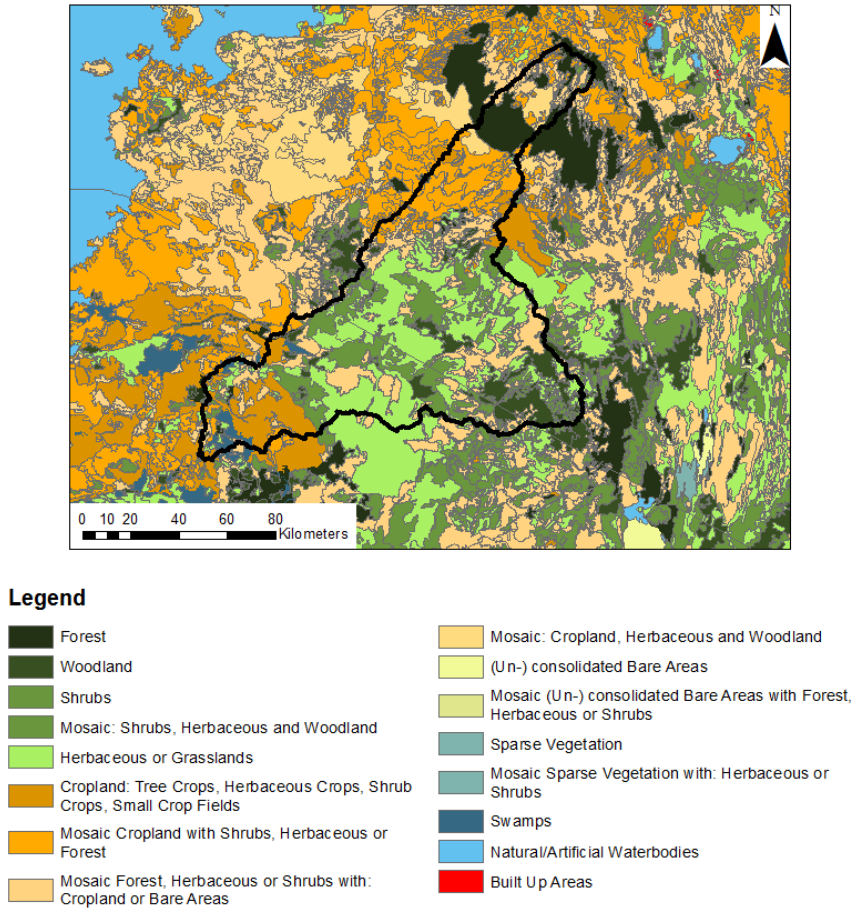

Figure 3-2: Land cover map of the Mara River Basin (FAO, 1998)

Soil type

For the soil classification, the product map SOTWIS is used; it is a combination of SOTER (Soil and Terrain database) and WISE (World Inventory of Soil Emmission Potentials). As this map is specifically made for Kenya, the soil characteristics of Tanzania are added by combining the classification method of SOTWIS with the Tanzanian soil type map available via ILRI (International Livestock Research Institute).

The soil is classified into five texture classes: course, medium, medium fine, fine and very fine, which are determined based on the content of sand, silt and clay (see Table 3-1 and Figure 3-3).

Table 3-1: Soil content for each texture class in the Mara River Basin in Kenya based on SOTWIS: average value and range within the catchment in brackets

Texture class	Sand content [%] (50 - 2000 µm)	Silt content [%] (2 - 50 µm)	Clay content [%] (<2 µm)	Organic carbon content [%]
Medium	40 (15 – 60)	36 (19 – 70)	25 (15 – 32)	3 (1 – 5)
Fine	29 (20 – 50)	25 (15 – 30)	46 (35 – 53)	2 (1 – 4)
Very fine	10 (9 – 20)	24 (20 – 28)	66 (60 – 67)	2 (2 – 2)

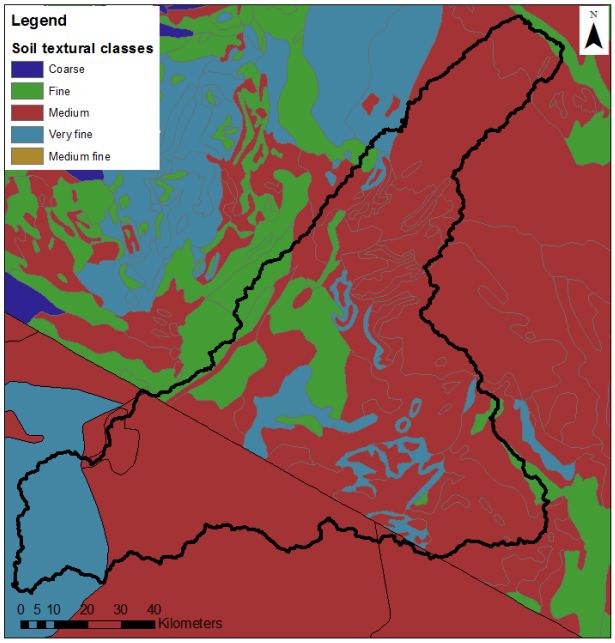

Figure 3-3: Soil textures in the Mara River Basin based on SOTWIS

Challenges in the catchment

As already indicated, human interventions have changed the natural environment, which can harm the ecology or pose a threat to the water users depending on the size of the change. A few examples of the challenges are:

- Land use change. In the past, deforestation (-32% between 1973 and 2000) and cultivation (+ 203%) have taken place. This is in itself not an issue as it contributes to economical growth, however, since it influences different processes as runoff, infiltration and evaporation, it can be a trigger for other issues; for example increased catchment erosion or inflow of fertilizer into the water system (Mati et al., 2008).
- Water scarcity. To ensure a healthy river system, minimum flow levels have been determined in studies called 'Environmental Flow Assessments' (EFA). By comparing these minimum levels to the actual ones, it was found that during droughts the water availability is critical or even insufficient (LVBC, 2012). This situation might become even severe as the water demand has increased with about 40% between 2000 and 2010 (Khroda, 2006). This larger water demand is caused by population growth and increased livestock numbers (Mati et al., 2008).
- Decreasing water quality. In the EFA studies, it was also found that the water quality has declined in the past 15 years. Especially during extreme low flows the quality is poor. (Subalusky, 2011)
- Increased catchment erosion. Data on turbidity and sediment concentration are found to exceed the recommended standards. This results in decreased water quality and is expected to influence the river morphology and might have caused the increased area of wetlands (+387%) (Mati et al., 2008). This expectation still needs to be confirmed though.

These challenges are explained more detailed in the Appendix A: Site description.

3.2.Data availability

For this study, different data types were used: data series and spatial maps. For precipitation, temperature, water level, discharge and turbidity data series of multiple stations were used (Figure 3-4). In Table 3-2, the maximum time range of all stations combined and data coverage are indicated. For the precipitation and temperature series the average coverage of all stations is shown. In Appendix B: Data analysisthis is done for each station separately.

For the turbidity and sediment concentration, also data from single measurement points were collected based on literature. Their coverage is indicated by the number of samples within the entire Mara River Basin (MRB) or at certain stations. These stations are at the same locations where the water levels are measured.

Moreover, different maps were used: digital elevation map (DEM), NDVI (Normalized Difference Vegetation Index) maps, land cover maps and soil maps (see Table 3-2). For the land cover, different products are compared with each other in Appendix C: Observed erosion features. This comparison shows that there are many inconsistencies between the products. For the study, the product Africover was used, a map that uses groundtruth and satellite images.

Table 3-2: Overview of available data series

	Data type	Nr of stations	Source	Time range	Date coverage/samples
Precipitation	Time series	30	Station data	1959-2011	82%
Temperature	Time series	9	NOAA, Station data	1957-2014	68%
Water level	Time series	3	Station data	1955-2013	Amala: 73% Nyangores: 86% Mines: 69%
Discharge	Time series	4	Station data	1955-2008	Amala: 73% Nyangores: 85% Mines: 69%
Turbidity	Time series	2	Station data (Mulot headquarter and Bomet Water Supply Station)	2012-2014	Amala: 92% Nyangores: 92%
Turbidity	Single measurements	19	Data from literature	2012-2014; 2007-2009	Amala: 45 Nyangores: 55 Mines: 2 MRB: 347
Sediment concentration	Single measurements	10	Station data from literature	2006-2008	Amala: 38 Nyangores: 34 Mines: 8 MRB: 96

Table 3-3: Overview of available spatial maps

	Data type	Source
DEM	SRTM map	USGS
NDVI	Map	USGS; derived from Landsat images
Land cover	Map	Africover (1998), Agristat, AVHRR (1982-1993), GLC (2000-2007), Globcover (2005 & 2009), GLCNMO (2003 & 2008)
Soil type	Map	KENSOTER 2.0 (2007), SOTWIS (2004)

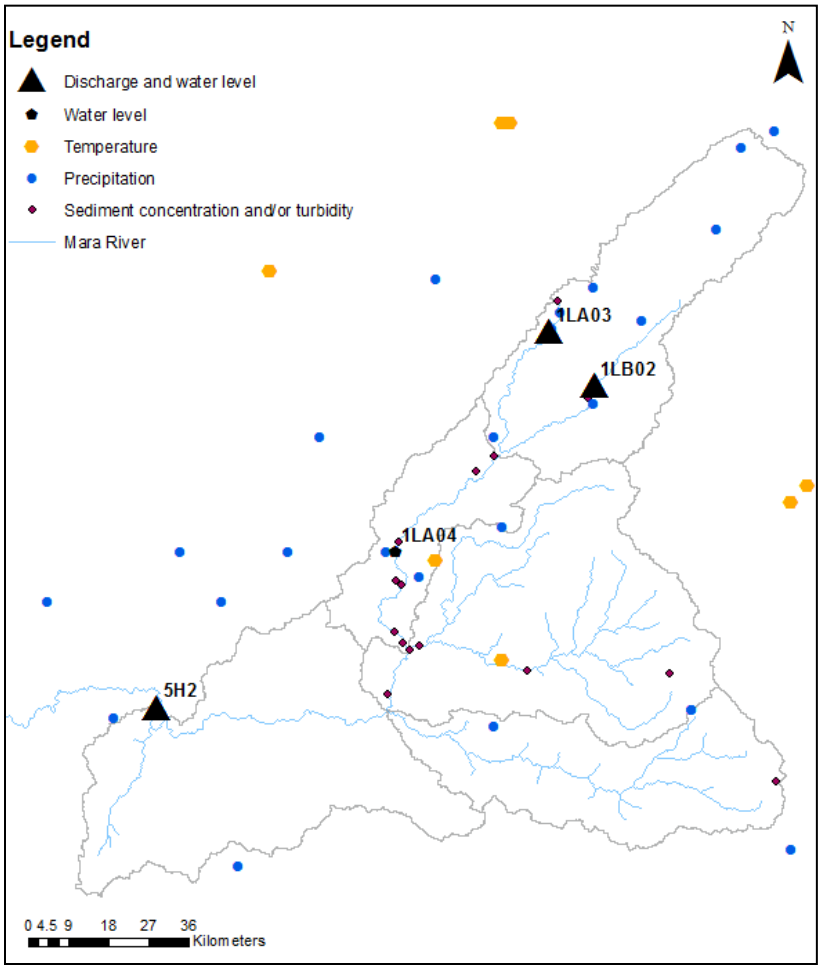

Figure 3-4: Map with all the data stations

3.3.Data analysis

Precipitation

The precipitation stations were checked using a double mass analysis in which the cumulative annual rainfall of two stations is plotted against each other. This curve should be approximately a straight line otherwise there is a change in observation in one of these two stations; hence the data are inconsistent. Additionally, the cumulative annual rainfall of a certain station was plotted against the average annual cumulative rainfall of all stations. If there are inconsistencies that cannot be corrected, then this station is discarded. In Figure 3-5, the double mass curves of two stations are shown as an example: the first has no inconsistencies (right figure), whereas the second does have inconsistencies (left figure); see Appendix B: Data analysis for the remaining double mass curves.

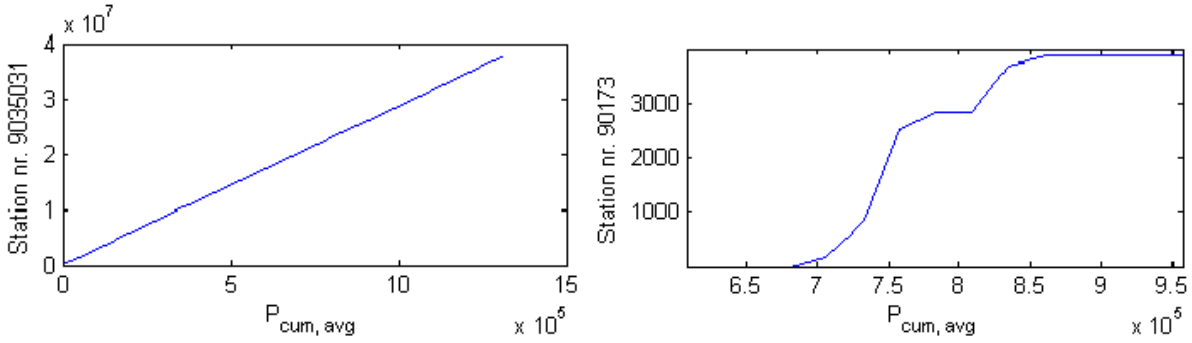

Figure 3-5: Double mass curve: comparing the cumulative annual rainfall at station 9035031 (left) and 90173 (right) with the average cumulative rainfall at all stations in [mm]

Water level and discharge

Often, the discharge is determined based on the stream water level through a rating curve. This curve is checked by plotting the discharge against the water level. As shown in Figure 3-6, the rating curve has been adjusted multiple times in the Amala tributary and at Mara Mines, where the observed water level height has decreased significantly. In the Nyangores tributary, only one rating curve has been used. This means that only for this location, the discharge data can be used whereas at the other two stations new rating curves need to be created to determine the discharge. In Appendix B: Data analysis, the water level and discharge is plotted for all three stations.

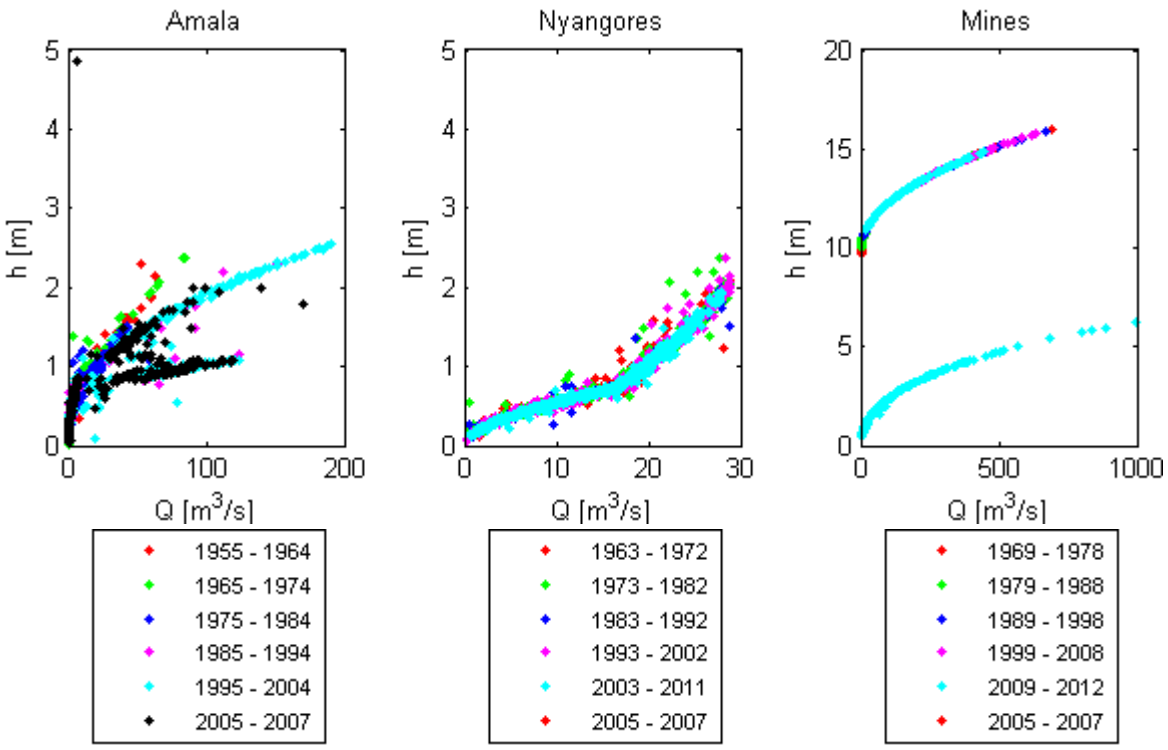

Figure 3-6: Rating curve for the stations Amala (1LB02), Nyangores (1LA03) and Mines (5H2)

Turbidity

In the Nyangores and Amala, the turbidity was measured daily in 2014 and between 2012 and 2014 respectively (see Figure 3-7). At these locations, the turbidity was also measured in 2007 as part of an MSc thesis (Kiragu, 2009). At other locations in the catchment, various data points were collected from previous studies (McCartney, 2010; Subalusky, 2011).

As shown in *Appendix C: Observed erosion features*, these few field measurements were used to calculate the average annual turbidity. This is equal to 48 NTU in the Nyangores, 307 NTU at the Talek confluence and 101 NTU in the Mara River upstream of the Talek. Moreover, the data series collected by Kiragu also contain water level data on the same dates. These were used to convert the turbidity data to sediment concentrations. With this analysis, sediment loads can be estimated more easily.

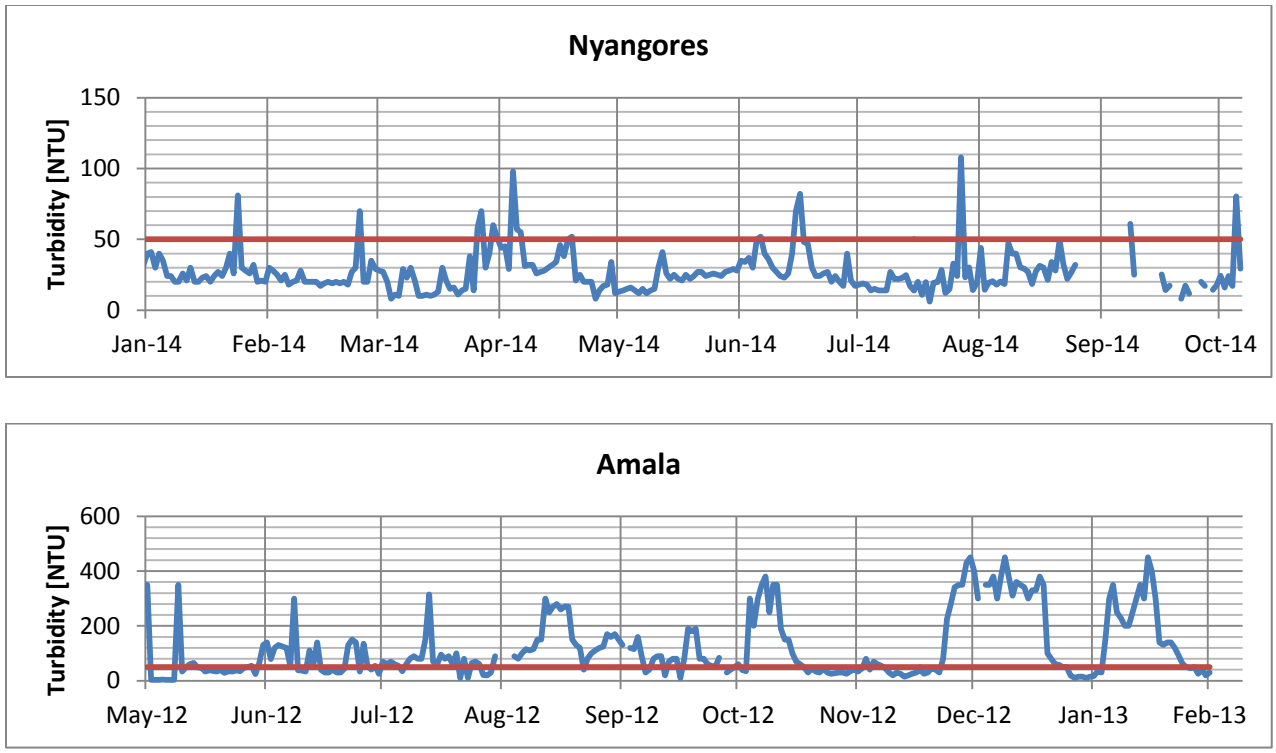

Figure 3-7: Turbidity measured in the Nyangores River at Bomet and in the Amala River at Mulot. The red line indicates the Kenyan standard of 50 NTU. In both tributaries there are large peaks however these are more extreme in the Amala River where the standard is exceeded almost continuously.

Sediment concentration

The sediment concentration was measured regularly in the Nyangores and Amala tributaries. These data were collected as part of an MSc thesis (Kiragu, 2009). As shown in Figure 3-8, the sediment concentration frequently exceeds the recommended standard in Kenya of 30 mg/l (Minister for Environment and Natural Resources, 2006).

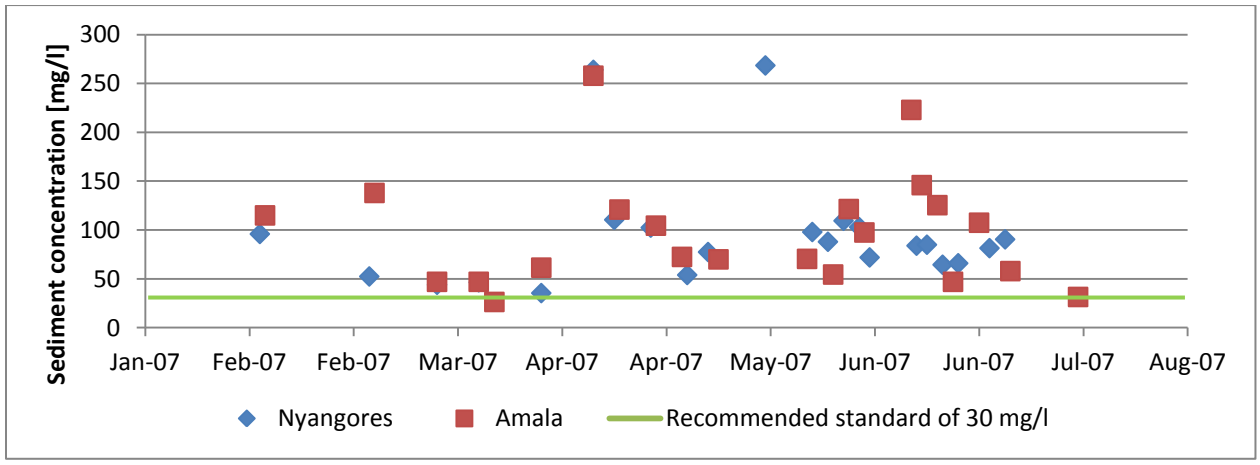

Figure 3-8: Sediment concentration measured in the tributaries Nyangores and Amala (Kiragu, 2009)

Observed erosion features

Based on interview results with local people, information from the SCMPs (Sub-Catchment Management Plans), field observations and measurements, a general impression was obtained on the occurrence of erosion in the catchment; see Table 3-4. In general, there are two main groups: croplands and Masai land. In the first case, sheet erosion is observed whereas in the second case there are gullies in addition to sheet erosion from the overgrazed fields. See *Appendix C: Observed erosion features* for a more detailed analysis.

Table 3-4: General overview: main sources, problems, causes and solutions related to erosion based on interviews, SCMPs and field observations

	Croplands	Masai land
Main sources	- Crop fields	- Grazing fields - Along roads and animal tracks
Problems	- Loss of fertile soil - River pollution - Siltation	- Loss of fertile soil - Gullies: threat for animals, decrease land area - Siltation
Suspected causes	- Poor land use management - Encroachment of riparian zone	- Overgrazing
Currently applied or suggested solutions	- Improved agricultural practices - Soil conservation practices - Forestation - Spring protection - River bank protection	- Improved agricultural practices - Soil conservation practices - Forestation - Spring protection - River bank protection - Block gullies - Reduce pressure - Construction of cut off drains, retention ditches and check dams

4. Hydrology

4.1.Model explanation

For this study, the modelling concept of FLEX-Topo is applied. This is a semi-distributed rainfall runoff model that distinguishes hydrological response units (HRUs) based on the topography. In this study, however, the HRUs are not only based on the topography, but also on the land cover. Each HRU is then represented by a lumped conceptual model. The advantage of the model is the limitation of the amount of parameters compared to distributed models and the addition of internal information compared to fully lumped models. (Savenije, 2010)

Within the Mara River Basin, the following HRU are defined for each sub-catchment:

1. Forested hill slopes
2. Shrubs on hill slopes
3. Agriculture
4. Grassland

In Figure 4-1, the resulting map of the HRUs is shown and in Table 4-1, the percentages of each unit within a sub-catchment. In *Appendix D: Classification*, results preceding this final classification are described: the creation of a landscape map based on the DEM using a threshold for the slope and HAND (Height Above Nearest Drain), the sensitivity of the applied threshold parameters and analyses on the land cover.

Table 4-1: Classification results: area percentage of each hydrological response unit per sub-catchment in the Mara River Basin

Sub-catchment	Agriculture	Shrubs on hill slopes	Grassland	Forested hill slopes
North	73%	0%	0%	27%
Middle	19%	16%	65%	0%
Talek	0%	21%	79%	0%
Sand	0%	42%	58%	0%
Lower	26%	23%	52%	0%

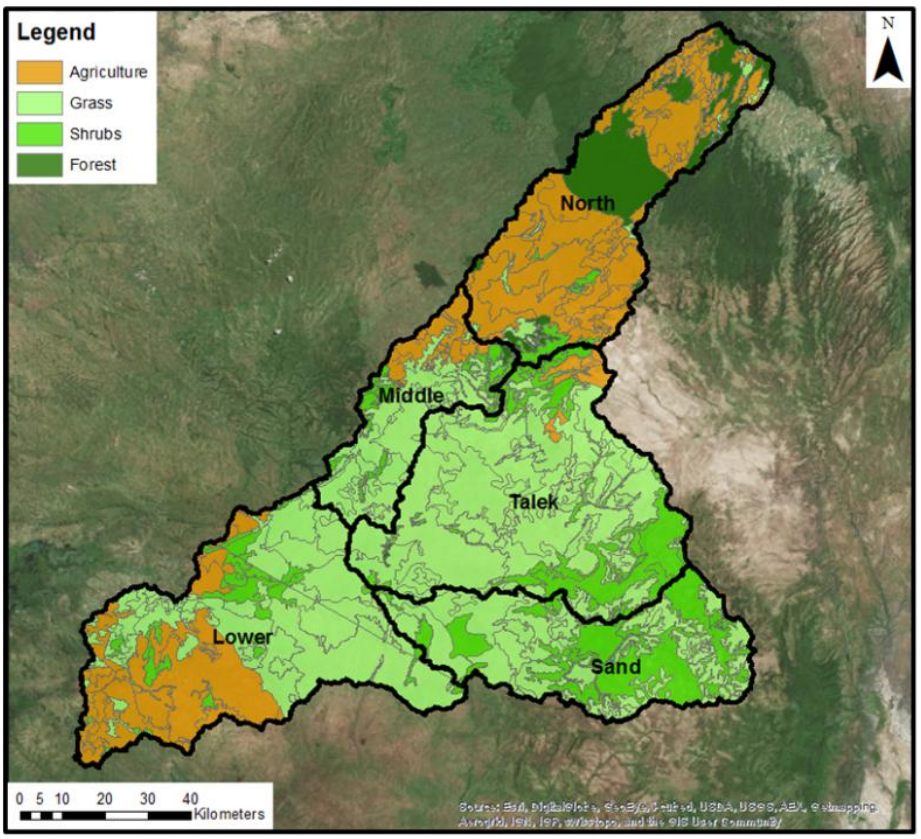

Figure 4-1: Classification of the Mara River Basin into four hydrological response units for each of the five sub-catchments

In the first two HRUs, Shallow subsurface flow (SSF) is perceived to be the dominating flow mechanism. Rainwater infiltrates into the soil and flows through root channels and animal burrows into the river. In contrast, barely any infiltration is assumed to take place in the other two HRUs. There the observed soil compaction is assumed to limit the infiltration capacity resulting in overland flow during heavy rainfall. Consequently, there Hortonian overland flow (HOF) is assumed to be the dominant flow mechanism. This assumption on the dominant flow mechanisms is used to find a suitable model structure. The model concept is visualized in Figure 4-2 and the model structure for each HRU is shown in Figure 4-3.

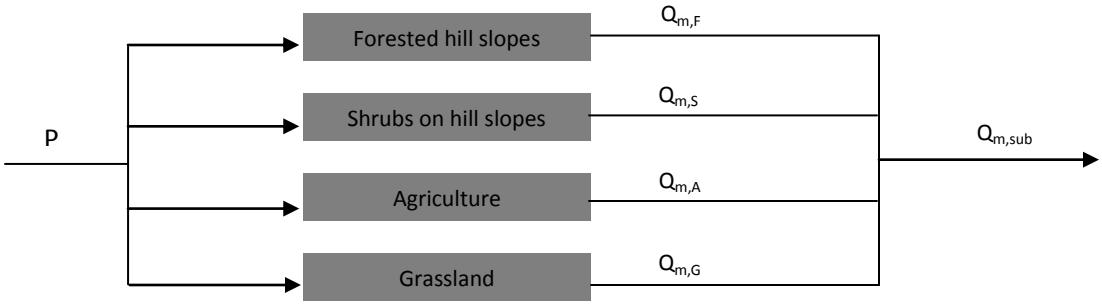

Figure 4-2: Schematization of the model concept for one sub-catchment. The model structure for the HRU *Forested hill slopes* and *Agriculture* are shown in Figure 4-3.

As shown in the model structure, the model consists of multiple storage components which are schematised as reservoirs. For each reservoir, the inflow, outflow and storage are determined for each time step using water balance equations as shown in Table 4-2. Thus, with this model the fluxes between each reservoir and the storage are simulated as a function of time. Each HRU responds independently, however, they are connected through the groundwater system. To find the total runoff at the sub-catchment outlet $Q_{m,sub}$, the outflow $Q_{m,i}$ of each HRU is multiplied by its area percentage and then summed up together with the groundwater discharge Q_s. The area percentage is the area of a specific HRU divided through the entire sub-catchment area. Then, the modelled discharge at the catchment outlet is determined by applying a simple river routing technique in which a delay from the sub-catchment outlet to the catchment outlet is added by assuming an average river flow velocity of 0.5 m/s.

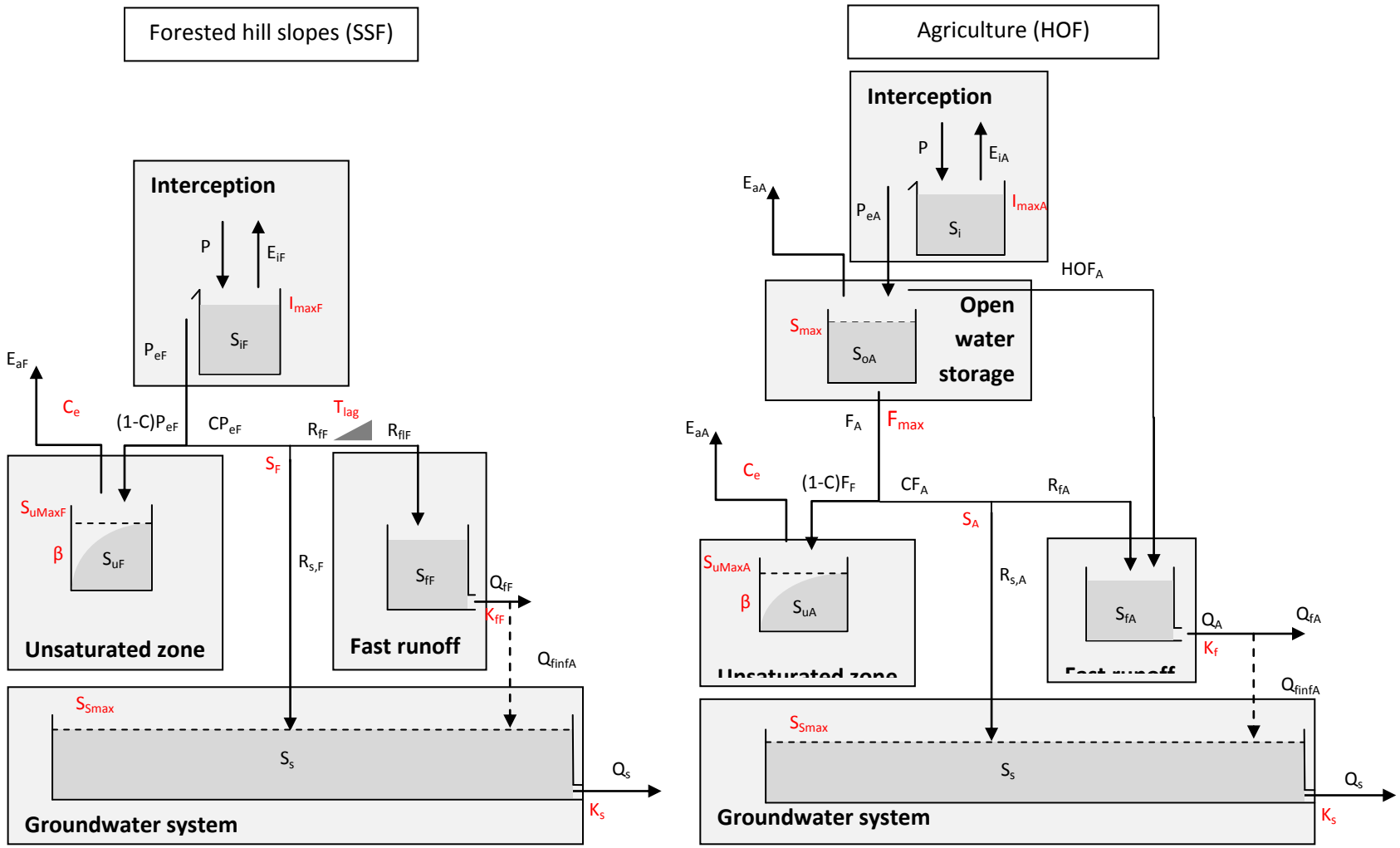

Figure 4-3: Model structure for the HRU *Forested hill slopes* (left) and for *Agriculture* (right). The structure for *Shrubs on hill slopes* is similar to the left one replacing the indices F with S. The structure for *Grassland* is similar to the right one replacing the indices A with G. Parameters are marked in red, storages and fluxed in black. Symbol explanation: Fluxes: precipitation (P), evaporation of the interception zone (E_i), actual evaporation (E_a), effective precipitation (P_e), infiltration into the unsaturated zone (F_A), discharge from unsaturated zone to the fast runoff zone (R_f), groundwater recharge (R_s), discharge from the fast runoff (Q_f), infiltration into groundwater system only applied in the sub-catchment Sand ($Q_{f,\,inf}$), discharge from the slow runoff (Q_s). Storages: storage in the interception zone (S_i), open water storage (S_{oA}), storage in the unsaturated zone (S_u), storage for the slow runoff (S_s), storage for the fast runoff (S_f). Remaining symbols: splitter (S), splitter (C), soil moisture distribution coefficient (β), transpiration coefficient (C_e = 0.5), reservoir coefficient (K); indices f and s indicate the fast and slow runoff. Units: fluxes [mm/d], storages [mm], reservoir coefficient [d], remaining parameters [-].

Table 4-2: Equations applied in the hydrological model. The formulas for the unsaturated zone are written for the hydrological response units: *Forested hill slopes* and *Shrubs on hill slopes*; for grass and agriculture, the inflow P_e changes to F.

Reservoir system	Applied equations
Interception	$E_i = \min(E_p, \min(P, I_{max}))$ $P_e = \max(P - E_i, 0)$
Surface water	$\frac{dS_o}{dt} = P_e - F - HOF - E_o$ $F = \min(S_o, F_{\max})$ $HOF = \max(0, S_o - S_{max})$ $E_o = \max(0, \min(E_p - E_i, S_o))$
Unsaturated zone	$\frac{dS_u}{dt} = (1 - C) * P_e - E$ $C = 1 - \left(1 - \frac{S_u}{S_{u,max}}\right)^{\beta}$ $E = \min\left((E_p - E_i), \min\left(S_u, (E_p - E_i) * \frac{S_u}{S_{u,max}} * \frac{1}{C_e}\right)\right)$
Groundwater recharge	$R_s = S * C * Pe$
Fast runoff	$\frac{dS_f}{dt} = R_{fl} - Q_f$ $R_{fl} = T_{lag}(C * Pe - R_s)$ → delay added using a linear function T_{lag} $Q_f = \frac{S_f}{K_f}$
Groundwater	$\frac{dS_s}{dt} = R_{s,tot} - Q_s$ $R_{s,tot} = \sum_{i=1}^{i=4} R_{s;HRU_i}$ $Q_s = \frac{S_s}{K_s}$
Total runoff	$Q_m = Q_s + \sum_{i=1}^{i=4} Q_{f;HRU_i}$

4.2.Parameter constraints and estimation

By adding estimating parameters or constraining them, unrealistic results are excluded. The applied parameter constraints are related to the interception and the reservoir coefficient K. For example, the largest interception is expected in the forest and the groundwater system is expected to respond the slowest, hence the reservoir coefficient is the largest. The applied parameter constraints are:

- $I_{max,forest} > I_{max,grass}, I_{max,shrubs}, I_{max,cropland}$
- $I_{max,shrubs} > I_{max,grass}, I_{max,cropland}$
- $K_s > K_{f,\ forest/shrubs}$, $K_{f,\ cropland/grassland}$
- $K_{f,\ forest/shrubs} > K_{f,\ cropland/grassland}$

The following parameters are estimated: $S_{u,max}$, K_s, S_{max}

Maximum storage capacity $S_{u,max}$

The parameter $S_{u,max}$ represents the amount of water stored in the root zone. This storage is equal to the maximum deficiency between precipitation input and output which is the water demand or the evaporation (Gao et al., 2014). Assuming a linear relation between the evaporation and the NDVI (Normalized Difference Vegetation Index), the evaporation during a dry season E_d is calculated as follows:

$$\frac{E_d}{E_a} = \frac{NDVI_D}{NDVI_A}\ thus\ E_d = E_a * \frac{NDVI_D}{NDVI_A}$$

The NDVI is a vegetation indicator used to analyse remote sensing measurements. Its values range from -1 to 1; NDVI = -1 corresponds to water, NDVI = 0 to bare areas and NDVI = 1 to forests. In this formula, E_d is the evaporation during a dry season, E_a the actual evaporation, $NDVI_A$ the long-term average annual NDVI and $NDVI_D$ the same parameter but during dry periods. As a result, the parameter $S_{u,max}$ is estimated for each HRU regardless the location within the catchment (see Table 4-3).

Table 4-3: Estimated values for the parameter $S_{u,max}$ for each HRU

HRU	$S_{u,max}$ [mm]
Forested hill slopes	122
Agriculture	94
Shrubs on hill slopes	89
Grass	83

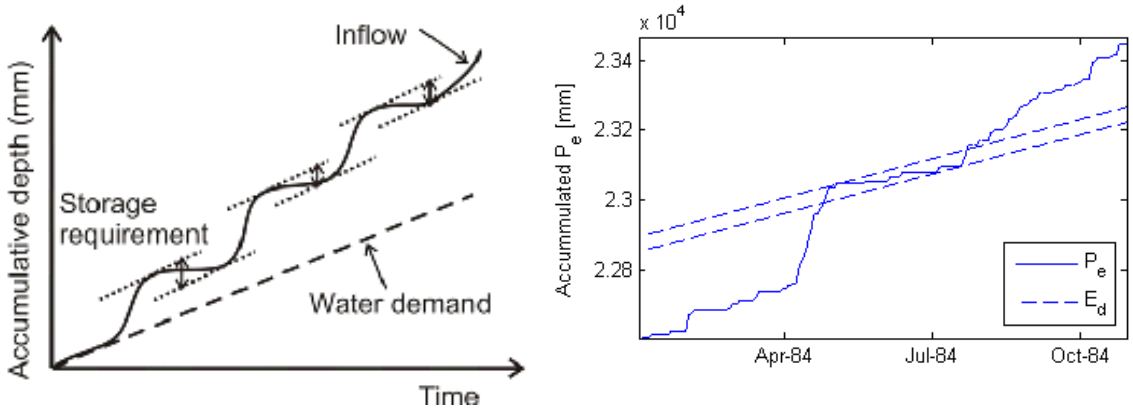

Figure 4-4: Cumulative plot of the inflow which is the effective rainfall P_e and the water demand which is the long-term average dry season water demand E_d. Left: Schematization (Gao et al., 2014). Right: Application to precipitation station nr. 9035085 in the sub-catchment North (right).

Reservoir coefficient for the groundwater system K_s

The parameter K_s is the reservoir constant that relates the outflow Q of a reservoir to its storage S: $S = -K_s * Q$. This parameter is estimated by doing a hydrograph recession analysis. During low flows the following relation between discharge and storage holds:

$$Q_s = \frac{dS_s}{dt} = \frac{d(-K_s * Q_s)}{dt}$$

$$Q_s = \mathrm{Q_{t=0}} * \exp\left(-\frac{t}{K_s}\right)$$

$$\ln(Q_s) = \ln(Q_{t=0}) + \ln\left(\exp\left(-\frac{t}{K_s}\right)\right)$$

Therefore, the reservoir coefficient is estimated during low flows and is found to be 28 d. See *Appendix E: Hydrological modelling* for more details.

The maximum surface water storage S_{max}

In the grasslands and cultivated areas, part of the water cannot infiltrate due to rainfall intensities exceeding the infiltration capacity. At first, this water is stored on the surface in pools and sinks. Only when this storage capacity is exceeded, hortonian overland flow takes place. This storage capacity is estimated with an elevation map. With this map, a flow direction map is built and sinks are located. Each sink has a certain volume equal to the height difference multiplied with the number of cells and the grid size. This volume divided through the sub-catchment area results in the storage capacity S_{max}. In Table 4-4, the parameter values are shown for each sub-catchment.

Table 4-4: Maximum surface water storage capacity

Sub-catchment	Maximum surface water storage capacity S_{max} [mm]
North	35
Middle	53
Talek	49
Sand	16
Lower	26

The estimation of these parameters is explained in more detail in *Appendix E: Hydrological modelling*. The remaining parameters that are not estimated or constrained, are freely calibrated; these are: β, S_F, S_A, S_{smax} and F_{max}.

4.3.Process constraints

To eliminate more unrealistic results, process constraints are applied. In this section, a short overview of the applied constraints is given; a more detailed explanation is done in *Appendix E: Hydrological modelling*.

Constraint on the total runoff and evaporation using the Budyko curve

The total annual runoff and evaporation is estimated based on the Budyko curve. These fluxes should be almost the same as the model results. Using standard deviations, a bandwidth is created around the estimations based on the Budyko curve. The model results are expected to be within this range otherwise the results are unrealistic and therefore discarded. In formula form, this means:

$$R_{mean} - 5 * R_{std} < Q_{m,mean} < R_{mean} + 5 * R_{std}$$
$$E_{mean} - 5 * E_{std} < E_{m,mean} < E_{mean} + 5 * E_{std}$$

In this formula, R is the runoff and E the evaporation calculated with the Budyko curve; see Table 4-5 for the numerical results. The indices mean and std indicate that the average or standard deviation is taken.

Table 4-5: Estimated runoff and evaporation for each sub-catchment based on the Budyko curve: mean and standard deviation

Sub-catchment	R_{mean} [mm/d]	R_{std} [mm/d]	E_{mean} [mm/d]	E_{std} [mm/d]
North	0.23	0.08	779.64	96.46
Middle	0.30	0.10	766.06	107.52
Talek	0.18	0.07	824.59	92.67
Sand	0.22	0.07	917.61	89.61
Lower	0.23	0.03	856.98	32.80

Constraint on the transpiration using the NDVI

The transpiration in each HRU is correlated with each other in the same way as the NDVI. Assuming a linear relation between transpiration and NDVI, the following relation is derived:

$$\frac{E_{forest}}{E_{grassland}} = \frac{a * NDVI_{forest}}{a * NDVI_{grassland}} = \frac{NDVI_{forest}}{NDVI_{grassland}}$$

Using this relation, the transpiration in each HRU is constraint based on their NDVI. Expressed in formulas:

$$\left(\frac{\mathrm{NDVI_i}}{\mathrm{NDVI_j}}\right)_{\mathrm{mean}} - 5 * \left(\frac{\mathrm{NDVI_i}}{\mathrm{NDVI_j}}\right)_{\mathrm{std}} < \frac{\Sigma \mathrm{E_i}}{\Sigma \mathrm{E_j}} < \left(\frac{\mathrm{NDVI_i}}{\mathrm{NDVI_j}}\right)_{\mathrm{mean}} + 5 * \left(\frac{\mathrm{NDVI_i}}{\mathrm{NDVI_j}}\right)_{\mathrm{std}}$$

The indices i and j indicate two different HRUs. $NDVI_{mean}$ is equal to the temporal average and $NDVI_{std}$ the standard deviation in 2014 averaged over the catchment; see Table 4-6 for the numerical results.

Table 4-6: Results on the estimation of $NDVI_{mean}$ and $NDVI_{std}$. Both parameters are dimensionless.

Hydrological unit	$NDVI_{mean}$	$NDVI_{std}$
Forested hill slopes	0.7365	0.0662
Shrubs on hill slopes	0.5352	0.0559
Cropland	0.5838	0.0433
Grassland	0.4936	0.0679

Constraint on the groundwater recharge

The groundwater recharge in forests and shrub lands are expected to be larger than in croplands and grasslands. Hence, the following constraints are applied:

- $R_{s,F} > R_{s,C}, R_{s,G}$
- $R_{s,S} > R_{s,C}, R_{s,G}$

Constraint on the fast runoff infiltration

In the Sand sub-catchment, a large fraction of the fast runoff is assmued to infiltrate through the river bed into the groundwater system. Therefore, only during very heavy rainfall, runoff in the river is observed. This occurs only a few times a year. During the remaining rain events, the water is infiltrated recharging a sub-surface river system.

This observation is included as a constraint. The number of large storms causing runoff in the river should be less than 5. A storm is considered large as soon as the runoff is larger than 2 mm/d. Hence, the constraint is: $Nr_{Q_{f,storm>Q_{peak}}} < 5$

4.4.Model results and discussion

4.4.1. Calibration methodology

For the determination of the remaining parameters, the model is calibrated and validated. In the calibration step, a large amount of parameter combinations within the defined constraints are selected randomly applying the Monte Carlo method. Using a precipitation and temperature time series as input, each combination is run through the model to calculate the total runoff, which is the model output. This simulated runoff is then compared with the observed discharge using objective functions to evaluate the performance of each parameter set. Then by applying the MOSCEM-UA algorithm, offspring are generated to find parameter sets with a better performance (Vrugt et al., 2003). Finally, the parameter set with the best performance is selected and used for validation.

The applied objective functions are:

$$NS_{FDC} = 1 - \frac{\sum(FDC_{obs} - FDC_{sim})^2}{\sum\left(FDC_{obs} - mean(FDC_{obs})\right)^2}$$

$$NS_{\log(FDC)} = 1 - \frac{\sum(\log(FDC_{obs}) - \log(FDC_{sim}))^2}{\sum\left(\log(FDC_{obs}) - mean\left(\log(FDC_{obs})\right)\right)^2}$$

In the objective functions, the observed flow duration curve (FDC) is compared with the modelled one. In the second formula, the logarithm of the FDC is taken before calculating the Nash Sutcliffe (NS) value. With these two objective functions, the flow duration curve is evaluated based on high and low flows.

For the observed runoff, a new rating curve needs to be created as there is no data of good quality available at the station Mara Mines (see section *3.2 Data*). That is why this discharge is estimated based on the water levels applying the Stevens method: According to Strickler, the discharge is equal to:

$$Q = k * i^{\frac{1}{2}} * A * R^{\frac{2}{3}}$$

$$Q = a * A * R^{\frac{2}{3}}$$

With:

- k Strickler roughness coefficient [$m^{1/3}/s$]
- i slope [-]
- A cross-section [m^2]
- R hydraulic radius [m]

The cross-sectional profile was measured in previous studies (GLOWS-FIU, 2012) therefore both the cross-section and the hydraulic radius are known as a function of the water depth. Only the parameter *a* is unknown and which is calibrated. To evaluate the result of this calibration, this parameter is also estimated based on the slope and the roughness: $a=k*i^{1/2}$. A similar value for this parameter should be found with both methods.

4.4.2. Modelling results

As shown in Figure 4-5, the model performs well in both the calibration and validation. The values of the objective functions are: $NS_{log(FDC)}$ = 0.91 and NS_{FDC} = 0.71. During the calibration, the model does not simulate the abrupt increase in the high flows or the sudden decrease in the low flows. The validation shows that the model simulates the high flows better and the low flows worse: $NS_{log(FDC)}$ = 0.74 and NS_{FDC} = 0.93.

With the dot plots, it is possible to assess whether the calibrated parameters are uniquely defined. If none of the parameters are defined well, then equifinality can be expected. As shown in Figure 4-7, all parameters except for T_{lag} and S_{smax} are well defined; the one more clear than the other though.

This model also performed well when calibrating and validating it on the Nyangores sub-catchment: the objective functions are equal to $NS_{log(FDC)}$ = 0.98 and NS_{FDC} = 0.60 for the calibration and $NS_{log(FDC)}$ = 0.74 and NS_{FDC} = 0.76 for the validation. Also, the model is calibrated on the entire Mara River Basin and validated on the Nyangores and vice versa. The resulting values of the objective functions are:

- Validating the model for the MRB based on parameter results of the calibration of Nyangores $NS_{log(FDC)}$ = 0.29 and NS_{FDC} = 0.00
- Validating the model for Nyangores based on parameter results of the calibration of the MRB $NS_{log(FDC)}$ = 0.97 and NS_{FDC} = 0.75

The second validation, in which Nyangores is validated based on the results of the MRB, gives a better model performance. The reason is that the entire MRB includes HRU that occur in the Nyangores as well. However, the Nyangores does not include all HRUs of the MRB, hence when validating MRB based on Nyangores, worse model performances are expected. The hydrographs and flow duration curves (FDC) for these model results are shown in *Appendix E: Hydrological modelling*.

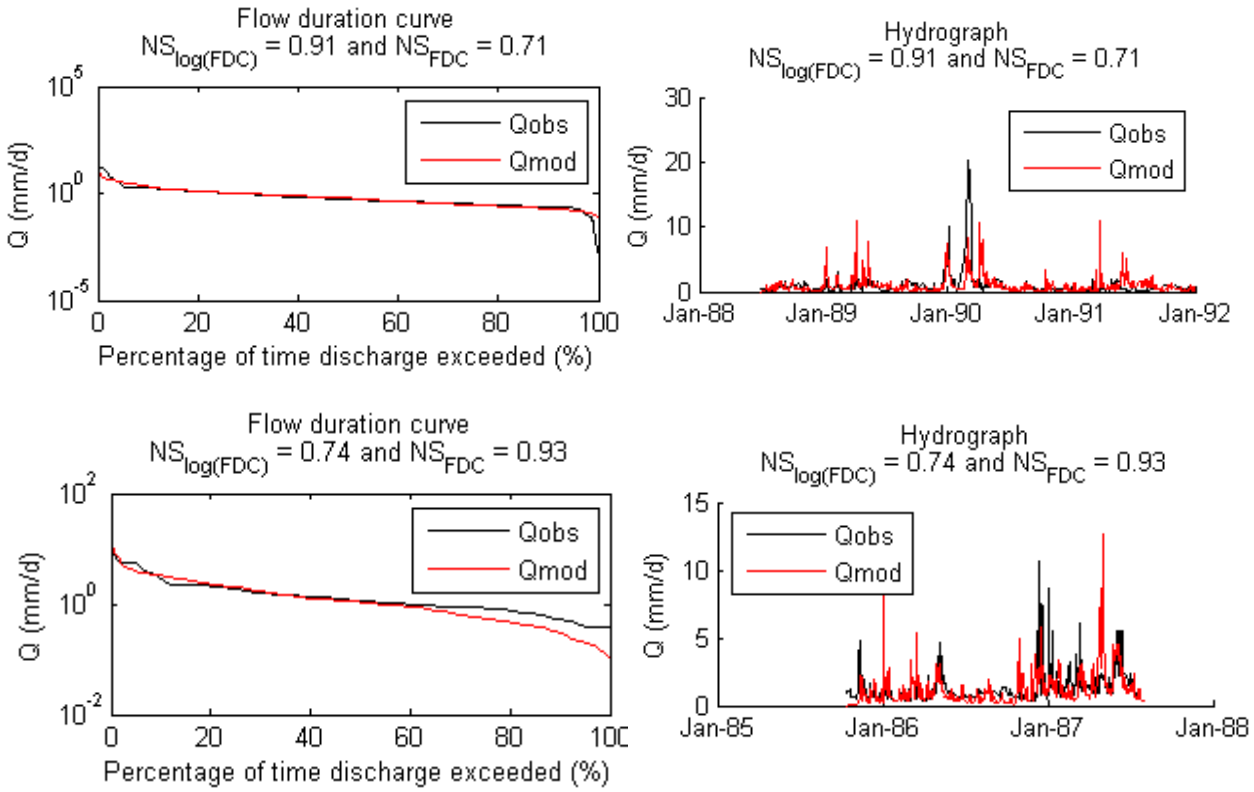

Figure 4-5: Calibration (upper) and validation (lower) results for the Mara River Basin: flow duration curve (left) and hydrograph (right)

Also, all the calibration results with $NS_{FDC} \geq 0.6$ and $NS_{log(FDC)} \geq 0.6$ are plotted to indicate their maximum range. This range is 9 mm/d at maximum during high flows and around 0.1 mm/d during low flows before it rapidly decreases to zero.

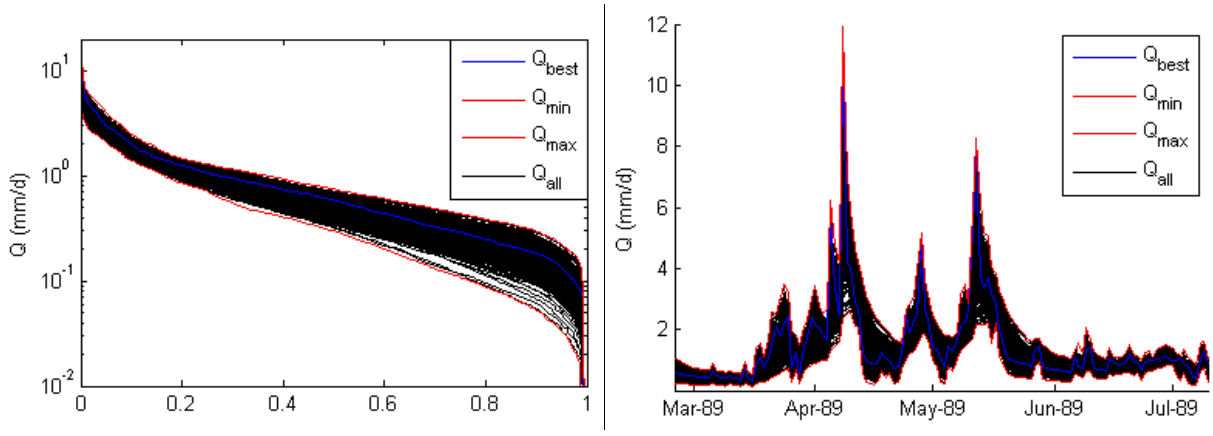

Figure 4-6: Plot of all the calibration results with $NS_{FDC} \geq 0.6$ and $NS_{log(FDC)} \geq 0.6$. The red lines indicate the lower and upper limit: Flow duration curve (left) and part of the hydrograph (right)

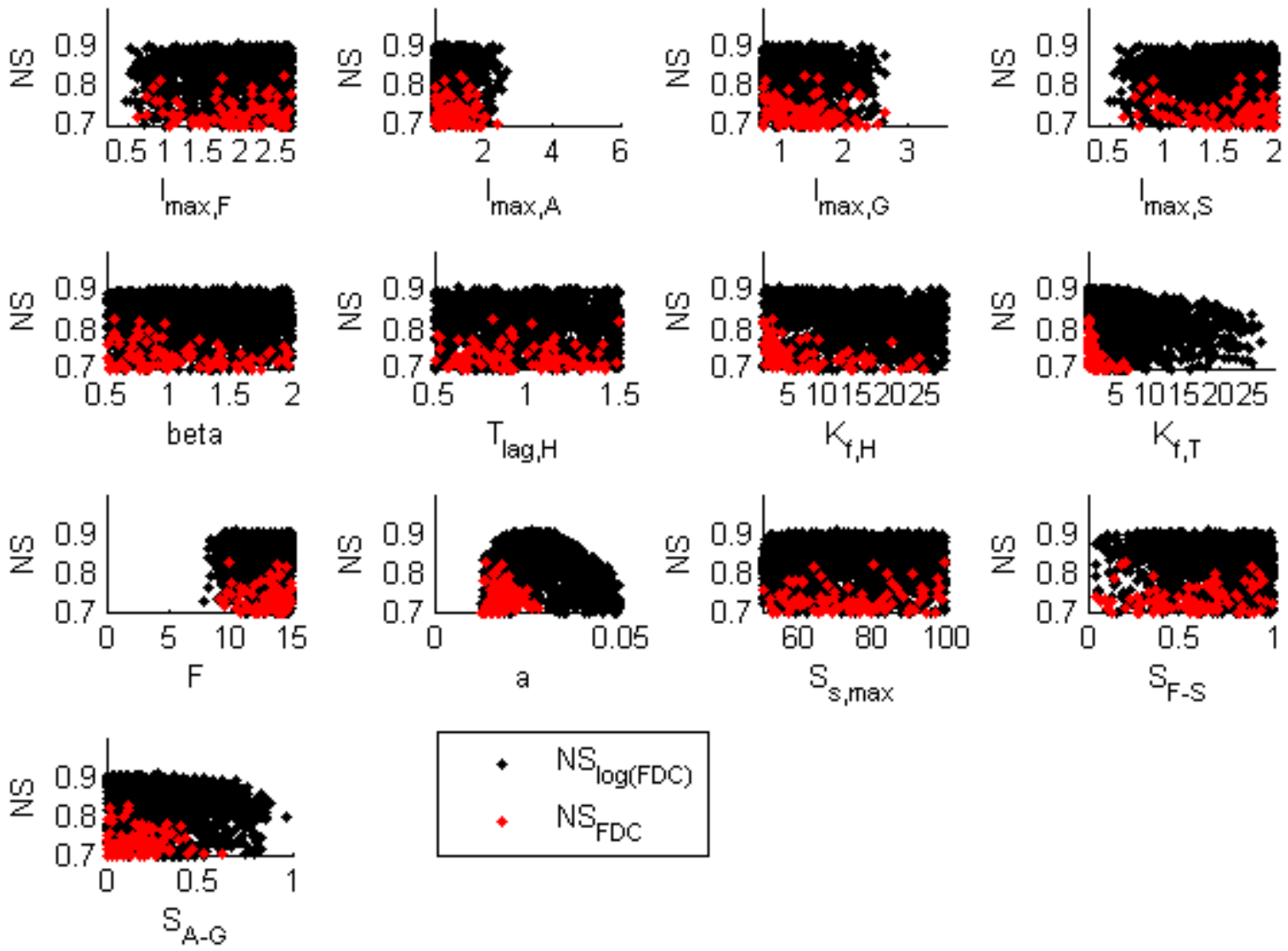

Figure 4-7: Dot plots for all calibrated parameters for the Mara River Basin. The minimum and maximum value on the horizontal axis is equal to the defined parameter boundaries for the calibration

4.4.3. Discussion

In the previous sections, the following aspects are shown:

- The model performs well during calibration and validation for the entire Mara River basin and the Nyangores sub-catchment
- Validation of the Nyangores sub-catchment based on parameters found while calibrating the entire Mara River Basin results in good model performances.
- Validation of the Mara River Basin based on parameters found while calibrating the Nyangores sub-catchment results in poorer model performances. The cause probably is the lack of grassland and shrubs in the Nyangores.

Additional, the following aspects are analysed:

- Sensitivity of the parameter a: This parameter is used to estimate the discharge applying the Stevens method: $Q=k \cdot i^{1/2} \cdot A \cdot R^{2/3} = a \cdot A \cdot R^{2/3}$. Calibrating this parameter gives a different result when estimating it based on the roughness and slope. This difference is caused by rapids near the measuring point. At these rapids, the parameter is found to increase locally during low flows. During high flows however, the effect of rapids is negligible. See *Appendix E: Hydrological modelling* for more information and a graphical illustration.
- Influence of the constraints: Excluding each constraint decreases the model performance. Hence, parameter sets are excluded for the right reason. See *Appendix E: Hydrological modelling* for the number of samples rejected through each constraint and the decrease of the model performance when excluding a constraint.
- Influence of semi-distributing the catchment: A splitting the model into five sub-catchments and four HRUs improves the model results compared to a lumped model. In *Appendix E: Hydrological modelling*, the hydrographs, flow duration curves and objective functions are shown for the scenarios in which the model is lumped to one catchment or lumped to a single HRU.

4.4.4. Recommendations

The main restriction in this study is the limited data availability. There are only a few rainfall stations available in the catchments and they all have a lot of gaps and stop around the year 2000. As a result, the calibration and validation is done for the 80s. Moreover, due to the limited number of stations and the large heterogeneity even within a sub-catchment, it is not possible to capture all peaks well.

To improve the model performance, it is advised to study the following aspects more detailed:

- Use the data that are measured in the catchment since October 2014. These new data cover the entire catchment and includes: precipitation, temperature and water level. With this data, it is possible to perform more detailed analysis within the catchment to check for example the expected preferential flow paths and the typical delay times. Also, multiple rainfall stations in a sub-catchment instead of a single one can be used to reduce the effects of heterogeneity.

- Check the rating curve at Mara Mines, the outlet of the MRB in Tanzania. In this study, the discharge is determined based on the water level applying the Stevens method. Hence, a new rating curve is created. However, it is found that the parameter *a* depends on the water level instead of being constant. This is a result of rapids near the measuring location. For a more accurate rating curve, it is advised to analyse this parameter more detailed.
- Suitability of using satellite data on rainfall instead of station data. For the precipitation, a limited number of stations are available for 1960 to 2000 is available. Therefore, satellite data might be useful for the calibration and validation of more recent time series. Also, with satellite data effects of heterogeneity could be reduced. However, the quality of these data needs to be assessed before using it.
- Suitability of using satellite data on evaporation. These could be used as an additional process constraint. However, these data first need to be analysed to assess their quality.

5. Sedimentology

The river transports both coarse and fine particles. Coarse particles participate in bed load and suspended load whereas fine particles in wash load. The transition between them is between 50 µm and 70 µm (Vriend et al., 2011). All suspended load influences the water quality, therefore, both the coarse and fine particles have an influence.

To improve the water quality, the sediment load needs to be lowered. Preferably, this is done by applying measures at the source of the sediments. Therefore, in this section possible sources of the coarse and fine sediments are evaluated.

5.1. Coarse sediments

In this section, different possible sources of coarse sediments in the river are analysed. Unfortunately, no data are available on the actual amount of coarse sediments transported in the river. That is why it is assumed that the transport of coarse sediments is capacity limited; hence this load is equal to the maximum capacity. This assumption is generally valid as it is found that the transport of coarse sediments is largely capacity-limited (Knighton, 1998).

Sources for coarse sediments

Coarse sediments can only be transported if the flow velocities are sufficiently high, which is the case in streams, the river itself or in gullies. This means that coarse sediments found in the river might originate from gullies or from the river itself. In this section, the main sources for coarse sediments are assessed.

To determine whether gullies are a significant source, the maximum capacity in a typical gully is compared with the river capacity. The transport capacity calculation is based on the formulas of Engelund and Hansen and Van Rijn. In *Appendix F: Sediment transport modelling*, these formulas are explained and the required parameters are estimated. Through a sensitivity analysis, it is shown that the roughness is the most sensitive parameter.

As shown in Figure 5-1 and Figure 5-2, the river capacity is much larger than the capacity in an average or extremely large gully. Only if there would be more than 10^5 average gullies flowing on average every 4 m into the Sand and Talek tributaries, then total capacity would be similar to the one in the Mara River. Also, only if there would be more than $5 \cdot 10^3$ extremely large gullies every 75 m, then the influence of gullies would be significant. However, this hypothetical quantity is much larger than the reality. This means that gullies are not a significant source for the coarse sediments. See *Appendix F: Sediment transport modelling* for a more detailed explanation of this analysis.

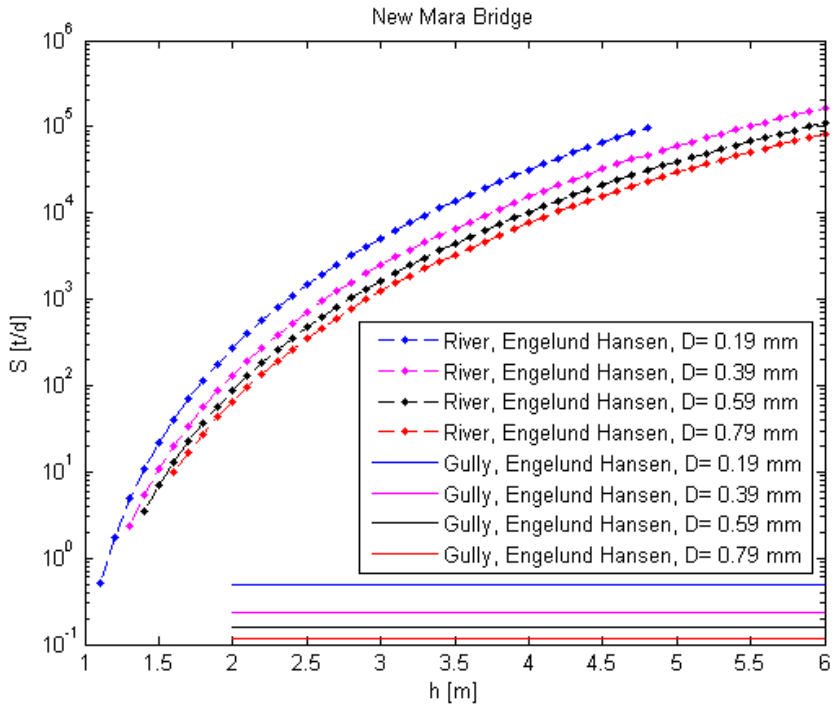

Figure 5-1: Comparison of the transport capacity in the river with the maximum load of an average gully applying the Engelund Hansen formula

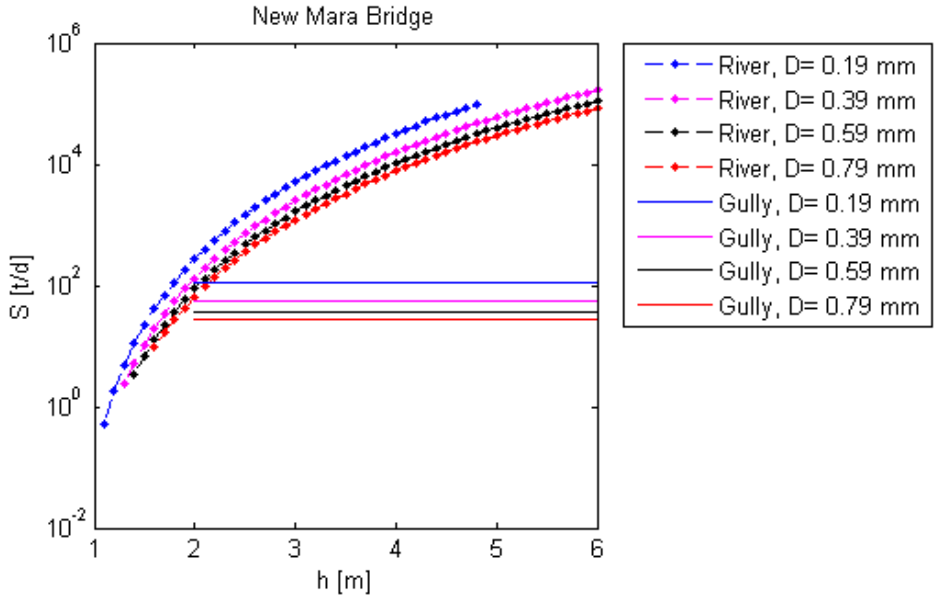

Figure 5-2: Comparison of the transport capacity in the river with the maximum load of an extremely large gully applying the Engelund Hansen formula

Alternatively, the coarse sediments might originate from the river bed itself. If this is the case, then the river is expected to meander. With the help of two DEMs for the years 2014 and 1996, the occurrence of meandering is confirmed: A maximum movement of 8.7 km is found along the Sand tributary. Along the Nyangores and Amala, this maximum movement is found to be 2 km and 1 km respectively (see Figure 5-3).

Therefore, it is concluded that the coarse suspended sediments mainly originate from the river bed and that the sources from the catchment itself are insignificant. This means that measures limiting erosion in gullies have no significant influence on the sediment load in the river. That is why it is recommended to apply measures in the river itself to minimize the load of coarse sediments.

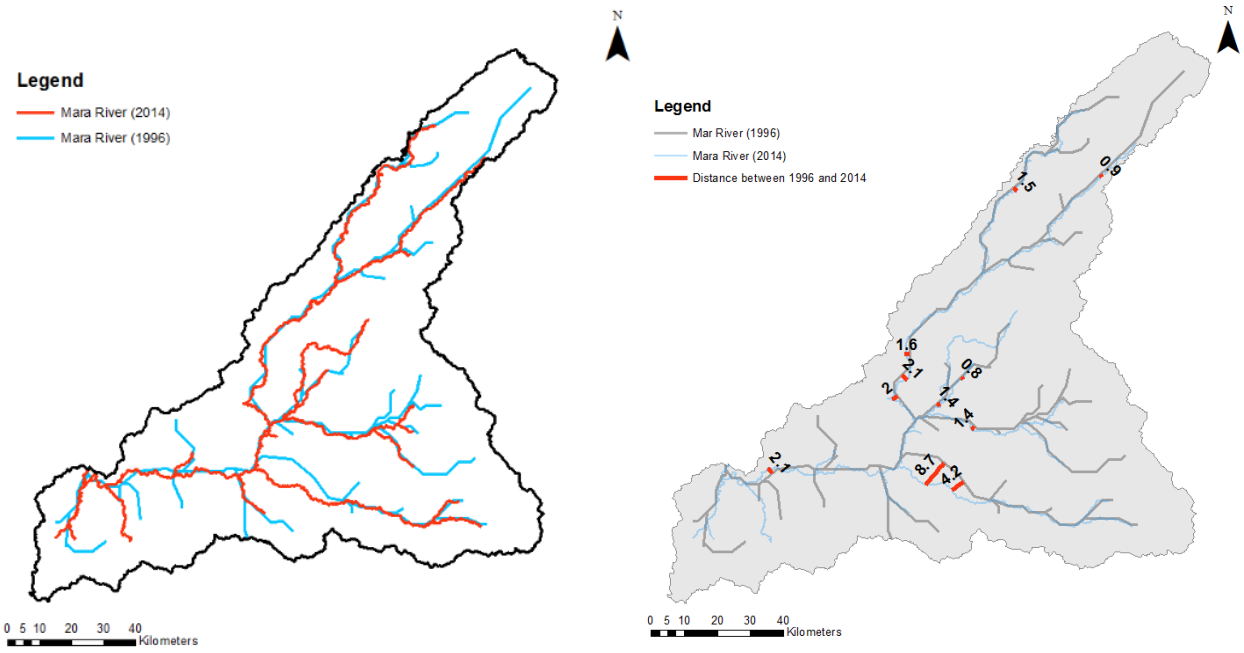

Figure 5-3: Location of the Mara River in 1996 and 2014 (left) and maximum river movement (right)

5.2.Fine sediments

In this section, the possible sources of fine sediments found in the river are determined. In general, it is assumed that these fine sediments originate from topsoil that is loosened and transported through overland flow. This is possible as about 60% of the topsoil consists of silt or clay which has a diameter of 62.5 µm or smaller.

5.2.1. Model explanation

For the modelling of the fine sediments originating from the topsoil, the empirical formula MUSLE (Modified Universal Soil Loss Equation) is applied. This model is chosen for its minor data requirements and its popular application throughout the world. The disadvantage is that this model has been calibrated for catchments in the US. See *Appendix F: Sediment transport modelling* for a more detailed explanation on the model choice and this specific model.

In the MUSLE model, the potential soil loss S is estimated based on the runoff, soil type, slope, land cover and land practice as shown in the formula below. Another disadvantage of this model is that it is dimensionally incorrect (Cârdei, 2010). In the runoff factor, two discharges are multiplied with each other and the power 0.56 is taken which results in the dimension $[L^{3.36}/T^{1.12}]$. This model does give reasonable responses though for larger peak runoffs and longer storms the soil loss increases. See *Appendix F: Sediment transport modelling* for more information. Despite this inconsistency, this model is still widely used in case of data shortage and/or lack of better models.

$$S = R * K * LS * C * P$$

$$R = 11.8 * \left(Q * q_p * A\right)^{0.56}$$

With:

- S : potential sediment loss [t/(d ha)]
- Q : surface runoff volume of a single storm [mm/storm]
- q_p : peak runoff [m^3/s]
- A : area [ha]
- K : soil erodibility factor [ton m^2 h/(m^3 ton cm)]
- LS : land topographic factor [-]
- C : land cover and management factor [-]
- P : support practice factor [-]

With the assumption that all the loosened sediment ends up the river, this soil loss is presumed to be equal to the fine sediment load in the river. The parameters K, LS and C are estimated based on the soil map KENSOTER, the DEM and NDVI maps. For the latter, a linear correlation between the NDVI and the land cover factor C is assumed. The land practice factor is estimated based on standard tables. The estimation of these factors is explained in detail in *Appendix F: Sediment transport modelling*. In Table 5-1 and Table 5-2, the results for these parameters are presented.

Table 5-1: Results for the estimation of the factors K in [ton m^2 hr/(m^3 ton cm)], LS in [-] and P in [-]

	Nyangores	North	Middle	Talek	Sand	Lower
K	0.017-0.028	0.018-0.036	0.0098-0.020	0.024-0.052	0.013-0.035	0.020-0.047
$LS_{agriculture}$	4.99	3.29	0.65	0.74	NA	1.36
$LS_{grassland}$	NA	3.70	1.44	1.11	2.29	1.35
P	0.8	0.8	0.8	0.8	0.8	0.8

Table 5-2: Estimation of the land cover and management factor C [-] based on the NDVI [-]

Land cover type	Mean NDVI	Factor C
Forest	0.74	0.00
Agriculture	0.58	0.27
Shrubs	0.53	0.36
Grass	0.49	0.43
Bare	0.17	1.00

5.2.2. Modelling results

Combining the MUSLE model with the hydrological model yields the simulation of the soil loss on a daily scale. This simulation is compared with sediment concentration data available for the Nyangores tributary, which is the only location where sufficient data are available. This comparison shows that the model is able to capture the order of magnitude of the soil loss, though not the exact patterns (see Figure 5-4). The root mean square error is equal to 58 t/d.

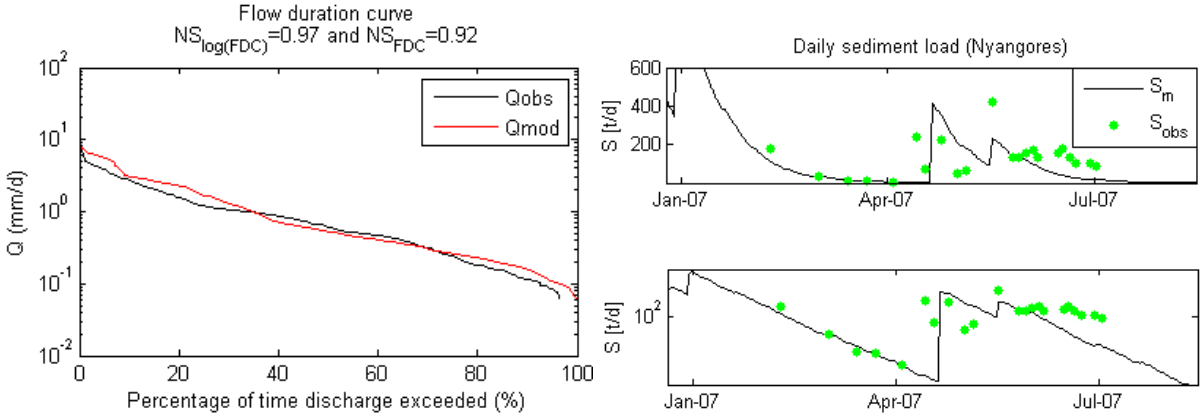

Figure 5-4: Model results for the Nyangores sub-catchment: flow duration curve (left) and suspended sediment load (right)

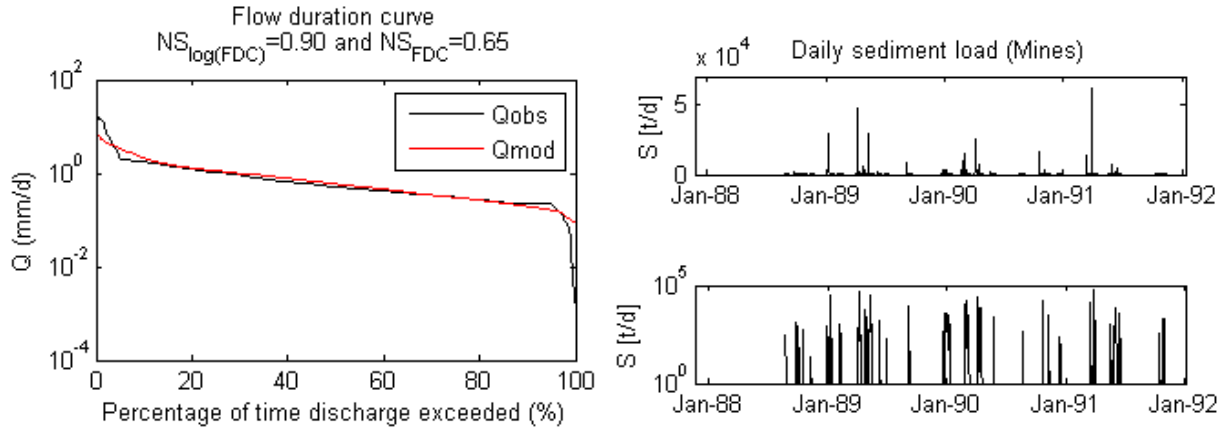

Figure 5-5: Model results for the Mara River Basin: flow duration curve (left) and suspended sediment load (right)

This model is then applied to the entire Mara River Basin (see Figure 5-5). Also, this total soil loss is converted to the average loss over the catchment (see Table 5-3 and Figure 5-6). As shown in the table, the largest loss of 0.30 mm/yr is found in the Sand sub-catchment on grasslands. Also, in this sub-catchment the largest average loss of 0.10 mm/yr is observed and at its outlet the largest daily average load of 714 t/d. Therefore, to reduce the sediment load in the river as efficiently as possible, it is recommended to focus on the Sand and the Lower sub-catchment when searching for potential measures reducing the soil loss. However, currently most studies seem to focus on the cultivated areas of the North sub-catchment instead where decreasing crop yields are observed in the past 20 years. It is assumed that this is caused by the loss of fertile top soil.

Just to give an example, potential measures are the reduction of the grazing pressure on grasslands due to massive livestock numbers, the construction of cut off drains and retention basins. Further studies are recommended for the most efficient measures reducing the soil loss in the Sand sub-catchment.

Table 5-3: Soil loss per HRU (Agriculture or Grassland) and per sub-catchment, and average daily sediment load at the outlet of each sub-catchment

	Agriculture [mm/yr]	Grassland [mm/yr]	Total [mm/yr]	Average daily sediment load [t/d]
North	0.00040	NA	0.00022	2
Middle	0.077	0.078	0.036	144
Talek	NA	0.033	0.020	238
Sand	NA	0.30	0.10	714
Lower	0.20	0.15	0.054	608

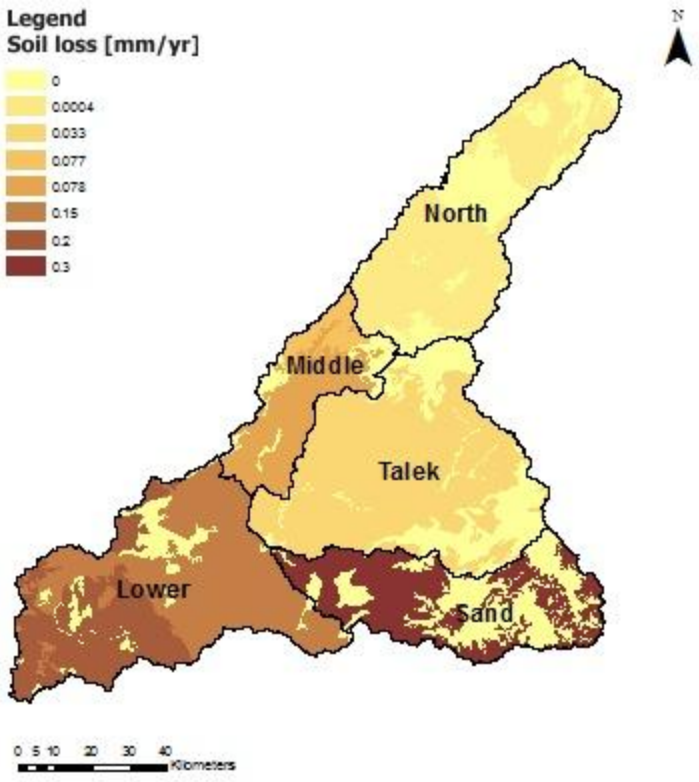

Figure 5-6: Map of the soil loss per HRU per sub-catchment

5.2.3. Discussion

In order to evaluate the model, different analyses are performed. First, different estimation possibilities for the runoff factor are analysed. Then a sensitivity and uncertainty analysis is carried out.

Runoff factor

For the estimation of the runoff factor a surface volume $Q_{surface}$ and peak runoff q_p are needed. The peak runoff can be estimated based on:

- The rational method: $q_p = C \cdot i \cdot A$
- The modelled river outflow Q_m averaged over the entire day
- The modelled river outflow Q_m averaged over several hours of the day
- The modelled runoff for hortonian overland flow (HOF) averaged over the entire day

The surface volume can be estimated based on:

- The modelled river outflow on a day
- The modelled total fast runoff on a day
- The modelled HOF on a day

These options are all modelled and compared with each other. It is found the model results are closest to the data if Q_{surfac}=HOF and q_{peak}= HOF regardless of over how many hours the peak runoff is averaged.

See Figure 5-7 for the results of two extreme options and *Appendix F: Sediment transport modelling* for more details on this analysis.

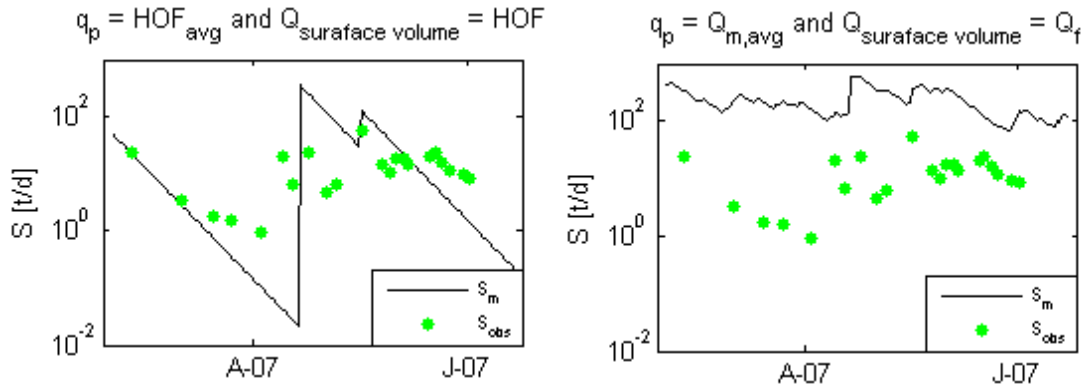

Figure 5-7: Results for two different estimation methods for the peak runoff q_p and the surface volume $Q_{surface\ volume}$ with extremely different results in the soil loss

Parameter sensitivity

In the sensitivity analysis, the parameters α, β, t(q_p), K, LS, C and P are varied within a certain maximum range. This range is equal to the expected uncertainty of this parameter. The conceptual parameters α and β are the constants 11.8 and 0.56 respectively. They have been calibrated for the US, but are actually sight specific. For parameter β, two ranges are analysed: a maximum one based on literature (Odongo et al., 2013) and a limited one based on data analysis. By varying these two parameters within their maximum boundaries, the smallest errors (RMSE) are found for $0.3 < \beta < 0.6$. The parameter t(q_p) is the number of hours over which the discharge is averaged to estimate the peak runoff. In Table 5-4, the minimum and maximum value for each parameter is indicated as well as the resulting difference in sediment load for the Nyangores and Mara River Basin (MRB). As shown in this table, the two conceptual parameters α and β are the most sensitive.

Table 5-4: Parameter values used for the sensitivity analysis and the resulting sensitivity range; the units are: α [ton/d^2], β [-], t(q_p) [d], K [ton m^2 hr/(m^3 ton cm)], LS [-], C [-], P [-]

	Min	Max	Sensitivity range [%] Nyangores	Sensitivity range [%] MRB
α	0	65	5.51	5.51
β	0 (0.3)	1 (0.6)	5069 (2.05)	38485 (2.54)
t(q_p)	24 h	1 h	1.54	1.54
K	K_{min}	K_{max}	0.49	0.60
LS, C	-10%	+10%	0.10	0.28
P	0.06 (terrace)	1 (no practices)	1.18	1.18

Model uncertainty

Using these uncertainties in the parameters, the model uncertainty is determined. The maximum uncertainty is found when including all parameter uncertainties (see Figure 5-8). This uncertainty can be limited most efficiently by fixing the two conceptual parameters following a more accurate estimation of the peak runoff. By fixing the conceptual parameters, the uncertainty is reduced from 608 000% to 3.6%. Only then it is worth focusing in more detail on the estimation of the factors P and C. The factors LS and K do not cause significant model uncertainties, hence at this stage it is recommended to focus on the other parameters. In *Appendix F: Sediment transport modelling*, more details can be found on this analysis.

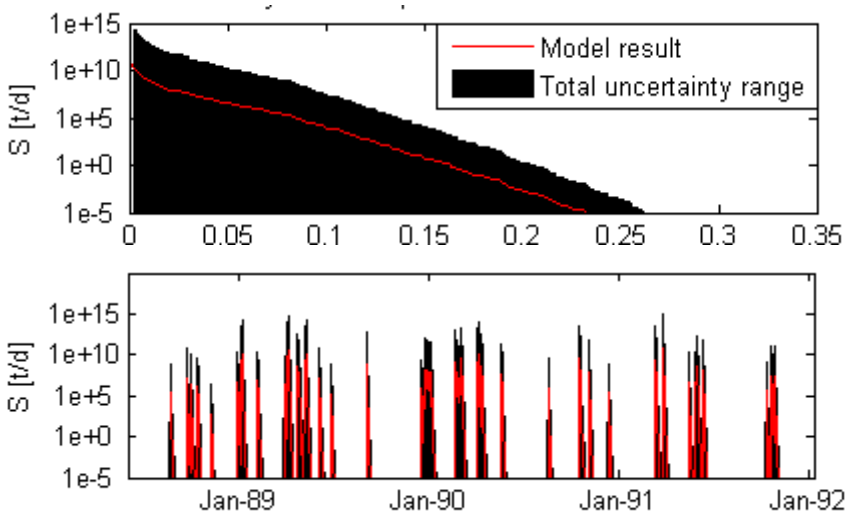

Figure 5-8: Maximum uncertainty of the MUSLE model: sediment load sorted (upper) and unsorted (lower) in logarithmic scale

5.2.4. Recommendations

In this study, the created hydrological and sediment transport model is compared to the limited data available for the Nyangores tributary. Due to the limited amount of data, no calibration is possible. For further studies, it is recommended to collect turbidity data series combined with water level data. Then the sediment load can be estimated by converting the turbidity data to sediment concentrations and multiplying it with the discharge. If these two types of data would be collected daily for at least a year in the Nyangores and different points in the Mara River, significant model improvements are possible. With these new data, the model for the entire Mara River Basin could be compared with data as well and model uncertainties caused by the conceptual parameters could be reduced significantly. Additionally, it is advised to study the peak runoff in more detail to reduce the model uncertainties it causes.

With the hydrological and sediment transport, it is found that the grasslands in the Sand sub-catchment contribute the most to the wash load in the Mara River. In this same area, very large cattle herds with about thousand animals are walking around looking for grass and water. At other locations such as the North, negligible soil loss is found in the model. There the land use is agriculture instead of livestock farming, hence only a few or no animals are owned.

6. Conclusion

In this research, the main areas contributing to the suspended sediment load in the Mara River are assessed. This suspended load in the Mara River consists of coarse sediments in the river bed and fine sediments in the wash load originating from the top soil in the entire catchment. The main sources of the coarse sediments are assessed hydraulically whereas for the fine sediments a hydrological model is combined with an empirical sediment yield model.

The coarse sediments in the Mara River are mainly found in the bed and can originate from gullies or the river itself as high flow velocities are needed for their transport. To determine the main source, the sediment transport capacity of the river was compared with the one of a typical gully observed locally and the occurrence of river meandering was analysed.

The fine sediments in the Mara River are mainly found in the wash load and are assumed to originate from eroded topsoil. To assess the main sources, a semi-distributed hydrological model based on the concept of FLEX-Topo was created and combined with the empirical model MUSLE (Modified Universal Soil Loss Equation). With this hydrological and sediment transport model, the soil loss was calculated on daily time-scale. It is assumed that this soil loss is equal to wash load in the river. In the hydrological model five sub-catchments and four hydrological response units (HRUs) were defined; the sub-catchments are: North, Middle, Talek, Sand, Lower and the HRUs are: forested hill slopes, shrubs on hill slopes, agriculture and grasslands. Only for croplands and grasslands, the MUSLE model were applied to calculate the soil loss as no significant erosion was observed in forests and shrub lands.

This model simulated the hydrology well and also captured the order of magnitude of the soil loss; however not the exact patterns. As shown in Table 6-1, the largest soil losses were found in the Sand and Lower sub-catchment: the soil loss is 0.30 mm/yr in the grasslands in the Sand and 0.2 mm/yr in the cultivated areas in the Lower sub-catchment. It is recommended to increase the model accuracy by using additional field measurements at multiple locations in the catchment, for example precipitation, temperature and discharge to improve the hydrological part and turbidity data to improve the sediment part of the model.

This means that the main sources for the fine suspended sediments are the grasslands in the Sand and the crop lands in the Lower sub-catchment. It is recommended to focus on these areas for decreasing the fine suspended sediment load most efficiently. However, currently most studies seem to focus on the cultivated areas in the North where local people have observed decreased crop yields in the past 20 years and suspect it is a result of eroded fertile top soil. The coarse sediments are found to originate from the river itself which has caused and still causes meandering.

Table 6-1: Soil loss per HRU (Agriculture or Grassland) and per sub-catchment, and average daily sediment load at the outlet of each sub-catchment

	Agriculture [mm/yr]	Grassland [mm/yr]	Total [mm/yr]
North	0.00040	NA	0.00022
Middle	0.077	0.078	0.036
Talek	NA	0.033	0.020
Sand	NA	0.30	0.10
Lower	0.20	0.15	0.054

7. Literature

Abdel-Fattah, S., Amin, A., & Rijn, L. C. V. (2005). Sand Transport in Nile River, Egypt. *Journal of Hydraulic Engineering, 130*(6), 488-500.

Ankum, I. (2002). Design of open-channels and hydraulic structures.

Ankum, P. (2002). Design of open-channels and hydraulic structures (Lecture Notes CT3410). Faculty of Civil Engineering, Delft University of Technology.

Anonymous (2009). Water Resources Users Association Develment Cycle (WDC): Water Services Trust Fund.

Anonymous (2013). Maps of World: Kenya River Map. Retrieved March 2014, from www.mapsofworld.com

Ascough, J. C., Baffaut, C., Barfield, B., Deer-Ascough, L. A., Flanagan, D. C., Kidwell, M. R., et al. (1995). WEPP User Summary: USDA- Water Erosion Prediction Project.

Cârdei, P. (2010). THE DIMENSIONAL ANALYSIS OF THE USLE - MUSLE SOIL EROSION MODEL. *Proc. Rom. Acad., 3*, 249-253.

Defersha, M. B., Melesse, A. M., & McClain, M. E. (2012). Watershed scale application of WEPP and EROSION 3D models for assessment of potential sediment source areas and runoff flux in the Mara River Basin, Kenya. *CATENA, 95*(0), 63-72. doi: http://dx.doi.org/10.1016/j.catena.2012.03.004

Dessu, S. B., Melesse, A. M., Bhat, M. G., & McClain, M. E. (2014). Assessment of water resources availability and demand in the Mara River Basin. *CATENA, 115*(0), 104-114. doi: http://dx.doi.org/10.1016/j.catena.2013.11.017

FAO (Cartographer). (1998). Africover.

FIU GIS-Center. Photographs of land cover and land use from different reference points in the Mara Basin. Retrieved May 2014, from www.gisrs.fiu.edu

Gao, H., Hrachowitz, M., Fenicia, F., Gharari, S., & Savenije, H. H. G. (2013). Testing the realism of a topography driven model (FLEX-Topo) in the nested catchments of the Upper Heihe, China. *Hydrol. Earth Syst. Sci. Discuss, 10*, 12663-12716.

Gao, H., Hrachowitz, M., Schymanski, S. J., Fenicia, F., & Savenije, H. H. G. (2014). Ecosystems and societies use similar strategies to manage water supply.

Gharari, S., Hrachowitz, M., Fenicia, F., & Savenije, H. H. G. (2011). Hydrological landscape classification: investigating the performance of HAND based landscape classifications ina central European meso-scale catchment. *Hydrol. Earth Syst. Sci., 15*, 3275-3291.

GLOWS-FIU (2012). Environmental Flow Recommendation for the Mara River, Kenya and Tanzania: Global Water for Sustainability program (GLOWS). Miami, FL.

GLOWS (2014). Transboundary Water for Biodiversity and Human Health in the Mara River Basin, Kenya & Tanzania (TWB-MRB). Retrieved March 2014, from www.globalwaters.net

Haan, C. T., Barfield, B. J., & Hayes, H. C. (1994). *Design Hydrology and Sedimentology for Small Catchments*. ACADEMIC PRESS, INC.

Karaburun, A. (2010). Estimation of C factor for soil erosion modeling using NDVI in Buyukcekmece watershed. *Ozean Journal of Applied Sciences, 3*, 77-85.

Khroda, G. O. (2006). Mara River Catchment Basin Initiative *Preliminary Phase: Project Development and Stakeholders Analysis, The Hydrology of Mara River*: WWF – Eastern Africa Regional Programme Office (EARPO).

Kiragu, G. M. (2009). Assessment of Suspended Sediment Loadings and their Impact on the Environmental Flows of Upper Transboundary Mara River, Kenya.

Knighton, D. (1998). *Fluvial Forms and Processes: A new Perspective*: Hodder Arnold.

Landsberg, F. (2007). Nature's Benefits in Kenya: An Atlas of Ecosystems and Human Well-Being. Retrieved March 2014, from www.wri.org

Larson, M., Camenen, B., & Nam, P. T. (2011). A Unified Sediment Transport Model for Inlet Application. *Journal of Coastal Research*(Special Issue 59), 27-38.

Lidén, R. (1999). A new approach for estimating suspended sediment yield. *Hydrol. Earth Syst. Sci., 3*(2), 285-294.

LVBC (2012). Environmental Flow Recommendations for Reserve Flow in the Mara River, Kenya and Tanzania. Lake Victoria Basin Commission, Kisumu, Kenya.

Mango, L. M., Melesse, A. M., McClain, M. E., Gann, D., & Setegn, S. G. (2011). Land use and climate change impacts on the hydrology of the upper Mara River Basin, Kenya: results of a modeling study to support better resource management. *Hydrol. Earth Syst. Sci., 15*(7), 2245-2258. doi: 10.5194/hess-15-2245-2011

Mati, B. M., Mutie, S., Gadain, H., Home, P., & Mtalo, F. (2008). Impacts of land-use/cover changes on the hydrology of the transboundary Mara River, Kenya/Tanzania. *Lakes & Reservoirs: Research and Management, 13*(2), 169-177.

McCartney, B. A. (2010). Evaluation of Water Quality and Aquatic Ecosystem Health in the Mara River Basin East Africa.

McClain, M. E., Subalusky, A. L., Anderson, E. P., Dessu, S. B., Melesse, A. M., Ndomba, P. M., et al. (2013). Comparing flow regime, channel hydraulics and biological communities to infer flow-ecology relationships in the Mara River of Kenya and Tanzania. *Hydrological Sciences Journal, 59 (3-4)*, 1-19. doi: 10.1080/02626667.2013.853121

Melesse, A. M., McClain, M., Wang, X., Abira, M., & Mutayoba, W. (2008). Modeling the Impact of Land-Cover and Rainfall Regime Change Scenarios on the Flow of Mara River, Kenya. *World Environmental and Water Resources Congress 2008*, pp. 1-10.

Minister for Environment and Natural Resources (2006). THE ENVIRONMENTAL MANAGEMENT AND CO-ORDINATION (WATER QUALITY); REGULATIONS, 2006 *ARRANGEMENT OF REGULATIONS*. Kenya Law.

Ministry of Foreign Affairs (2013). Order of the Minister for Foreign Trade and Development Coordination of 11 July 2013, no. MinBuZa-2013.207602, laying down administrative rules and a ceiling for grants awarded under the Ministry of Foreign Affairs Grant Regulations 2006 (SWMM). *Staatscourant, Nr. 20290*.

Muthike, J. (2007). Starter Document for Geomorphology Component. Mara River Research Database.

Ndomba, P. M. (2009). Critical/Extreme Low Flows EFA, Mara River Basin: Hydraulics Component Final Report: Phase III. Mara River Research Database.

Neitsch, S. L., Arnold, J. G., Kiniry, J. R., & Williams, J. R. (2011). Soil & Water Assessment Tool Version 2009.

Odongo, V. O., Onyando, J. O., Mutua, B. M., van Oel, P. R., & Becht, R. (2013). Sensitivity analysis and calibration of the Modified Universal Soil Loss Equation (MUSLE) for the upper Malewa Catchment, Kenya. *International Journal of Sediment Research, 28*(3), 368-383. doi: http://dx.doi.org/10.1016/S1001-6279(13)60047-5

Savenije, H. H. G. (2010). Topography driven conceptual modelling (FLEX-Topo). *Hydrol. Earth Syst. Sci., 14*, 2681-2692.

SerengetiPark (2000). National Park's Official Site Serengeti. Retrieved July 2014, from www.serengeti.org

Strużyński, A., Kulesza, K., & Strutyński, M. (2013). Bed Stability as a Parameter Describing the Hydromorphological Balance of a Mountain River. In P. Rowiński (Ed.), *Experimental and Computational Solutions of Hydraulic Problems* (pp. 249-260): Springer Berlin Heidelberg.

Subalusky, A. (2011). Refining Flow Recommendations for the Mara River, Kenya and Tanzania: GLOWS.

Tilahun, S. A., Guzman, C. D., Zegeye, A. D., Engda, T. A., Collick, A. S., Rimmer, A., et al. (2013). An efficient semi-distributed hillslope erosion model for the subhumid Ethiopian Highlands. *Hydrol. Earth Syst. Sci., 17*, 1051-1063.

U.S. Geological Survey. (2014). Digital Elevation Map. from www.earthexplorer.usgs.gov

UNEP (2009). *Kenya: Atlas of Our Changing Environment*: Division of Early Warning and Assessment (DEWA) and United Nations Environment Programme (UNEP).

Ven, F. H. M. van de (2011). Water Management in Urban Areas. TU Delft.

Vriend, H. J. de, Havinga, H., Prooijen, B. C. van, Visser, P. J., & Wang, Z. B. (2011). River Engineering (Lecture Notes CT4345). Faculty of Civil Engineering, Delft University of Technology.

Vrugt, J. A., Gupta, H. V., Bastidas, L. A., Bouten, W., & Sorooshian, S. (2003). Effective and efficient algorithm for multiobjective optimization of hydrologic models. *Water Resources Research, 39*(8), n/a-n/a. doi: 10.1029/2002WR001746

WREM International Inc. (2008). Mara River Basin Monograph, Mara River Basin Transboundary Integrated Water Resources Management and Development Project, Final Technical Report (pp. 446p.).

Appendices

Appendix A: Site description

Table of Contents

1. Description of the Mara River Basin

1.1. Geographic location

The Mara River originates in Kenya in the Mau Escarpment which is in the province Rift Valley and flows into Lake Victoria in Tanzania at Musima Bay (see Figure 1-1). This lake is the second largest freshwater lake of the world and covers an area of about 69 000 km^2 of which 6% is in Kenya, 45% in Uganda and 49% in Tanzania (UNEP, 2009). The main tributaries of the Mara River are the Nyangores and Amala Rivers in the upper reach and the Talak, Sand, Tabora, Somonche and Tigite River in the middle and lower reaches (see Figure 1-2). (McClain et al., 2013) The first two tributaries are perennial rivers while the remaining tributaries are ephemeral rivers, thus they often dry up in rainless periods (Dessu et al., 2014).

In total the river is 395 km long (Dessu et al., 2014) and its catchment covers an area of about 11,500 km^2 (McClain et al., 2013) of which about 65% is located in Kenya (Mati et al., 2008).

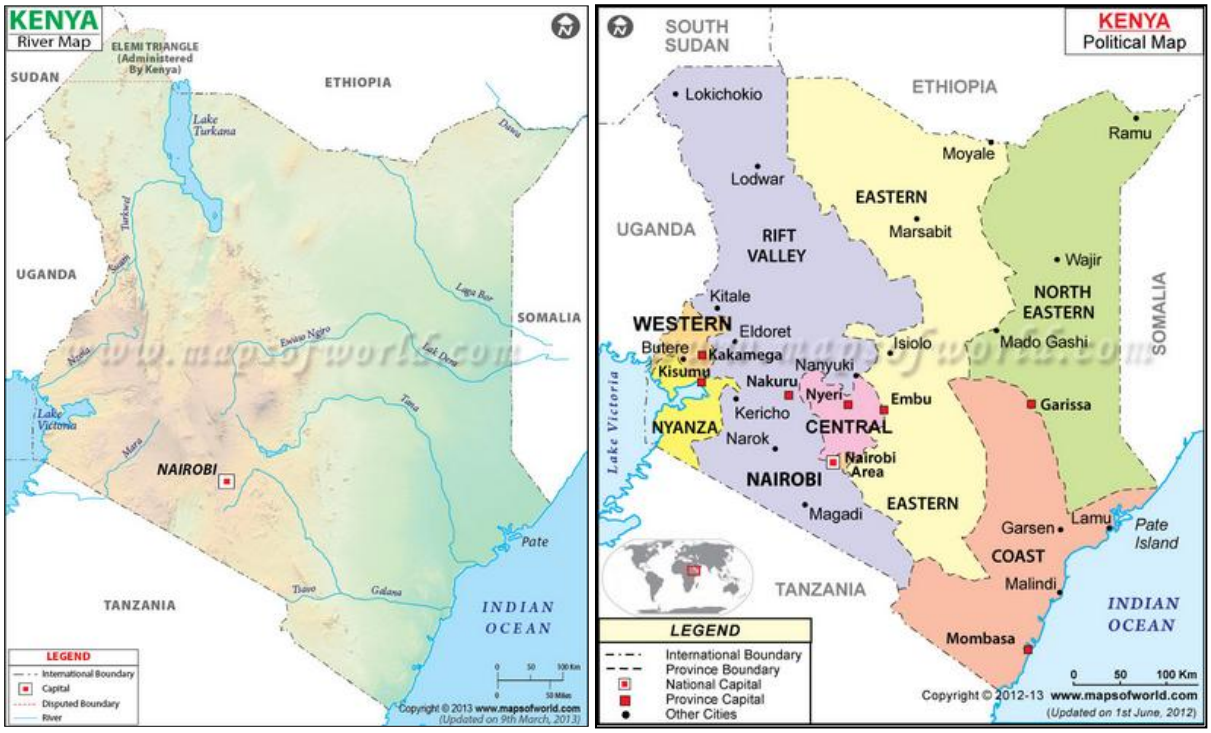

Figure 1-1: Geographical map of Kenya showing the main rivers (left) or the provinces of Kenya (right) (Anonymous, 2013)

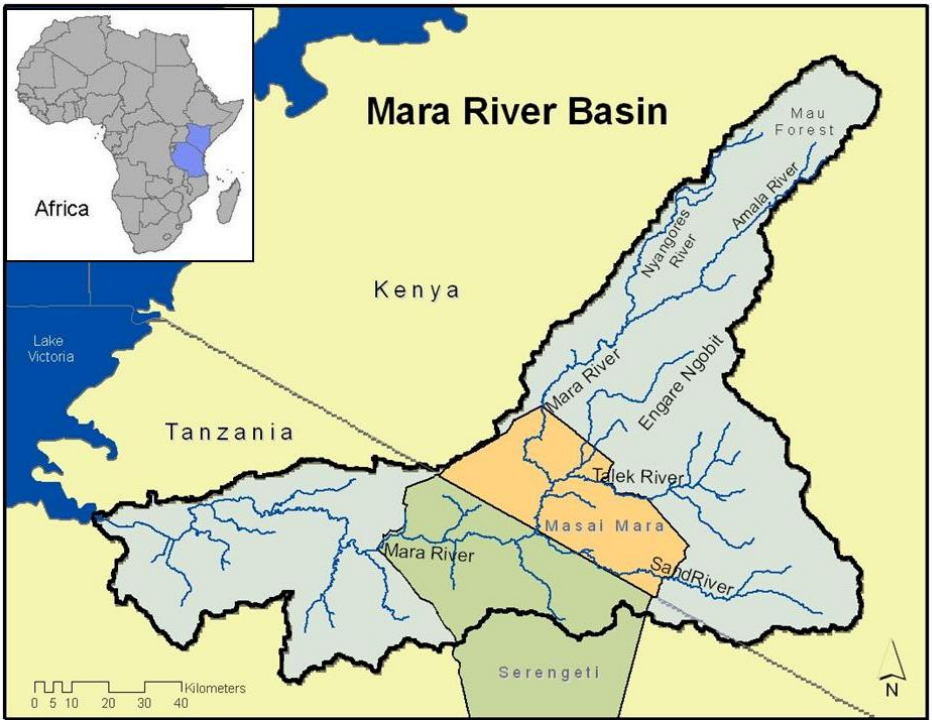

Figure 1-2: Map of the Mara River Basin with its tributaries (GLOWS, 2014)

1.2.Climatic condition

Within the Mara River Basin, there are two wet seasons linked to the annual oscillations of the ITCZ (Inter-tropical Convergence Zone). The first wet season is approximately from March to May and the second from October to December (McClain et al., 2013). The precipitation varies spatially over the catchment following the local topography. The largest annual rainfall can be found in the upstream area of the catchment; there it is between 1000 to 1750 mm. In the middle and downstream areas, the annual rainfall is between 900 to 1000 mm and 300 to 850 mm, respectively (Dessu et al., 2014). The map in Figure 1-3 gives an indication of the spatial variation of the precipitation.

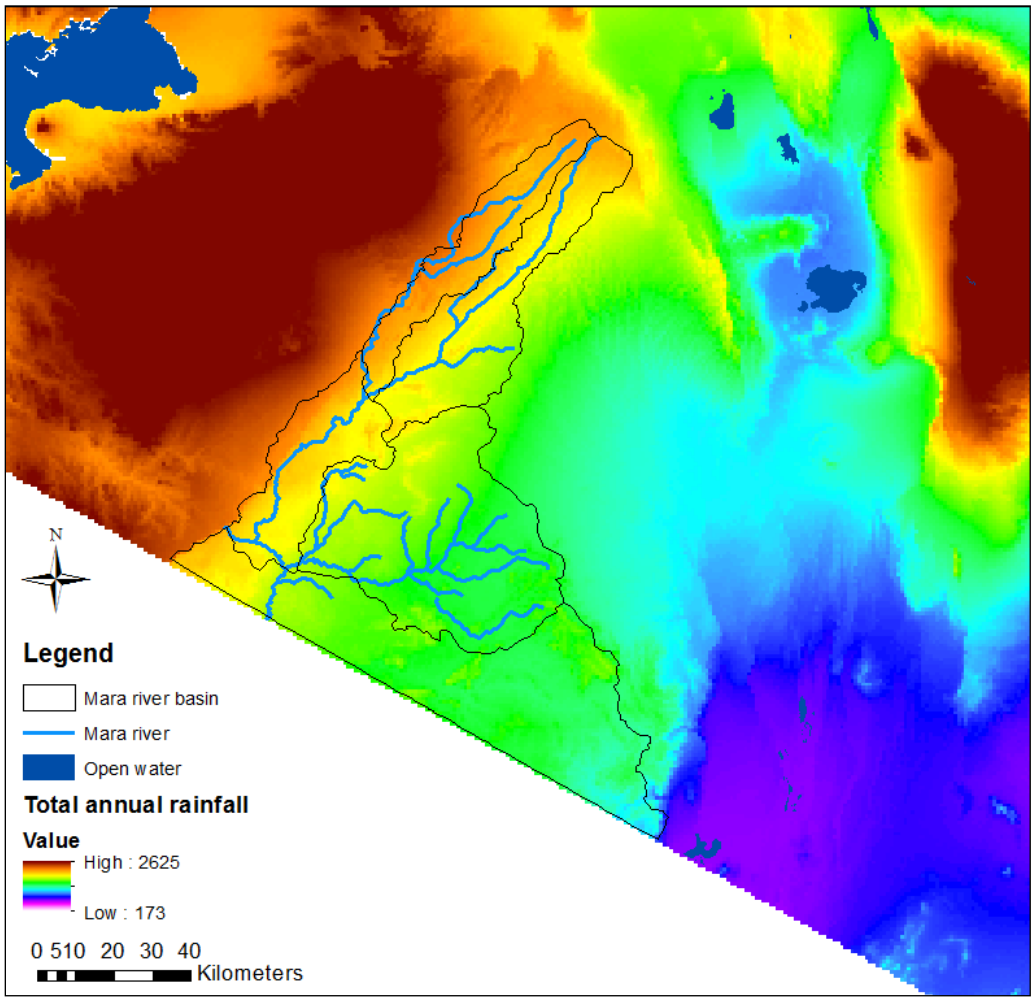

Figure 1-3: Annual precipitation in the Mara River Basin in Kenya (Landsberg, 2007)

1.3.Topography

The elevation varies in the river basin between 3000 masl (metres above sea level) at the Mau Escarpment, 1480 masl at the border to Tanzania and 1130 masl at Lake Victoria (McClain et al., 2013). For the modelling a digital elevation map (SRTM) as shown in Figure 3-1 will be used with a resolution of 90 m and vertical accuracy of 16 m (U.S. Geological Survey, 2014).

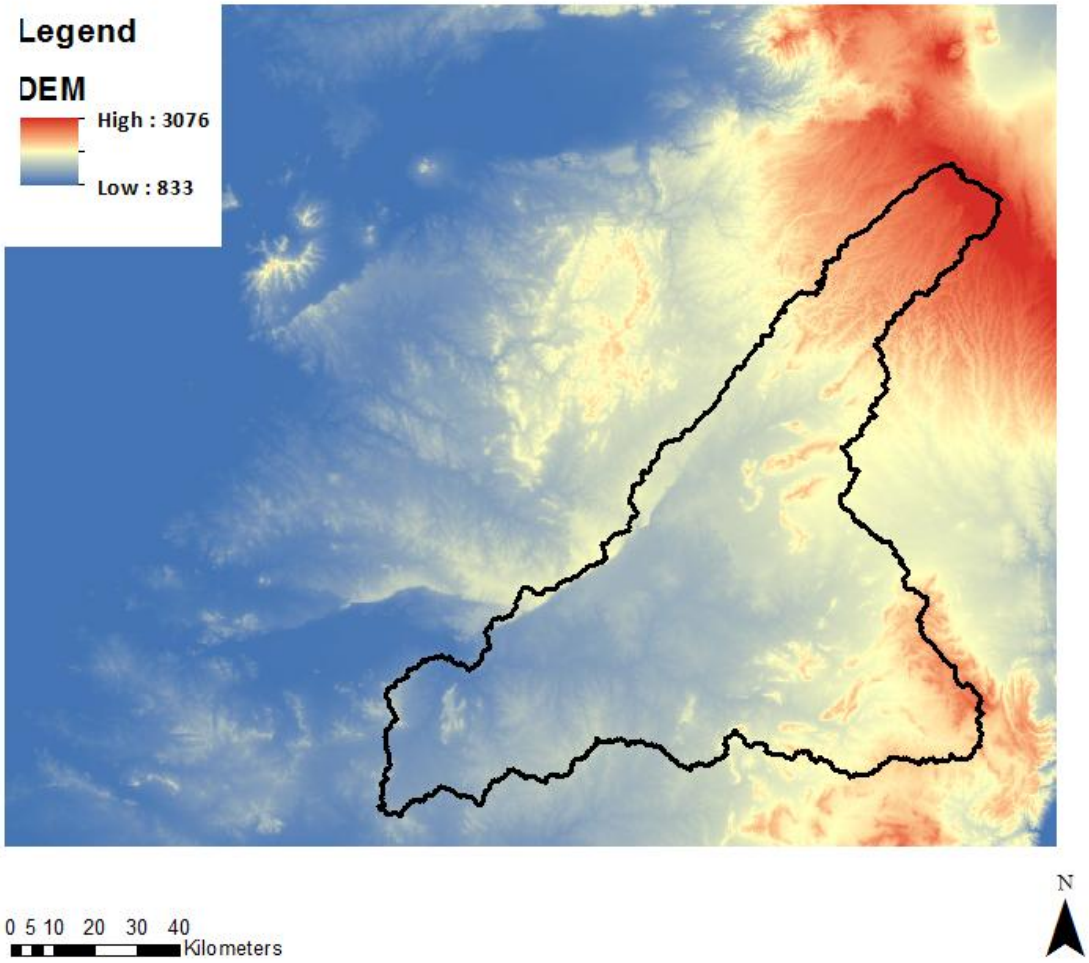

Figure 1-4: Digital elevation map (DEM) of the Mara River Basin (U.S. Geological Survey, 2014)

2. Challenges in the Mara River Basin

As indicated in the site description, several changes in the past due to human interventions have changed the natural environment which can harm the ecology or pose a threat to the water users depending on the size of the change. A few examples of challenges that will be explained more detailed are:

- Insufficient water and of decreasing quality during droughts as found in Environmental Flow Assessments (EFAs) studies for the determination of minimum flow requirements assuring sufficient water quantity and quality for basic human needs and the ecosystem
- Increasing water demand due to the rising population density requiring more water for agricultural, livestock and industrial sectors
- Increased catchment erosion resulting in decreased water quality and increased area of wetlands (+387%)
- Land use change in the form of deforestation (-32% between 1973 and 2000) and cultivation (+ 203%). This is in itself not an issue in itself as it contributes to economic growth, however since it influences different processes as runoff, infiltration and evaporation, it can be a trigger for other issues; for example increased catchment erosion or inflow of fertilizer into the water system.

2.1. Minimum flow requirements

To sustain both basic human needs and aquatic ecosystems, the Kenyan and Tanzanian water policies and laws have called for 'the protection of a reserve in all aquatic ecosystems'(LVBC, 2012). This reserve is minimum flow level needed to assure a healthy river system that can provide services for communities as clean drinking water, food or building materials. (LVBC, 2012)

For the determination of the minimum flow levels, the approach called Environmental Flow Assessments (EFAs) is applied. It is an accepted science-based approach combining hydrological, social, physical and biological indicators. This approach is applied in the project called *Transboundary Water for Biodiversity and Human Health in the Mara River Basin* (TWB-MRB) which is implemented under the Global Water for Sustainability Program (GLOWS) between 2006 and 2012 and was funded by the U.S. Agency for International Development (USAID). (LVBC, 2012)

The studies done in this project show that there is sufficient water to meet all demands, both for humans and the ecosystem. For Sites 1, 3 and 5, the reserve flow accounts for 28%, 45% and 42% respectively of the mean annual runoff. As shown in the map in Figure 2-2, Site 1 is located in the Amala River, Site 3 at the border between Kenya – Tanzania and Maasai Mara National Reserve – Serengeti National Park and Site 5 at Mara Mine in Tanzania. However, during droughts, the reserve flows exceed the historic average flows for 3 months, 2 months and 1 month for Sites 1, 2 and 3-5 respectively. In the remaining months, there is only little water available for extraction (see Figure 2-1). (LVBC, 2012)

Moreover, when focusing on the water quality, it is found that this parameter has declined significantly during extreme low flow levels as experienced in 2009. Also, measurements in the Amala River have shown greater declines in the average monthly flow levels over the last 15 years, higher sediment load

per unit catchment area and lower water quality compared to in the Nyangores River. This suggests the responsibility of land degradation in the Amala sub-catchment to the local water quality decline. Furthermore, the lowest water quality is found in the Talek River. (Subalusky, 2011)

In short, the river flows are found to be critical or insufficient during droughts, the water quality is found to decrease significantly during low flows and may decline also as a response to land degradation.

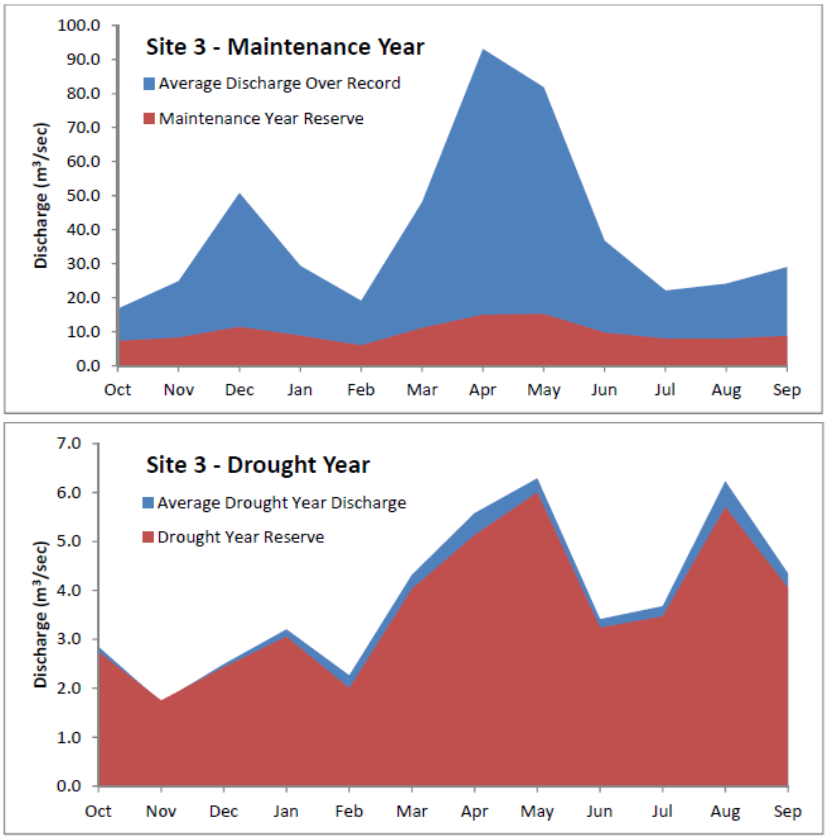

Figure 2-1: EFA recommendations at Site 3 for a) average discharge over period of record and maintenance year reserve flows, b) average drought year discharge and drought year reserve flows (LVBC, 2012)

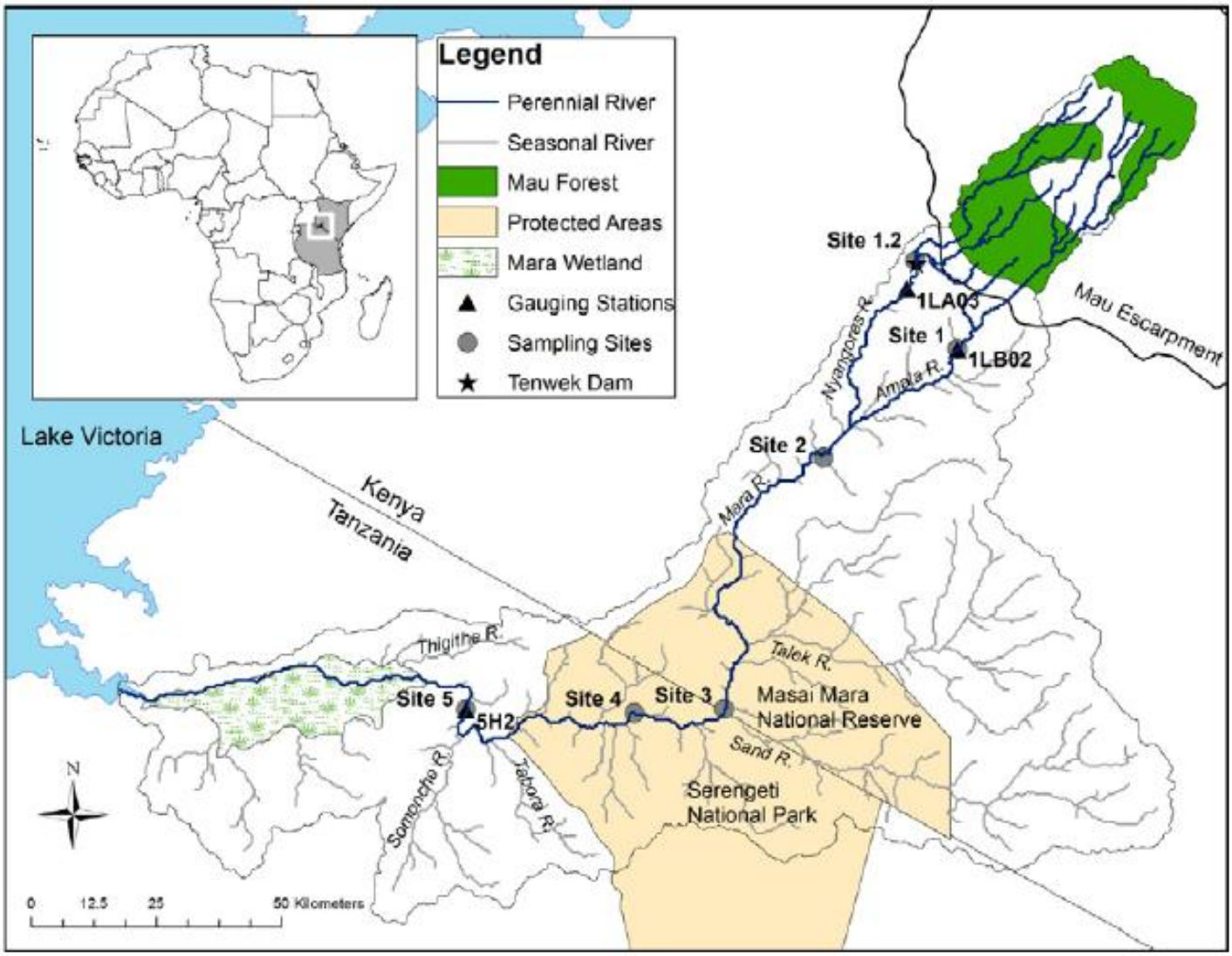

Figure 2-2: Map of the measuring sites (LVBC, 2012)

2.2.Water demand

For the Mara River Basin, different studies are done on the water availability and demand and conclude the existence of water scarcity. Khroda for example shows that with an average domestic and industrial water demand of 107l/day/cap to 109l/day/cap for the Narok district, the total water demand for the population in the Mara River Basin would double within 20 years, from 1990 to 2010 (see Table 2-1). In 2010, the available water however would amount 10,179 m^3/day from groundwater and 21,750 m^3/day from surface water. (Khroda, 2006)

Table 2-1: Estimated water demand [m^3/day] (Khroda, 2006)

Year	Population	Rural	Urban	Stock	Industrial	Total
1990	407,099	10,715	2,530	32,127	228	45,600
2000	644,338	19,472	8,559	44,700	422	73,153
2010	840,605	31,929	16,903	54,809	606	104,247

In a different study, Dessu estimates the water budget by comparing the water demand with the water availability for 12 sub-catchments in a monthly timescale to capture the seasonal variation. The water demand is estimated for six water consumptive sectors: residential, livestock, wildlife, tourism, irrigation and industry. In this study in contrast to the previous one of Khroda, the residential water demand is estimated based on the recommendations of the KWRMA: 25 l/day/cap and 45 l/day/cap for minimum basic human need and for rural water supply purposes respectively. As a result, the annual water demand is largest for the agricultural purposes in the sub-catchments 3, 4 and 11 (see Figure 2-3). (Dessu et al., 2014)

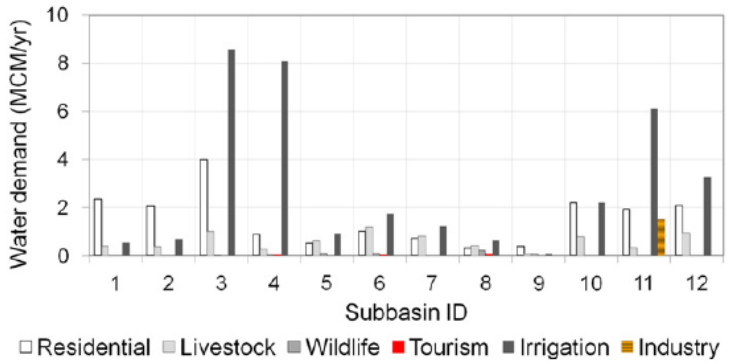

Figure 2-3: Annual water demand in 2009 for each sector and each sub-basin (Dessu et al., 2014)

Comparing the water demand with the water availability indicates the water scarcity which is largest under extreme dry conditions (case b) and smallest under flood conditions (case d); see Figure 2-4. However, not all sub-catchments respond equally in those extreme cases: under extreme dry conditions, sub-catchments 1, 2 and 9 do not experience any significant water stress while sub-catchment 8 experiences high water stresses also under flood conditions. The first may be a result of low water demands while the latter a result of high water demands relative to the water availability.

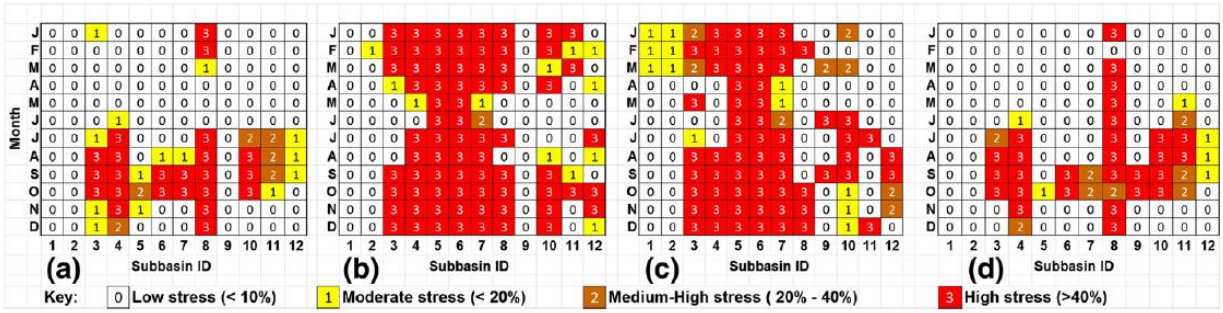

Figure 2-4: Monthly water budget status for each sub-catchment; the four groups of stress levels are based on the percentage of demand of the available water resource; a) total water availability vs. total water demand, b) reserve volume vs. basic water demand, c) Normal water availability vs. normal water demand, d) flood volume vs. flood demand (Dessu et al., 2014)

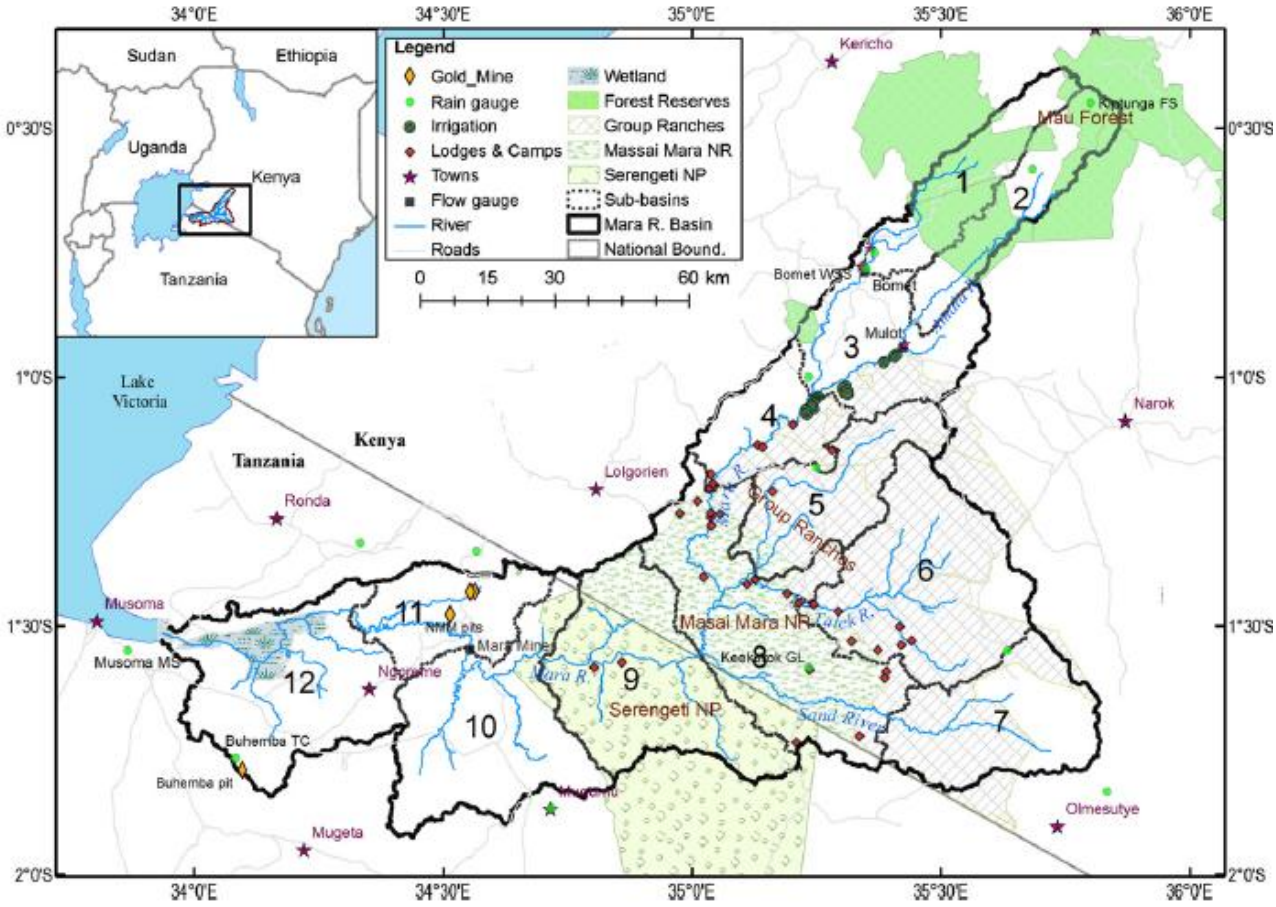

Figure 2-5: Sub-catchments in the Mara River Basin based on topography, climate, land use, soil type and administrative boundaries (Dessu et al., 2014)

2.3.Population growth

Through a rapid population growth and high immigration rates, the population and settlement increased in the basin and the water demand increased as well. Between 1999 and 2002 for example, the number of households increased by 13% in the upper catchments. The increased water demand is also caused by the larger demand by livestock: it increased approximately from 159 m^3/year to 190 m^3/year between 1990 and 2000. (Mati et al., 2008)

Also, the population change between 1960 and 2005 is mapped in an atlas of Kenya by the United Nations Environment Programme (UNEP); Figure 2-6. In these maps it is shown that the population density has increased from medium/high to high; the medium class indicates a density of 25-100 people/km^2 and the high class >100 people/km^2. (UNEP, 2009)

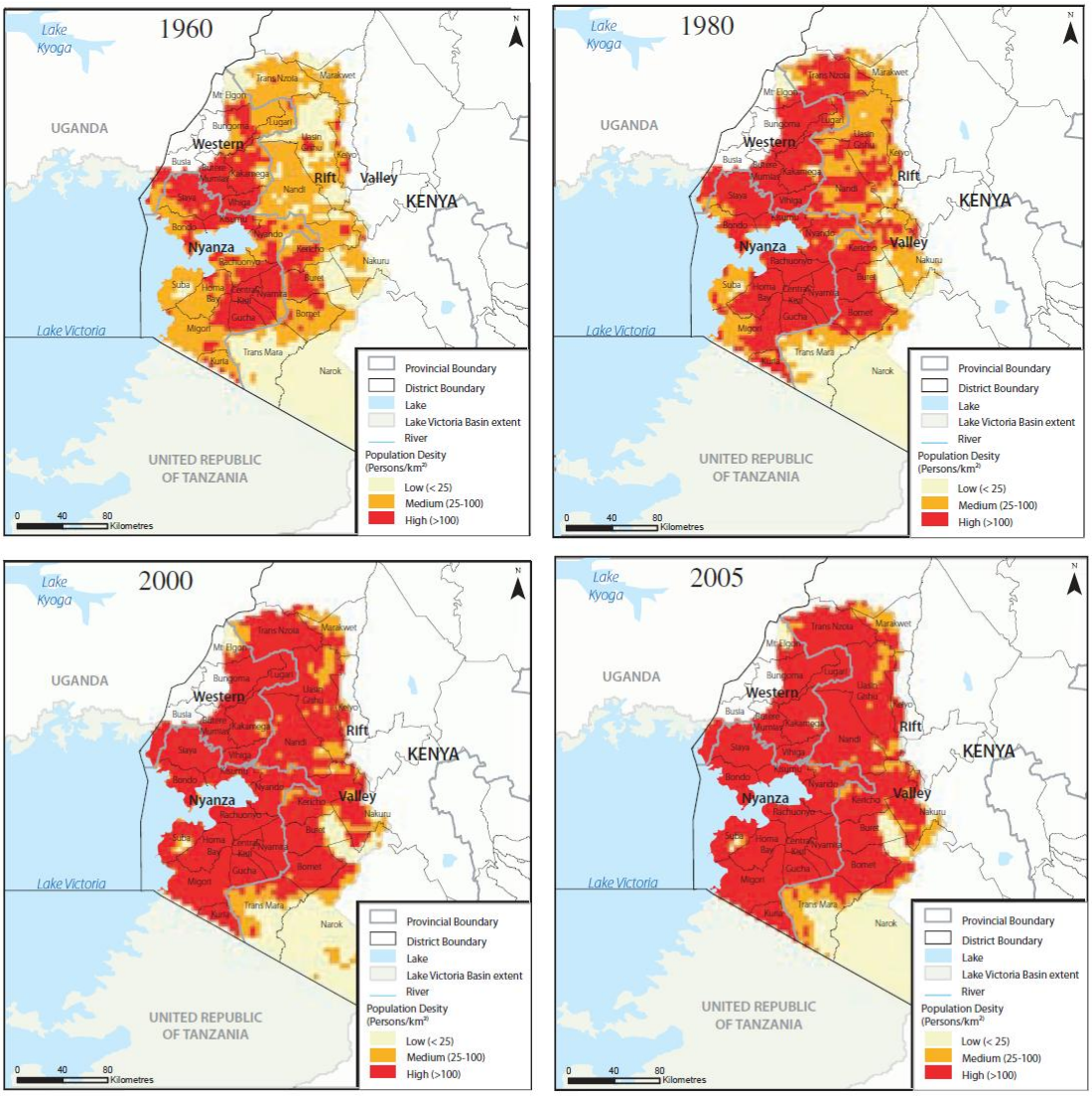

Figure 2-6: Population density change within the Kenyan portion of Lake Victoria Basin, 1960-2005 (UNEP, 2009)

2.4.Catchment erosion

In the Mara River Basin (MRB), human interventions have led to deforestation and the increase of agricultural areas. This change, combined with the application of poor agricultural practices, has led to an increased rapid runoff of rainwater and the pollution of the river with eroded topsoil (see Figure 2-7). As a result, fertile soil is lost and the sediment load in the river increases. The latter is a result of a larger suspended load due to increased erosion in the catchment and larger bed load due to increased discharges in the river. With the increased suspended sediment load in the river, the water quality decreases as water becomes more turbid and as more nutrients are encapsulated by the sediments; these nutrients decreasing the water quality are especially phosphorus, heavy metals and pesticides(Kiragu, 2009).

As the turbidity is a measure of the amount of suspended sediments in the water, this parameter can be used to assess that amount. In Kenya and Tanzania, the water quality standards include a turbidity of 50 NTU and 30 NTU respectively (McCartney, 2010). However, studies by Lake Victoria Basin Commission (LVBC) have shown a turbidity range of 17.5 NTU and 686 NTU for low and high flows respectively (LVBC, 2012); see also Table 2-2 and Figure 2-8. The low flow turbidity was measured in February 2009 and the high flows in October 2008.

Also, a study by Kiragu shows an average daily sediment concentration of 95.16 mg/l and 97.43 mg/l in the Nyangores River and Amala River respectively which is above the recommended standard of 30mg/l in Kenya; see also Figure 2-9 (Kiragu, 2009). This sediment concentration measured between February 2007 and July 2007 shows an increase in sediment concentration with the discharge for the Amala River. However, this relation is not visible in the measurements done for the Nyangores River.

Figure 2-7: Pictures showing the gullies or very river banks in the Mara Rive Basin. Top left: Soil erosion near the Maasai Mara National Reserve (UNEP, 2009). Top middle: Deep gully along the riparian zone at the border between Kenya and Tanzania, and the Maasai Mara National Reserve and Serengeti National Park (LVBC, 2012). Remaining pictures (FIU GIS-Center) and their location from top middle to bottom right: A) Kagawet Bridge (pic571), B) Kagawet Bridge (pic574), C) LOITA 04 (pic 1179), D) Mau 03- forest at swamp (pic1214)

Table 2-2: Water quality measurements (LVBC, 2012)

Site	Flow Conditions	pH	DO (mg/L)	EC (µs/cm)	TDS (µg/L)	Turbidity (NTU)	Temp (°C)	TN (mg/L)	NH_4 (µg/L)	TP (µg/L)	SRP (µg/L)
Site 1	Low	8.6	8.7	239	155	45.9	21.4		103	20	<100
	High	7.1	8.2	53	34	67.2	17.8		145	<20	<100
Site 1.2	Low	9.0	7.3	81	53	17.5	17.8		51	30	<100
	High	7.0	7.8	42	27	51.7	18.5		203	<20	<100
Site 2	Low	7.8	2.4	431	280	72.1	24.5		76	<20	<100
	High	7.3	8.1	82	54	91.9	20.5		152	50	<100
Site 3	Low	8.0	2.8	567	368	74.5	25.4		135	100	<100
	High	7.1	6.1	122	79	330	24.2		291	<20	<100
Site 4	Low	8.7	8.6	362	234	53.4	26.3	1.03	395	260	64
	High	8.2	8.5	74	48	686.0	20.1	1.25	300	680	150
Site 5	Low	8.9	7.3	368	239	27.6	26.9	0.63	201	160	28
	High	7.9	8.5	121	78	647.5	22.3	2.37	165	560	190

*Analysis instruments and methods varied between Sites 1-3 and Sites 4-5, which may account for some minor differences in parameter measurements across sites

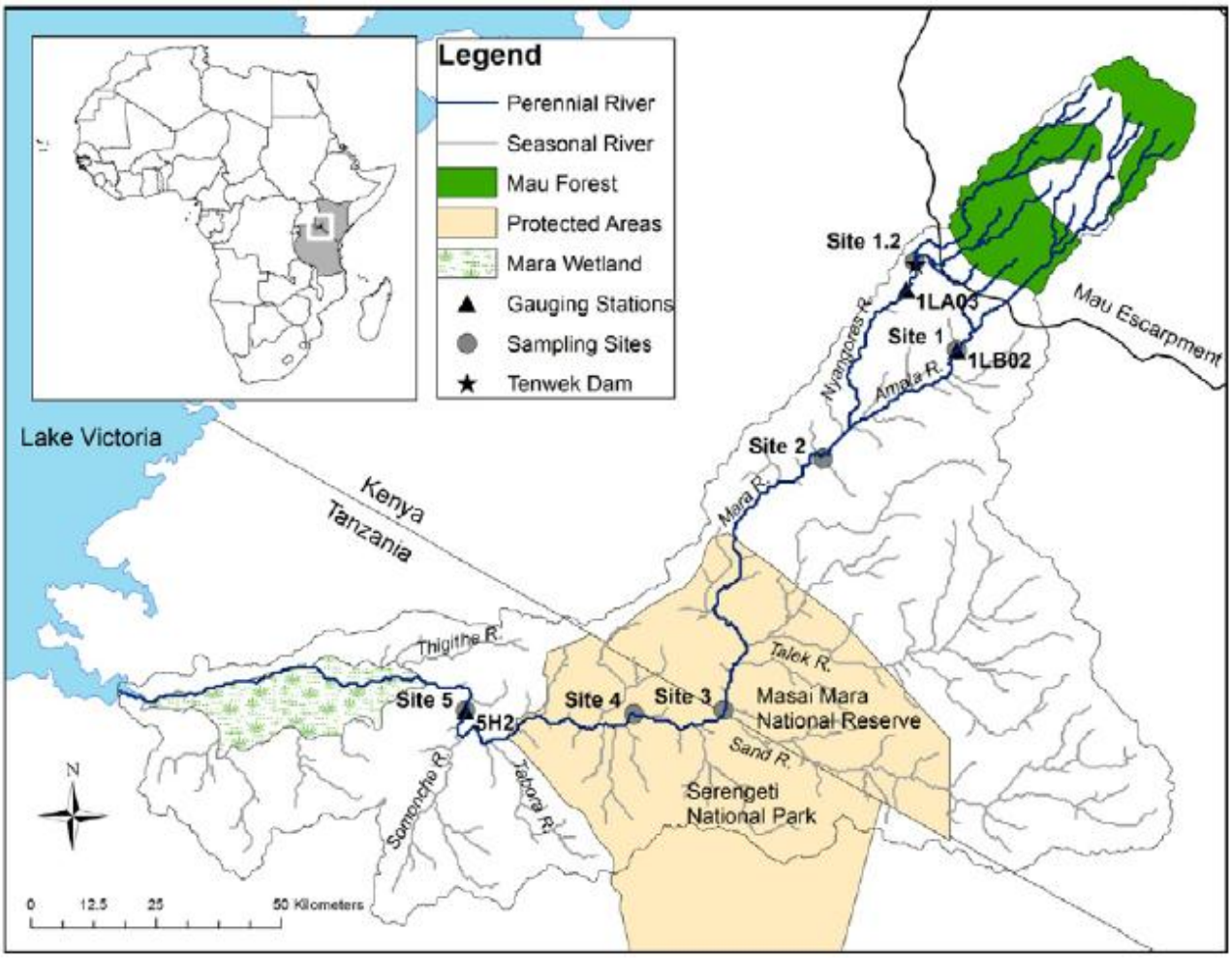

Figure 2-8: Location of water quality measurements (LVBC, 2012)

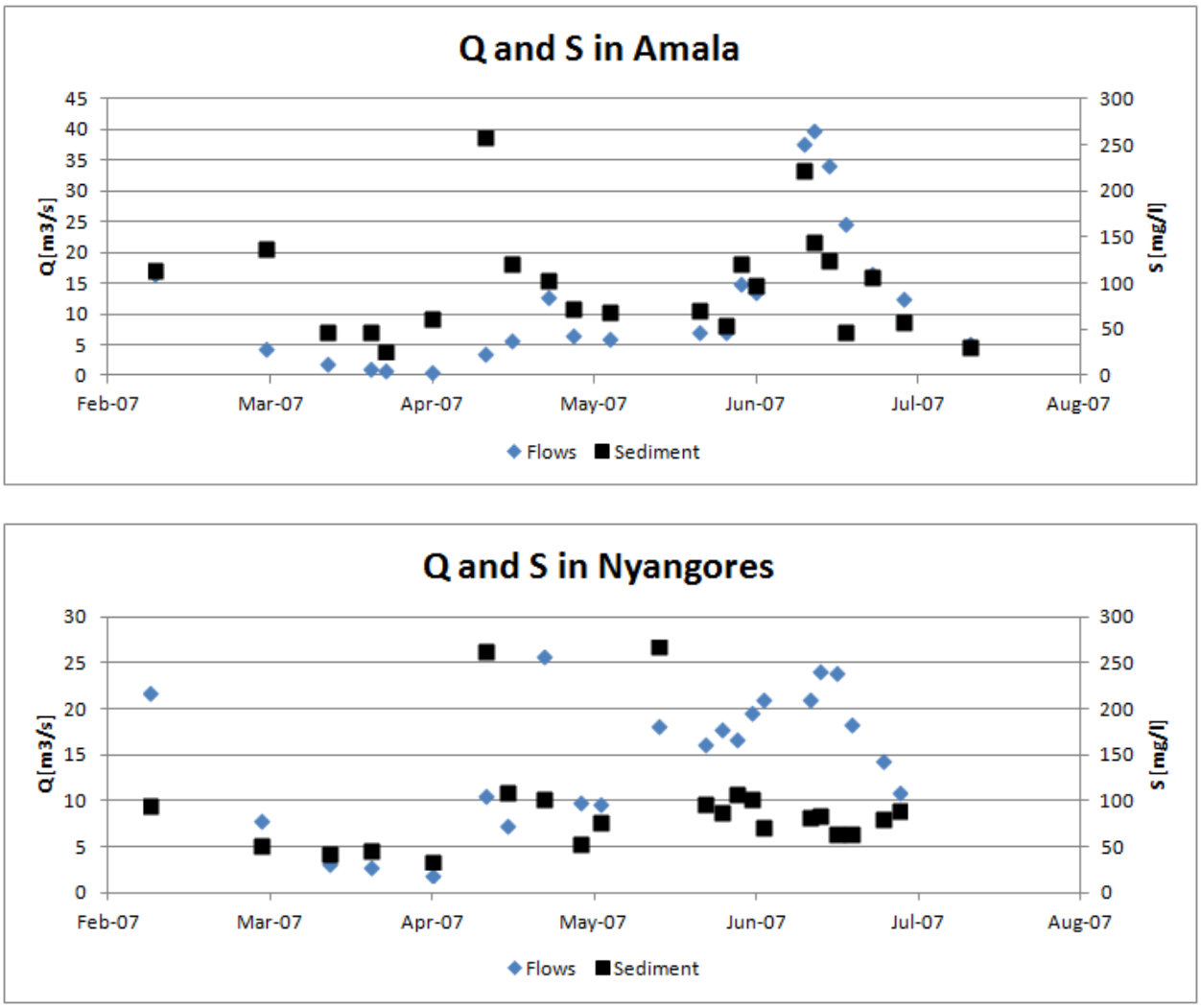

Figure 2-9: Measured discharge Q and sediment concentration S in the tributaries Amala (Site 1) and Nyangores (Site 1.2) (Kiragu, 2009)

2.5.Land use change

Originally, the area mainly contained forested areas and rangeland, but in the past more and more land is cultivated: In 1973, the forest had an area of 1000 km^2, the rangeland 11,000 km^2 and the cultivated land 1500 km^2, that is about 7%, 81% and 11% of the basin. However, the farmland increased to 45,000 km^2 (33%) in 2000.(McClain et al., 2013)

Mati et al. (2008) shows that in the past 30 years (1973 to 2000) the agricultural area has increased with +203% and the forested area and rangeland decreased with -32% respectively -27% (see Table 2-3). Also, it is found that peak flows have increased with 7% and occur 4 days earlier within the studied time range. Moreover, evidence is found for increased soil erosion in the upper catchments, increased silt build-up in downstream floodplains and for wetland expansion with +387%. (Mati et al., 2008)

With the deforestation and change to farmland, less rainwater is infiltrated in the soil resulting in faster and higher runoffs. The result in a reduction of dry season flows and an increase of peak flows. With the larger peak flows, more erosion occurs especially in the upper catchments and a higher sediment load flows into the river which results among other things in the eutrophication of the receiving wetlands and Lake Victoria.

Table 2-3: Land-use/cover area changes in the Mara River Basin, 1973 – 2000 (Mati et al., 2008)

Land-cover type	1973 (km^2)	1986 (km^2)	2000 (km^2)	Change (1973–2000) (km^2)	Change (%)
Forests	1008	893	689	–319	–32
Tea/Open forests	621	1073	1948	+1327	+214
Agricultural land	826	1617	2504	+1678	+203
Shrubland	5361	5105	3546	–1815	–34
Grassland	2465	1621	1345	–1120	–45
Savannah	3163	2867	2354	–809	–26
Wetlands	286	604	1394	+1108	+387
Waterbodies	104	54	55	–49	–47

Appendix B: Data analysis

Table of Contents

1. Data availability

1.1. Map of all the station

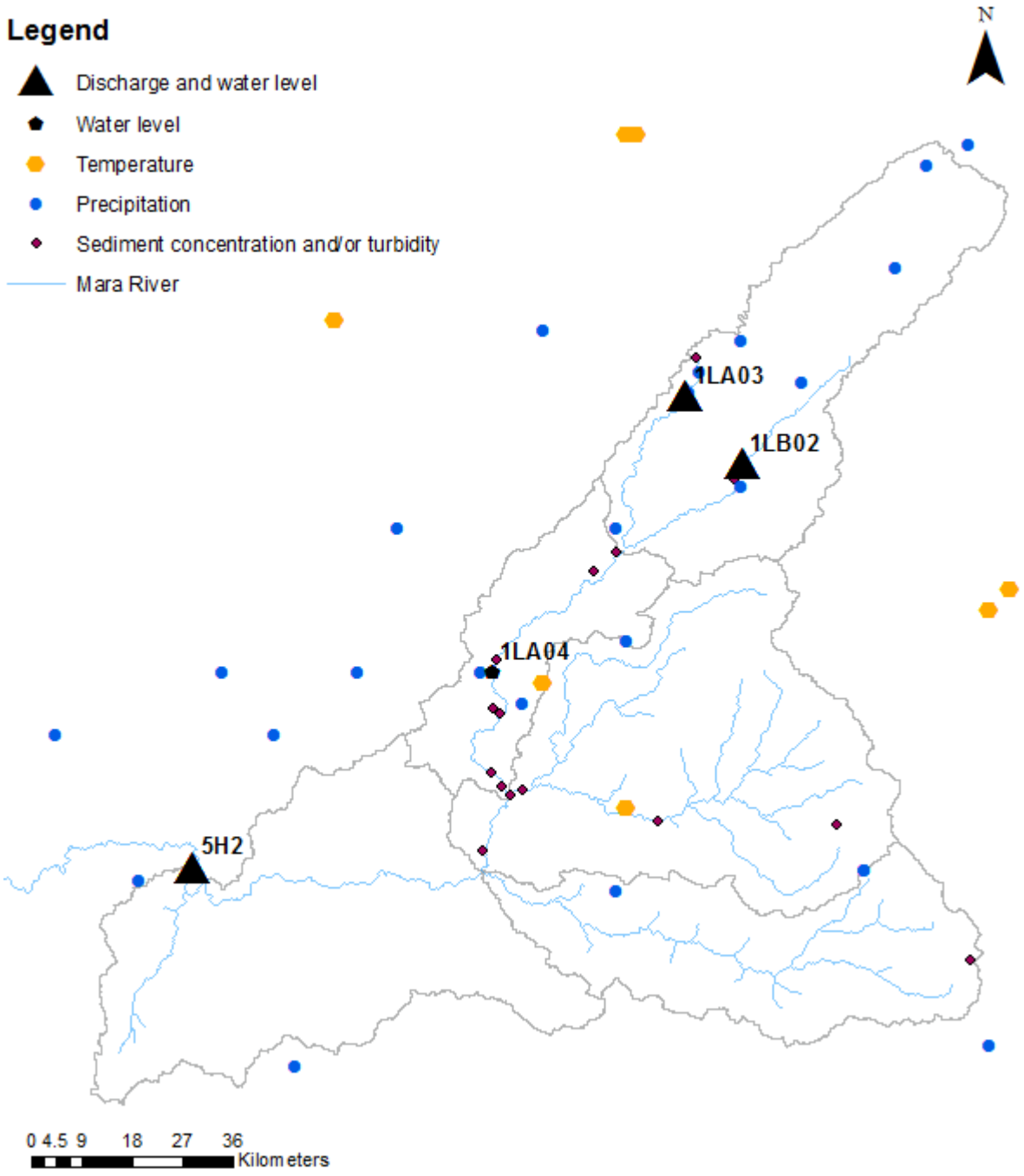

1.2.Precipitation data

Figure 1-1: Map of all the stations measuring precipitation

Table 1-1: Precipitation data availability

Station name	Station ID	Country	Coordinate	Coordinate	Start	End	Data coverage
DANSON K.NGUGI SAW MILL,ELBURG.	9035031	Kenya	35.8	-0.38333	1959	1987	75%
MULOT POLICE POST	9135022	Kenya	35.43333	-0.93333	1969	1988	85%
NAIKARA AFRICA GOSPEL CHURCH	9035284	Kenya	35.63333	-1.55	1973	1998	96%
ELBURGON,BARAGET FOREST STATION	9035241	Kenya	35.73333	-0.41667	1969	1992	100%
SOTIK, TENWIK MISSION	60579	Kenya	35.36667	-0.75	1970	1983	98%
NAIKARA AFRICA GOSPEL CHURCH	60754	Kenya	35.63333	-1.55	1970	1988	90%
SOTIK,KABOSON GOSPEL MISSION	60745	Kenya	35.23333	-1	1970	1986	86%
SOTIK, AITONG VET. HOUSE	60747	Kenya	35.25	-1.18333	1981	1997	70%
NAROK,KEEKOROK GAME LODGE	60750	Kenya	35.23333	-1.58333	1970	1997	97%
KICHWA TEMBO CAMP	9135035	Kenya	35.01667	-1.23333	1988	2002	68%
NAROTIA FOREST STATION	9035303	Kenya	35.53333	-0.76666	1979	2003	66%
NYANGORES FOREST STATION	9035302	Kenya	35.43333	-0.7	1979	1990	99%
SOTIK WATER SUPPLY	9035264	Kenya	35.11667	-0.68333	1965	2004	84%
BOMET WATER SUPPLY	9035265	Kenya	35.35	-0.78333	1965	2008	72%
OLEGURUOE D.O'S OFFICE	9035085	Kenya	35.68333	-0.58333	1959	1984	95%
TALEK CAMP NAROK	9135012	Kenya	35.25	-1.45	1988	2011	99%
MARA SERENA LODGE	9135030	Kenya	35.11667	-1.25	2008	2011	99%
GOVERNOR'S CAMP	9135026	Kenya	35.08333	-1.28333	2011	2011	100%
SOTIK DIV AGRI OFFICE	60727	Kenya	34.88333	-1	1970	1988	93%
TARANGANYA SEC. SCHOOL	60728	Kenya	34.6	-1.23333	1983	1990	85%
LOLGORIEN POLICE POST	60734	Kenya	34.81667	-1.23333	1981	1987	56%
ENTASEKERA CHIEF'S CAMP	60753	Kenya	35.83333	-1.83333	1986	1992	53%
NTIMARU CHIEF'S OFFICE	9134019	Kenya	34.68333	-1.33333	1959	2000	88%
BUHEMBA TR.CENTRE	90172	Tanzania	34.08333	-1.76667	1970	1997	90%
KISAKA NGURUIME	90173	Tanzania	34.46667	-1.56667	1970	1979	64%
MUSOMA MET.	90045	Tanzania	33.8	-1.5	1970	1974	8%
NYABANGI MISSION	90049	Tanzania	33.86667	-1.55	1970	1994	92%
TARIME HYDROMET	90062	Tanzania	34.33333	-1.33333	1970	1994	66%
MUGUMU PRIMARY SCHOOL	90063	Tanzania	34.71667	-1.86667	1970	1997	96%

1.3.Temperature data

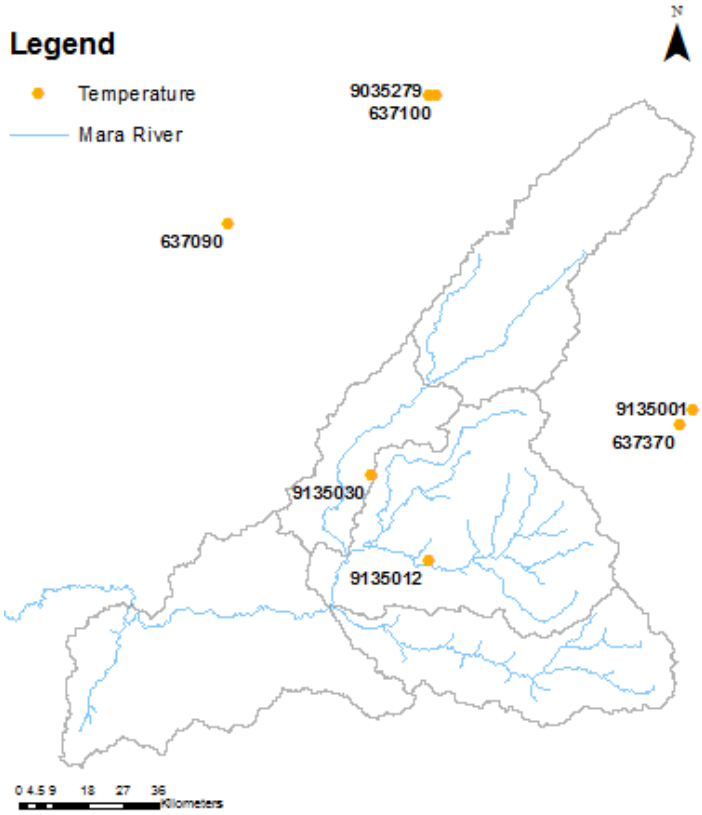

Figure 1-2: Map of all the stations measuring temperature

Table 1-2: Temperature data availability

STATION NAME	Station ID	Country	BEGIN	END	Coordinate	Coordinate	Source	Data coverage
MUSOMA	637330	Tanzania	1957	2014	-1.5	33.8	NOAA	30%
NAROK	637370	Kenya	1957	2014	-1.133	35.833	NOAA	33%
KISII	637090	Kenya	1984	2014	-0.667	34.783	NOAA	43%
KERICHO	637100	Kenya	1973	2014	-0.367	35.267	NOAA	36%
NAKURU	637140	Kenya	1957	2014	-0.267	36.1	NOAA	73%
HAIL RESEARCH STATION KERICHO	9035279	Kenya	1992	2003	-0.36667	35.25	Station data	100%
NAROK METEOROLOGICAL STATION	9135001	Kenya	1992	2003	-1.1	35.86667	Station data	99%
TALEK CAMP NAROK	9135012	Kenya	1984	2007	-1.45	35.25	Station data	98%
MARA SERENA LODGE	9135030	Kenya	2004	2007	-1.25	35.11667	Station data	96%

1.4.Discharge and water level data

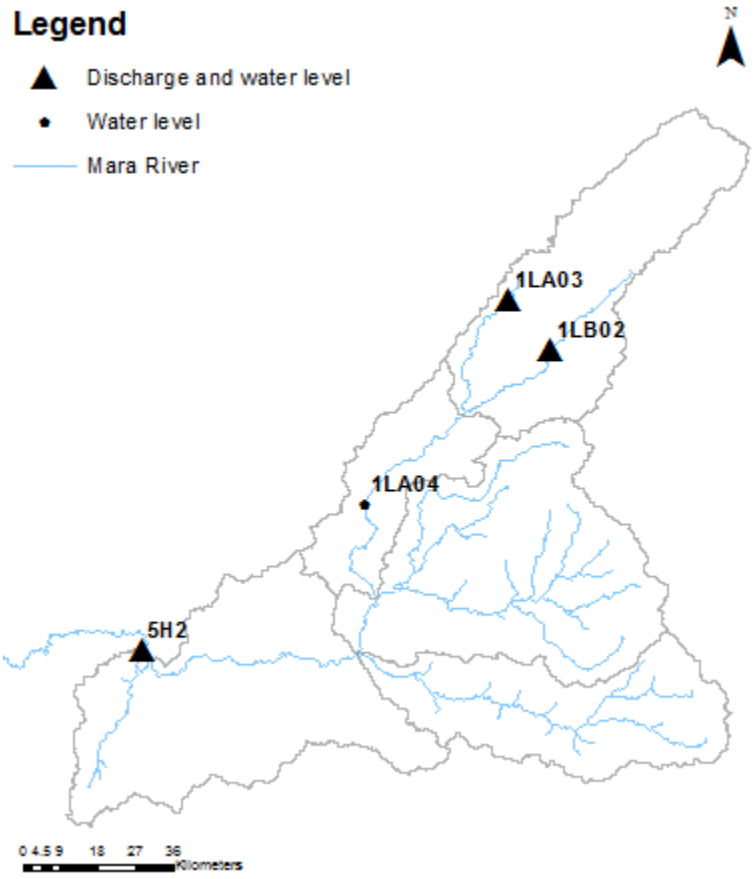

Figure 1-3: Map of all the stations measuring discharge and water level

Table 1-3: Discharge data availability

Station Name	Station ID	Coordinate	Coordinate	Start	End	Data coverage
Amala at Kapkimolwa Bridge	1LB02	-0.89895	35.43739	1955	2008	73%
Nyangores at Bomet Bridge	1LA03	-0.78986	35.34651	1963	2008	85%
Mara at Mara Mine	5H2	-1.548	34.554	1969	2013	69%

Table 1-4: Water level data availability

Station Name	Station ID	Coordinate	Coordinate	Start	End	Data coverage
Amala at Kapkimolwa Bridge	1LB02	-0.89895	35.43739	1955	2008	73%
Nyangores at Bomet Bridge	1LA03	-0.78986	35.34651	1963	2008	86%
Mara	1LA04	-1.233	35.036	1970	1992	37%
Mara at Mara Mine	5H2	-1.548	34.554	1969	2013	69%

1.5.Sediment concentration and turbidity

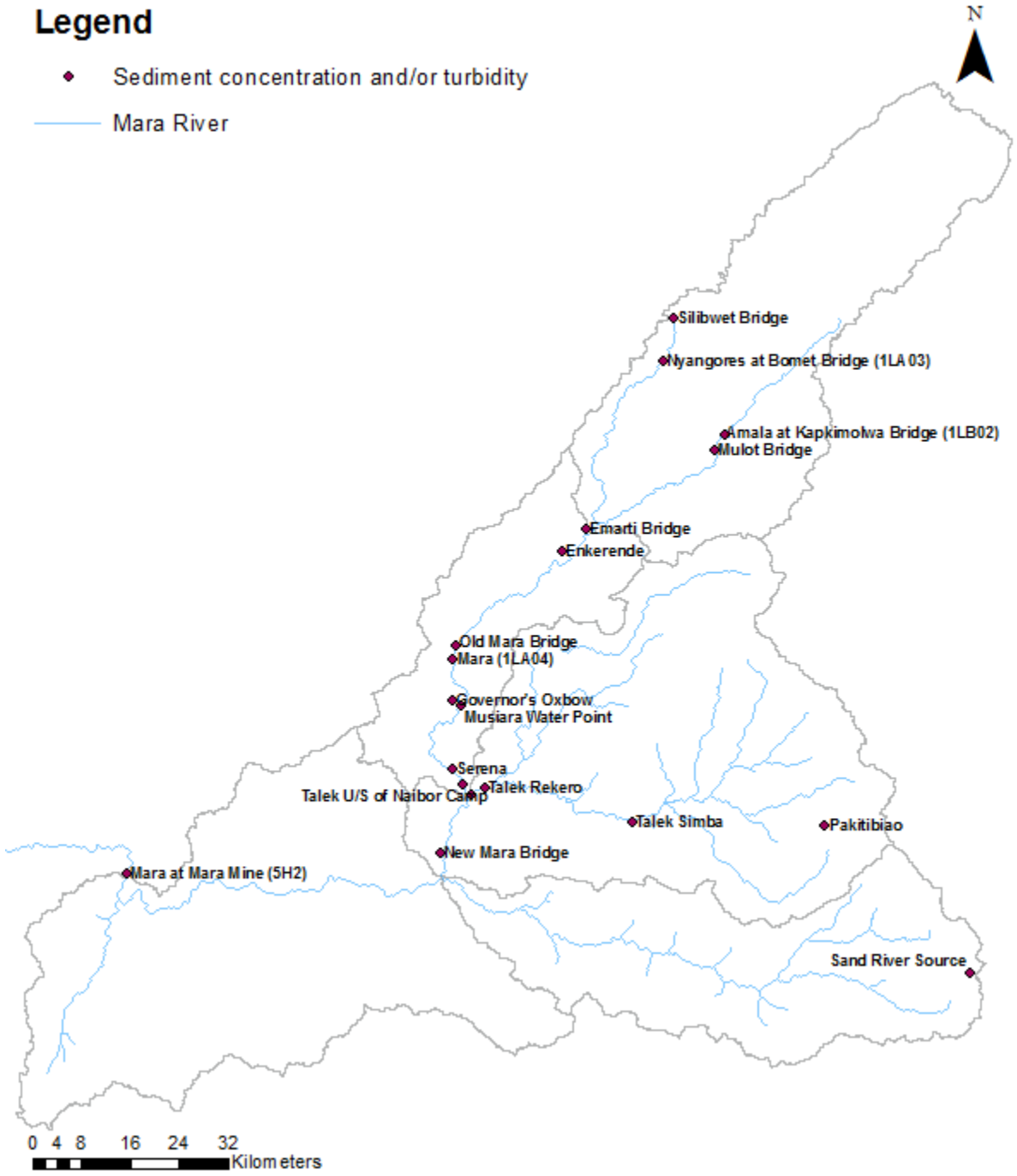

Figure 1-4: Map of all the stations measuring sediment concentration and/or turbidity

Table 1-5: Turbidity and sediment concentration data availability

Location	Coordinate	Coordinate	Source	Year	Number of sample points	Data recorded
Amala at Kapkimolwa Bridge (1LB02)	-0.89895	35.43739	Station data (Mulot headquarter)	2012-2014	825 (97% coverage)	Turbidity
			(Kiragu, 2009)	2007	22	TSS, turbidity, water level
			WWF	2006, 2007	16	TSS
			(WREM International Inc, 2008)	2000-2003	4	Sediment load, water level
			(Subalusky, 2011)	2008, 2009	23	Turbidity, water level
Nyangores at Bomet Bridge (1LA03)	-0.78986	35.34651	Station data (Bomet Water Supply Station)	2013-2014	262 (92% coverage)	Turbidity
			(Kiragu, 2009)	2007	22	TSS, turbidity, water level
			(McCartney, 2010)	2007, 2008	2	Turbidity, TSS
			WWF	2006, 2007	10	TSS
			(Subalusky, 2011)	2008, 2009	31	Turbidity, water level
			(WREM International Inc, 2008)	1980, 2000-2004	10	Sediment load, water level
Mara at Mara Mine (5H2)	-1.548	34.554	WWF	2004	6	TSS
			(McCartney, 2010)	2007, 2008	2	Turbidity, TSS
Mara (1LA04)	-1.233	35.036	(WREM International Inc, 2008)	1980, 2000-2004	23	Sediment load, water level
Mara at Kirumi Bridge			WWF	2004, 2003	5	TSS
				1999	6	Turbidity
Mulot Bridge	-0.922	35.424	(Subalusky, 2011)	2008, 2009	21	Turbidity, water level
			(McCartney,	2007,	2	Turbidity, TSS

			2010)	2008		
Emarti Bridge	-1.039	35.233	(Subalusky, 2011)	2008	1	Turbidity
			(McCartney, 2010)	2007, 2008	2	Turbidity, TSS
New Mara Bridge	-1.519	35.018	(Subalusky, 2011)	2008, 2009	44	Turbidity, water level
			(McCartney, 2010)	2007, 2008	2	Turbidity, TSS
Old Mara Bridge	-1.212	35.041	(Subalusky, 2011)	2008, 2009	22	Turbidity, water level
			(McCartney, 2010)	2007, 2008	2	Turbidity, TSS
Silibwet Bridge	-0.728	35.362	(Subalusky, 2011)	2008, 2009	23	Turbidity, water level
			(McCartney, 2010)	2007, 2008	2	Turbidity, TSS
Enkerende	-1.072	35.197	(Subalusky, 2011)	2008, 2009	24	Turbidity, water level
Governor's Oxbow	-1.292	35.035	(Subalusky, 2011)	2008, 2009	18	Turbidity, water level
Mara at the Talek Confluence	-1.432	35.064	(Subalusky, 2011)	2008, 2009	23	Turbidity, water level
Talek Rekero	-1.422	35.084	(Subalusky, 2011)	2009	9	Turbidity
Talek Simba	-1.472	35.302	(Subalusky, 2011)	2008, 2009	17	Turbidity, water level
Talek U/S of Naibor Camp	-1.416	35.05	(Subalusky, 2011)	2008, 2009	19	Turbidity, water level
Mara Swamp, Tanzania	-1.529	33.979	(Subalusky, 2011)	2008, 2009	4	Turbidity, water level
Musiara Water Point	-1.301	35.048	(Subalusky, 2011)	2009	1	Turbidity
Pakitibiao	-1.478	35.587	(Subalusky, 2011)	2008	1	Turbidity
Sand River Source	-1.697	35.802	(Subalusky, 2011)	2008	1	Turbidity
Serena	-1.394	35.034	(McCartney, 2010)	2008	1	Turbidity, TSS

2. Data analyses: plots

2.1.Flow duration curve

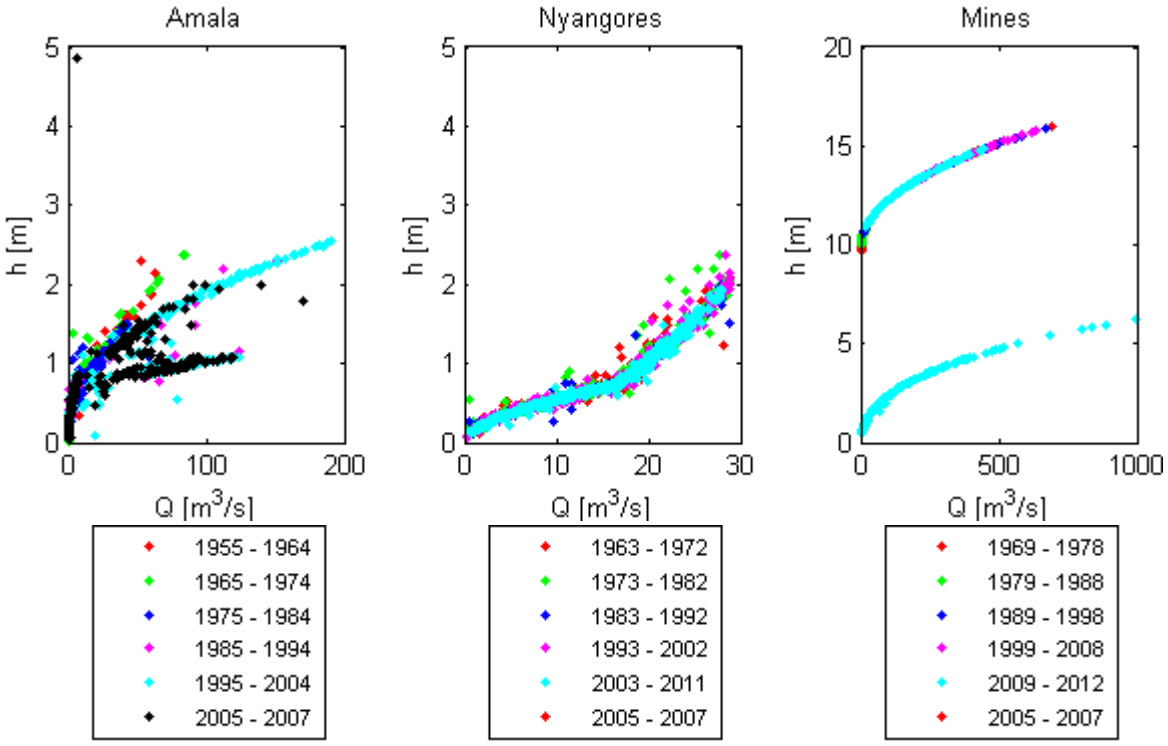

Figure 2-1: Discharge water level plot for three stations: Amala (1LB02), Nyangores (1LA03) and Mara Mines (5H2)

2.2.Water level

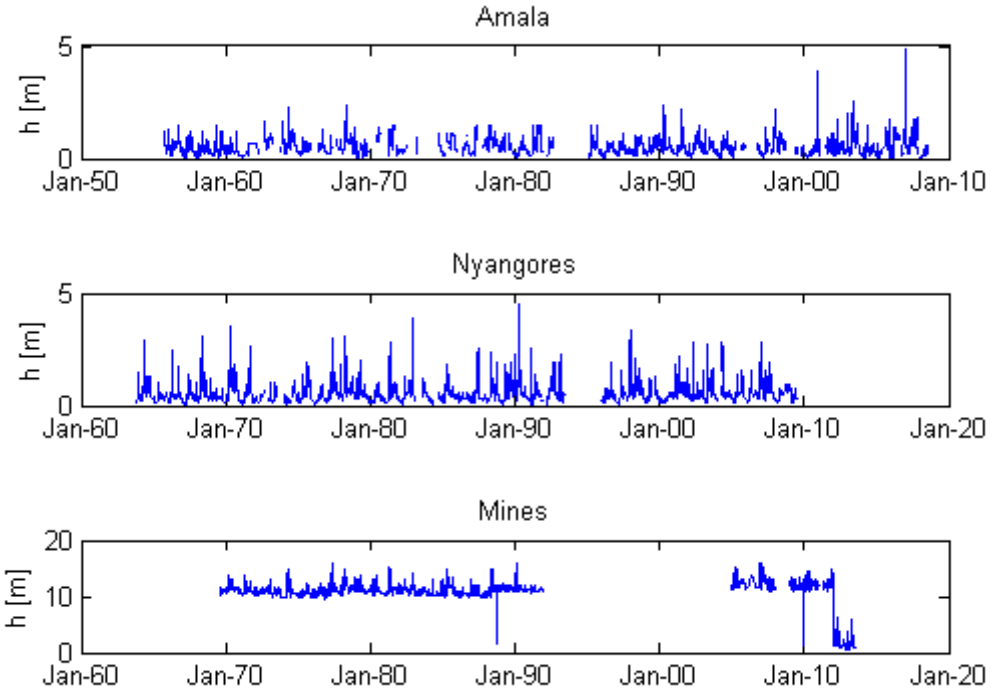

Figure 2-2: Water level measured at three stations: Amala (1LB02), Nyangores (1LA03) and Mara Mines (5H2)

2.3.Hydrograph

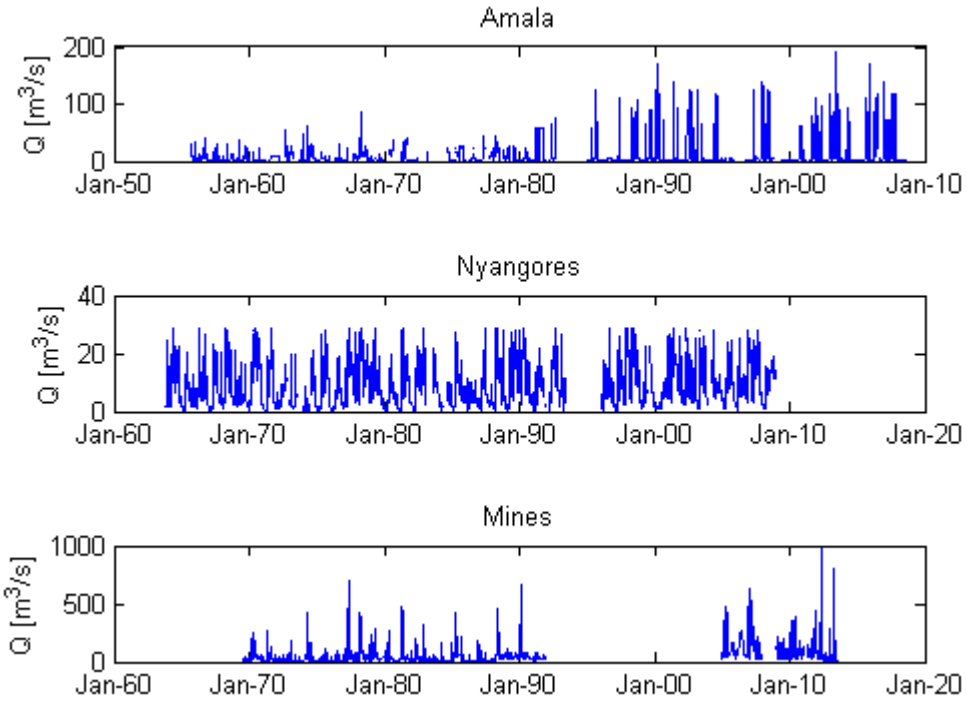

Figure 2-3: Discharge determined at three stations: Amala (1LB02), Nyangores (1LA03) and Mara Mines (5H2)

2.4.Double mass curves

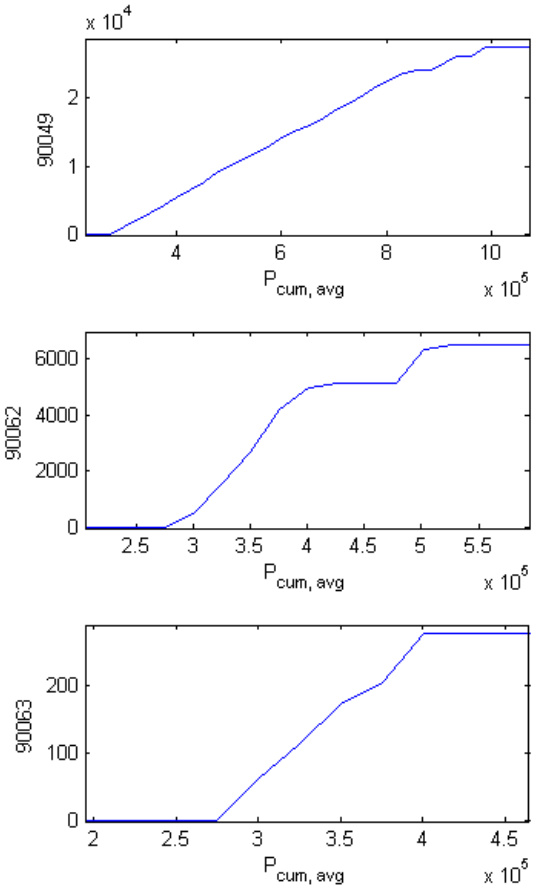

Figure 2-4: Double mass curves for the stations 90049, 90062 and 90063. In each plot the annual cumulative rainfall is plotted against the average annual cumulative rainfall $P_{cum,\ avg}$ of all stations in [mm]

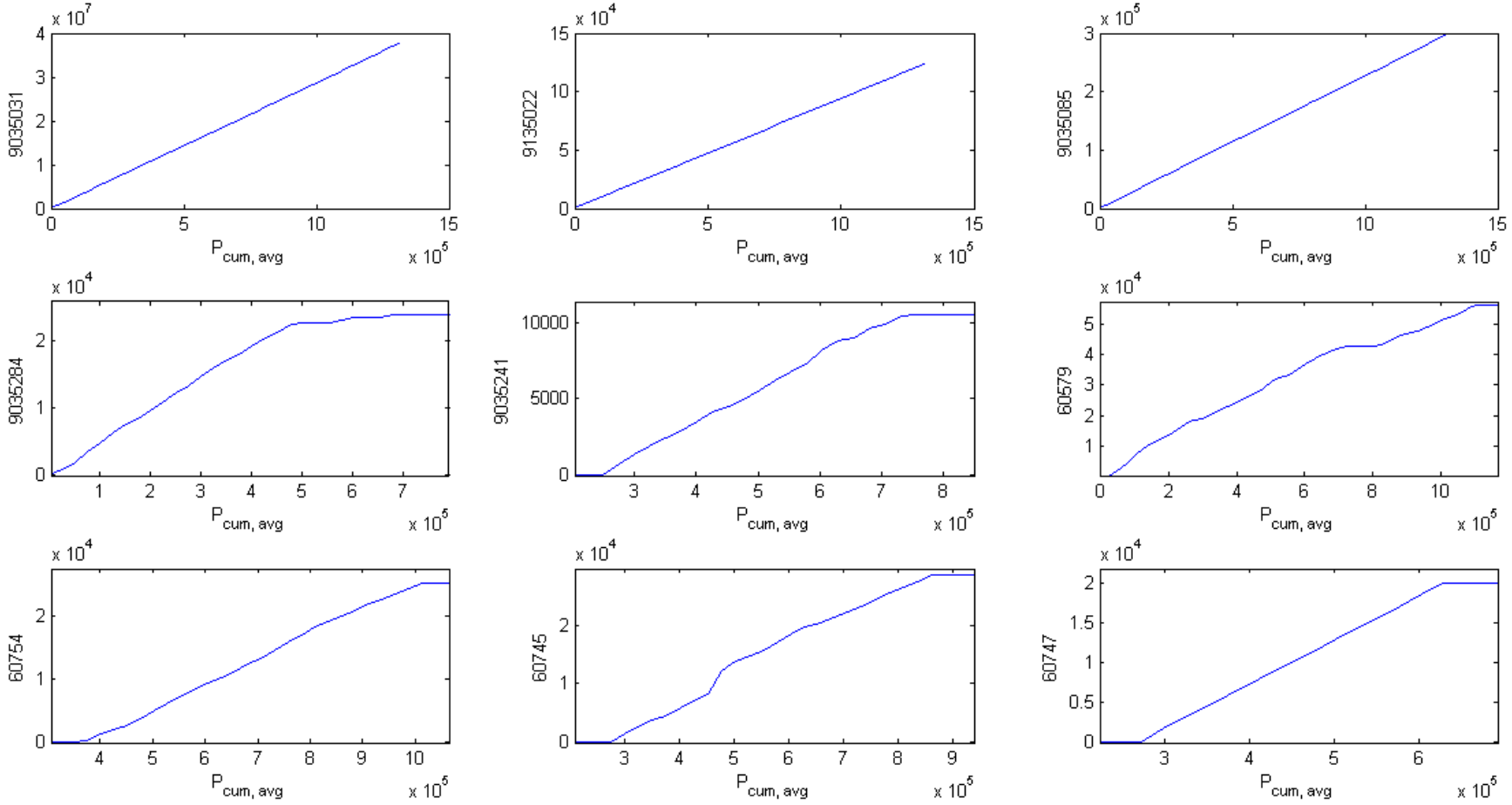

Figure 2-5: Double mass curves for the stations 9035031, 9135022, 9035085, 9035284, 9035241, 60579, 60754, 60745 and 60747. In each plot the annual cumulative rainfall is plotted against the average annual cumulative rainfall $P_{cum, avg}$ of all stations in [mm]

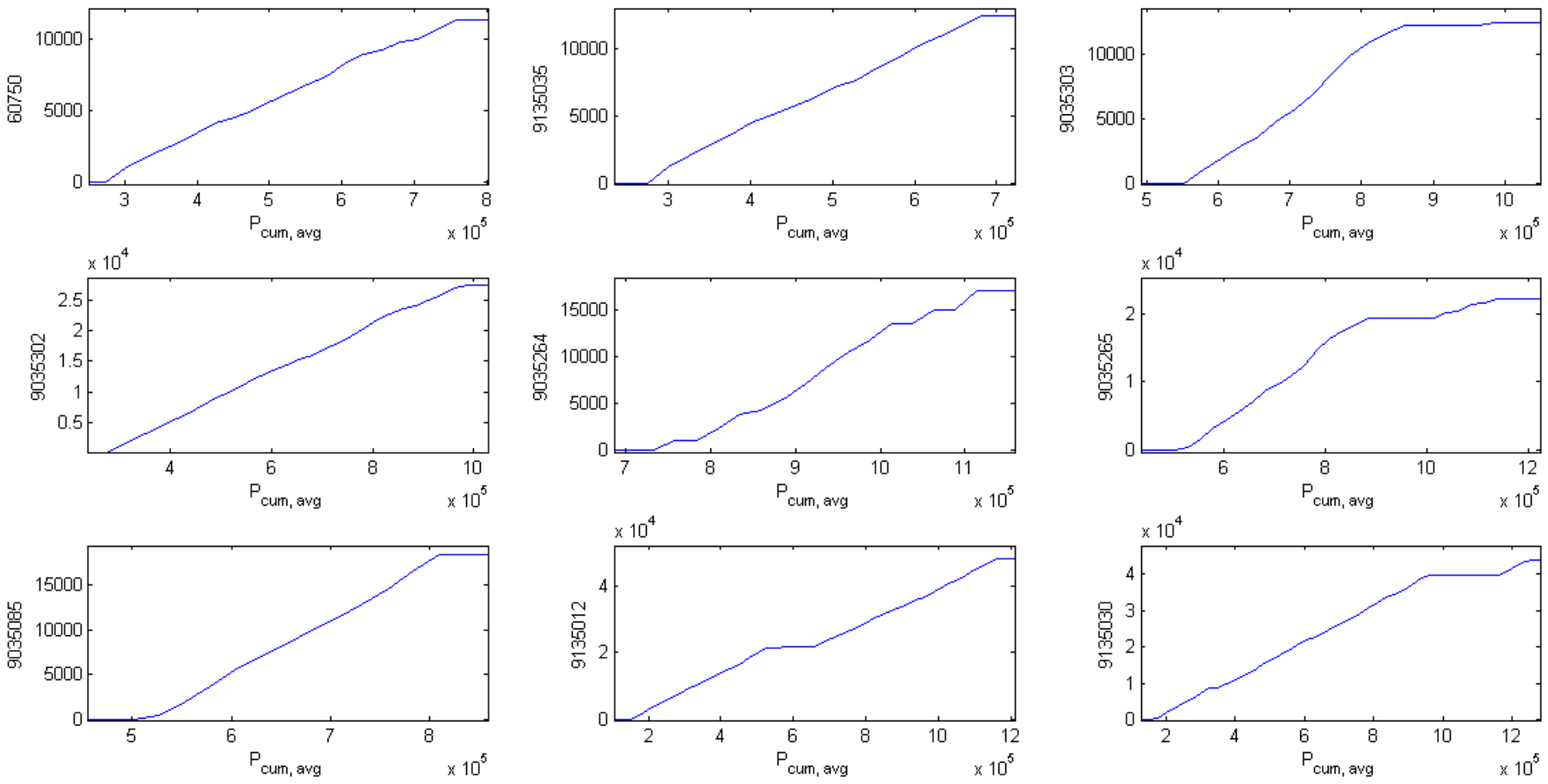

Figure 2-6: Double mass curves for the stations 60750, 9135035, 9035303, 9035302, 9035264, 9035265, 9035085, 9135012 and 9135030. In each plot the annual cumulative rainfall is plotted against the average annual cumulative rainfall $P_{cum, avg}$ of all stations in [mm]

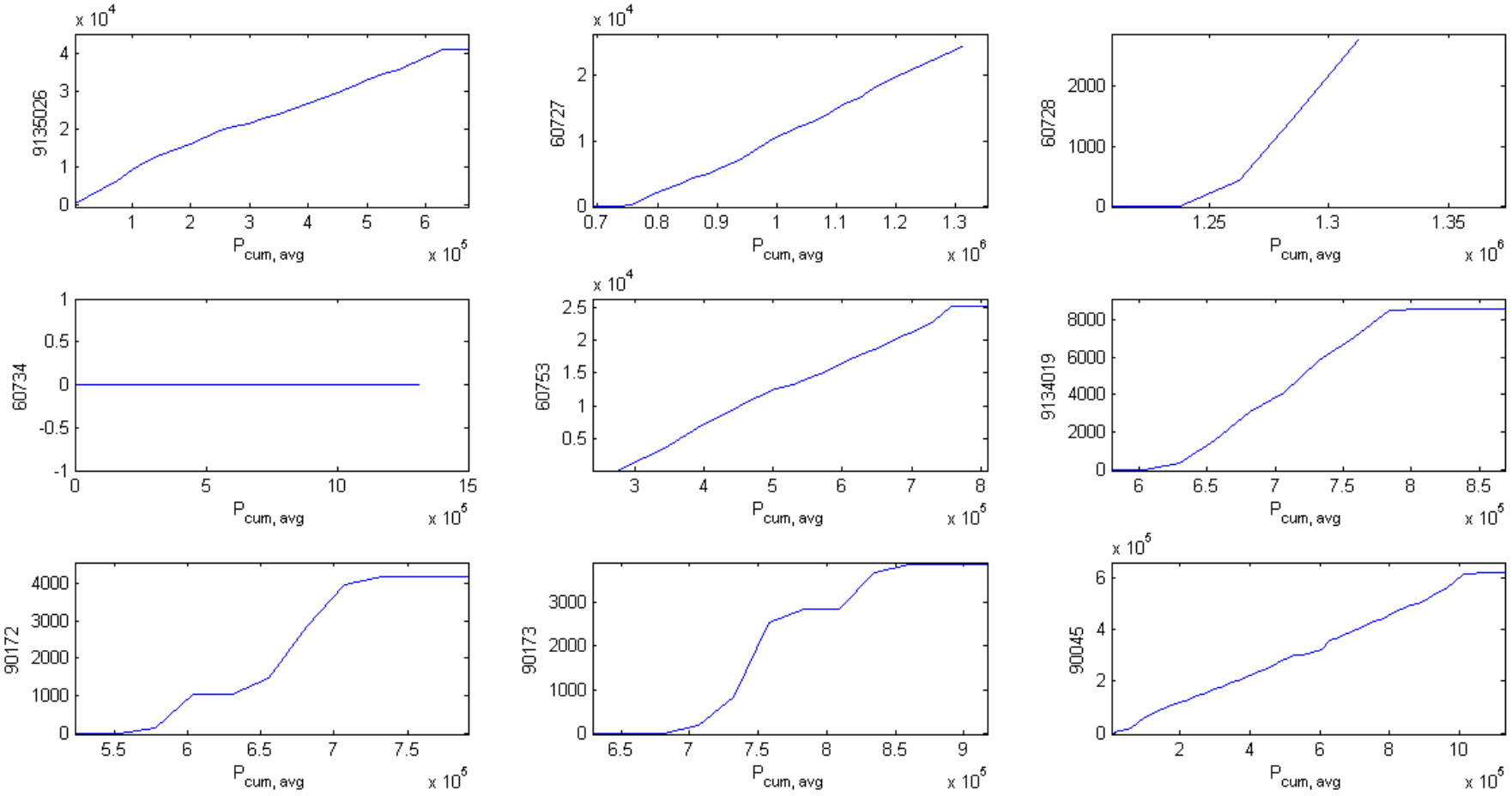

Figure 2-7: Double mass curves for the stations 91350269135026, 60727, 60728, 60734, 60753, 9134019, 90172, 90173 and 90045. In each plot the annual cumulative rainfall is plotted against the average annual cumulative rainfall $P_{cum, avg}$ of all stations in [mm]

Appendix C: Observed erosion features

Table of contents

In this section, the occurrence of sediment transport in the Mara River Basin is assessed. This assessment is based on:

- Interviews results conducted while visiting the different sites in the Mara River Basin
- Personal field observations
- Sub-catchment Management Plans (SCMP)
- Data on turbidity and sediment concentration

1. Assessment based on: Interview results

To estimate the occurrence of sediment transport in the catchment, members of different Water Resources Users Associations (WRUAs) throughout the catchment are interviewed. A WRUA is a community of volunteers, water users and stakeholders, that work together to improve the water resources management (Anonymous, 2009). In total, members of 10 WRUAs are interviewed; see Figure 1-1 for their location:

- Head of the WRUAs covering mainly the upper sub-catchment
- Amala WRUA
- Lower Nyangores WRUA
- Mara Emarti WRUA
- Ildungishu Siana WRUA
- Olderkesi WRUA
- Naikarra WRUA
- Leshuta WRUA
- Oloolaimutia WRUA
- Engare Ngito WRUA

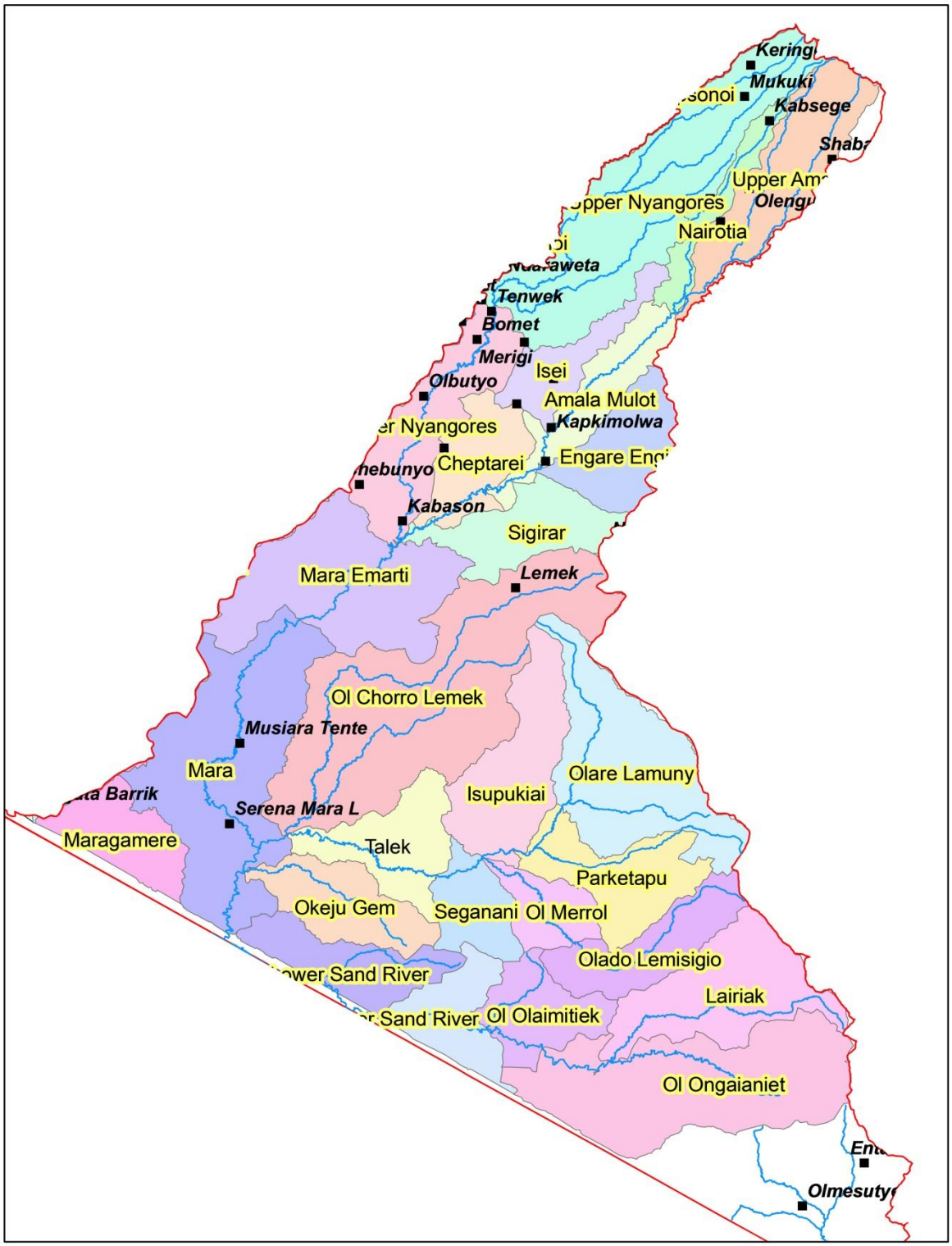

Figure 1-1: Map of the WRUAs in Kenya

During the interviews, the members described their observations of erosion regarding form and location. Also, they mentioned related problems they experience and solutions they either apply or propose. In Table 1-1 an overview is given of the interview results. To clarify this table, several aspects will be explained now.

Observations

First, each interviewee explained whether they observed erosion by describing visual features, for example:

- the turbidity of the water which might change with the water level
- the occurrence of rills
- the collapsing of river banks
- the occurrence of landslides

With these observations, the locations of erosion can be assessed. These are for example: along the riverbank, along roads and animal tracks, on crop fields or on plain field due to wind erosion.

Problems

Then the interviewees were asked to explain all the problems they experienced related to erosion. In general, their answers could be grouped into four categories:

- loss of top soil
- siltation of pans or water supply systems which may get blocked by the sediments
- river pollution
- gullies; large gullies reduce the space available for roads or grazing and are a threat for animals who can fall in them and get stuck

These problems seem to have intensified over the past 30 years. Not all WRUA members were able to describe the change as they have not lived long enough in the area of their WRUA. The members, who did describe it, gave different explanations:

1. In areas governed by pastoralists. In the past 30 years, the pressure on the land increased due to the population growth and the larger numbers of livestock. Through this change, overgrazing started to become a problem as the number of animals grazing on a land exceeded its capacity. As a result of overgrazing, larger areas become bare and more vulnerable to soil erosion.
2. In areas governed by farmers, the population growth resulted in smaller fields per person. In the past, farmers did apply agricultural practices as terraces. However these were removed to increase the area available for crops. After this removal, the top soil started to erode which was noticed by the decline of the soil fertility. Nowadays a lot of manure and fertilizers need to be used to obtain similar crop yields whereas 30 years ago neither of them was used.
3. Another reason for this change might be the land ownership regulation; according to the large scale farmer Hugo Wood. Currently, part of the land owned by Maasai is leased to farmers. However, the leasing agreements are very flexible as the Maasai might change suddenly with no warning from tenant as soon as there is a higher offer. Therefore, it is not realistic for such

farmers to think on the long run and for example to apply soil conservation techniques. The result is land deterioration which is visible on several locations.

Solutions

After having described the observations and problems related to erosion, the WRUA members explained different solutions they either currently apply or would like to in the future. These solutions are:

- Bring in expertise, as they lack in knowledge to solve this problem
- Block gullies; the means are quite diverse: some apply sticks and branches others stones, again others propose the construction of gabions, or the planting of trees
- Improve agricultural practices, for example:
    - Terracing
    - Contour ploughing
    - Agroforestry
    - Mulching
    - Contour and minimum tillage
    - Plant grass on contours
    - Mixed farming
    - Crop rotation
    - Application of manure
    - Application of drought tolerant crops
    - Cover cropping after harvests
    - Leaving grass strips
- Forestation
- River bank protection
- Soil conservation practices; for example crop rotation, cover cropping, mulching, cross-slope farming, grassed waterways, buffer strips along watercourses etc. These practices are very similar to the agricultural practices proposed since in both cases the goal is to conserve the topsoil.
- Promote alternative livelihoods
- Reduce the pressure on watering points or grazing locations to minimize gully developments along cattle tracks. This can be achieved by creating more watering points, applying rotational grazing schemes and/or reducing the number of livestock.
- Create (wide) livestock pathways to reduce the pressure on the narrow paths currently available
- Spring protection by building a construction around them combined with troughs for animals. The aim is to prevent it from getting polluted through animals trampling in the water or even clogged or dried up. By protecting the existing springs and making sure they do not get exhausted, the number of watering points does not decrease. This is closely related to the solution of reducing the pressure on watering points.

Table 1-1: Overview of the interview results; the marking 'x' indicates that the interviewee mentioned the corresponding aspect

	Olderkesi WRUA	Head of WRUAs	Amala WRUA	Lower Nyangores WRUA	Mara Emarti WRUA	Ildungishu Siana WRUA	Naikarra WRUA	Leshuta WRUA	Oloolaimutia WRUA	Engare Ngito WRUA
Observation										
Turbid water	X					X				
Rills						X				
Collapse of river bank										X
Landslides										X
Locations										
Riverbank										X
Along roads/tracks	X				X	X	X	X	X	X
Crop field		X	X	X				X		X
Wind erosion										X
Problems										
Loss of fertile soil	X	X		X		X	X	X	X	X
Siltation	X					X		X		
River pollution					X					
Gullies						X	X	X	X	X
Change past 30 years										
Increased pressure				X				X		X
More erosion						X	X	X		X
Solutions										
Bring in expertise	X						X		X	
Block gullies	X		X		X	X	X	X	X	X
Agricultural practices		X	X						X	
Forestation		X								X
River bank protection		X								X
Soil conservation				X						
Alternative livelihoods		X								
Pressure reduction								X		
Create livestock tracks										X
Spring protection								X		

2. Assessment based on: Sub-catchment management plans (SCMPs)

For several WRUAs, a sub-catchment management plan is written. In this plan water resources management problems are described as also activities proposed to solve them (Anonymous, 2009). For this analysis 7 SCMPs are available; these are for the WRUAs:

- Engare Ngiito
- Amala
- Nyangores
- Isei
- Mara Emarti
- Naikarra
- Talek

Based on these plans, the occurrences of erosion, related problems and proposed solutions are put together in an overview as shown in Table 2-1.

Also, it is mentioned that the average sediment load is between 113-432 tonnes/day in the Amala River and 6.3-424.3 tonnes/day in the Nyangores River. In the Engare Ngito WRUA, the soil loss is estimated to be 0.08-521.8 tonnes/ha/year; this estimation is done by applying the USLE method.

To clarify the table, all new entries not used in the previous table will be explained.

- Observation
  - Turbid water
  - Rills
  - Collapse of river bank
  - Landslides
  - Gullies
- Locations
  - Riverbank
  - Along roads/tracks
  - Crop field
  - Wind erosion
- Problems
  - Loss of fertile soil
  - Siltation
  - River pollution
- Change past 30 years
  - Increased pressure
  - More erosion
- Solutions
  - Bring in expertise
  - Block gullies
  - Agricultural practices
  - Forestation
  - River bank protection
  - Soil conservation
  - Alternative livelihoods
  - Reduce the pressure
  - Create livestock tracks

Causes

In the SCMPs, different causes for the erosion are mentioned. These are:

- Overgrazing resulting in the increasing size of bare areas that are more vulnerable to soil erosion
- Poor land use management especially in agricultural areas
- Encroachment of the riparian zone. This zone is along the riverbanks is meant to be 30 m wide to ensure a stable river bank thus to ensure negligible soil erosion from the banks.
- Deforestation
- Sand harvesting; on different locations, sand is harvested for construction. These locations however have become bare and therefore more vulnerable to soil erosion.

Solutions

As solutions, several options are given in the SCMPs, the ones that were not mentioned during the interviews are:

- Desiltation of the pans already silted in order to be able to use them in their full capacity
- Construction works; this includes the building of: cut off drains, retention ditches and check dams

Table 2-1: Overview based on the SCMPs; ; the marking 'x' indicates that the corresponding aspect is mentioned in the SCMP

	Olderkesi WRUA	Amala WRUA	Isei WRUA	Lower Nyangores WRUA	Mara Emarti WRUA	Naikarra WRUA	Engare Ngito WRUA	Talek WRUA
Locations								
Riverbank						X		
Along roads/tracks		X				X		X
Crop field		X		X	X		X	
Problems								
Loss of fertile soil			X	X			X	
Siltation			X	X	X		X	
River pollution		X	X					
Gullies			X			X		
Causes								
Overgrazing			X	X		X	X	X
Poor land use management			X	X				
Riparian zone encroachment						X		
Deforestation						X		
Sand harvesting						X		
Solutions								
Agricultural practices		X	X	X			X	
Forestation		X	X	X	X	X	X	X
River bank protection		X	X	X	X	X	X	X
Soil conservation		X	X	X	X	X	X	X
Pressure reduction					X		X	
Desiltation			X					
Construction works							X	
Spring protection		X		X	X	X		X

3. Assessment based on: Field observations

During a visit in the Mara River Basin, a clear difference in land use is noticed between the sub-catchments North and Talek/Sand.

Land use

In the sub-catchment North, there is mainly cropland and the Mau forest, while the sub-catchments Talek and Sand are mostly Maasai land who own large numbers of livestock. The Middle sub-catchment however is owned by farmers, both small and large scale, but also by pastoralists with again large numbers of livestock.

Erosion features

Corresponding to the land use, mostly sheet erosion is found in the cultivated areas resulting in the loss of top soil. In the Maasai land however, cattle tracks are seen near watering points with large gullies along the river bank or next to the tracks (see Figure 3-1). Also along roads many large gullies are seen. Depending on how dry it is, the area is found to be dusty and extremely vulnerable to wind erosion especially by driving cars.

Figure 3-1: Examples of observed erosion features. From left to right: Gullies along roads, gullies at a watering point, dusty roads

4. Assessment based on: Data analysis

On different locations within the Mara River Basin, data related to sediment transport is collected from various previous studies:

- Turbidity and sediment concentration data (see Figure 3-8) measured in the Nyangores and Amala tributaries from February to July 2007 (Kiragu, 2009)
- Turbidity data measured on various locations in the entire catchments and on different moments of the year between June 2008 and May 2010. This data is collected as part of a consultant report to refine the reserve flow recommendations in the Mara River (Subalusky, 2011)
- Turbidity and sediment concentration data measured on various locations in the entire catchment between July/Aug 2007 and June/July 2008 (McCartney, 2010)
- Turbidity data series measured for the Amala tributary between May 2012 and September 2014 and for the Nyangores tributary between January and September 2014 (see Figure 3-7). This data is measured by local people and is collected during the field visit.

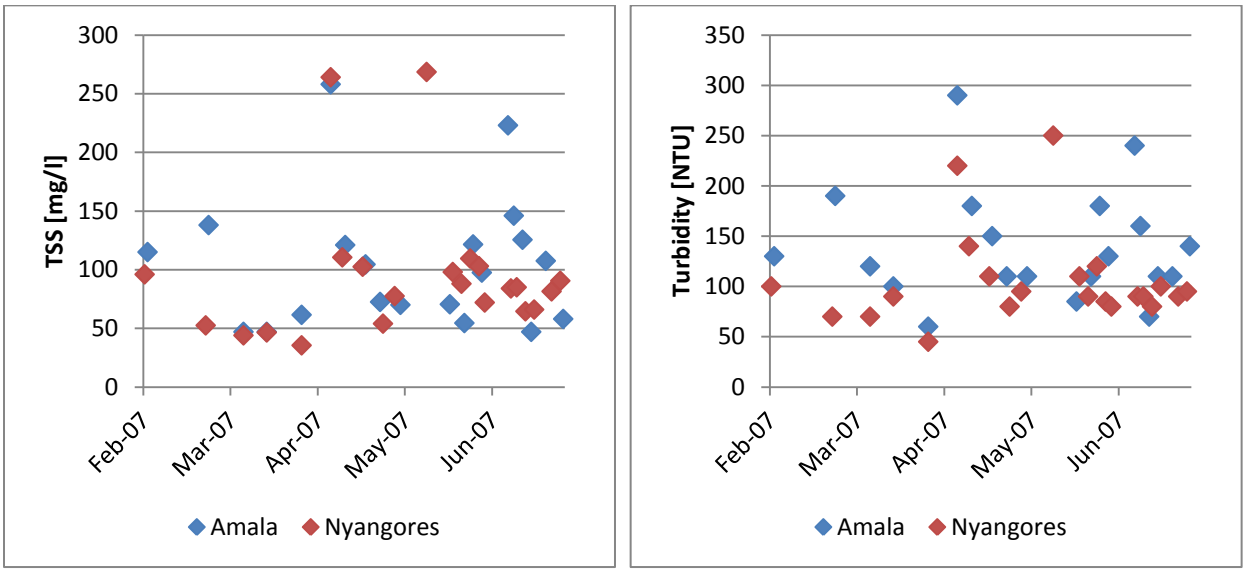

Figure 4-1: Sediment concentration and turbidity measured in the tributaries Nyangores and Amala (Kiragu, 2009)

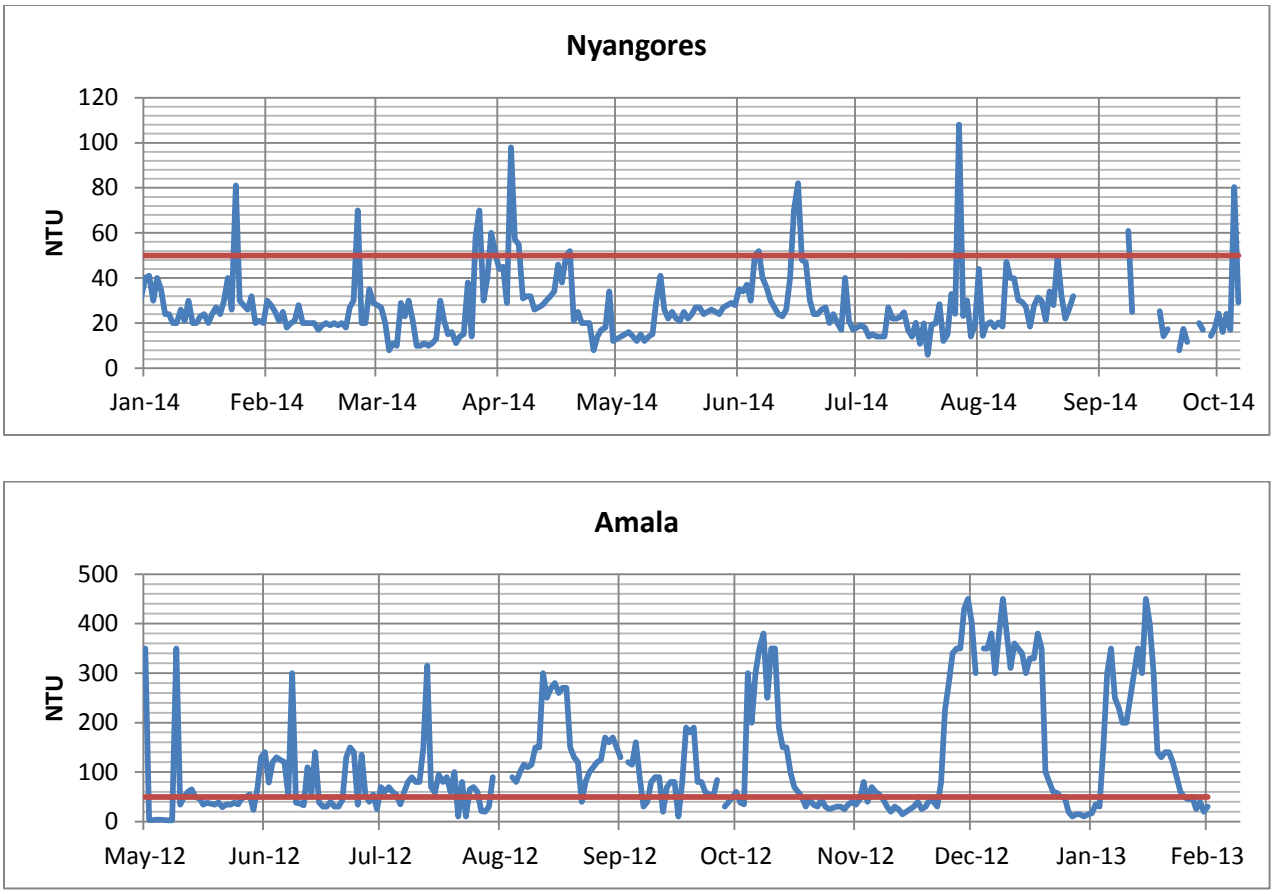

Figure 4-2: Turbidity in NTU measured in the Nyangores River at Bomet and in the Amala River at Mulot. The red line indicates the Kenyan standard of 50 NTU. In both tributaries there are large peaks however these are more extreme in the Amala River where the standard is exceeded almost continuously.

Turbidity data series in the entire catchment

The available turbidity data is used to analyse its spatial variability throughout the entire catchment. For this analysis data covering the entire year is selected for several stations from the dataset of Subalusky and McCartney. Then the average is calculated for each station and plotted as shown in see Figure 4-3. This plot shows that the average turbidity is around 45NTU in the northern part of the catchment. Further south before the confluence with the Talek tributary, the turbidity doubles and after the confluence it increases with a factor 8 at maximum. This relation between the sub-catchments is used while evaluating the model simulating the sediment transport.

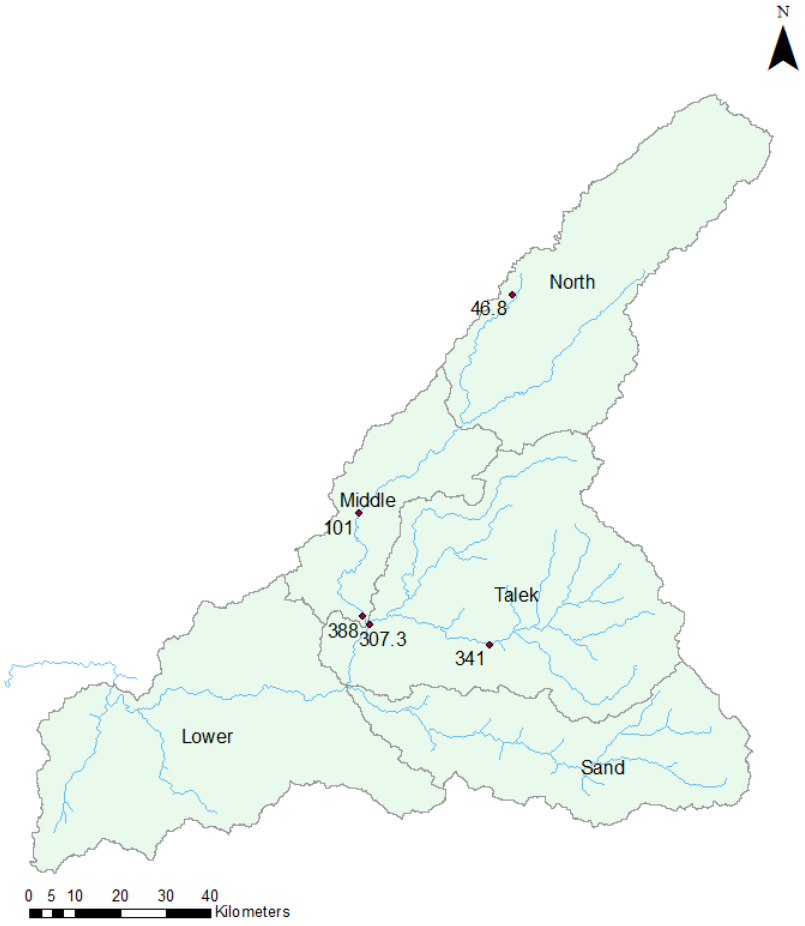

Figure 4-3: Average turbidity in the Mara River Basin

Conversion of turbidity data to sediment concentration

With this turbidity data of Kiragu, the sediment concentrations are estimated using a polynomial relation. Multiplication with the discharge then results in the sediment load which can be used as comparison tool to verify the model.

With the study of Kiragu data on the turbidity and sediment concentration is available from February to July 2007 for the tributaries Nyangores and Amala (Kiragu, 2009). Before converting this turbidity data to sediment concentrations, it is analysed to ensure its reliability regarding the following aspects:

- The devices' capacity should not be exceeded
- Outliers should be eliminated

For the dataset used, the devices capacity is not exceeded and there are no outliers. Furthermore, the relation between turbidity and concentration is only valid within the range of the available data. In this case it's for a turbidity between 50 and 300 NTU. Also, the relation is most reliable in the months in which the turbidity is measured, which is from February to July in this case.

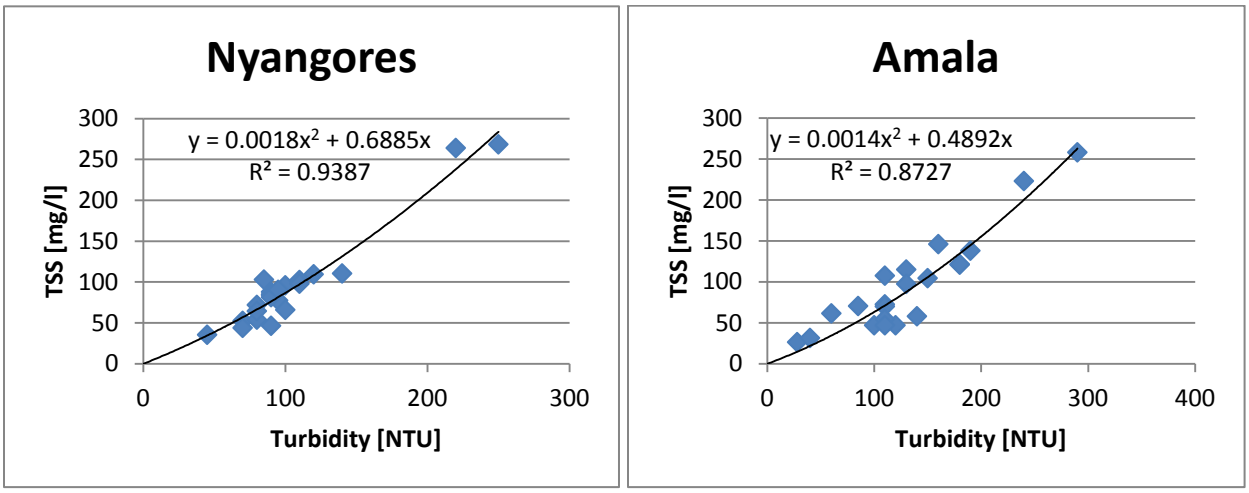

Figure 4-4: Estimation of the relation between turbidity and the sediment concentration TSS in the tributaries Nyangores and Amala using a polynomial relation

5. Total overview

The interview results, information from the SCMPs, field observations and data points are put together to obtain a general overview of the catchment as shown in Table 1-1. In general there are two main groups: croplands and Maasai land. In the first case, a lot of sheet erosion is observed while in the second case there are a lot of gullies in addition to sheet erosion from the overgrazed fields.

Table 5-1: General overview of the catchment

	Croplands	Maasai land
Main location	- Crop fields	- Grazing fields - Along roads and animal tracks
Problems	- Loss fertile soil - River pollution - Siltation	- Loss fertile soil - Gullies: threat for animals, decrease land area - Siltation
Causes	- Poor land use management - Encroachment riparian zone	- Overgrazing
Solutions	- Improved agricultural practices - Soil conservation practices - Forestation - Spring protection - River bank protection	- Improved agricultural practices - Soil conservation practices - Forestation - Spring protection - River bank protection - Block gullies - Reduce pressure - Construction of cut off drains, retention ditches and check dams

Appendix D: Classification

Table of contents

1. Methodology

The area is classified into different hydrological units based on the landscape and land cover. As each unit is expected to respond differently to rainfall, different model structures are created for each unit. Also, the parameters are expected to be different for each hydrological unit. This is taken into account through the choice of parameter ranges and by adding parameter constraints.

In each hydrological unit, different preferential flow paths are expected (Gao et al., 2013). For example subsurface flow is expected on the hill slopes with forest or shrubs whereas hortonian overland flow is expected on the hilly grasslands and cultivated land. To take such differences in dominant flow mechanisms into account, different model structures are applied for each hydrological unit.

2. Landscape classification

Based on the topography, the landscape is determined by using the slope (s) and the height above the nearest drain (HAND). In total, the landscape can be split into four classes: plateau/terrace, hill slope, sloped wetland and flat wetland. An area is characterized as plateau if it is flat, thus the slope is lower than a certain threshold value and located high above the ground water level thus the HAND is higher than a certain threshold. For hill slopes however, both the slopes and HAND are high (see Table 2-1). (Savenije, 2010)

Table 2-1: Characteristics regarding the slope and HAND for each landscape

Landscape	Characteristics for slope and HAND
Plateau/terrace	$s < s_{threshold}$ and $HAND > HAND_{threshold}$
Hill slope	$s > s_{threshold}$ and $HAND > HAND_{threshold}$
Sloped wetland	$s > s_{threshold}$ and $HAND < HAND_{threshold}$
Flat wetland	$s < s_{threshold}$ and $HAND < HAND_{threshold}$

The landscape depends on the chosen thresholds parameters; therefore the sensitivity of the catchment to these values is assessed in the next section. Based on this assessment in comparison with field observations, appropriate values are chosen for the thresholds to obtain the landscape classification of the Mara River Basin.

3. Sensitivity analysis on the threshold parameters in the landscape classification

In this section, the sensitivity of the Mara River Basin on the threshold parameters $s_{threshold}$ and $HAND_{threshold}$ are assessed. According to Gharari, the optimal values are found to be $s_{threshold}$ = 0.0129 and $HAND_{threshold}$ = 5.9 m for a central European meso-scale catchment based on statistical analyses (Gharari et al., 2011). For the sensitivity analysis, a range for both parameters is chosen:

- $0.001 < s_{threshold} < 0.25$
- $0 < HAND_{threshold} < 10$

For the lower and upper end of these ranges, extreme values are chosen to ensure the realistic values are included as well.

By changing these two parameters, their sensitivity is assessed:

- For the parameter $s_{threshold}$ an optimal value can be found as for hill slope and terrace, the area percentage approaches a certain value. Approximately for $s_{threshold}$=0.15 this asymptotic value is reached. For wetland, the area percentage is completely independent of $s_{threshold}$ as can be seen in Figure 3-1.
- For the parameter $HAND_{threshold}$, no optimal value can be found. The percentage of hill slope and terrace increases with $HAND_{threshold}$ while the percentage of wetland decreases (see Figure 3-2). However this increase or decrease does not behave asymptotically as $s_{threshold}$.

Based on this analysis, the parameter $s_{threshold}$ is chosen to be 0.15. The parameter $HAND_{threshold}$ is chosen to be zero as there are no wetlands with a significantly large area. Therefore based on the landscape classification, two classes can be distinguished: hill slopes and terraces Figure 3-3.

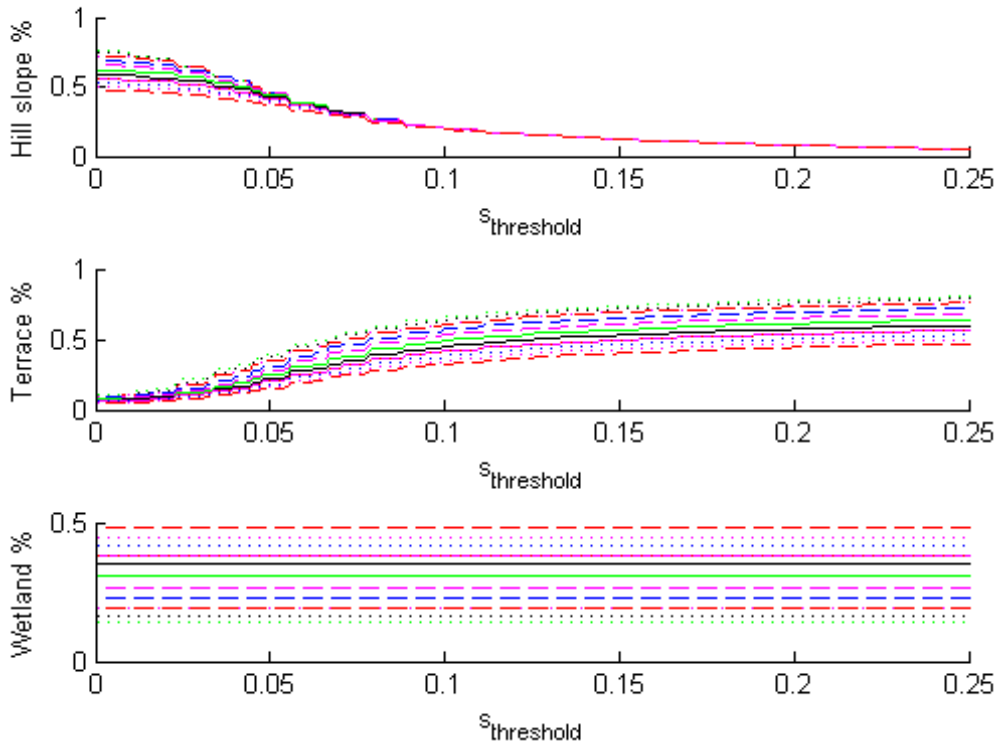

Figure 3-1: Sensitivity of the slope threshold

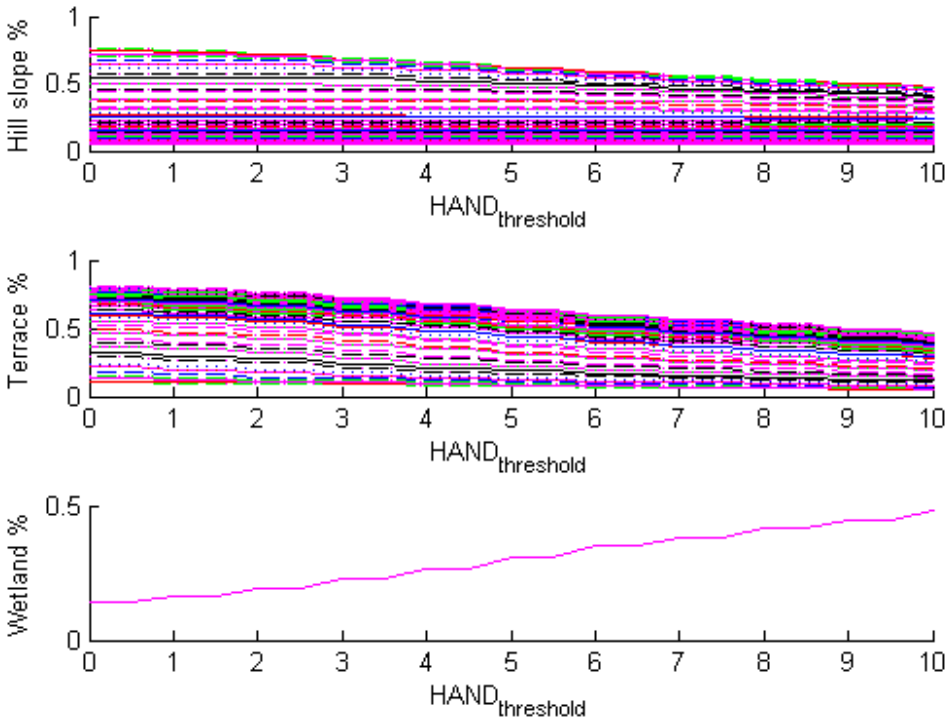

Figure 3-2: Sensitivity of the HAND (height above nearest drain) threshold

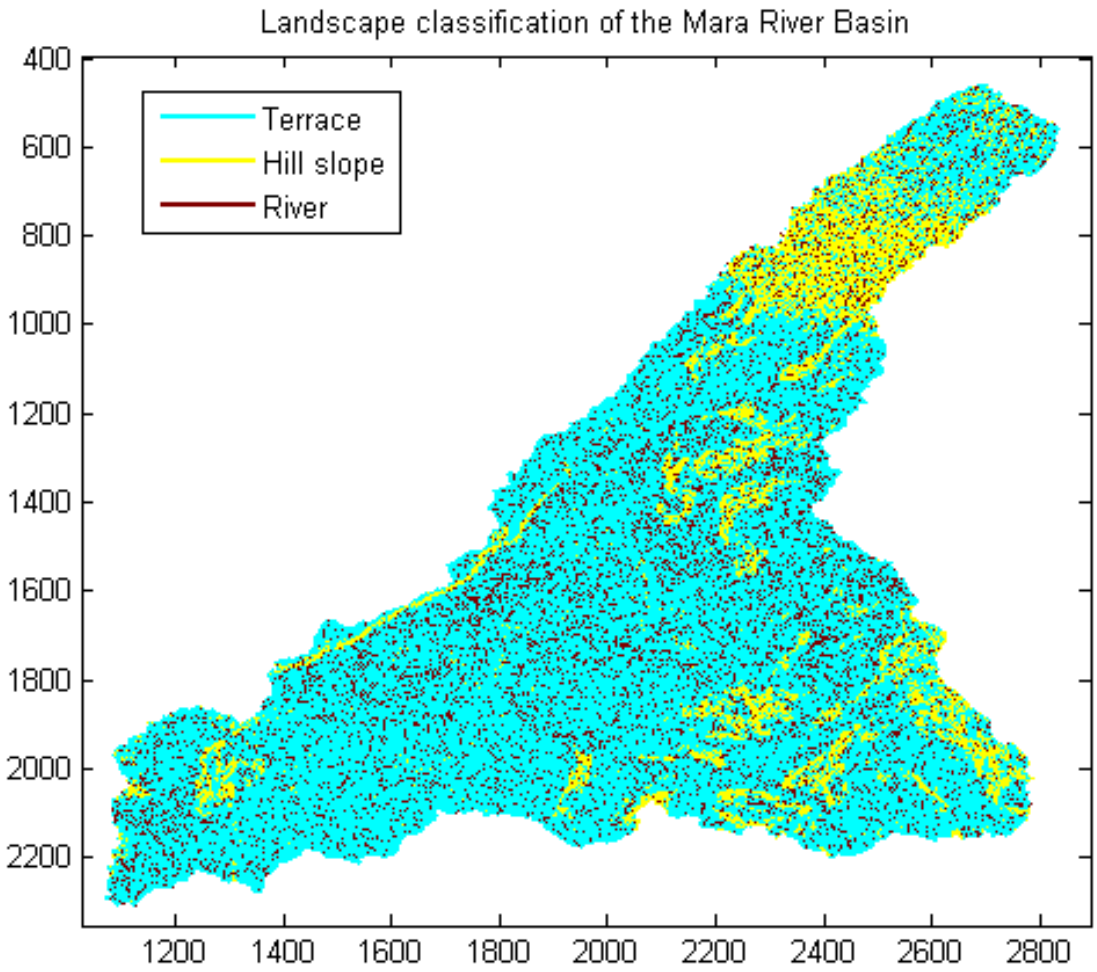

Figure 3-3: Landscape classification based on the slope alone

4. Land cover classification

For the land cover classification, product maps and a description formulated by the Ministry of Foreign Affairs are taken into consideration.

4.1.Land cover product maps

Three different products are compared with each other to assess their suitability as also the land cover changes in the past. The products taken under consideration are: Africover, Global Land Cover and Globcover; see Table 4-1 for the product specification.

Table 4-1: Product map specifications

Product name	Year	Resolution/grid size	Source	Source
Africover	1998	1:200,000	Derived from LANDSAT TM images, confirmed with field data	FAO
Global Land Cover	2000-2007	Year 2000: 1 km Years 2001-2007: 0.5 km	Derived from EGA2000 dataset acquired by the VEGETATION instrument	DAAC (Distributed Active Archive Center for Biogeochemical Dynamics)
Globcover	2005, 2009	300 m	Derived from MERIS FR mosaics (Medium Resolution Imaging Spectrometer Instrument; Fine Resolution)	ESA (European Space Agency)

Since the land cover maps are derived differently for each product type, inconsistencies can occur with the definition of the land cover classes. Therefore, the mosaic classes for example are defined slightly differently for each product resulting in unrealistic developments. That is why a detailed comparison of the maps is not possible. However, through a rough comparison of the maps, past land use changes are estimated.

A visual comparison of the maps shows (see Figure 4-1 and Figure 4-2):

- General deforestation, especially in the north, but also lower catchment
- Increased cultivated areas , especially in the north
- Forestation in the lower and middle catchment between 1998 and 2000 (unrealistic)
- Increased herbaceous areas and decreased mosaic croplands from 1998 to 2000 and from 2005 to 2009; possibly due to a change in the class definition even within the product Globcover

These trends are also found when analysing the land cover distribution shown in Table 4-2. In the remaining part of the study, the map Africover is used as it's based not only on satellite data, but also on field data which is confirmed during the field visit.

Table 4-2: Land cover distribution in the Mara River Basin

	Cropland	Mosaic crop	Forest	Herbaceous	Shrubs	Other
1998 Africover	8%	9%	22%	40%	16%	5%
2000 Global Land Cover	13%	3%	26%	26%	32%	0%
2005 Globcover	11%	58%	18%	3%	10%	1%
2009 Globcover	9%	49%	15%	17%	8%	1%

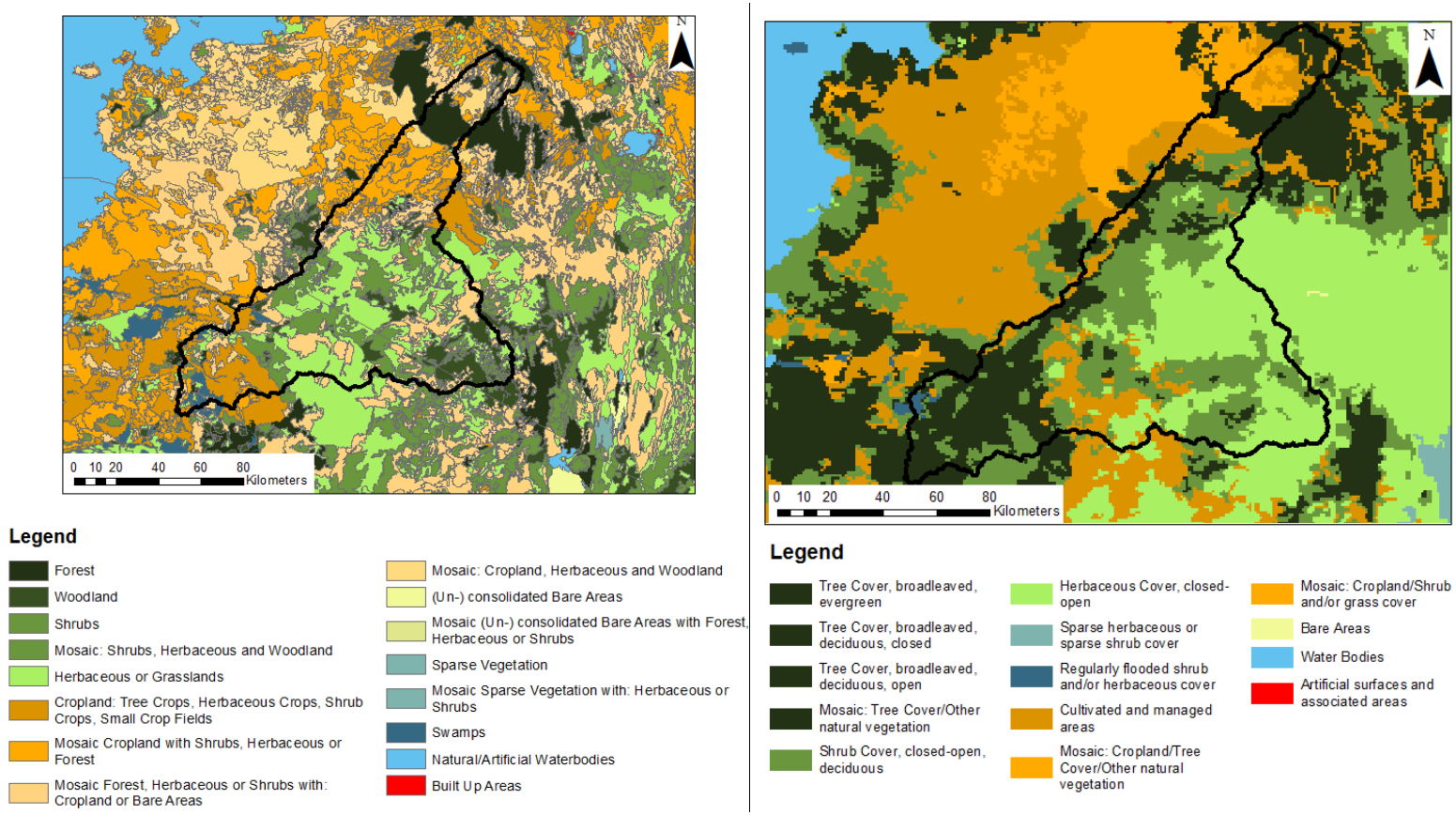

Figure 4-1: Land cover maps: Africover (left) and Global Land Cover (right)

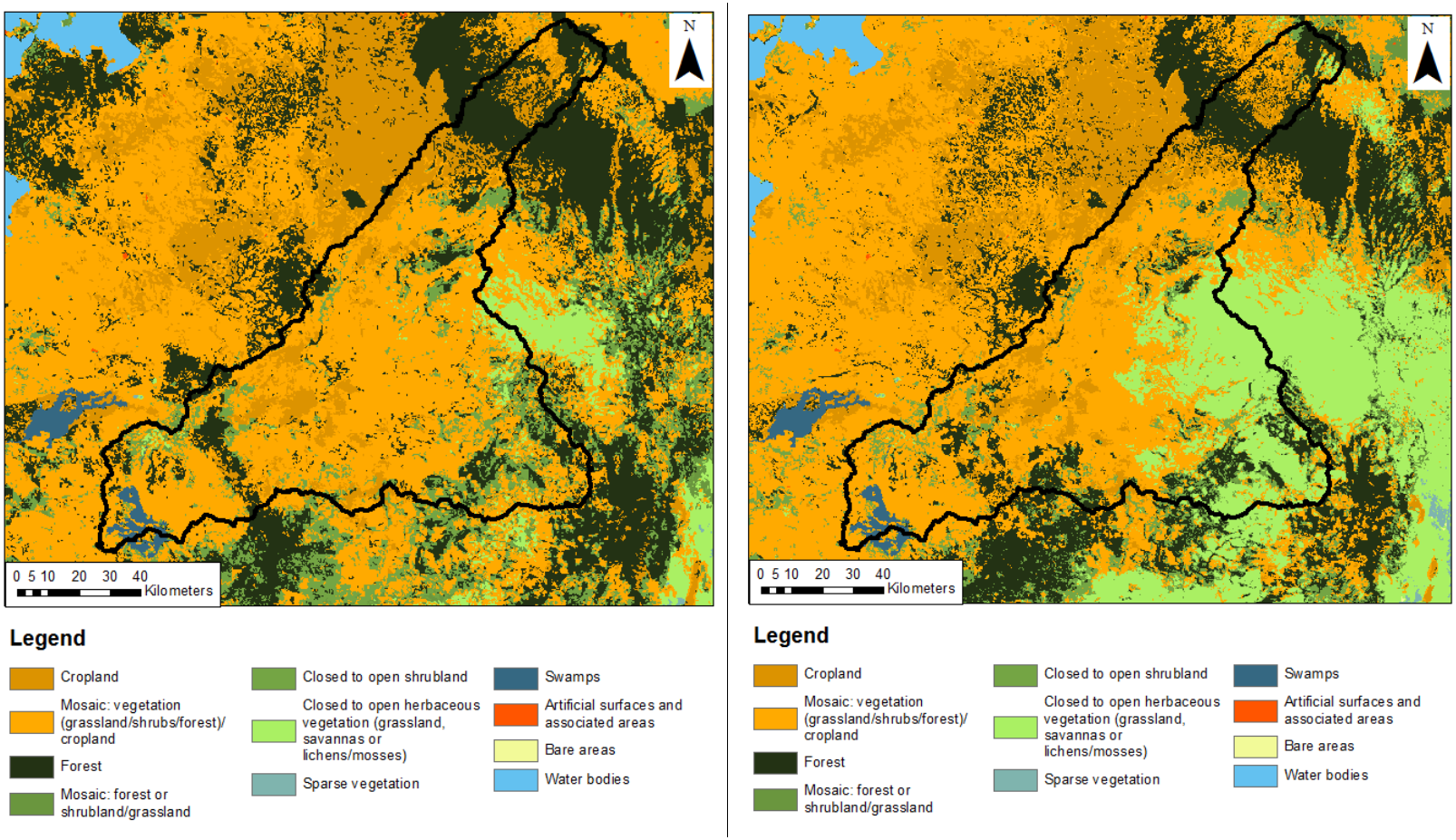

Figure 4-2: Land cover maps: Globcover 2005 (left) and 2009 (right)

4.2.Current land cover according to the Ministry of Foreign Affairs

The current land uses according to the Dutch Ministry of Foreign Affairs, are stated in Overview 4-1 (Ministry of Foreign Affairs, 2013); see also Figure 4-3 for the location of each elevation class mentioned in the overview.

As can be seen with the areas for the nature reserves, this is merely a rough classification based on elevation classes. Compared with the product maps, this classification confirms the existence of agriculture and forest in the north and shows that the cultivated areas are spread over the entire catchment except where the Mau forest and nature reserves are located.

Overview 4-1: Current land uses according to the Dutch Ministry of Foreign Affairs (Ministry of Foreign Affairs, 2013)

Upper catchment:

- 2932 – 2400 m above mean sea level: Deforested and degraded agricultural land. Frost occurs several times per year. Outside Mau Forest complex but marginal agricultural land.
- 2200 – 2400 m above mean sea level: Forest reserve of Maasai Mau Forest block. Relatively intact forest, bound by 50 m wide strips of tea plantations owned by the Moi family.
- 1800 – 2200 m above mean sea level: Small scale farms. Farm size 2-3 acres, being subdivided. High soil erosion resulting in high silt loads in the rivers (Nyangores: 162 tonnes of soil per year is lost, more in the Amala river).

Middle catchment:

- 2200 – 1700 m above mean sea level: Large wheat farms (>10.000 ha), characterized by leased lands, high erosion rates, use of pesticides and loss of grazing land. Irrigation is coming up.
- 1700 m above mean sea level: private conservancies, grazing land. Risk of degradation because of overgrazing.
- 1700 – 1500 m above mean se level: protected area of Maasai Mara Reserve and Serengeti National Park (Tanzania). There are about 200 tourist facilities in and near the protected areas, most without any water treatment.

Lower catchment (Tanzania):

- 1500 - 1134 m above mean sea level: dry lands and Mara wetland. The wetland is expanding due to siltation. Also some encroachment leading to conversion of wetland to agricultural land. There are plans to construct an irrigation scheme in this area.

Source: Ministry of Foreign Affairs, 2013

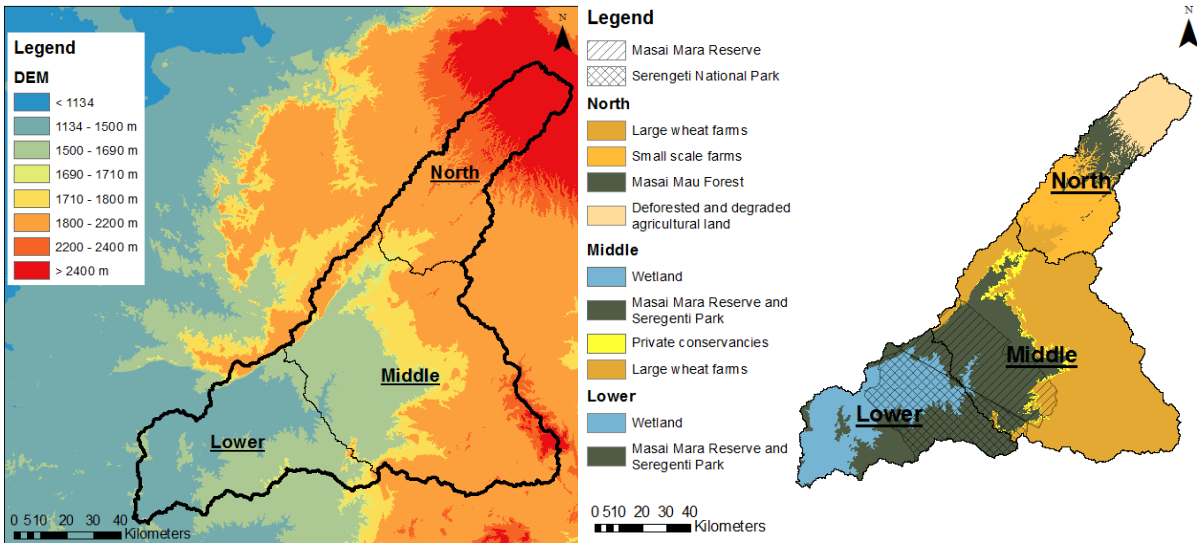

Figure 4-3: Digital elevation map (SRTM) with elevation classes (left) and land use classification (right) according to the Dutch Ministry of Foreign Affairs

5. Classification results

Based on the landscape classification, two distinct classes are found: hill slopes and terraces. Based on the land cover classification using the map Africover, four types are distinguished: cropland, grassland, shrub land and forest. A comparison of both classification shows that there is a high resemblance: forests are found on hill slopes as also shrubs whereas grasslands are mainly found terraces. Croplands are found on both sloped and flat areas.

Using both the landscape and land cover classification results, four hydrological units are defined for the remaining of the study:

- Forests steep slopes
- Shrubs on steep slopes
- Grasslands on flat slopes
- Cultivated land

In Figure 3-2, the final classification for the Mara River Basin is shown graphically and in Table 4-1 the area percentage of each hydrological unit in a sub-catchment. This classification is also applied to the catchments of the tributaries Nyangores and Amala (see Table 5-2).

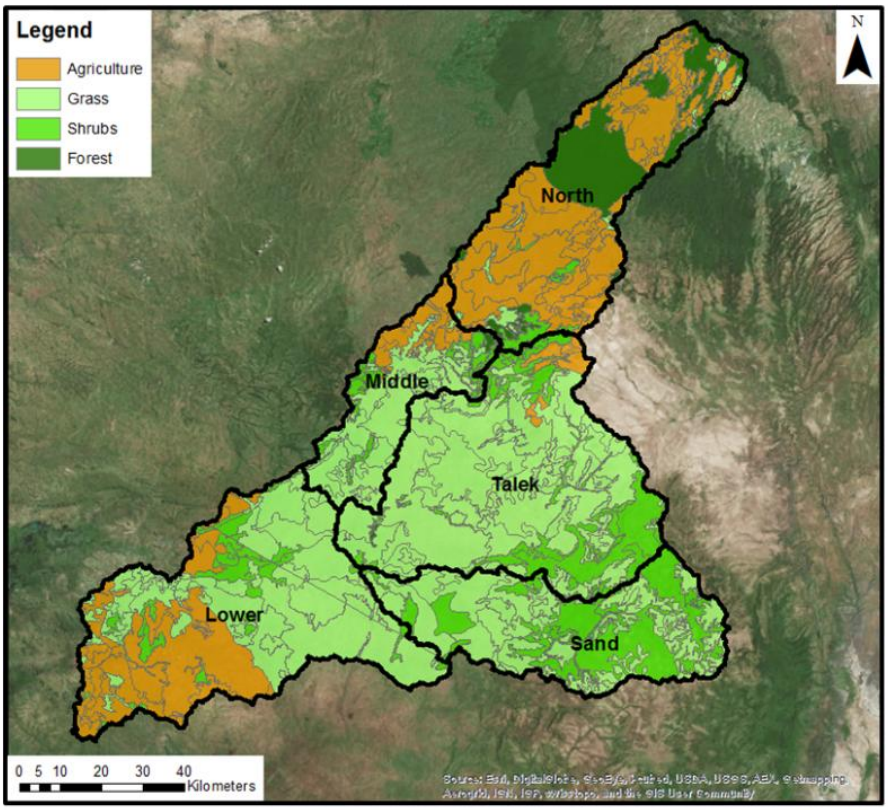

Figure 5-1: Classification of the Mara River Basin into four hydrological units

sTable 5-1: Classification results: area percentage of each hydrological unit per sub-catchment in the Mara River Basin

	Crops	Shrubs	Grass	Forest
North	73%	0%	0%	27%
Middle	19%	16%	65%	0%
Talek	0%	21%	79%	0%
Sand	0%	42%	58%	0%
Lower	26%	23%	52%	0%

Table 5-2: Classification results: area percentage of each hydrological unit within the catchments Nyangores and Amala

	Crops	Shrubs	Grass	Forest
Nyangores	53%	0%	0%	47%
Amala	63%	0%	0%	37%

Appendix E: Hydrological modelling

Table of Contents

1. Model choice

In general, the different types of models can be classified based on two aspects:

1. The model is lumped or (semi-) distributed; as shown in Table 1-1 a lumped is fast and easy with no internal information whereas a distributed model is slow, shows equifinality, but does include internal information. A semi-distributed is a combines of these two types.
2. The model is empirical, conceptual, process based or stochastic; as shown in Figure 1-1 the complexity, data requirements and calculation time increase for each model type.

For this study, a topography driven conceptual the model called FLEX-Topo will be applied which is a semi-distributed model. In this model, a limited number of landscapes are distinguished based on the topography. Each landscape class is then represented by a lumped conceptual model. The advantage of the model is the limitation of the amount of parameters compared to distributed models and the addition of internal information compared to fully lumped models.(Savenije, 2010)

Table 1-1: Comparison of lumped, distributed and semi-distributed models

	Lumped	Distributed	Semi-distributed
Advantages	Fast, easy	Includes distributed data sources and results	Includes distributed data sources, fast
Disadvantages	No internal information	Slow, equifinality	Little internal information, equifinality possible

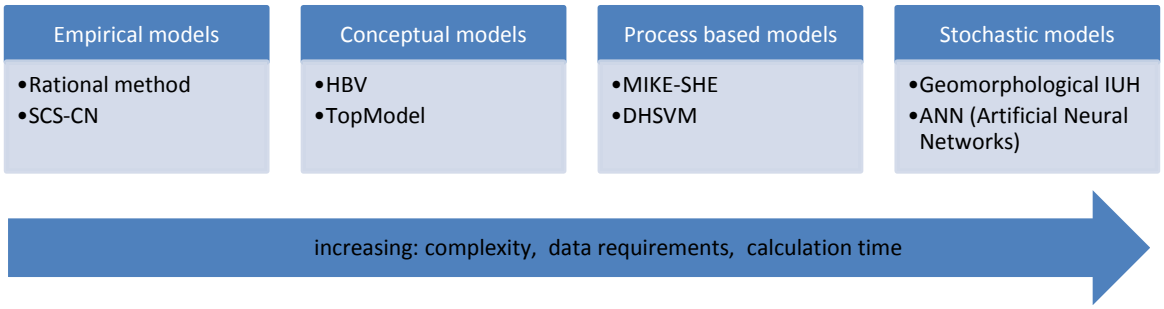

Figure 1-1: Overview of the different model types

2. Model methodology

In short, the following steps are taken to set up a hydrological model:

3. Data collection
    a. Digital elevation map (DEM)
    b. Land cover maps from different years
    c. Precipitation data series
    d. Water level data series
    e. Discharge data series
    f. Temperature data series
4. Data analysis
    a. Land cover maps from different years need to show a logical development in land cover change; for example agricultural area is expected to increase, not decrease in time
    b. Precipitation data series from different stations need to correlate with each other
    c. Precipitation data from satellite images may be used if station data sees shows to be lacking for a certain time period, however the quality of satellite data needs to be estimated using station data series for other and available time periods
    d. Water level and discharge need to correlate with each other, otherwise the discharge will be calculated based on water level time series by making a new rating curve
5. Classification into hydrological response units. These are areas that are expected to respond similarly.
    a. Classify the catchment into different landscapes, for example plateau, hill slope, terrace and wetland using a digital elevation map
    b. Classify the catchment into different land covers with the help of an existing land cover product
    c. Divide the catchment into different hydrological units based on the landscape and land cover.
6. Set up the hydrological model
    a. Define the model structure for each hydrological unit
    b. Estimate as much parameters as possible to limit the number of calibration parameters
    c. Limit the ranges of each calibration parameter
    d. Define parameter and process constraints
7. Run, evaluate and improve the model
    a. Model the hydrological system for each HRU
    b. Check whether modelling results are logical and adjust the model structure if necessary. Control it by checking the hydrograph, flow duration curve, water balance, total evaporation compared to measured actual evaporation and each individual discharge component, thus the fast runoff for each class and the groundwater flow
    c. Validate the model using a data series set of a different time span of for a different location

3. Process constraints

The process constraints applied to the total runoff, evaporation and groundwater recharge. First each constraint is explained, then their impact is analysed.

Constraints based on the Budyko curve

With the Budyko curve, the annual average runoff R_{mean} and evaporation E_{mean} are estimated using only rainfall data; see Table 4-5 for the results. The following formula is applied:

$$\frac{E}{P} = 1 - \exp\left(-\frac{E_p}{P}\right) = 1 - \frac{R}{P}$$

Hence the runoff and evaporation can be estimated with:

$$R = P * \exp\left(-\frac{E_p}{P}\right)$$

$$E = P * (1 -* \exp\left(-\frac{E_p}{P}\right))$$

The modelled runoff Q_m and evaporation E_m on annual scale should close to the estimation based on the Budyko curve. As the modelled results won't be exactly the same as the estimations, a range is applied using the standard deviation as shown with the formulas below.

$$\mathrm{R_{mean}} - 5 * \mathrm{R_{std}} < \mathrm{Q_{m,mean}} < \mathrm{R_{mean}} + 5 * \mathrm{R_{std}}$$
$$\mathrm{E_{mean}} - 5 * \mathrm{E_{std}} < \mathrm{E_{m,mean}} < \mathrm{E_{mean}} + 5 * \mathrm{E_{std}}$$

Table 3-1: Estimated runoff and evaporation for each sub-catchment based on the Budyko curve: mean and standard deviation

Sub-catchment	R_{mean}	R_{std}	E_{mean}	E_{std}
North	0.23	0.08	779.64	96.46
Middle	0.30	0.10	766.06	107.52
Talek	0.18	0.07	824.59	92.67
Sand	0.22	0.07	917.61	89.61
Lower	0.23	0.03	856.98	32.80

Constraint based on the NDVI

In forested areas, more evaporation is expected than in grasslands. This evaporation is assumed to be a linear function of the NDVI (Gao et al., 2013). Hence, the relation between the evaporation in forests and in grasslands is equal to the relation between their NDVI:

$$\frac{E_{forest}}{E_{grassland}} = \frac{a * NDVI_{forest}}{a * NDVI_{grassland}} = \frac{NDVI_{forest}}{NDVI_{grassland}}$$

Therefore, the evaporation in each HRU is constraint based on their mean NDVI and the standard deviation:

$$\left(\frac{NDVI_i}{NDVI_j}\right)_{mean} - 5 * \left(\frac{NDVI_i}{NDVI_j}\right)_{std} < \frac{\Sigma E_i}{\Sigma E_j} < \left(\frac{NDVI_i}{NDVI_j}\right)_{mean} + 5 * \left(\frac{NDVI_i}{NDVI_j}\right)_{std}$$

The indices i and j indicate two different HRUs. $NDVI_{mean}$ is equal to the temporal average and $NDVI_{std}$ the standard deviation in 2014 averaged over the catchment; see Table 4-6 for the numerical results.

Table 3-2: Results on the estimation of $NDVI_{mean}$ and $NDVI_{std}$

Hydrological unit	$NDVI_{mean}$	$NDVI_{std}$
Forest	0.7365	0.0662
Shrubs	0.5352	0.0559
Cropland	0.5838	0.0433
Grassland	0.4936	0.0679

Groundwater recharge

The groundwater recharge in forests and shrub lands are expected to be larger than in croplands and grasslands. Hence, the following constraints are applied:

- $R_{s,F} > R_{s,C}, R_{s,G}$
- $R_{s,S} > R_{s,C}, R_{s,G}$

Fast runoff infiltration

In the Sand sub-catchment, a large fraction of the fast runoff is expected to infiltrate through the river bed into the groundwater system. Therefore, only during very heavy rainfall, runoff in the river is observed. This occurs only a few times a year. During the remaining rain events, the water is infiltrated recharging a sub-surface river system.

This observation is included as a constraint. The number of large storms causing runoff in the river should be less than 5. A storm is considered large as soon as the runoff is larger than 2 mm/d. Hence, the constraint is: $Nr_{Q_{f,storm>Q_{peak}}} < 5$

4. Parameter estimation

4.1.1. Storage capacity in the unsaturated zone $S_{u,max}$

The storage capacity in the unsaturated zone is equal to the amount of water stored in the root zone depth by plants to avoid stress during dry periods. Therefore, by studying the water usage of vegetation, the required amount of water to overcome a typical dry period is estimated. It is then assumed that plants naturally store that amount of water to survive such droughts and that this quantity is equal to storage capacity $S_{u,max}$. (Gao et al., 2014)

For the calculation of the storage capacity, first the water demand in a dry season is determined as a function of the long-term water demand, NDVI and the NDVI in a dry season assuming a linear relation between E_{td} /E_{ta} and $NDVI_D$/$NDVI_A$ as shown in the formulas below. The long-term water demand E_{ta} is calculated by subtracting the discharge from the effective rainfall.

$$P_e = P - E_i$$

$$\frac{E_{td}}{E_{ta}} = \frac{NDVI_D}{NDVI_A} \; thus \; E_{td} = E_{ta} * \frac{NDVI_D}{NDVI_A}$$

$$E_{ta} = P_e - Q$$

With:

- P precipitation [mm/d]
- P_e effective precipitation [mm/d]
- E_i interception threshold, set to 2 mm/d [mm/d]
- E_{td} water demand in dry season [mm/d]
- E_{ta} long-term average annual plant water demand [mm/d]
- $NDVI_A$ long-term average annual NDVI
- $NDVI_D$ NDVI in dry season

For the precipitation, stations are spatially distributed by creating a Thiessen Network (see Figure 4-1). For the actual evaporation, satellite data is used.

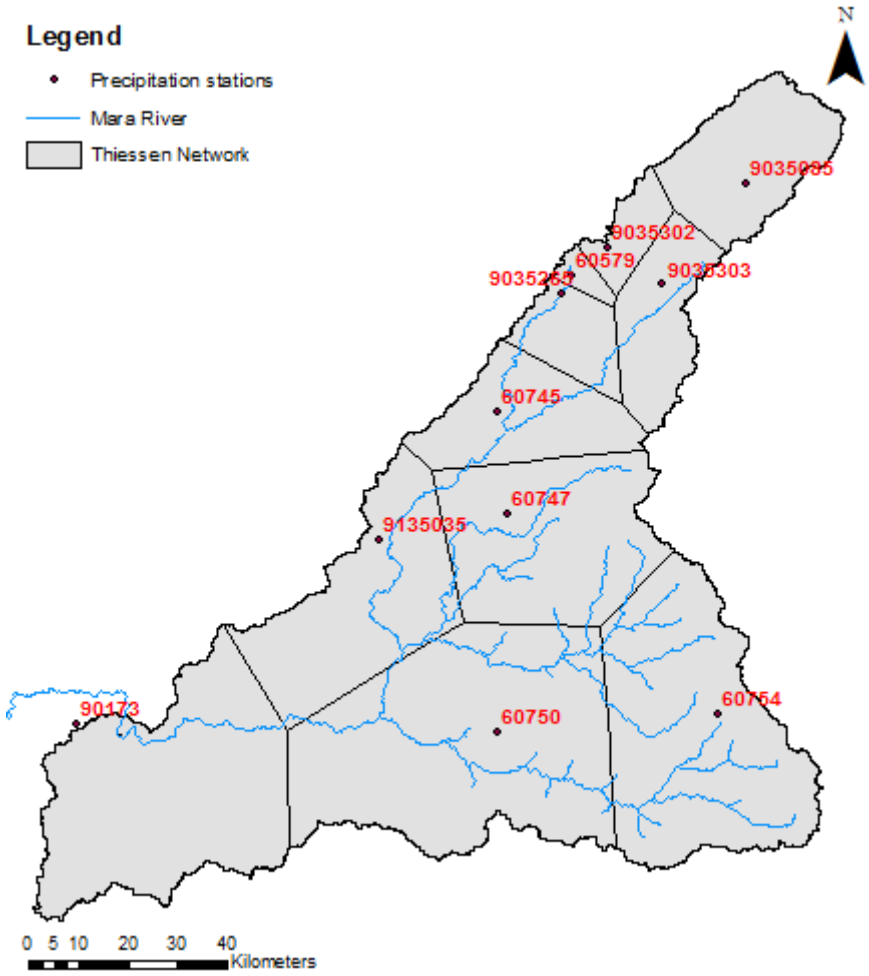

Figure 4-1: Thiessen network of the precipitation stations

Then, the cumulative effective rainfall P_e which is the water inflow and the water demand E_{td} are plotted. The required storage is determined for each year based on the maximum water stress when the demand exceeds the inflow (see Figure 4-4). Through a statistical analysis using the Gumbel distribution, the storage capacity S_R with a return period of 20 years is calculated; see Overview 4-1.

With this method, the maximum storage capacity is calculated for each cell in the MRB. For each HRU, the average over the entire MRB is calculated. This is the parameter S_R used in the model:

- Forested hill slopes : 122 mm
- Agriculture : 94 mm
- Shrubs on hill slopes : 89 mm
- Grass : 83 mm

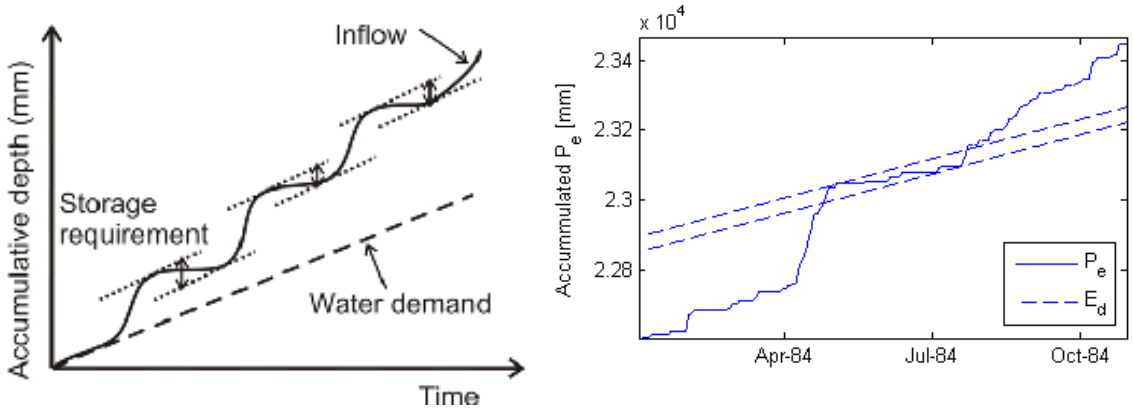

Figure 4-2: Cumulative plot of the inflow which is the effective rainfall P_e and the water demand which is the long-term average dry season water demand E_d. Schematization (left) and application to precipitation station 9035085 in the sub-catchment North (right).

Overview 4-1: Statistical analysis: Gumbel distribution

For each season, the required storage is calculated. With this dataset, a statistical analysis is done to determine the storage capacity with a return period of 20 years. First, the reduced variate y is calculated for each data sample using its return period using the formula:

$$y = -\ln\left(-\ln\left(1 - \frac{1}{T}\right)\right)$$

This reduced variate is a function of the sample data X and two coefficients a and b:

$$y = a * (X - b)$$

$$a = \frac{s_y}{s}$$

$$b = X_m - s * \frac{y_m}{s_y}$$

With:

- y : reduced variate
- y_m : mean value of the reduced variate
- X : value of the sample
- X_m : mean sample value
- s : standard deviation of the sample
- s_y : standard deviation of the reduced variate

Now, the two coefficients a and b are calculated to determine the sample value X with T=20 years. This is the storage capacity S_R.

4.1.2. Reservoir coefficient Ks

The reservoir coefficient for slow runoff K_s is estimated by studying the hydrograph of the catchment during low flows. During these periods, only the slow flows contribute to the river flow and there is no inflow into the groundwater which is the slow flow reservoir S_s. Thus as indicated with the formulas below, the reservoir coefficient is the slope of the discharge in a log scale during dry periods. For the Mara River Basin, this parameter is estimated to be 28 d.

$$Q = Q_s = \frac{dS_s}{dt}$$

$$S_s = -K_s * Q_s$$

$$Q_s = -\frac{d(K_s * Q_s)}{dt}$$

$$Q_s = \mathrm{Q_{t=0}} * \exp\left(-\frac{t}{K_s}\right)$$

$$\ln(Q_s) = \ln(Q_{t=0}) + \ln\left(\exp\left(-\frac{t}{K_s}\right)\right)$$

The substituting $\log(Q_s)$ with y, $\log(Q_{t=0})$ with C and $\log(e^{-t/Ks})$ with a*t yields a general formula for the trend line with slope a:

$$y = C + a * t$$

Hence, the slope is equal to:

$$a * t = \log\left(\exp\left(-\frac{t}{K_s}\right)\right) = -\frac{t}{K_s} * \log(\exp(1))$$

$$a = -\frac{1}{K_s} * \log(\exp(1))$$

Therefore, the parameter K_s is equal to:

$$K_s = -\frac{1}{a} * \log\left(\exp(1)\right)$$

The average slope of the trend lines is found to be -0.016 resulting in K_s= 28 d.

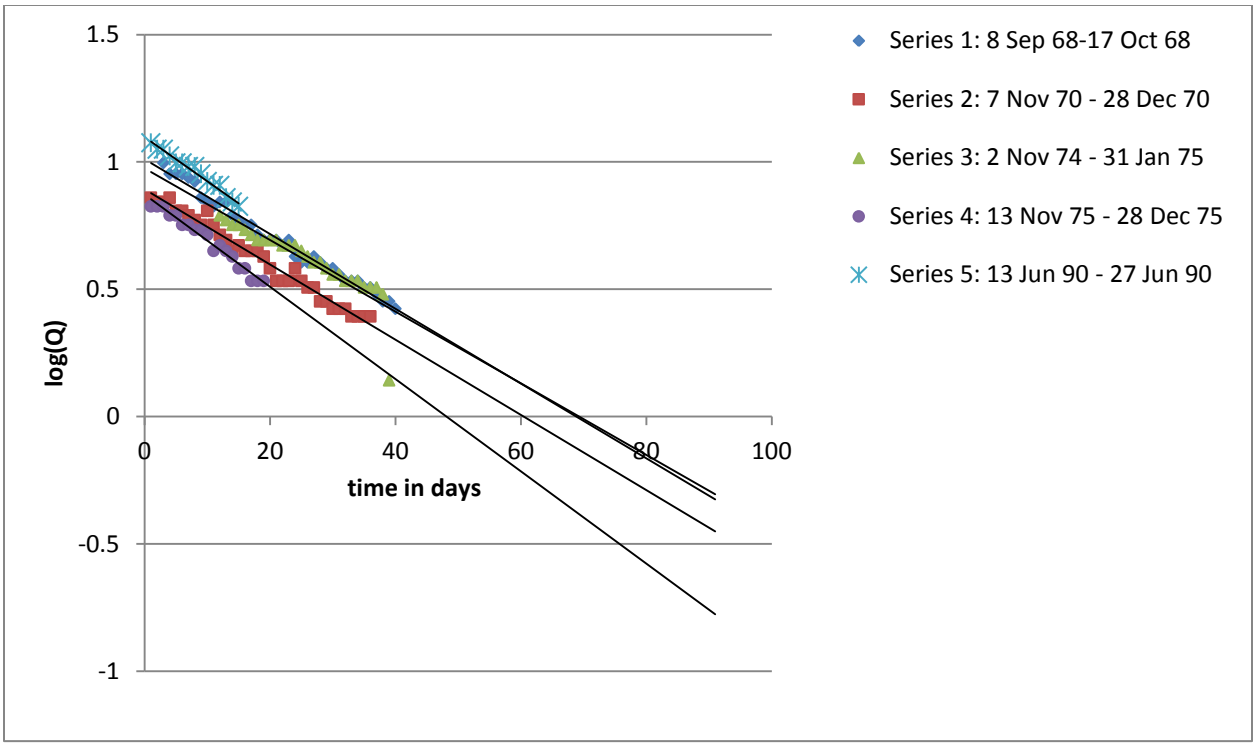

Figure 4-3: Plot of the discharge in logarithmic scale for five dry periods. Each section starts at t=0.

4.1.3. Maximum surface water storage in pools S_{max}

In the grasslands and cultivated areas, part of the water cannot infiltrate due to rainfall intensities exceeding the infiltration capacity. At first, this water is stored on the surface in pools and sinks. Only when this storage capacity is exceeded, hortonian overland flow takes place. This storage capacity is estimated with an elevation map. With this map, a flow direction map is built and sinks are located. Each sink has a certain volume equal to the height difference multiplied with the number of cells and the grid size. This volume divided through the sub-catchment area results in the storage capacity S_{max}. In In the grasslands and cultivated areas, part of the water cannot infiltrate due to rainfall intensities exceeding the infiltration capacity. At first, this water is stored on the surface in pools and sinks. Only when this storage capacity is exceeded, hortonian overland flow takes place. This storage capacity is estimated with an elevation map. With this map, a flow direction map is built and sinks are located. Each sink has a certain volume equal to the height difference multiplied with the number of cells and the grid size. This volume divided through the sub-catchment area results in the storage capacity Smax. In Table 4-4, the parameter values are shown for each sub-catchment.

Table 4-4 the parameter values are shown for each sub-catchment.

Table 4-1: Maximum surface water storage capacity

Sub-catchment	Maximum surface water storage capacity S_{max} [mm]
North	35
Middle	53

Talek	49
Sand	16
Lower	26

5. Model calibration and validation

For the determination of the remaining parameters, the model is calibrated and validated. In the calibration step, a large amount of parameter combinations within the defined constraints are selected randomly applying the Monte Carlo method. Using a precipitation and temperature time series as input, each combination is run through the model to calculate the total runoff which is the model output. This simulated runoff is then compared with the observation using objective functions to evaluate the performance of each parameter set. Then by applying the MOSCEM-UA algorithm, offspring are generated to find parameter sets with a better performance. Finally, the parameter set with the best performance is selected and used for validation.

The applied objective functions are:

$$NS_{FDC} = 1 - \frac{\sum(FDC_{obs} - FDC_{sim})^2}{\sum\left(FDC_{obs} - mean(FDC_{obs})\right)^2}$$

$$NS_{\log(FDC)} = 1 - \frac{\sum(\log(FDC_{obs}) - \log(FDC_{sim}))^2}{\sum\left(\log(FDC_{obs}) - mean\left(\log(FDC_{obs})\right)\right)^2}$$

In the objective functions, the observed flow duration curve (FDC) is compared with the modelled one. In the second formula, the logarithm of the FDC is taken before calculating the Nash Sutcliffe (NS) value. With these two objective functions, the flow duration curve is evaluated based on high and low flows.

6. Model results

In this section, the modelling results are presented. First, the calibration and validation results are shown. Then, the improvement caused by splitting the catchment into HRU and sub-catchments will be demonstrated. The resulting values for the objective functions and calibration parameters for all model runs are put together in a table in section '6.6 Overview model results'.

6.1. Model results for the Mara River Basin

As shown in Figure 4-5, the model performs well in both the calibration and validation. Also the slope of the hydrograph during low flows in similar in both the observation and simulation (see Figure 6-2) which implicates that the reservoir coefficient for the slow runoff K_s is estimated well. During the calibration, the model does not simulate the abrupt increase in the high flows or the sudden decrease in the low flows. Also, the validated model simulates the high flows better, but the low flows worse.

With the dot plots, it is possible to assess whether the calibrated parameters are clearly defined. If none of the parameters are defined well, then equifinality can be expected. As shown in Figure 4-7, all parameters except for T_{lag} and S_{smax} are well defined; the one more clear than the other though.

The model also performs well when switching up the data series: hence the data series originally used for validation is now used for calibration and vice versa; see Figure 6-4 and Figure 6-5.

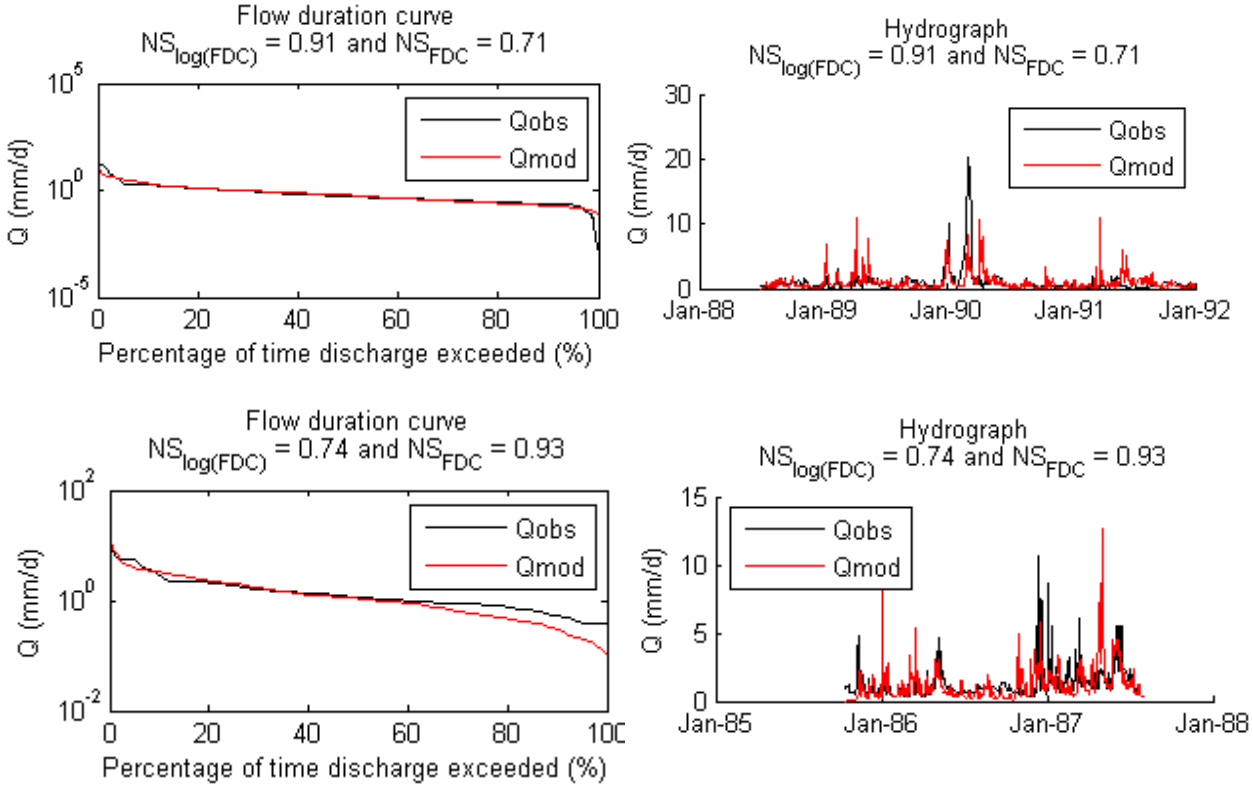

Figure 6-1: Calibration (upper) and validation (lower) results for the Mara River Basin: flow duration curve (left) and hydrograph (right)

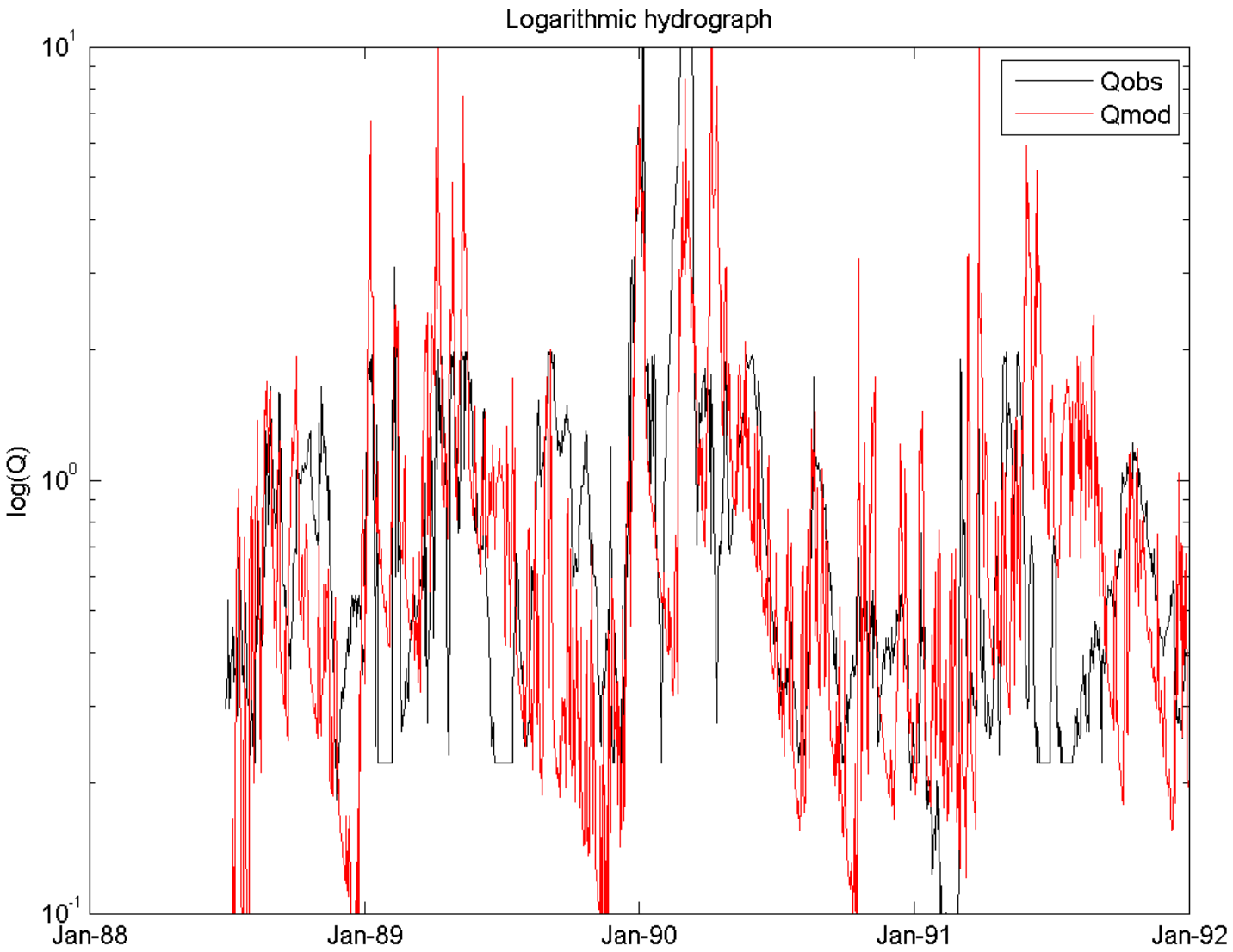

Figure 6-2: Logarithm of the hydrograph

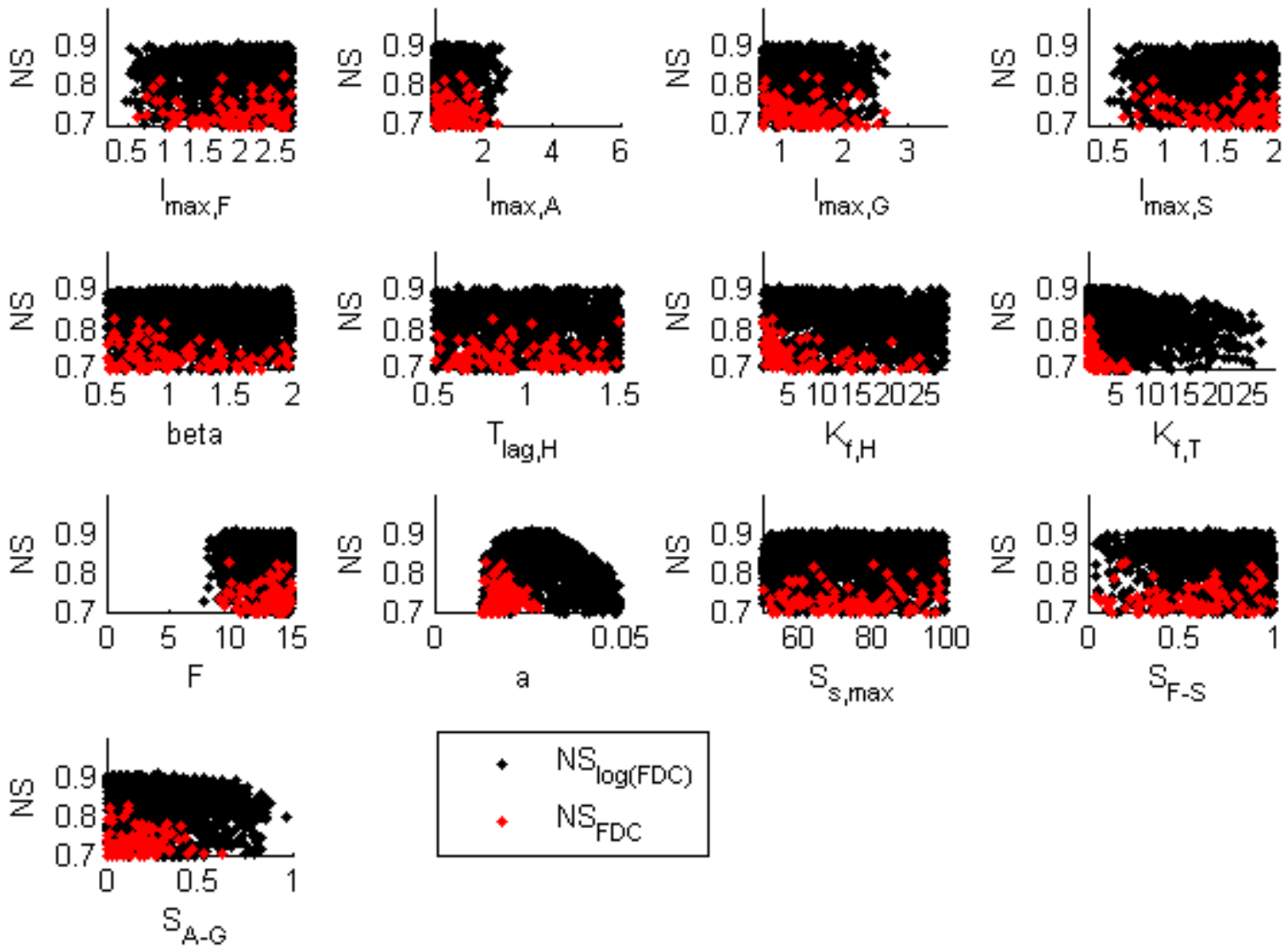

Figure 6-3: Dot plots for all calibrated parameters for the Mara River Basin. The minimum and maximum value on the horizontal axis is equal to the defined parameter boundaries for the calibration

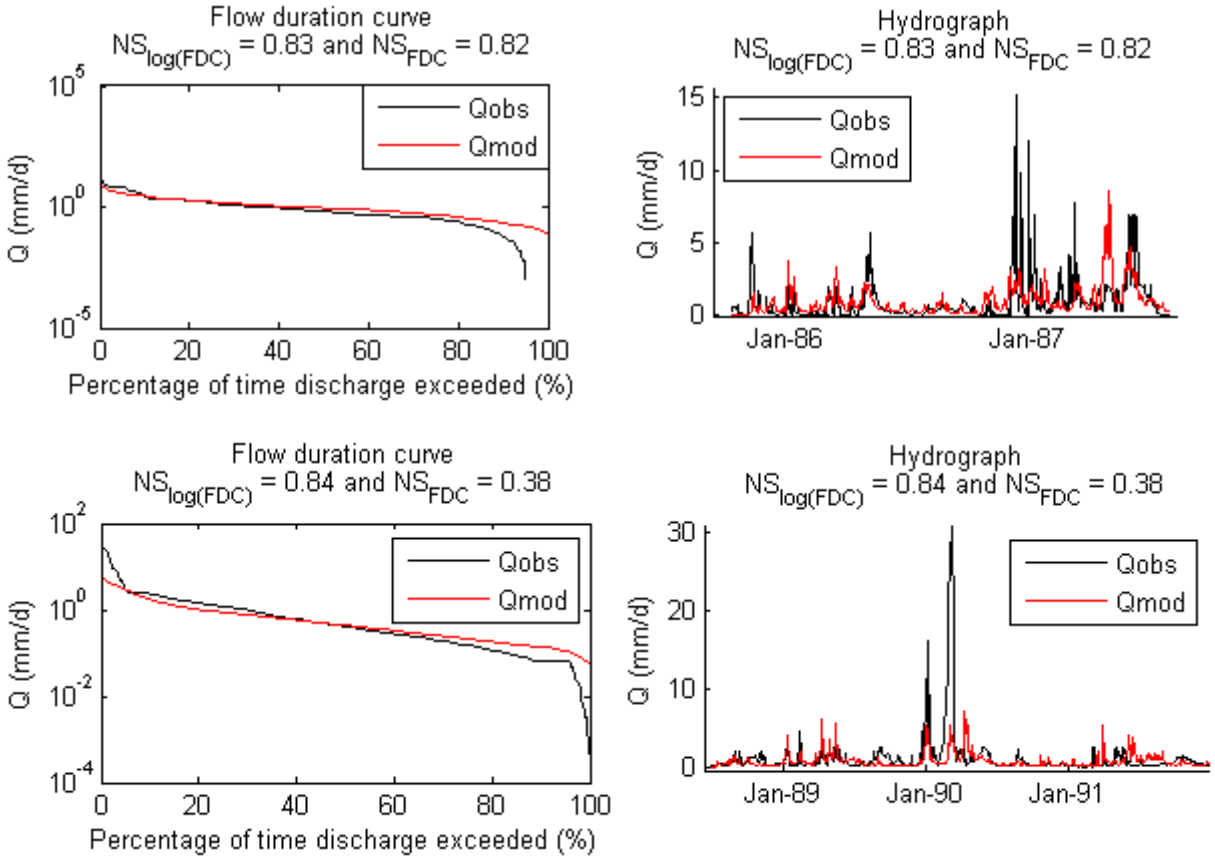

Figure 6-4: Calibration (upper) and validation (lower) results for the Mara River Basin: flow duration curve (left) and hydrograph (right) with new data series. The data series originally used for validation is now used for calibration and vice versa.

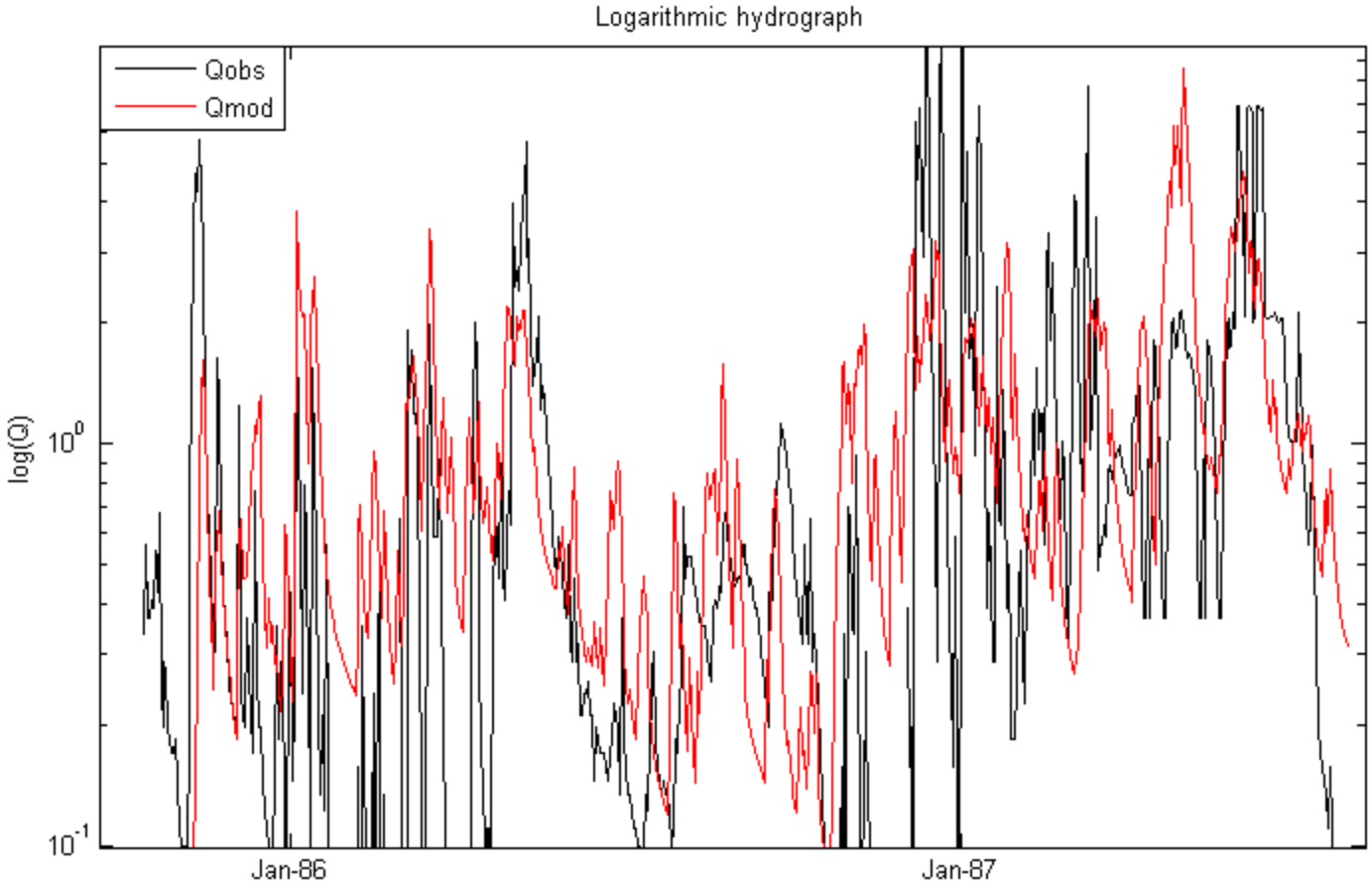

Figure 6-5: Logarithm of the hydrograph with new data series. The data series originally used for validation is now used for calibration and vice versa.

The parameters obtained from this calibration on the Mara River Basin are used to validate the sub-catchment Nyangores. As shown in Figure 6-6, also for this run the model performs well.

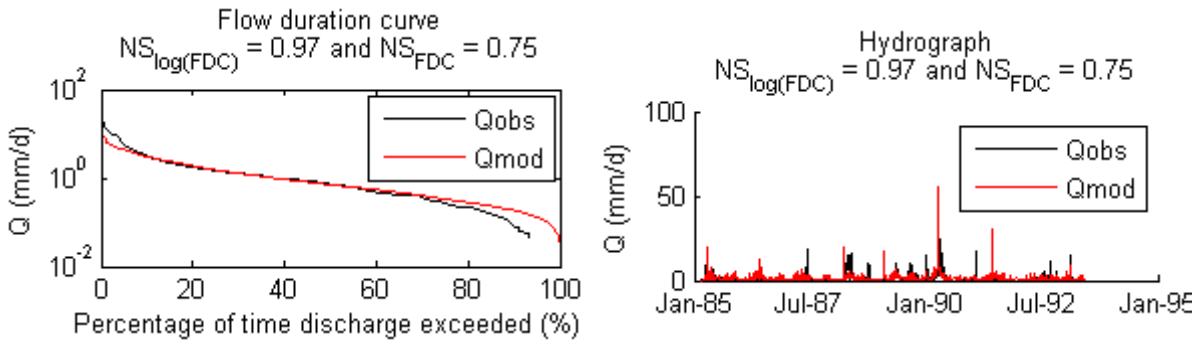

Figure 6-6: Validation results of the Nyangores sub-catchment using the parameters based on the calibration of the Mara River Basin: flow duration curve (left) and hydrograph (right)

6.1.1. Verification of the parameter a

One of the calibrated parameters is the parameter a used to estimate the discharge from the water level and a given cross-section using the formula of Strickler:

$$Q = k * A * R^{2/3} * i^{1/2} = a * \left(A * R^{\frac{2}{3}}\right)$$

Calibrating this parameter yields: a=0.03. However this parameter is estimated to be 0.01 using an average roughness of 35 $m^{1/3}/s$ and a slope of $1.90 \cdot 10^{-3}$ based on the digital elevation map. Only when increasing the roughness to 90 $m^{1/3}/s$ or increasing the slope to $1.25 \cdot 10^{-2}$, this value of a=0.03 could be found. These however are unrealistic values.

However, looking at satellite images of the river, several rapids are found. These rapids might influence the slope and therefore also the parameter a. That is why the influence of rapids on this parameter is analysed by modelling a simple rectangular channel with several jumps in the bed level. At such a jump, rapids occur during low flows. For this analysis, the software SWAT is used.

With this simulation, the velocity is found to increase at the bed level difference. Therefore, the discharge is much larger with similar water level. Hence, the parameter a increases locally to increase the discharge (see Figure 6-7). The influence of the jump in the bed level depends on the discharge: during very high flows, this jump is barely noticeable (see Figure 6-8) whereas the opposite is the case during low flows. That is why, the parameter a only increases significantly at rapids during low flows whereas it is constant along the river during high flows.

In conclusion, an increase of the parameter from a=0.01 to a=0.03 as found through calibration is possible through the existence of rapids. This means that this parameter depends on the discharge. However, more studies are needed to determine the influence specific for the Mara River more accurately.

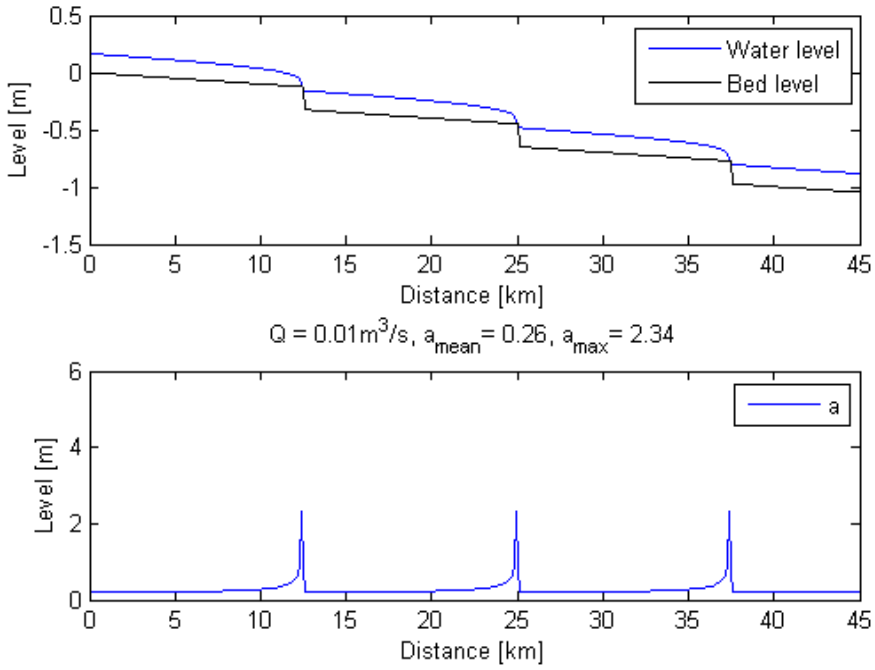

Figure 6-7: Longitudinal profile of a river with rectangular cross-section with the water level (upper) and local value for the parameter a (lower) during low flows

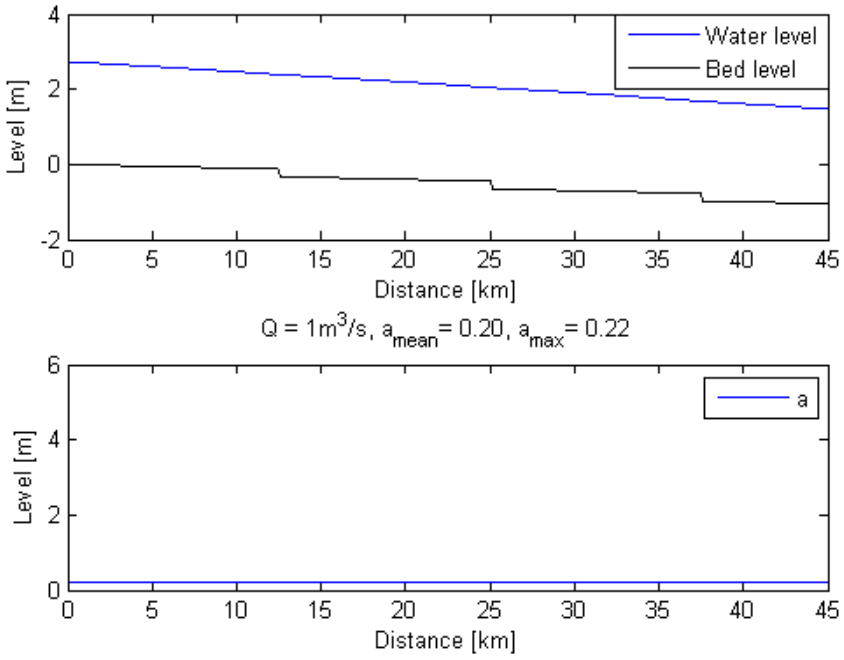

Figure 6-8: Longitudinal profile of a river with rectangular cross-section with the water level (upper) and local value for the parameter a (lower) during high flows

6.2.Model results for the Nyangores sub-catchment

The model also performs well when calibrating it on the Nyangores sub-catchment (see Figure 6-9).

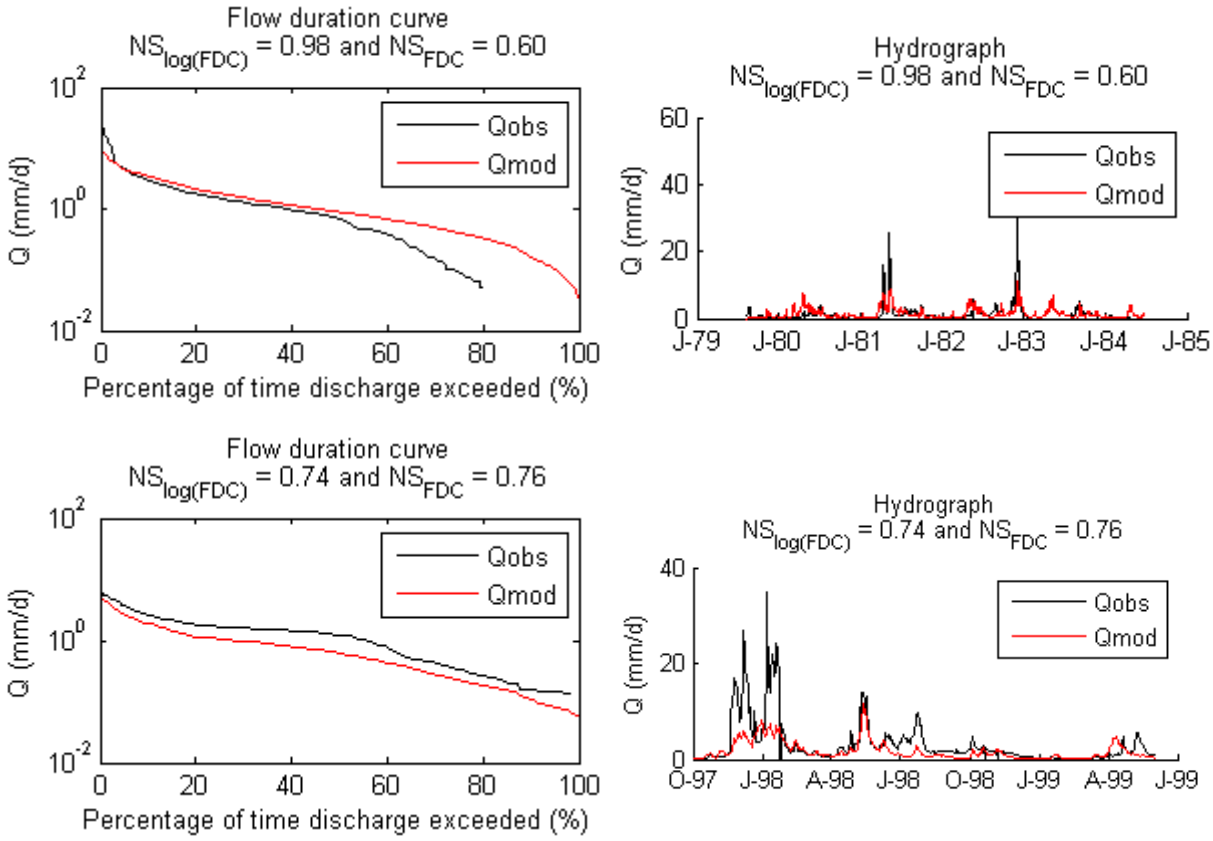

Figure 6-9: Calibration (upper) and validation (lower) results for the Nyangores sub-catchment: flow duration curve (left) and hydrograph (right)

The calibration results of this model are used to validate the model on the entire Mara River Basin. As shown in Figure 6-10, the model performance has decreased significantly. This is not surprising as in the Nyangores sub-catchment, mainly forested and cultivated areas are found whereas in the remaining catchment the land cover is dominated by grassland and shrubs.

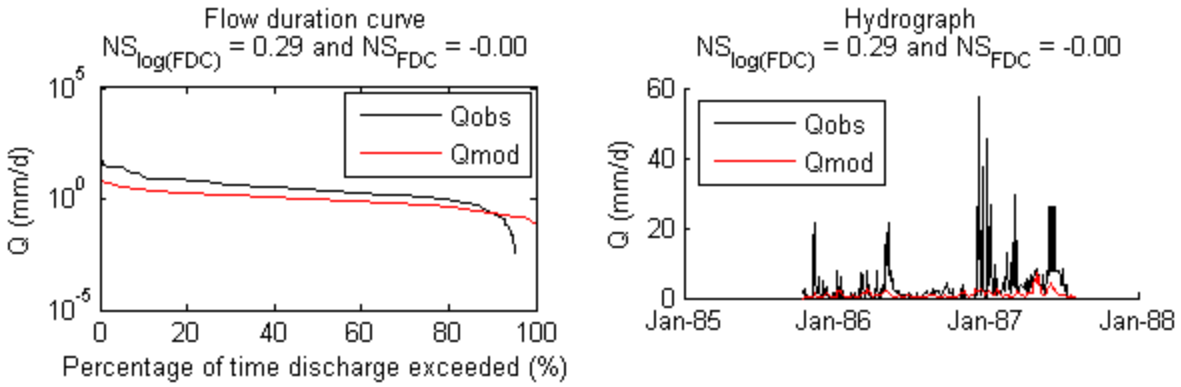

Figure 6-10: Validation results of the Mara River Basin using the parameters based on the calibration of the Nyangores sub-catchment: flow duration curve (left) and hydrograph (right)

6.3.Influence of the introduction of HRU

In this section, the influence of multiple HRU is analysed. This is done by lumping the model using a single HRU. For this analysis two scenarios are compared with the original one:

1. The model structure of the hydrological unit 'Forest' is used. This means that there is shallow subsurface flow (SSF) in the entire catchment.
2. The model structure of the hydrological unit 'Grassland' is used. This means that there is hortonian overland flow (HOF) in the entire catchment.

Compared with the original model, both scenarios give worse model results (see Figure 6-11 and Figure 6-12). Hence, the introduction of four HRU improves the model performance significantly.

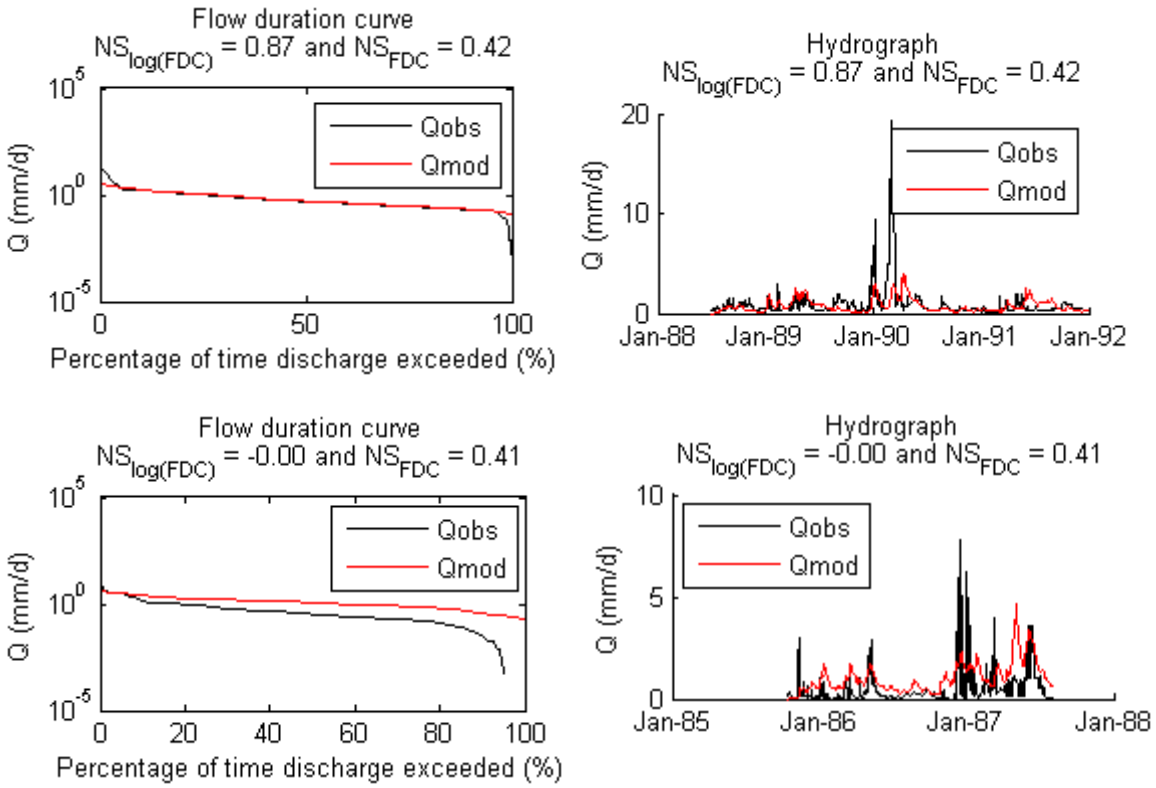

Figure 6-11: Calibration (upper) and validation (lower) results for the Mara River Basin using a single HRU with SSF: flow duration curve (left) and hydrograph (right)

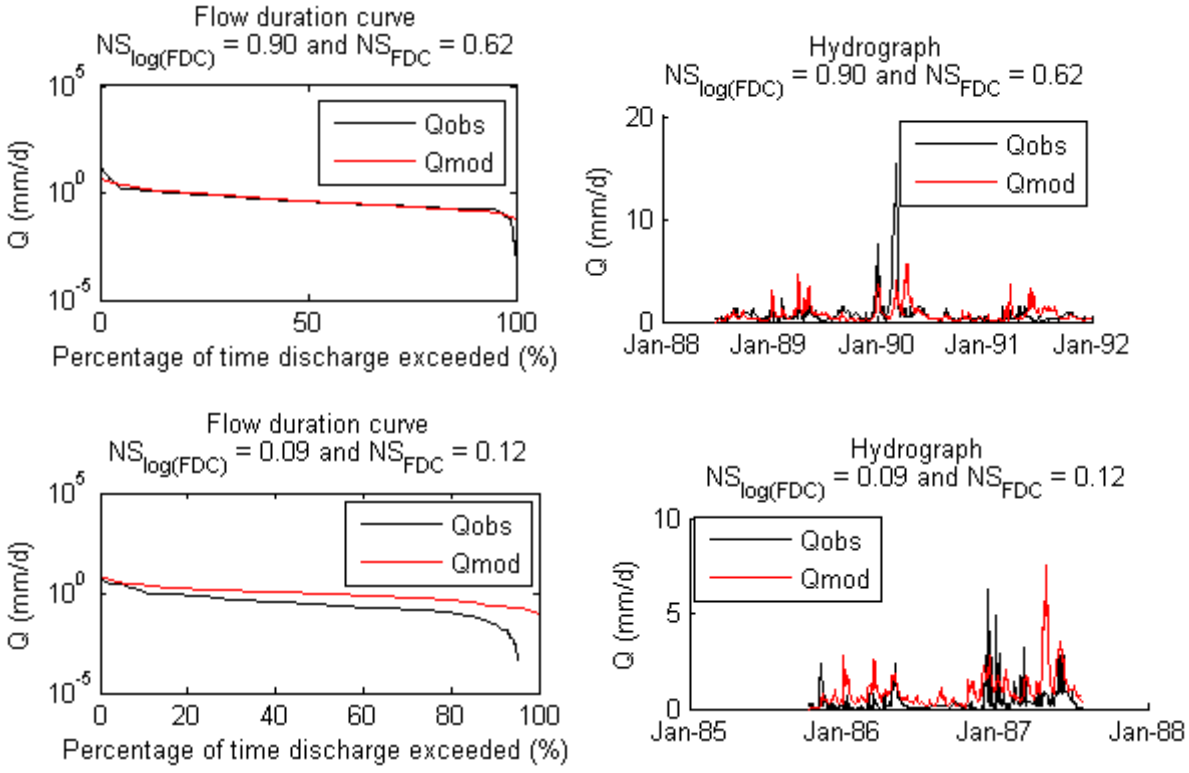

Figure 6-12: Calibration (upper) and validation (lower) results for the Mara River Basin using a single HRU with HOF: flow duration curve (left) and hydrograph (right)

6.4.Influence of the introduction of sub-catchments

In this section, the influence of splitting the catchment into five sub-catchments is analysed. This is done by lumping the model to a single catchment. As shown in Figure 6-13, this decreases the model performance. Hence, splitting the catchment into sub-catchments improves the model significantly.

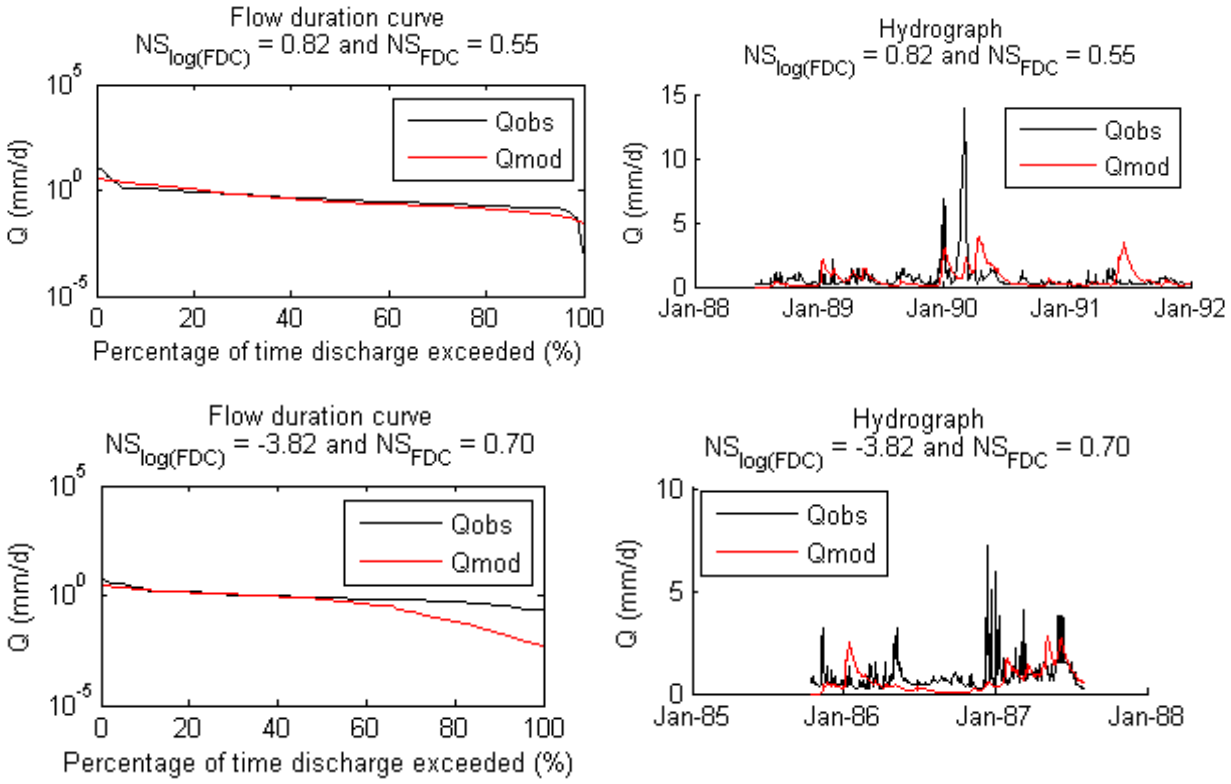

Figure 6-13: Calibration (upper) and validation (lower) results for the Mara River Basin lumping the model to a single catchment: flow duration curve (left) and hydrograph (right)

6.5.Influence of each constraint

To assess the impact of each constraint, the number of samples rejected through a specific constraint is counted and divided through the total number of samples. For this analysis, each constraint is given a number:

- Constraint 1: Runoff close to estimation based on Budyko curve
- Constraint 2: Total evaporation close to estimation based on Budyko curve
- Constraint 3: Sand river flow limited based on observation
- Constraint 4: Transpiration relation between HRUs based on NDVI
- Constraint 5: Expected preferential recharge relation

As shown in Table 6-1, the constraint on the evaporation using the NDVI is the one rejecting most samples. In total, about 90% of the samples are rejected.

Table 6-1: Impact of each constraint for the entire catchment and for each sub-catchment separately: percentage of rejected samples per constraint

	MRB	North	Middle	Talek	Sand	Lower
Rejected samples through constraint 1	0%	0%	0%	0%	0%	0%
Rejected samples through constraint 2	0%	0%	0%	0%	0%	0%
Rejected samples through constraint 3	0%	0%	0%	0%	0%	0%
Rejected samples through constraint 4	66%	52%	12%	0%	2%	0%
Rejected samples through constraint 5	25%	25%	0%	0%	0%	0%

To assure that these samples are excluded for the right reasons, the effect of excluding each constraint is analysed. It is found that the excluding of each constraint results in good results in the calibration, but poorer model results in the validation (see Table 6-2). For example, when excluding the fourth constraint, the calibration performance increases however the validation results decreases. Hence, for each constraint samples are rejected for the right reasons. This decrease in model performance is also visible in the FDCs; see Figure 6-15 for these curves for the calibration and validation with and without all constraints. Also, the calibration parameters are less well defined when excluding all constraints (see Figure 6-14).

Table 6-2: Impact of excluding a constraint on the objective function Nash Sutcliffe

	Calibration results	Validation results
All constraints included	$NS_{log(FDC)}$ = 0.91; NS_{FDC} = 0.71	$NS_{log(FDC)}$ =0.74; NS_{FDC} = 0.93
Constraint 1 excluded	$NS_{log(FDC)}$ =0.90; NS_{FDC} = 0.59	$NS_{log(FDC)}$ =0.71; NS_{FDC} = 0.93
Constraint 2 excluded	$NS_{log(FDC)}$ =0.90; NS_{FDC} = 0.67	$NS_{log(FDC)}$ =0.57; NS_{FDC} = 0.96
Constraint 3 excluded	$NS_{log(FDC)}$ =0.89; NS_{FDC} = 0.51	$NS_{log(FDC)}$ =0.52; NS_{FDC} = 0.81
Constraint 4 excluded	$NS_{log(FDC)}$ =0.92; NS_{FDC} = 0.90	$NS_{log(FDC)}$ =-0.31; NS_{FDC} = 0.39
Constraint 5 excluded	$NS_{log(FDC)}$ =0.89; NS_{FDC} = 0.51	$NS_{log(FDC)}$ =0.47; NS_{FDC} = 0.77
All constraints excluded	$NS_{log(FDC)}$ =0.90; NS_{FDC} = 0.63	$NS_{log(FDC)}$ =0.60; NS_{FDC} = 0.48

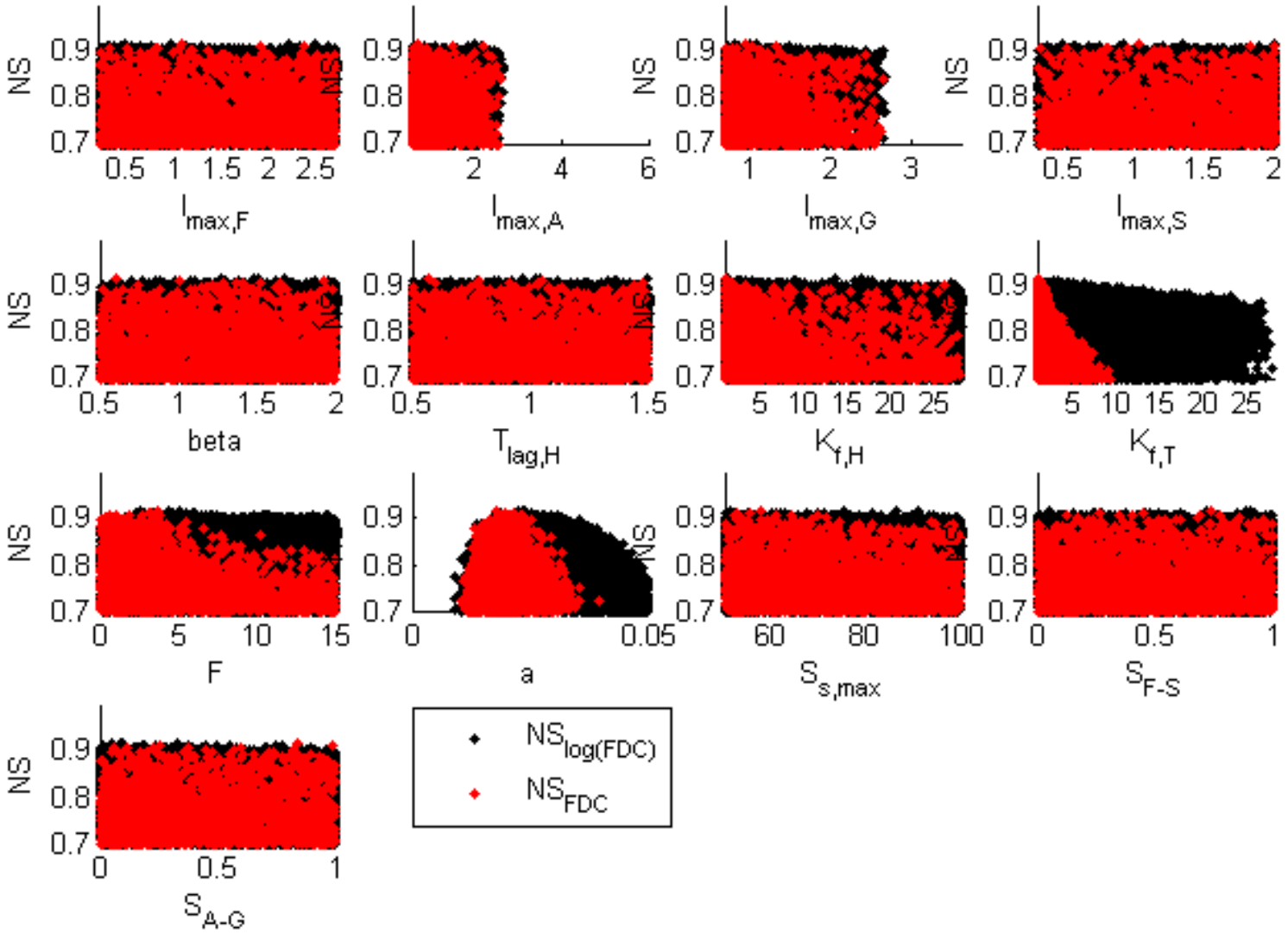

Figure 6-14: Dot plots for all calibrated parameters for the Mara River Basin for a model run in which all constraints are excluded. The minimum and maximum value on the horizontal axis is equal to the defined parameter boundaries for the calibration

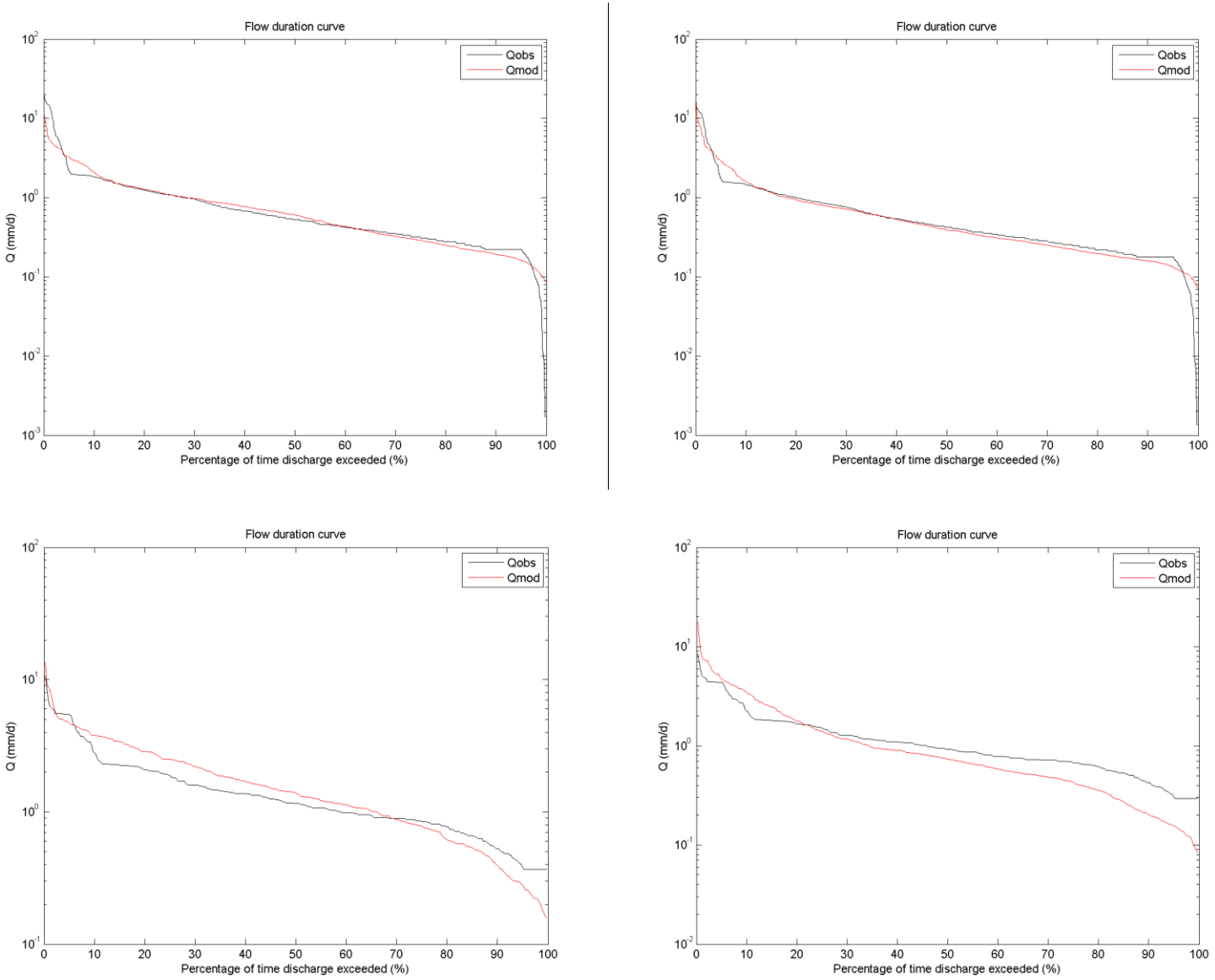

Figure 6-15: FDC with all constraints (left) and with no constraints (right) for the calibration (upper) and validation (lower)

6.6.Overview model results

In this table, all the values found for the objective functions and the calibration parameters are put together for all model runs explained in the previous sections.

Table 6-3: Overview of all the modelling results: values for the objective functions $NS_{log(FDC)}$ and NS_{FDC} and for the calibration parameters

	MRB: Semi-distributed	MRB: Semi-distributed	MRB: Semi-distributed, $S_{u,max}$ per HRU & sub-catchment	MRB: 1 HRU (SSF), 5 sub-catchments	MRB: 1 HRU (HOF), 5 sub-catchments	MRB: 1 HRU (SSF), 1 sub-catchment	MRB: 1 HRU (HOF), 1 sub-catchment	MRB: 4 HRUs, 1 sub-catchment	Nyangores: Semi-distributed	Nyangores: Semi-distributed
	Calibration (Validation)	Validation based on Nyangores	Calibration (Validation)	Calibration (Validation)	Calibration (Validation)	Calibration (Validation)	Calibration (Validation)	Calibration (Validation)	Calibration (Validation)	Validation based on MRB
$NS_{log(FDC)}$	0.91 (0.74)	0.29	0.92 (0.63)	0.87 (0.00)	0.90 (0.09)	0.89 (-1.98)	0.85 (-2.94)	0.82 (-3.82)	0.98 (0.74)	0.94
NS_{FDC}	0.71 (0.93)	0.00	0.88 (0.42)	0.42 (0.41)	0.62 (0.12)	0.47 (0.66)	0.76 (0.48)	0.55 (0.70)	0.60 (0.76)	0.83
$I_{max,F}$	1.96	2.52	1.70	2.21	2.35	1.67	1.96	1.90	2.52	1.96
$I_{max,A}$	0.92	1.20	0.88	1.39	1.77	0.60	1.67	0.73	1.20	0.92
$I_{max,G}$	1.50	0.79	1.50	1.24	1.70	1.34	1.80	1.21	0.79	1.50
$I_{max,S}$	1.78	1.37	1.55	1.94	1.94	1.38	1.87	1.57	1.37	1.78
β	1.55	0.80	1.26	1.18	0.69	1.72	1.83	0.62	0.80	1.55
T_{lag}	0.64	1.16	1.11	1.00	1.33	1.19	0.90	0.78	1.16	0.64
$K_{f,FS}$	3.68	14.20	6.57	8.72	6.29	27.19	10.28	27.25	14.20	3.68
$K_{f,AG}$	1.06	4.55	1.01	4.57	3.90	19.62	1.74	22.28	4.55	1.06
F	10.45	12.04	3.56	12.49	11.32	12.12	12.96	12.68	12.04	10.45
a	0.03	0.18	0.02	0.03	0.02	0.02	0.02	0.02	0.18	0.16
S_{smax}	70.54	91.14	78.45	70.67	73.20	78.49	94.55	97.76	91.14	70.54
S_{FS}	0.65	0.52	0.68	0.63	0.84	0.89	0.84	0.86	0.52	0.65
S_{AG}	0.28	0.10	0.14	0.24	0.46	0.64	0.50	0.64	0.10	0.28

Appendix F: Sediment transport modelling

Table of contents

The river transports both coarse and fine particles. Coarse particles participate in bed load and suspended load whereas fine particles in wash load and suspended load. The transition between them is between 50 µm and 70 µm (Vriend et al., 2011). Both the suspended load and the wash load influences the water quality, therefore, both the coarse and fine particles have an influence.

To improve the water quality, the sediment load needs to be lowered. Preferably, this is done by applying measures at the source of the sediments. Therefore, in this section possible sources of the coarse and fine sediments are evaluated.

1. Coarse sediments

In this section, different possible sources for coarse sediments in the river are analysed. Unfortunately, there is no data available on the actual amount of coarse sediments in the river. That is why it is assumed that the river the actual sediment load regarding the coarse material is equal to the transport capacity. This assumption is generally valid as it is found that the transport of coarse sediments is largely capacity-limited (Knighton, 1998).

Coarse sediments can only be transported through very high flow velocities which can be found streams, the river itself or in gullies. In this section, the influence of gullies on the sediment load in the river is evaluated. This is done by comparing the sediment transport capacity of the river with the one of typical gullies found in the catchment.

1.1. Sediment transport capacity of the river

For the Mara River, the total sediment transport capacity is calculated based on the formulas of Engelund Hansen and Van Rijn. In both formulas, the bed load and the suspended load are included hence the total transport capacity is estimated.

1.1.1. Data used to calculate the sediment transport capacity

In this section an overview is given of all the data used to estimate the sediment transport capacity in the Mara River. As not all the required data is available, some of it is estimated based on literature.

Overview 1-1: Required data for the calculation of the sediment transport capacity

Constants	
$\rho = 1000$ kg/m^3	(water density)
$\Delta = 1.65$	(=(ρ_s-ρ)/ρ)
$\nu = 10^{-6}$ m^2/s	(kinematic viscosity)
$\epsilon_p = 0.4$	(porosity for quarts granules)
$\kappa = 0.4$	(von Karmen constant)
Grain diameter	
$D_{16} = 0.62*D_{50}$	(grain diameter for which 16% of the mixture is finer)
$D_{50} = 0.5$ mm	(grain diameter for which 50% of the mixture is finer)
$D_{84} = 1.70*D_{50}$	(grain diameter for which 84% of the mixture is finer)
$D_{90} = 1.90*D_{50}$	(grain diameter for which 90% of the mixture is finer)
Roughness	
k=35 m$^{1/3}$/s	(Strickler roughness coefficient)
Hydraulic characteristics	
Q	(river discharge)
h	(water depth)
u	(flow velocity)
B	(river width)
a	(reference level at time t_1; it is chosen to be 0.1 m below the water surface at all times)

Grain diameter

Data on the sediment distribution of the river bed is lacking, therefore, it is not possible to estimate the diameters D_{16}, D_{50}, D_{84} and D_{90} accurately. That is why the relation between these four diameters is estimated based on literature. In previous studies, the sediment distribution is determined for the Bialy Dunajec River, Czarny Dunajec River and Skawa River in Poland (Strużyński et al., 2013) and the Nile River in Egypt near the cities Aswan, Sohag, Quena and Beni Suef (Abdel-Fattah et al., 2005). In these

rivers, the sediment distribution is analysed detailed and show a similar distribution even despite the differences in the diameter D_{50}. By comparing these three rivers with each other and with the scarce data available for the Mara River (Muthike, 2007), a relation is found as shown in Overview 1-1. For the diameter D_{50}, the value 0.5 mm is chosen randomly as there is insufficient reliable data on the local sediment distribution.

Roughness

For the Strickler roughness coefficient, the average value for a natural channel with short grass is taken; that is 35 $m^{1/3}/s$ (P. Ankum, 2002).

Hydraulic characteristics

At several locations along the Mara River, the cross-sectional river profile is measured as shown in Figure 1-1 (Ndomba, 2009). This data is used to determine the river with at different water levels. In the same study, the discharge, velocity and water level are measured multiple times at Site 1.2 which is in the Nyangores tributary (see Table 1-1).

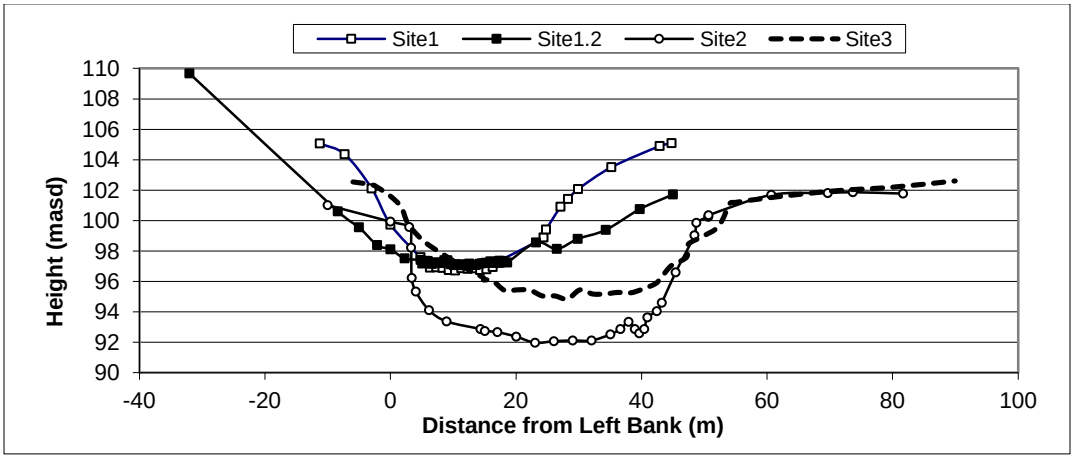

Figure 1-1: Cross-sectional profile of the Mara River in the Amala River at Mulot (Site 1), Nyangores River at Bomet (Site 1.2), Mid Mara at Old Mara Bridge (Site 2) and Lower Mara at New Mara Bridge (Site 3) (Ndomba, 2009)

Table 1-1: Hydraulic characteristics Site 1.2 which is in the Nyangores River (Ndomba, 2009)

Stream Discharge (m3/s)	Water Surface Level (masd)	Average Velocity (m/s)	Hydraulic depth (m)	Wetted Width (m)	Wetted perimeter (m)	Cross section Area (m2)
0.2	97.3122	0.1006	0.209	14.9438	15.2148	3.3586
0.25	97.3276	0.1094	0.2188	15.5258	15.8124	3.5872
0.3	97.341	0.1182	0.2276	16.0722	16.3716	3.7972
0.5	97.385	0.1464	0.2646	16.7568	17.09	4.5238
0.646	97.4112	0.1648	0.2862	17.1496	17.5008	4.968
1	97.4646	0.2008	0.3282	17.9554	18.3324	5.903
2	97.5672	0.2812	0.4092	19.2962	19.7118	7.8208
3	97.6426	0.3448	0.4726	19.8448	20.2886	9.2914
4	97.7044	0.399	0.5242	20.287	20.7542	10.5334
5	97.7598	0.4458	0.5698	20.65	21.1384	11.665
6	97.8088	0.4886	0.6108	20.9484	21.4556	12.6872
7	97.8536	0.528	0.6474	21.2206	21.745	13.6332
7.943	97.8932	0.5622	0.6798	21.4608	22.0002	14.4782
8	97.8952	0.5644	0.6814	21.4734	22.0138	14.5238
10	97.9714	0.63	0.7428	21.9356	22.5052	16.1772
15	98.1324	0.767	0.8598	23.1146	23.747	19.7976
20	98.2876	0.857	0.934	25.3032	26.0012	23.5522
27	98.4564	0.9652	0.9716	29.0102	29.7862	28.1518
50	98.85	1.2328	1.2026	33.9232	34.848	40.7332
100	99.4406	1.6134	1.6096	38.663	39.7864	62.2262
200	100.2354	2.0944	2.1084	45.4396	46.7916	95.8584

1.1.2. Sediment transport capacity: Methodology

In this section the methodology for the calculation of the sediment transport capacity is explained, first according to Engelund Hansen, then Van Rijn.

Sediment transport capacity: methodology according to Engelund Hansen

With the formula of Engelund Hansen the total transport capacity is calculated, thus both the suspended and the bed load are included. This formula however is only valid for grain diameters between 0.19 mm and 0.93 mm and for a Shields-parameter θ between 0.07 and 6. In Overview 1-2, the calculation of the transport capacity according to Engelund Hansen is explained.

Overview 1-2: Explanation of the sediment transport capacity calculation according to Engelund Hansen (Vriend et al., 2011)

According to Engelund Hansen, the total transport capacity S can be calculated with the following formula:

$$\Phi = 0.05 * \psi^{\frac{5}{2}}$$

In which Φ the flow parameter

$$\Phi = \frac{S}{\sqrt{(g * \Delta * D^3)}}$$

ψ the flow parameter

$$\psi = \mu * \frac{\tau_b}{\rho * g * \Delta * D}$$

and μ the ripple factor

$$\mu = \left(\frac{C^2}{g}\right)^{\frac{2}{5}}$$

Also, for each discharge it is determined whether sediment transport is expected because for very low flows this is not the case. Therefore, the Shields parameter θ is compared to its critical value using the Shields curve. Only if the critical value is exceeded, there is sediment transport.

$$\theta = \frac{u_*^2}{g * \Delta * D}$$

Sediment transport capacity: methodology according to Van Rijn

Also with the formula of Van Rijn the total transport capacity is calculated. This methodology however does not have any constraints and is therefore applicable for all diameters. In Overview 1-2, the calculation of the transport capacity according to Van Rijn is explained.

Also, it's worth mentioning that this formula tends to underestimate the transport capacity (Larson et al., 2011).

Overview 1-3: Explanation of the sediment transport capacity calculation according to Van Rijn (Vriend et al., 2011)

The total sediment load is estimated by calculating the bed load s_b and the suspended load s_s separately and then adding them up to each other:

$$s = s_b + s_s$$

Bed load

For the calculation of the bed load, the following empirical formula is applied:

$$\Phi_b = 0.053 * \frac{T^{2.1}}{D_*^{0.3}} \; if \; T < 3$$

$$\Phi_b = 0.1 * \frac{T^{1.5}}{D_*^{0.3}} \; if \; T \geq 3$$

$$s = \frac{\Phi}{\sqrt{g * \Delta * {D_{50}}^3}}$$

In this formula, T is the parameters for the bed shear stress and D_* the dimensionless parameter for the grain diameter. The first is calculated with the bottom shear stress related to the grains τ_b' and the critical shear stress $\tau_{cr.}$

$$D_* = D_{50} * \left(\Delta * \frac{g}{\nu^2}\right)^{\frac{1}{3}}$$

$$T = \frac{\tau_b' - \tau_{cr}}{\tau_{cr}}$$

$$\tau_b' = \left(\frac{C}{C'}\right)^2 * \tau_b$$

$$\tau_b = \rho * u_*^2$$

$$C' = C_{90} = 18 * \log\left(12 * \frac{h}{D_{90}}\right)$$

The Chézy friction coefficient C is estimated with the Strickler coefficient and the hydraulic radius:

$$C = k * R^{\frac{1}{6}}$$

Suspended load

The suspended sediment load is calculated with the following formula

$$s_s = F * u * h * c_a$$

For concentration c_a and the factor F the formulas are

$$c_a = 0.015 * \frac{D_{50}}{a} * \frac{T^{1.5}}{D_*^{0.3}}$$

$$F = \frac{\left(\frac{a}{h}\right)^{Z'} - \left(\frac{a}{h}\right)^{1.2}}{\left(1 - \frac{a}{h}\right)^{Z'} * (1.2 - Z')}$$

The factor Z' can be calculated with

$$Z' = \frac{w_s}{\left(1 + 2 * \left(\frac{w_s}{u_*}\right)^2\right) * \kappa * u_*} + 2.5 * \left(\frac{w_s}{u_*}\right)^{0.8} * \left(\frac{c_a}{1 - \epsilon_p}\right)^{0.4} \; for \; 0.01 \leq \frac{w_s}{u_*} \leq 1$$

The fall velocity is determined using the representative grain diameter in suspension D_s using the following formula.

$$\frac{D_s}{D_{50}} = 1 + 0.011 * \left(0.5 * \left(\frac{D_{84}}{D_{50}} + \frac{D_{50}}{D_{16}}\right) - 1\right) * (T - 25)$$

Also, for each discharge it is determined whether sediment transport is expected because for very low flows this is not the case. Therefore, the Shields parameter θ is compared to its critical value using the Shields curve. Only if the critical value is exceeded, there is sediment transport.

$$\theta = \frac{u_*^2}{g * \Delta * D}$$

1.1.3. Sediment transport capacity: Results

Applying both methodologies, Engelund Hansen and Van Rijn, the sediment transport capacity is calculated for different discharges. This is done for the Nyangores River at Bomet and for the Mara River at New Mara Bridge as shown in see Figure 1-2.

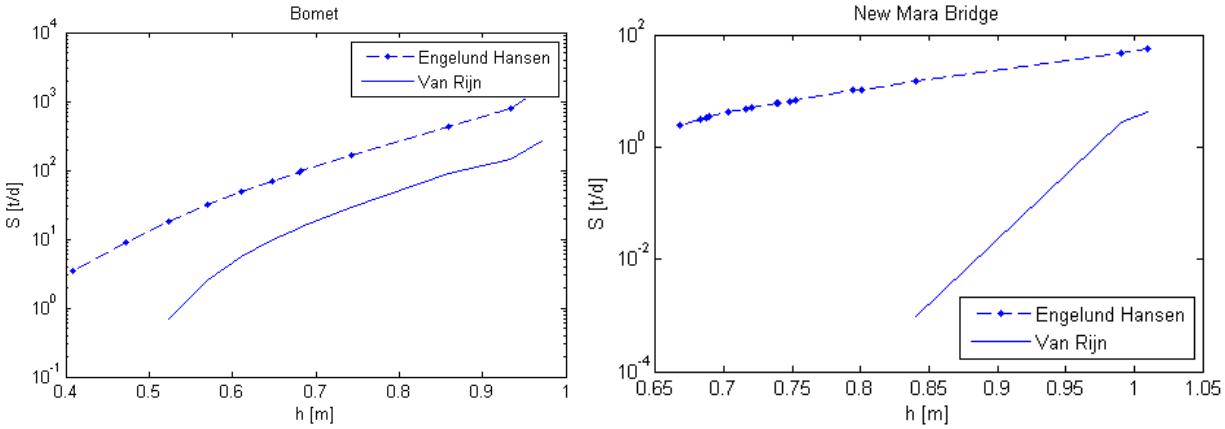

Figure 1-2: Sediment transport capacity according to Engelund Hansen and Van Rijn in the Nyangores at Bomet and Mara River at New Mara Bridge

1.1.4. Sediment transport capacity: Sensitivity analysis

In this section, the sensitivity of the Engelund Hansen en Van Rijn formulas is evaluated. This is done by using different values for the roughness and for the diameter. These two parameters are the ones with the largest uncertainties whereas the others are either measured, estimated based on measured or constants.

Roughness

The roughness is varied between 25 $m^{1/3}/s$ and 45 $m^{1/3}/s$. These are typical values found in natural channels with short grass (P. Ankum, 2002). Varying the roughness in this range results in a larger bandwidth in the transport capacity as shown in Figure 1-3. This bandwidth is larger for the Engelund Hansen formula than the Van Rijn formula. At New Mara Bridge, the change in roughness has no effect at all in the Van Rijn formula. This implies that the Van Rijn formula is not sensitive to the roughness, whereas the Engelund Hansen formula is sensitive.

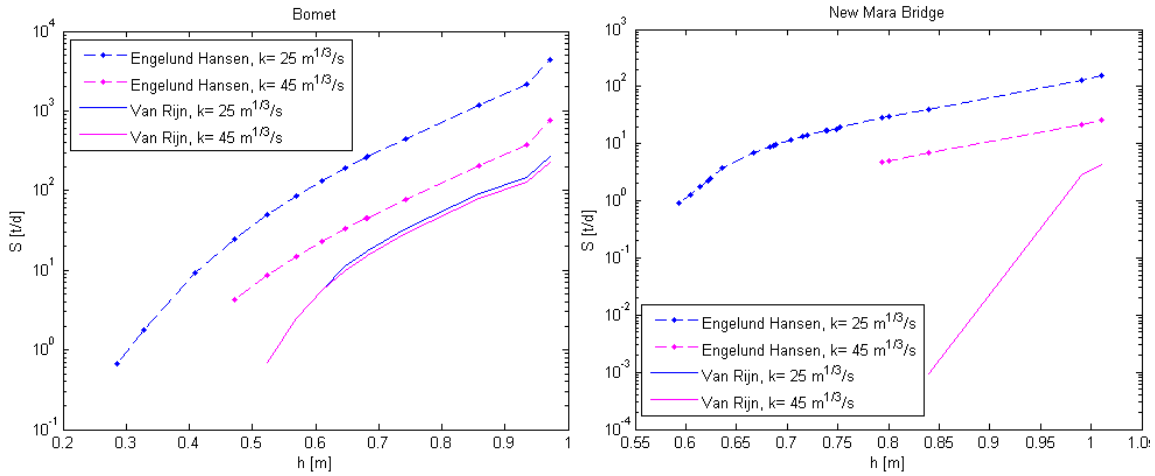

Figure 1-3: Sediment transport capacity according to Engelund Hansen and Van Rijn in the Nyangores at Bomet and Mara River at New Mara Bridge for three different values for k

Grain diameter

Different grain diameters between 0.5 mm and 0.93 mm are chosen for the diameter D_{50}. This choice is based on two aspects:

- The diameter should be between 0.19 mm and 0.93 mm to fulfil the restrictions of the formula of Engelund Hansen.
- With these formulas, the transport of coarse sediments is studied. These sediments have a grain diameter larger than 0.5-0.7 mm.

The transport capacity is calculated several times using different values for D_{50} within the given range. This results in a bandwidth for the transport capacity as shown in Figure 1-4 which is smaller than the one caused by the roughness.

At new Mara Bridge, the Van Rijn formula does not seem to be valid for all conditions: For too low velocities the critical shear stress exceeds the bed shear stress. In that case, there is no sediment flow. That is why results under this condition are excluded from the calculation as can be seen in the graph.

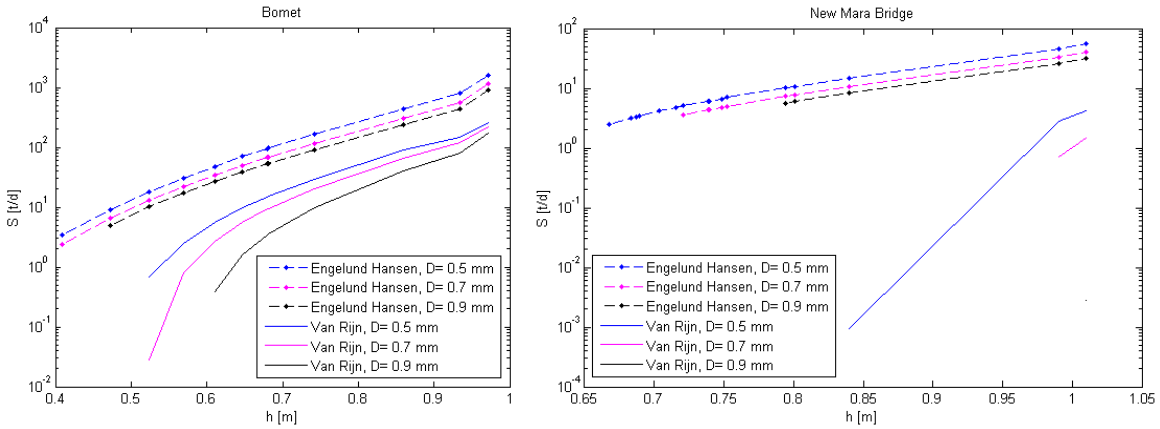

Figure 1-4: Sediment transport capacity according to Engelund Hansen and Van Rijn in the Nyangores at Bomet and Mara River at New Mara Bridge for three different values for D_{50}

1.2. Possible sources of coarse sediments

The coarse sediments in the river can origin from the river itself or from gullies. In this section, it is determined whether gullies or the river itself are a significant source.

1.2.1. Possible sources of coarse sediments: Gullies

To assess whether gullies are a significant source their sediment transport capacity are estimated and compared to the one in the river. Only if the capacity of the gullies is of the same order of magnitude as in the river, they are a significant source.

Average gully

An average gully seen in the sub-catchments Talek and Sand is about 0.5 m x 0.5 m large. For the velocity the value 0.2 m/s is chosen. This is the minimum velocity at which there is sediment transport. For such a gully, the maximum transport capacity is calculated, that is when it is completely filled with water that flows at maximum velocity. The transport capacity under that condition is then compared with the capacity in the river during peak flow. Based on water level measurements at New Mara Bridge between 21 Sep and 12 Nov 2014, it is found that the depth is at least 2 m during peak flow. For both the river and a gully, the transport capacity is calculated applying the methodology of Engelund Hansen.

Compared to the transport capacity in the river, the capacity of a single gully is negligible small (see Figure 5-2). Only if there would be more than 10^5 gullies flowing directly into the Talek or Sand River, the effect of gullies would be significant. This would mean that every 4 m a gully is flowing into the Talek or Sand, considering that the Talek River is 240.8 km long and the Sand River 212.9 km. This is much more frequent than observed; therefore it is possible to neglect the effect of average gullies.

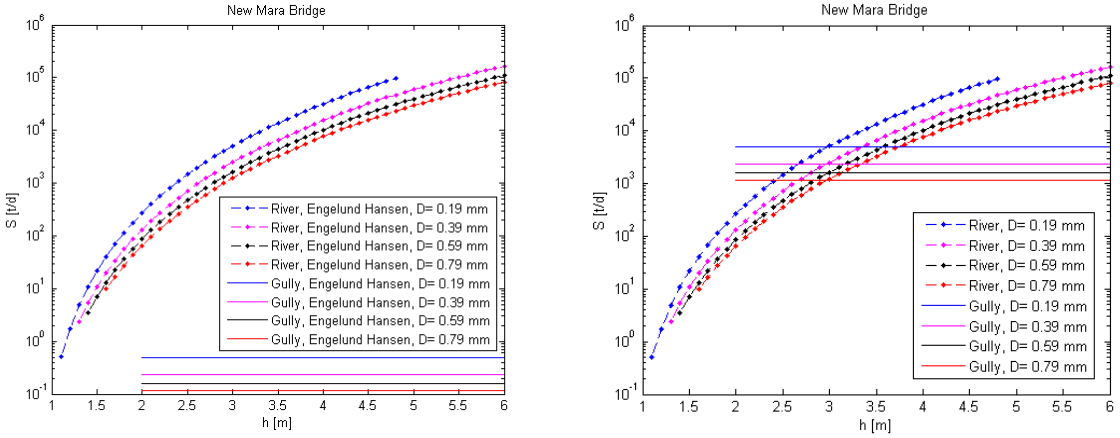

Figure 1-5: Comparison of the transport capacity in the river and A) of one average gully (left), B) of 10^5 average gullies (right) applying the Engelund Hansen formula

Large gully

The same analysis is done for a large gully as for an average one. Only now, the flow velocity is 0.3 m/s and the dimensions are 2 m x 4 m. Also the effect of a single large gully is negligible small (see Figure 1-6). The effect of large gullies would only be significant if there would be more than $5 \cdot 10^3$ that flow

directly into the Sand or Talek River, which is every 75 m. This is much more frequent than observed; therefore it is possible to neglect the effect of large gullies.

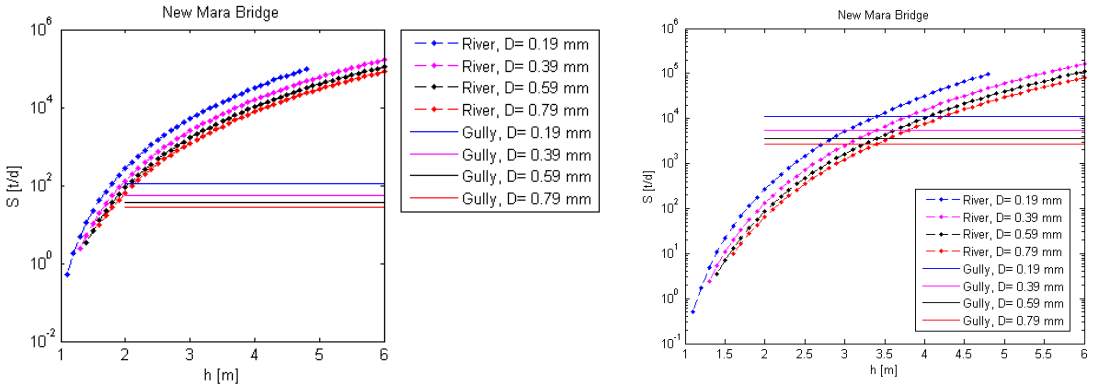

Figure 1-6: Comparison of the transport capacity in the river and A) of one large gully (left), B) of $5*10^3$ large gullies (right) applying the Engelund Hansen formula

1.2.2. Possible sources of coarse sediments: River

As gullies seem to be an insignificant source for the coarse sediments in the river, the source could be the river itself implying that the river meanders. To assess whether the river indeed is meandering, the location of the river in 2014 is compared to the one in 1996.For this comparison, a digital elevation map (DEM) is used. From this map, the flow accumulation map is created. By choosing an appropriate threshold, the river can be seen clearly in this map. For 1996, the DEM map used is obtained from GTOPO30 while for 2014 it is SRTM.

The location of the Mara River in 1996 and 2014 is shown in Figure 5-3. This figure shows that the river did meander. The maximum movement of 8.7 km is found along the Sand River (see Figure 1-8). Along the Mara River this movement is about 2 km and in the Nyangores and Amala River about 1 km at maximum.

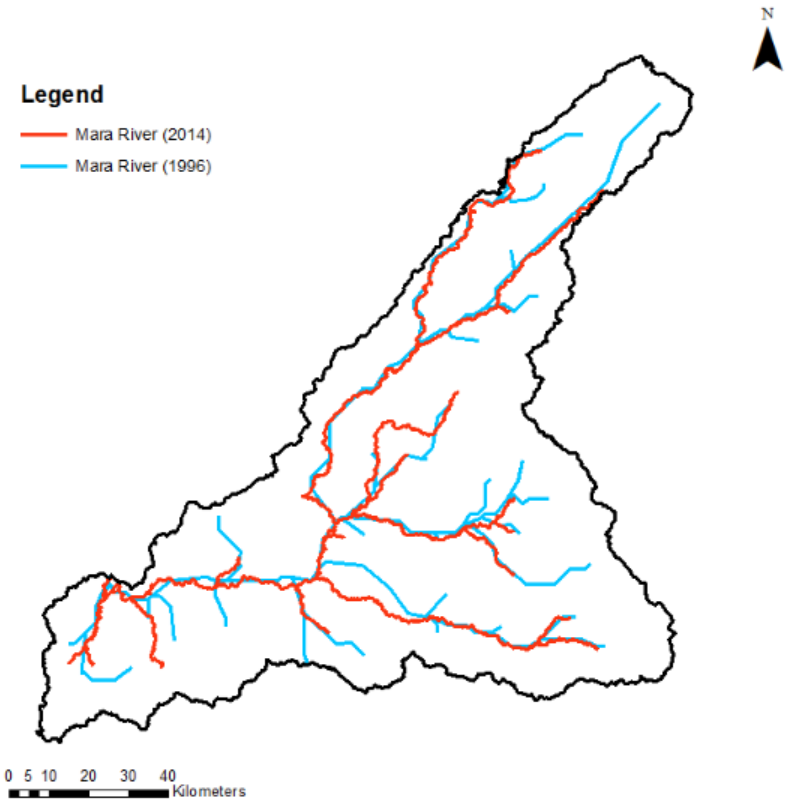

Figure 1-7: Location of the Mara River in 1996 and 2014

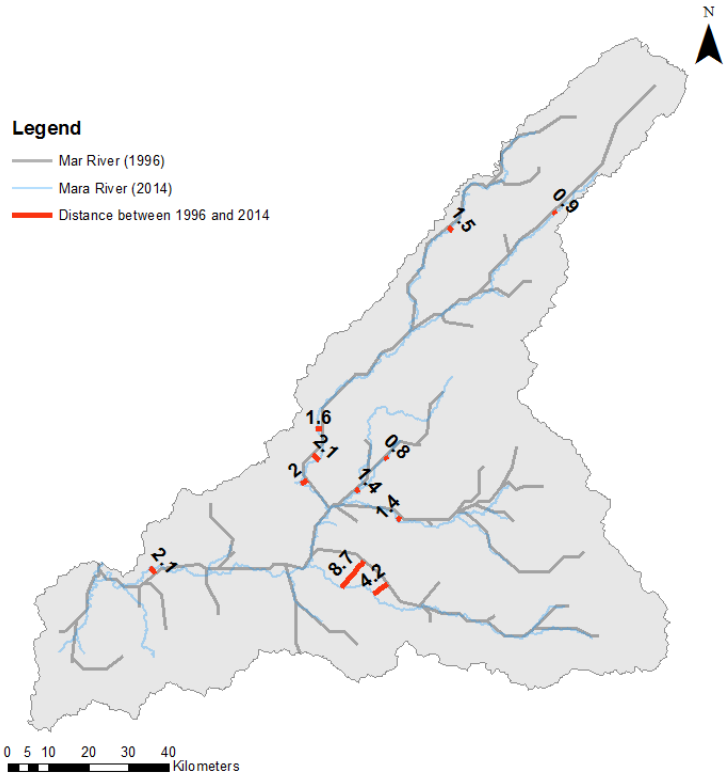

Figure 1-8: Difference in the location of the Mara River between 1996 and 2014

1.3.Results

Two possible sources for coarse sediments in the river are analysed: gullies and the river itself. This analysis shows that gullies have a negligible effect on the sediment load in the river whereas the river itself seems to be a more significant source which can be seen through the significant meandering in the past. To minimize the sediment load, it is therefore useless to prevent gully formations. More recommendable are measures in the river itself, for example: Decrease the flow velocity to decrease the transport capacity for example by increasing the river width. Unfortunately, this measure is more efficient for the decrease of the bed load transport capacity than the suspended load whereas the latter influences the water quality more.

2. Fine sediments

In this section, different possible sources for fine sediments found in the river are analysed. This is done by modelling the sediment transport and comparing it with the concentration of fine sediments measured in the river.

In general, it is assumed that these fine sediments origin from topsoil that are loosened and transported through overland flow. This is possible as about 60% of the top soil consists of silt or clay which has a diameter of 62.5 µm or smaller.

2.1.Model setup for the modelling of the transport of fine sediments

2.1.1. Model choice

Similar as to hydrological models, there are different types of sediment yield models. Also in this case, there are lumped and distributed models, and empirical, conceptual or physical models. An overview of a limited number of models is given in Table 2-1 and additional information on some of these models is given in the sections hereafter. As shown in this overview, the models USLE/RUSLE, MUSLE, WEPP, CREAMS and two conceptual models are compared with each other. This comparison is mainly based on the information given in the book by Haan, Barfield and Hayes called 'Design Hydrology and Sedimentology for Small Catchments'.

The models WEPP and CREAMS are physical based; therefore the complexity and data requirement is high. The empirical models USLE/RUSLE and MUSLE are based on data of storms in the United States, however are applied on many different situations around the world. A comparison between the two presented conceptual models show their close resemblance as they use a similar formula for the sediment yield, however in the second modelling method a balance for the sediment storage is added to include the process of sediment accumulation. A more detailed description on the two modeling methods is given in the next section.

For this study, the MUSLE model will be applied as it is requires minimum data and is widely applied. Therefore, different tables developed for this method are available to limit the parameter ranges of the different factors applied. Also, this model can be combined with the chosen hydrological model FLEX-Topo in contrast to the physical models.

Table 2-1: Overview of a limited number of sediment transport models (Haan et al., 1994)

	USLE/RUSLE (Revised) Universal Soil Loss Equation	MUSLE Modified Universal Soil Loss Equation	WEPP (Ascough et al., 1995) Water Erosion Prediction Project	CREAMS Chemical Runoff Erosion in Agricultural Management Systems	Conceptual model 1 (Tilahun et al., 2013)	Conceptual model 2 (Lidén, 1999)
Type	Empirical	Empirical	Physical	Physical	Conceptual	Conceptual
Input data	- climate data (e.g. P, E_p, Q) - DEM map - Land cover map - Land use map - Soil type map	- climate data (e.g. P, E_p, Q) - DEM map - Land cover map - Land use map - Soil type map	- climate data (e.g. P, E_p, Q) - DEM map - Cropping/management map - Soil type map - Channel topography, soils, management practices, Hydraulic characteristics	- climate data (e.g. P, E_p, Q) - DEM map - Cropping/management map - Soil type map - Channel topography, soils, management practices, Hydraulic characteristics	- climate data (e.g. P, E_p, Q) - DEM map	- climate data (e.g. P, E_p, Q) - DEM map
Output	Sediment loss	Sediment loss	Soil erosion	Soil erosion	Sediment yield	Sediment yield
Output timescale	Single-storm events/monthly/yearly output	Monthly/yearly output	Single-storm events/monthly/yearly output	Single-storm events/monthly/yearly output	Monthly/yearly output	Daily/monthly/yearly output
Method	Describes soil erosion as a function of rainfall energy & intensity, soil erodibility, slope length & steepness, soil cover, conservation practices	Predicts sediment yield; Parameters lumped for HRU, spatial distribution ignored	Predicts erosion in uniformly spaced rills	Estimates sum of all rill erosion on a slope segment by predicting interrill and rill erosion separately	Estimates the sediment yield based on the flow rate	Estimates the sediment yield based on the flow rate
Calibration parameters	-	-	-	-	2 parameters: n, α	4 parameters: a, b, c, d
Application: area scale	Large catchments	Large catchments	Small catchments	Field sized areas	Sloped catchments	Catchments
Assumption	Standard tables available for the estimation of the factors R, K,LS,C and P determined in the U.S. are applicable worldwide	Calibrated conceptual parameters (11.8 and 0.56) for the U.S. applicable worldwide	Uniform rill spacing of 1m; parameters are estimated the U.S. are applicable world wide	Assumes homogeneous land use, soil type, rain intensity	- linear relation between Sediment concentration and Velocity from (sub-) basin - dilution with interflow	No deposition or re-suspension in the river
Popularity	Widely used to predict the impact of land use on soil erosion	Applied in SWAT	Still under development, further testing on the application for watersheds conditions is needed		Case study: 113ha large catchment in the Ethiopian Highlands	Case study: 200 km^2 large catchment in Bolivia
Additional comments	Parameters based on small plot measurements, thus scaling up to watershed scale results in over-/underestimation of soil loss at the outlet (Tilahun et al., 2013)	Rainfall energy term in USLE replaced with a Runoff energy term	- Modification from CREAMS model - runoff predictions based on infiltration excess	Interrill erosion: predicted as function of rainfall energy, interril erodibility, slope steepness, interrill cover factor; Rill erosion: predicted as function of runoff volume, peak discharge, rill erodibility, slope steepness, slope length, rill cover, practice factors		No river routing included which was acceptable for this case as deposition and re-suspension in the river is negligible due to the small catchment size and large altitude differences

Additional information for the model: USLE/RUSLE/MUSLE

The models USLE, RUSLE and MUSLE calculate the potential sediment loss S based on different site specific parameters: the rainfall runoff, topography, soil type and land use. For the determination of each parameter, empirical formulas and tables are available. These empirical relations are based on data from storms in 24 states in the United States.(Haan et al., 1994)

$S = R * K * L * S * C * P$ USLE/RUSLE

$S = 11.8 * (Q * q_p * A)^{0.56} * K * LS * C * P$ MUSLE

With:

- S : potential sediment loss [t/(d ha)]
- Q : surface runoff volume of a single storm [mm/storm]
- q_p : peak runoff [m^3/s]
- A : area [ha]
- K : soil erodibility factor [ton m^2 hr/(m^3 ton cm)]
- LS : land topographic factor [-]
- C : land cover and management factor [-]
- P : support practice factor [-]

Cârdei performed a dimensional analysis of this formula and concluded that the dimensions have no physical meaning (Cârdei, 2010). Therefore this formula is dimensionally incorrect. However this model is still widely used due to lack of data and/or lack of better models.

This formula does give logical responses to increased storm volume or peak runoff. Simplifying the storm with a triangular [see Figure 2-1], volume can be estimated with

$$V = 0.5 * q_p * T$$

This simplification changes product $Q*q_p$ in the runoff factor to

$$0.5 * qp^2 * T$$

Hence, the runoff factor changes to

$$11.8 * (0.5 * q_p^2 * T)^{0.56} \approx 11.5 * q_p * (0.5 * T)^{0.5} = constant * q_p * T^{0.5}$$

Or

$$11.8 * \left(2 * \frac{V^2}{T}\right)^{0.56} \approx constant * V * T^{-0.5}$$

This simplification shows:

- The soil loss increases with the peak runoff and storm duration, however more extreme with the first.
- The soil loss increases with the storm volume and decreases with the storm duration.

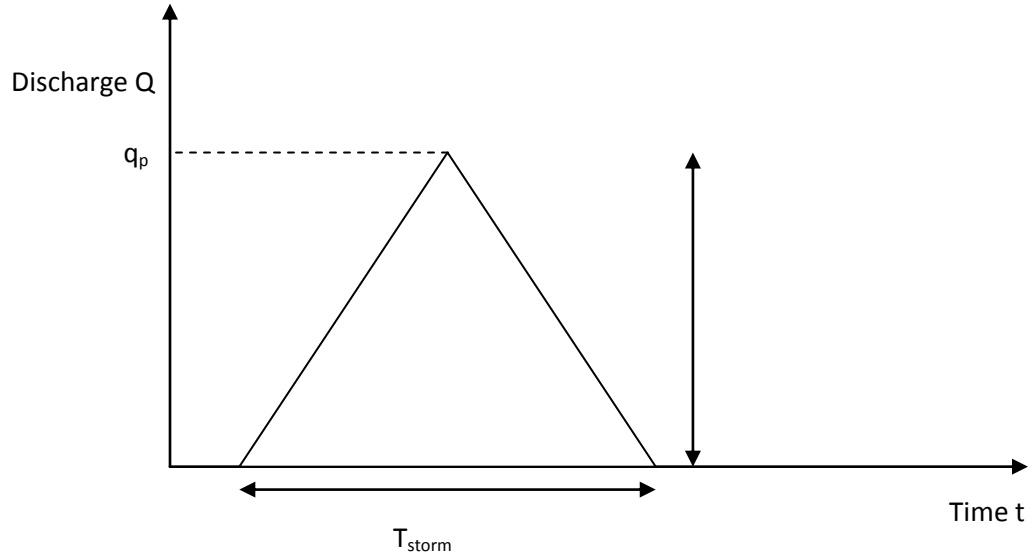

Figure 2-1: Simplification of a storm with duration T_{storm} and maximum runoff q_p

Additional information for the model: Conceptual model 1

In the first conceptual model, the sediment yield Y is calculated based on the runoff rate using two parameters. The physical justification of this conceptual model is based on the Hairsine and Rose model. This model is applied and tested by Tilahun in an 113ha large catchment in the Ethiopian Highlands. (Tilahun et al., 2013)

$$C_i = \alpha_i * q_i^n$$

$$Q_i = A_i * q_i$$

$$Y_i = C_i * Q_i = C_i * A_i * q_i = \alpha_i * q_i^n * A_i * q_i$$

$$Y_{tot} = \Sigma(C_i * Q_i) = \Sigma(\alpha_i * A_i * q_i^{n+1})$$

- C sediment concentration [kg/m^3]
- q runoff rate per unit area [m/day]
- Q runoff rate [m^3/day]
- Y_i sediment yield per sub-area [kg/day]
- α parameter: function of the slope, Manning's roughness coefficient, slope length, effective deposition and vegetation cover
- n parameter: n=0.4 if the width is much larger than the water depth

Additional information for the model: Conceptual model 2

Also in the second conceptual model, the sediment yield calculation is based on the runoff. Therefore also in this case, a hydrological model is used as basis as it is used for the calculation of the runoff. This model is applied by Lidén in a 200 km^2 large catchment in Bolivia. (Lidén, 1999)

$$SS_{acc} = a * P^b$$

$$SS_{yield} = H_{sed} * \left(\frac{Q}{c}\right)^d \quad if\ Q < c$$

$$SS_{yield} = H_{sed} \quad if\ Q \geq c$$

$$\frac{dH_{sed}}{dt} = a * [P(t)]^b - H_{sed}(t) * \left(\frac{Q(t)}{c}\right)^d \quad if\ Q < c$$

$$\frac{dH_{sed}}{dt} = a * [P(t)]^b - H_{sed}(t) \quad if\ Q \geq c$$

- SS_{acc} accumulated mobilized sediment [kg/day]
- P precipitation [mm/day]
- H_{sed} total sediment storage available to flush out [kg]
- SS_{yield} suspended sediment yield at outlet [kg/day]
- Q discharge [mm/day]
- a parameter [kg/mm^{-b}]
- b parameter [-]
- c parameter (upper limit at which whole H_{sed} is discharged) [mm/day]
- d parameter (describes the shape, see Figure 2-2) [-]

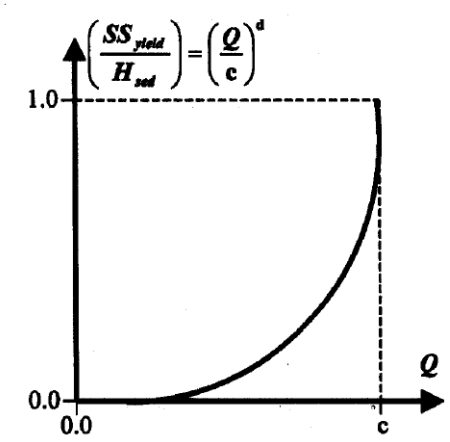

Figure 2-2: Graphical description of the release function for the suspended sediment yield (Lidén, 1999)

2.1.2. Modelling methodology applying MUSLE

The empirical model MUSLE (Modified Universal Soil Loss Equation) is based a modified version of the USLE. With this model, the sediment transport caused by sheet erosion is calculated depending on the following factors:

- Rain intensity
- Soil type
- Slope
- Land use
- Land management

The formula used in this model is (Neitsch et al., 2011):

$$S = 11.8 * \left(Q * q_p * A\right)^{0.56} * K * LS * C * P$$

With:

- Q : surface runoff [mm/d]
- q_p : peak runoff [m^3/s]
- A : area [ha]
- K : soil erodibility factor [ton m^2 hr/(m^3 ton cm)]
- LS : land topographic factor [-]
- C : land cover and management factor [-]
- P : support practice factor [-]

2.1.3. Estimation of the peak runoff according to the SWAT guidelines

To estimate the peak runoff the methodology explained in the SWAT guide is applied and summarized in this section (Neitsch et al., 2011). For this estimation the rational formula is used:

$$q_{peak} = C * i * A$$

With

- q_p : peak runoff [L^3/T]
- C : runoff coefficient [-]
- i : rainfall intensity [L/T]
- A : catchment area [L^2]

The runoff coefficient is equal to

$$C = \frac{Q_{\text{surface}}}{\text{R}_{\text{day}}}$$

With

- $Q_{surface}$: surface runoff for the day [L]
- R_{day} : rainfall for the day [L]

The rainfall intensity can be estimated with

$$i = \frac{R_{tc}}{t_c}$$

With

- t_c : time of concentration [T]
- R_{tc} : amount of rain falling during the time of concentration [L]

The amount of rain falling during the concentration time is a fraction of the daily rainfall:

$$R_{tc} = \alpha_{tc} * R_{day}$$

Combining the original formula of the peak discharge and the ones for the runoff coefficient and rainfall intensity results in the following equation for the q_{peak}:

$$q_{peak} = \frac{\alpha_{tc} * Q_{surf} * A}{t_c}$$

In Overview 2-1, the calculation of the fraction α_{tc} is explained and in Overview 2-2 the estimation of the concentration time t_c.

Overview 2-1: Estimation of the fraction α_{tc} according to the SWAT guide (Neitsch et al., 2011)

In SWAT, the fraction of rain falling in the concentration time is estimation with the following formula:

$$\boldsymbol{\alpha_{tc} = 1 - \exp\left[2 * t_c * \ln(1 - \alpha_{0.5})\right]}$$

With

- $\alpha_{0.5}$: the fraction of daily rain falling in the half-hour highest intensity [-]
- t_c : concentration time [T]

The maximum half-hour rainfall fraction of the day $\alpha_{0.5}$ is estimated with:

$$\boldsymbol{if\ rnd \leq \frac{\alpha_{0.5mon} - \alpha_{0.5L}}{\alpha_{0.5U} - \alpha_{0.5L}}}\ :$$

$$\boldsymbol{\alpha_{0.5} = \alpha_{0.5mon} * \frac{\alpha_{0.5L} + [rnd * (\alpha_{0.5U} - \alpha_{0.5L}) * (\alpha_{0.5mon} - \alpha_{0.5L})]^{0.5}}{\alpha_{0.5mon}}}$$

$$\boldsymbol{if\ rnd > \frac{\alpha_{0.5mon} - \alpha_{0.5L}}{\alpha_{0.5U} - \alpha_{0.5L}}}\ :$$

$$\boldsymbol{\alpha_{0.5} = \alpha_{0.5mon} * \frac{\alpha_{0.5U} - (\alpha_{0.5U} - \alpha_{0.5mon}) * \left[\frac{\alpha_{0.5U} * (1 - rnd) - \alpha_{0.5L} * (1 - rnd)}{\alpha_{0.5U} - \alpha_{0.5mon}}\right]^{0.5}}{\alpha_{0.5mon}}}$$

With

- $\alpha_{0.5mon}$: average maximum half-hour rainfall fraction for the month
- $\alpha_{0.5L}$: smallest half-hour rainfall fraction that can be generated, this is set to 0.02083
- $\alpha_{0.5U}$: largest half-hour fraction that can be generated
- rnd : random number between 0 and 1 generated by the number each day. Here both extremes are used to determine a upper and lower limit for the peak runoff and thus also for the sediment load.

The largest half-hour rainfall fraction $\alpha_{0.5U}$ is estimated with:

$$\boldsymbol{\alpha_{0.5U} = 1 - \exp\left(\frac{-125}{R_{day} + 5}\right)}$$

The average maximum half-hour rainfall fraction for the month $\alpha_{0.5mon}$ is estimated with:

$$\boldsymbol{\alpha_{0.5mon} = adj_{0.5\alpha} * \left[1 - \exp\left(\frac{R_{0.5sm(mon)}}{\mu_{mon} * \ln\left(\frac{0.5}{yrs} * days_{wet}\right)}\right)\right]}$$

With

- $adj_{0.5\alpha}$: an adjustment factor [-], here it is chosen to be 1 as no adjustments are desired at this stage
- $R_{0.5sm(mon)}$: smoothed half-hour rainfall amount for the month [L]
- μ_{mon} : mean daily rainfall [L]
- yrs : number of years of rainfall data used
- $days_{wet}$: number of wet days in the month

The smoothed half-hour rainfall amount for the month $R_{0.5sm(mon)}$ is estimated with:

$$\boldsymbol{R_{0.5sm(mon)} = \frac{1}{3} * (R_{0.5(mon-1)} + R_{0.5(mon)} + R_{0.5(mon+1)})}$$

With:

- $R_{0.5sm(mon)}$: smoothed maximum half-hour rainfall for a given month [L]
- $R_{0.5sm(x)}$: smoothed maximum half-hour rainfall for the specified month x [L]

Overview 2-2: Estimation of the concentration time t_c according to the SWAT guide (Neitsch et al., 2011)

The amount of time between the start of a rainfall event and the moment at which the entire area is contributing to the flow at the outlet is called the concentration time. Hence, it is the time a droplet needs to travel from the furthest place to the outlet. To estimate this concentration time, the overland flow time t_{ov} and the channel flow time t_{ch} are summed up. Then the traveling time of a droplet towards the nearest channel (t_{ov}) is taken into account, but also the time in the channel towards the outlet (t_{ch}) (Neitsch et al., 2011)

$$t_c = t_{ov} + t_{ch}$$

Overland flow time t_{ov}

The overland flow time depends on the slope length of the area L_{slp} [s] and the overland flow velocity v_{ov} [m/s]:

$$t_{ov} = \frac{L_{slp}}{v_{ov}}$$

The velocity can be estimated with the Manning's equation:

$$Q = \frac{1}{n} * A * R^{\frac{2}{3}} * i^{\frac{1}{2}}$$

Using the equations $Q = q * B$, $A = B * h$, $R \sim h$ and $q = u * h$ results in

$$q = \frac{1}{B} * \frac{1}{n} * h^{\frac{5}{3}} * i^{\frac{1}{2}} = \frac{1}{B} * \frac{1}{n} * \left(\frac{q}{u}\right)^{\frac{5}{3}} * i^{\frac{1}{2}}$$

$$u = \frac{1}{B^{\frac{3}{5}}} * \frac{1}{n^{\frac{3}{5}}} * q^{\frac{2}{5}} * i^{\frac{3}{10}}$$

Hence, the overland flow velocity is equal to

$$v_{ov} = \frac{1}{B^{0.6}} * \frac{1}{n^{0.6}} * q^{0.4} * i^{0.3}$$

With:

- n : Manning's roughness coefficient [s/m$^{1/3}$]; this is assumed to be between 0.07 and 0.24 s/m$^{1/3}$ which are typical values for crop fields with poor agricultural practices and grass lands (Neitsch et al., 2011).
- q : average overland flow rate [m^2/s]
- i : average slope in the area [-]
- A : wet cross-sectional area [m^2]
- R : hydraulic radius [m]
- h : water depth [m]
- u : velocity of the water [m/s]
- B : width, here a 1 m wide strip is considered

In the SWAT guide, the average overland flow rate is assumed to be 6.35 mm/hr, however here the average modelled value for hortonian overland flow is used.

Channel flow time t_{ch}

The channel flow time depends on the average flow channel length L_{ch} [m] and the average channel velocity v_{ch} [m/s]:

$$t_{ch} = \frac{L_{ch}}{v_{ch}}$$

The average channel length is estimated with

$$L_{ch} = \sqrt{L * Lcen}$$

With

- L : channel length from the most distant point to the basin outlet
- L_{cen} : channel length to the basin centroid. This is assumed to be equal to L_{cen}=0.5L

Thus, the average channel length can be estimated with $L_{ch} = 0.71 * L$.

The average velocity is estimated with the Manning's equation with the assumption:

- Trapezoidal channel with 2:1 side slopes
- Bottom width-depth ratio of 10:1

This results in an average velocity of

$$v_{ch} = \frac{0.489 * Q_{ch}^{0.25} * i^{0.375}}{n^{0.75}}$$

With:

- Q_{ch} : average channel flow rate [m^3/s]. In the SWAT manual this is estimated based on the assumed overland flow of 6.35 mm/hr, however here the average modelled value for the total outflow is taken.
- i : channel slope [-]
- n : Manning's roughness coefficient for the channel [s/m$^{1/3}$]; this is assumed to be 0.028 s/m$^{1/3}$ which is the average value for a natural channel (I. Ankum, 2002)

2.1.4. Estimation of the factors K, LS, C and P according to the SWAT guidelines

In this section, the estimation of the factors is explained. This is done based on the formulas used in the SWAT manual (Neitsch et al., 2011).

Soil erodibility factor K

Using the soil map called KENSOTER of the Mara River Basin, the soil erodibility factor K is estimated with the following formula:

$$K = \frac{0.00021 * M^{1.14} * (12 - OM) + 3.25 * (c_{soilstr} - 2) + 2.5 * (c_{perm} - 3)}{100}$$

With

- M : particle-size parameter
- OM : percent organic matter (%)
- $c_{soilstr}$: soil structure code
- c_{perm} : profile permeability class

The particle-size parameter is equal to:

$$M = (m_{silt} + m_{vfs}) * (100 - m_c)$$

With

- m_{silt} : percent silt content
- m_{vfs} : percent very fine sand content
- m_c : percent clay content

The percentage organic matter is estimated with:

$$OM = 1.72 * orgC$$

With

- orgC : percent organic carbon content

The codes assigned to the soil structures $c_{soilstr}$ are:

1. very fine granular
2. fine granular
3. medium or coarse granular
4. blocky, platy, prism like or massive

The codes for the permeability c_{perm} are:

1. rapid (>150mm/hr)
2. moderate to rapid (50-150 mm/hr)
3. moderate (15-50 mm/hr)
4. slow to moderate (5-15 mm/hr)
5. slow (1-5 mm/hr)
6. very slow (<1mm/hr)

In the Mara River Basin, the soil erodibility factor is found to be between 0.013 ton m^2 hr/(m^3 ton cm) and 0.047 ton m^2 hr/(m^3 ton cm). In Table 2-2, the results for this factor as also the used values for the calculation are shown. For the very fine sand content, a range is given between zero and a certain maximum for the following reason: In the KENSOTER database, only the percentage of sand is given which includes very fine sand with a diameter of 1/16-1/8 mm, but also coarser sand types with diameters between 1/8 and 2 mm. Therefore, the very fine sand content may vary between zero and the value given for sand in general. This range results also in a range in the erodibility factor K as shown in the table. For the first modelling run, the average value is used.

Table 2-2: Data used to calculate the soil erodibility factor K for each sub-catchment in the Mara River Basin and the Nyangores sub-catchment as well. These values are estimated based on the map KENSOTER

	Nyangores	North	Middle	Talek	Sand	Lower
m_{silt}	44.38%	33.69%	10.09%	28.67%	16.86%	29.73%
m_{vfs}	0-33.35%	0-27.95%	0-12.61%	0-44.23%	0-27.47%	0-41.14%
m_c	22.27%	17.55%	12.66%	31.11%	17.28%	29.07%
$c_{soilstr}$	3	3	4	3	3	3
c_{perm}	3	2.2	1.3	4.5	2.3	3.1
orgC	4.45%	2.67%	0.45%	1.48%	0.96%	1.58%
K	0.017-0.028	0.018-0.036	0.0098-0.020	0.024-0.052	0.013-0.035	0.020-0.047

Land topographic factor LS

To estimate the topographic factor, a digital elevation map is used. With this map, the slope is calculated for each cell. Based on the slope and the slope length which is equal to the grid size in this case, the topographic factor is calculated for each cell using the following formula:

$$LS = \left(\frac{L}{22.1}\right)^{m} * (65.41 * (\sin(\alpha_{hill}))^2 + 4.56 * \sin(\alpha_{hill}) + 0.065)$$

$$m = 0.6 * (1 - \exp(-35.835 * slp))$$

With:

- L : slope length [m]
- α_{hill} : angle of the slope
- slp : slope of the hill (slp=tan(α_{hill}))

This calculation is done for each sub-catchment and each land cover type separately as shown in Table 2-3. Only the land cover types are shown where significant soil erosion is expected, thus agricultural fields and grasslands.

Table 2-3: Average slope used to calculate the land topographic factor LS for each sub-catchment in the Mara River Basin and the Nyangores sub-catchment as well. These values are estimated based on the digital elevation map which has a resolution of 90 m

	Nyangores	North	Middle	Talek	Sand	Lower
Slope (agriculture)	0.13	0.09	0.03	0.03	NA	0.05
Slope (grassland)	NA	0.10	0.05	0.04	0.07	0.05
LS (agriculture)	4.99	3.29	0.65	0.74	NA	1.36
LS (grassland)	NA	3.70	1.44	1.11	2.29	1.35

Land cover and management factor C

The estimation of the land cover and management factor is based on the NDVI of the year 2014. It is known that for a forested area, this factor is equal to 0 as no erosion expected there whereas it is 1 for base areas where maximum erosion is expected. Using these two extremes the average NDVI per land cover type is related to this factor by assuming a linear relation. With this relation, the land cover factor is estimated for crop, grass and shrub lands. (Karaburun, 2010)

This methodology is applied since too little knowledge is available on the agricultural practices within the basin to estimate this factor as explained in the SWAT guide.

Table 2-4: Estimation of the land cover and management factor C based on the NDVI

Land cover type	Mean NDVI	Factor C
Forest	0.74	0.00
Agriculture	0.58	0.27
Shrubs	0.53	0.36
Grass	0.49	0.43
Bare	0.17	1.00

Support practise factor P

The support practise factor is estimated by using standard tables in which the influence of different practises as contour farming, strip cropping or terracing is documented; see for example Figure 2-3 which is taken from the SWAT guide. For instance the value 0.8 should be used if contour farming is applied on a slope between 17 and 20%.

Land slope (%)	P_{USLE}	Maximum length (m)
1 to 2	0.60	122
3 to 5	0.50	91
6 to 8	0.50	61
9 to 12	0.60	37
13 to 16	0.70	24
17 to 20	0.80	18
21 to 25	0.90	15

Figure 2-3: P factor values and slope-length limits for contouring (Neitsch et al., 2011)

2.2.Model results

In the previous section, the parameters are estimated applying the guidelines of SWAT. In this section, the first model results are shown. However, adjustments are done to the MUSLE formula as also the parameter estimation in order to obtain model results that are closer to the data. This analysis is done for the Nyangores sub-catchment as only there sufficient data is available. For the entire Mara River Basin, it is assumed that these analysis results are valid as well.

2.2.1. First model results for the Nyangores sub-catchment

Application of the MUSLE formula combined with the hydrological model results in the simulation of the suspended sediment flow on a daily scale with an upper limit S_{max} and a lower limit S_{min} (see Figure 2-4). This is the result of choosing a random of 0 and 1 in the estimation of the peak runoff (see section 2.1.3).

The data is compared with the model results graphically and by evaluating the root mean squared error (RMSE) which is calculated with the equation shown below. A graphical comparison of this model with the little data available shows that the data is between the two extremes: on average the observed load is 128 t/d whereas an 58 t/d to 201 t/d is simulated. The RMSE is between 182 t/d and 733 t/d.

$$RMSE = \left(\frac{1}{n}\Sigma(S_m - S_o)^2\right)^{0.5}$$

S_m is the modelled sediment load, S_o the observed load and n the total number of data points.

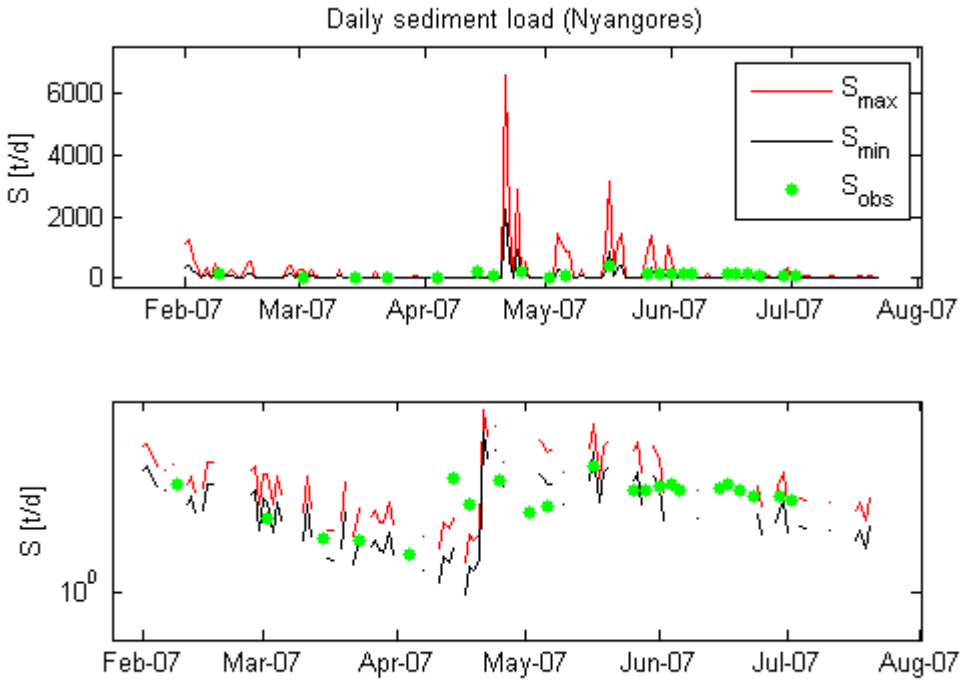

Figure 2-4: Daily suspended sediment load

2.2.2. Analysis on the estimation of the peak runoff

According to the SWAT manual, the peak runoff q_p (see formula) can be estimated by applying the rational formula. To approximate the parameters of this formula, physical and empirical relations are available. For these relations, detailed information on the precipitation, roughness and river cross-section. As this information is lacking, one is forced to make many assumptions and do simplifications. As a result, the accuracy of this estimation is doubtful.

$$S = 11.8 * \left(Q * q_p * A\right)^{0.56} * K * LS * C * P$$

Alternatively, the peak runoff can be estimated based on merely the modelled total runoff Q_m averaged over the entire day. As shown in Figure 2-5, the order of magnitude of the simulation results is similar in both cases: when using Q_m the average modelled load is 94 t/d and the RMSE is 154 t/d. Thus estimating the peak runoff based on Q_m has two advantages: 1) the assumptions and simplifications needed for the estimation of the peak runoff according to the SWAT manual is avoided, and 2) the RMSE is decreased. Therefore, this alternative methodology is preferred.

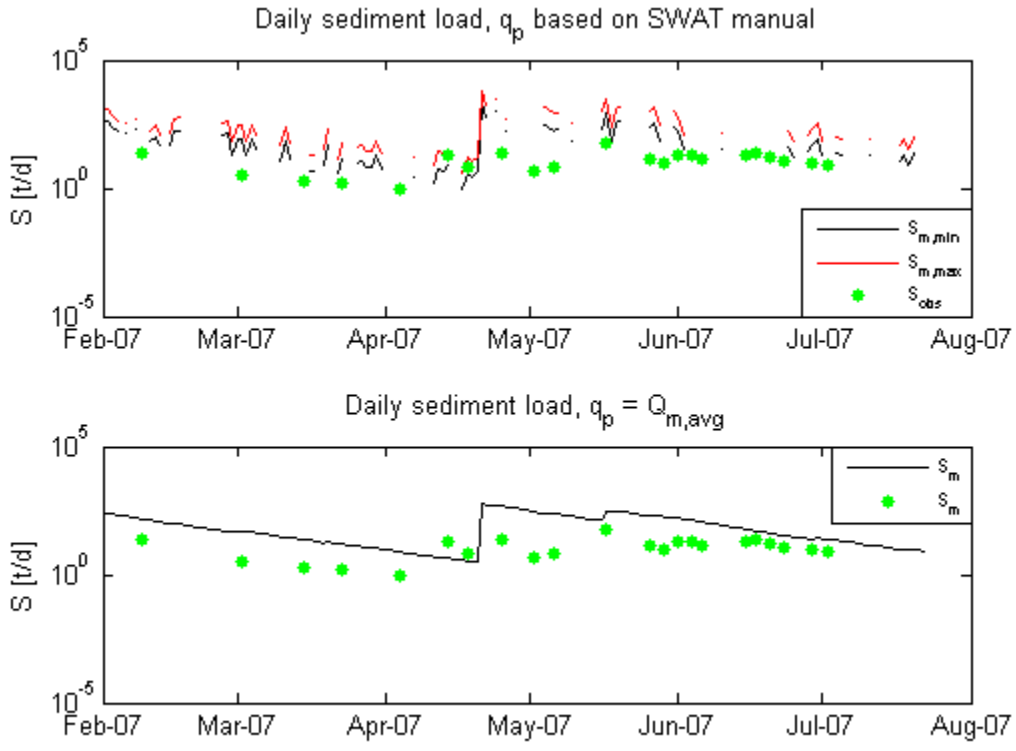

Figure 2-5: Model results applying the SWAT guideline (upper) and the average total runoff Q_m (lower) for the peak runoff

Instead of using the total modelled runoff Q_m, the average of the hortonian overland flow HOF might improve the model results with the assumption that the latter has a dominant impact on the sediment load. This is also the case as shown in Figure 2-6. Also the RMSE indicates that the model performance

increases: the RMSE decreased from 154 t/d and 58 t/d. Hence, graphical observation and the RMSE indicate that the peak runoff should be based on the hortonian overland flow HOF.

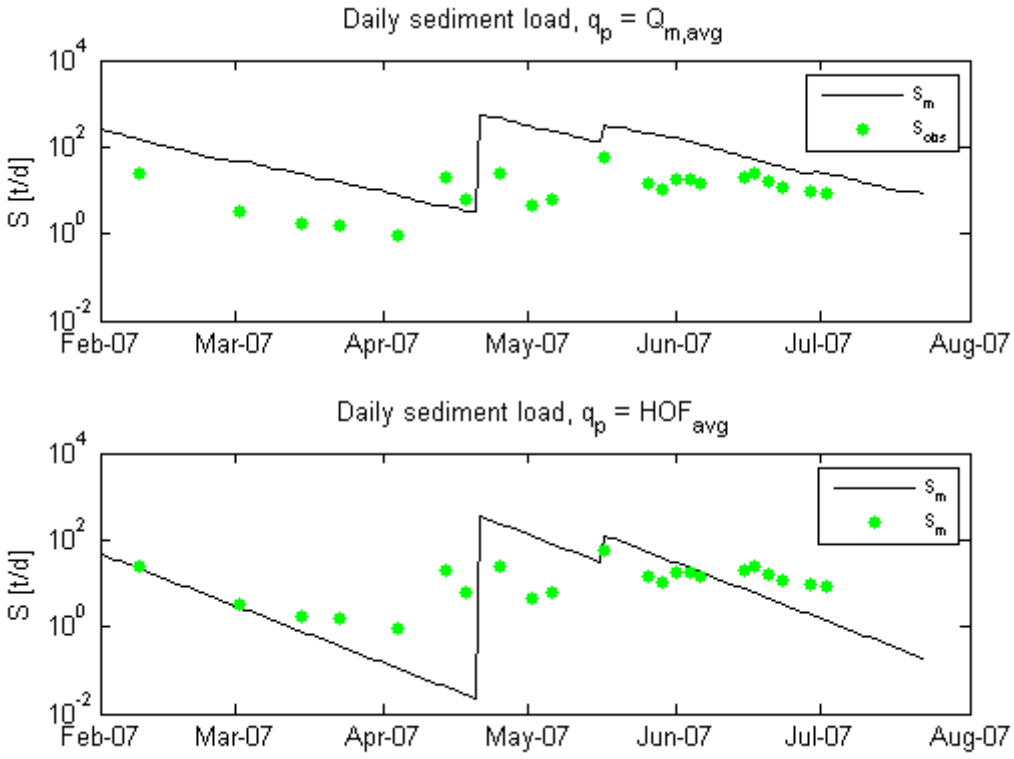

Figure 2-6: Model results using the average total runoff (upper) and the average hortonian overland flow (HOF; lower) (lower) for the peak runoff

By averaging the runoff over the entire day, peak runoff values are lost; hence the peak runoff as also the sediment load is under estimated. In reality, this peak runoff is larger however it is unknown how much larger. Therefore, the peak runoff is increased arbitrary to analyse the influence of such a change. Originally, the peak runoff is averaged over 24 hours, now however over 3 hours and 1 hour.

As shown in Figure 2-7, this does not improve the model clearly as all three options result in sediment loads of a similar order of magnitude. The RMSE implicates though that averaging over 24 hours yields the best performance; see Table 2-5. That is why this duration is used for the estimation of the peak runoff. It is recommended though to do more detailed studies on the peak runoff to obtain more accurate results.

Table 2-5: Results on the RMSE estimating for the peak runoff by averaging the total runoff Q_m averaged over 24 h, 3 h or 1 h

	RMSE
24 hours	58 t/d
3 hours	206 t/d
1 hour	391 t/d

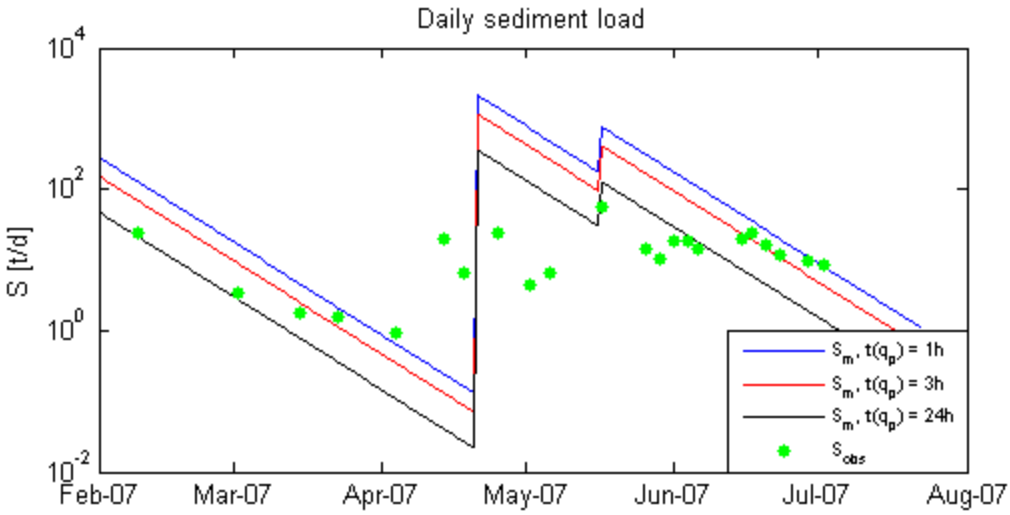

Figure 2-7: Model results using different estimation for the peak runoff: the total runoff Q_m averaged over 24 hours, 3 hours and 1 hour

2.2.3. Analysis on the estimation of the surface runoff volume

For the surface runoff volume Q (see formula), the fast runoff is applied. However, should this include merely the hortonion overland flow or all fast runoff components? To answer this question, the sediment load is simulated for both cases as shown in Figure 2-8.

$$S = 11.8 * \left(Q * q_p * A\right)^{0.56} * K * LS * C * P$$

Graphical comparison of both options shows that the use of only the hortonian overland flow for the surface runoff volume yields in slightly better results. Also, the RMSE increases to 77 t/d when using the total fast runoff; this value is equal to RMSE = 58 t/d using the HOF. That is why the usage of merely the HOF for the surface runoff volume is preferred.

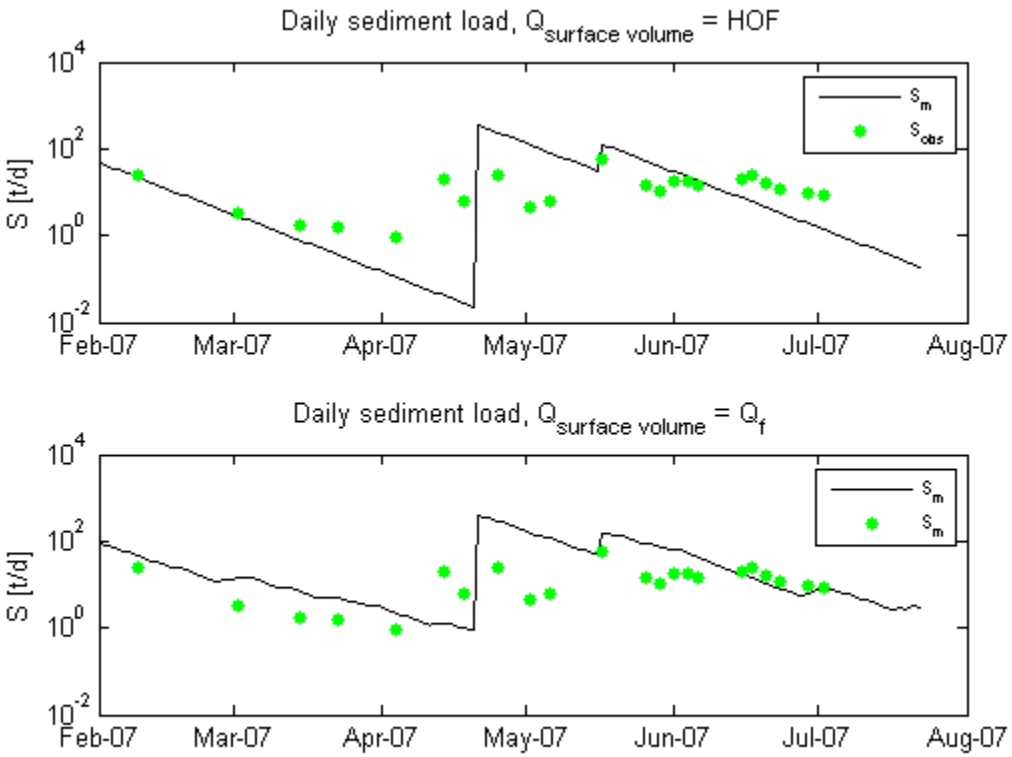

Figure 2-8: Model results applying the hortonion overland flow (upper) and the total fast runoff (lower) for the surface runoff

This choice is confirmed and becomes even clearer when reanalysis the choice of peak runoff in combination with the choice of surface runoff volume. In Table 2-6 these combinations and their results for the RMSE are indicated. With this table it can be seen that using the HOF for both the peak runoff and the surface runoff volume yields the lowest RMSE.

Table 2-6: Results for different estimation methods for the peak runoff q_p and the surface volume $Q_{surface\ volume}$

Tested combination for q_p and $Q_{surface\ volume}$	RMSE
$q_p = HOF_{avg}$ and $Q_{surface\ volume} = HOF$	58 t/d
$q_p = HOF_{avg}$ and $Q_{surface\ volume} = Q_f$	77 t/d
$q_p = Q_{m,avg}$ and $Q_{surface\ volume} = HOF$	154 t/d
$q_p = Q_{m,avg}$ and $Q_{surface\ volume} = Q_f$	259 t/d

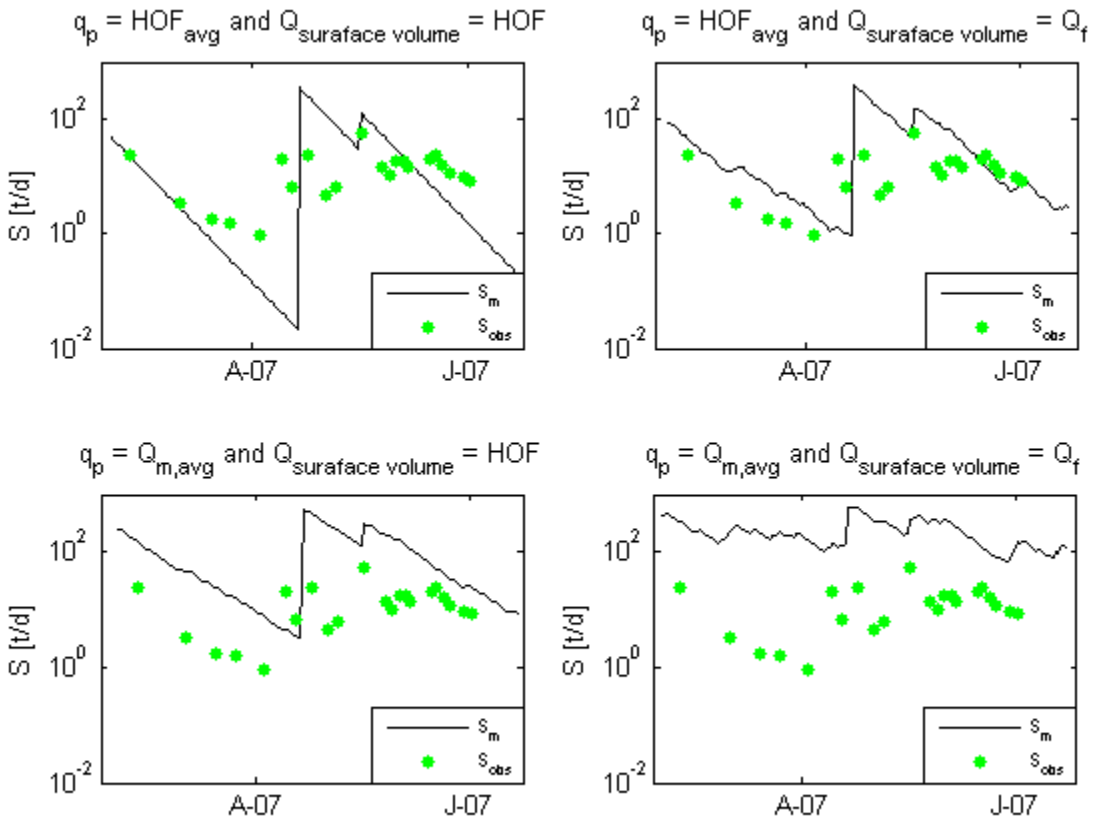

Figure 2-9: Results for different estimation methods for the peak runoff q_p and the surface volume $Q_{surface\ volume}$

2.2.4. Analysis on the estimation of the conceptual factors

In the MUSLE formula, the two conceptual parameters α and β are calibrated based on various catchments in the US. Based on this calibration, the values are found to be α =11.8 and β =0.56. However, Odongo calibrated these parameters as well, this time though for the upper Malewa catchment in Kenya (Odongo et al., 2013). He discovered that the sediment load is overestimated when applying the original values of the MUSLE and that these parameters should be equal to α =7.13-8.54 and β =0.32-0.42 based on his calibration results.

$$S = \alpha * (Q * q_p * A)^{\beta} * K * LS * C * P$$

The original parameter values are compared with the ones found by Odongo. This comparison shows that the values of Odongo increase the model performance slightly; see Table 2-7 and Figure 2-10. Therefore it is advised to estimate these parameters for this specific catchment to increase the model performance.

Table 2-7: Results on the RMSE using different values for the conceptual parameters a and b

	RMSE
Using original values of the MUSLE: α =11.8, β =0.56	58 t/d
Using values found by Odongo: α =7.13, β =0.32	17 t/d
Using values found by Odongo: α =8.54, β =0.42	14 t/d

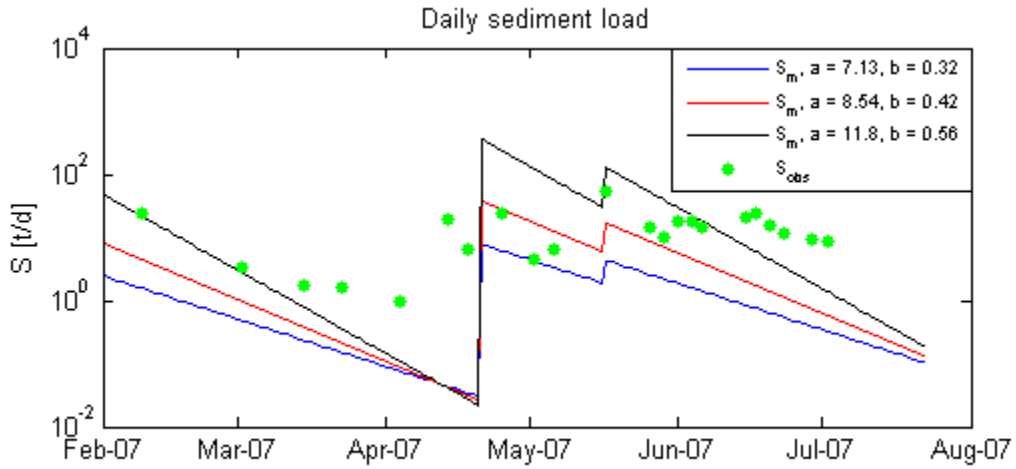

Figure 2-10: Model results with conceptual parameters according to the MUSLE formula (α=11.8, β=0.56) and according to Odongo

2.2.5. Final model results

With these adjustments explained in the previous sections, an improved model is obtained. These adjustments are applied for the Nyangores sub-catchment, but also the entire Mara River Basin (see Figure 5-5). Comparing the data with the model results in the Nyangores now shows that the RMSE has decreased from the starting value of RMSE = 128 t/d – 477 t/d to RMSE = 102 t/d.

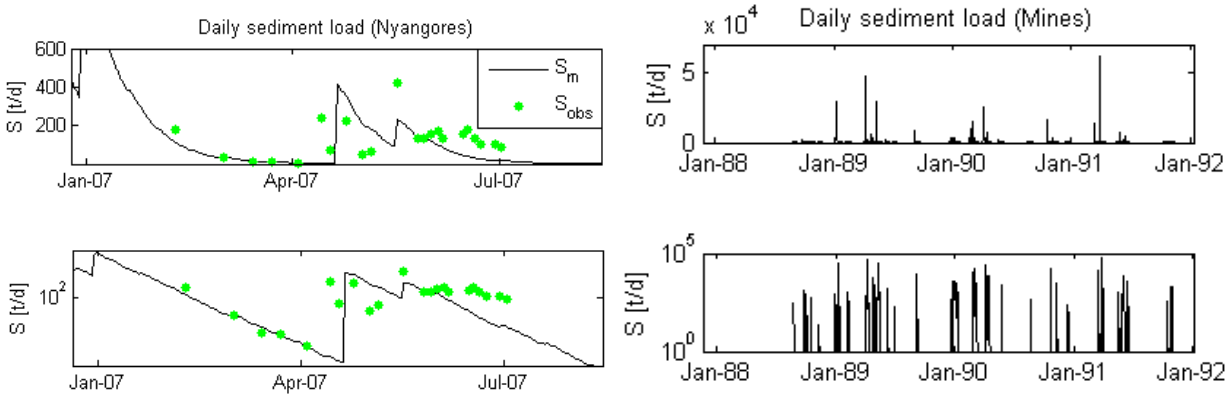

Figure 2-11: Model results for the Nyangores sub-catchment (left) and Mara River Basin (right)

For each sub-catchment within the Mara River Basin, the total and daily average sediment loads are calculated. As shown in Table 2-8, the largest sediment load is found at the outlet of the Sand sub-catchment.

Table 2-8: Sediment load at the river outlet of each sub-catchment: average daily value and total over the entire simulation period of 3.5 years

	Average daily sediment load [t/d]	Total sediment load [t/3.5yr]
North	1.95	2498
Middle	143.85	183981
Talek	238.93	305588
Sand	714.13	913372
Lower	608.26	777961

For a better comparison between the sub-catchment, the average soil loss over the sub-catchment in [mm/yr] is calculated. This is equal to the average sediment load divided through the area and the bulk density:

$$S_{avg} = \frac{S_{load}}{A * \rho_{bulk}}$$

With:

- S_{avg} : average soil loss [m/yr]
- S_{load} : average annual soil loss [t/yr]

- A : catchment area [m^2]
- ρ_{bulk} : bulk density [t/m^3]; for clay this value is typically 1.4 t/m^3

On average, the largest soil loss of 0.10 mm/yr is found in the Sand sub-catchment (see Table 5-3 and Figure 5-6). Also, the maximum per HRU is found in this sub-catchment for the grasslands areas: there the loss is 0.30 mm/yr.

Table 2-9: Soil loss per HRU (Agriculture or Grassland) and per sub-catchment in [mm/yr]

	Agriculture [mm/yr]	Grassland [mm/yr]	Total [mm/yr]
North	0.00040	NA	0.00022
Middle	0.077	0.078	0.036
Talek	NA	0.033	0.020
Sand	NA	0.30	0.10
Lower	0.20	0.15	0.054

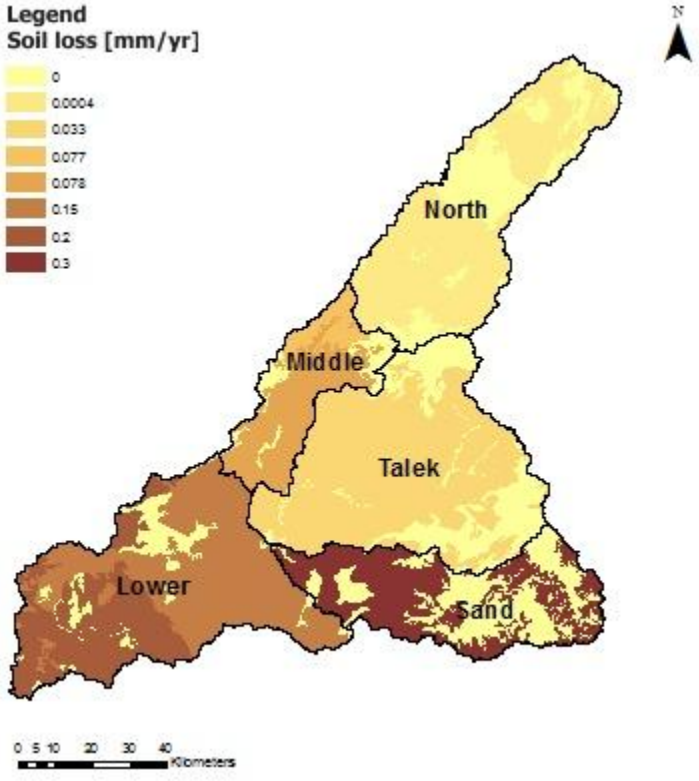

Figure 2-12: Map of the soil loss per HRU per sub-catchment

2.3.Sensitivity and uncertainty analysis

2.3.1. Parameter sensitivity

In this section, the parameter sensitivity is assessed. First, the maximum ranges of each parameter are determined as shown in Table 5-4. Then the model is run using the minimum and maximum value for each parameter separately and the sensitivity range is calculated with the formula shown below. This analysis is done for both the Nyangores sub-catchment and the entire Mara River Basin. As shown in Table 5-4, the model is the most sensitive to the parameter β.

$$sensitivity\ range = \frac{\Sigma(S_{max} - S_{min})}{\Sigma\ S_m}$$

With S_{max} and S_{min} the sediment load taking the maximum and minimum parameter value respectively and S_m the calculated load, using the chosen parameter value as shown in the table.

Table 2-10: Parameter values used for the sensitivity analysis and the resulting sensitivity range ΣΔS/S_m

	Min	Max	Chosen value	Sensitivity range Nyangores	Sensitivity range MRB
α	0	65	11.8	5.51	5.51
β	0 (0.3)	1 (0.6)	0.56	5069 (2.05)	38485 (2.54)
$t(q_p)$	24hr	1hr	24hr	1.54	1.54
K	K_{min}	K_{max}	K_{avg}	0.49	0.60
LS, C	-10%	+10%	+0%	0.10	0.28
P	0.06 (terrace)	1 (no practices)	0.8 (contour ploughing)	1.18	1.18

For the conceptual parameters, the minimum and maximum values are based on literature and narrowed based on data analysis. According to literature, α can range between 0 and 65; β ranges between 0 and 1 (Odongo et al., 2013). Within this data analysis, the sediment load is calculated with α and β ranging between their minimum and maximum. For each combination of α and β, the RMSE is calculated and evaluated. The lowest RMSE is found if β is between 0.3 and 0.6 regardless the value for α. Hence, the ranges for β are decreased accordingly. This reduces the sensitivity range ΣΔS/S_{avg} significantly as shown in the table.

2.3.2. Model uncertainty

There are many uncertainties in the estimation of the parameters used in the model. This results in uncertainties within the model as well. In this section, the model uncertainty is analysed. First, the maximum uncertainty is determined by taking the most extreme values for each parameter; hence the lowest and largest value possible. This range of the maximum uncertainty is shown in Figure 2-13 and is calculated using the same formula as the sensitivity range.

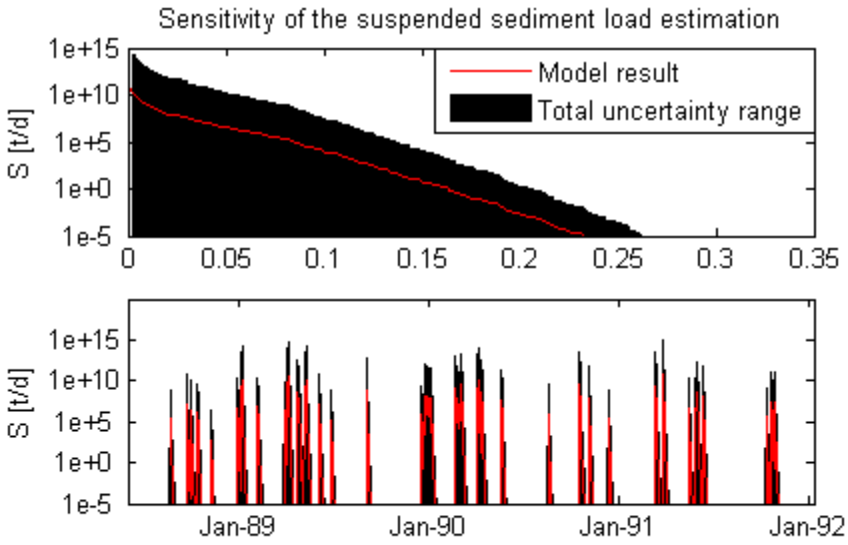

Figure 2-13: Maximum model uncertainty for the MRB with the sediment load sorted (upper) and unsorted (lower) in logarithmic scale

The aim is now to reduce this uncertainty as much as possible. This reduction can be achieved by reducing the uncertainty in each parameter. However, it is more effective to reduce merely the uncertainty of those parameters that have the largest impact on the entire model uncertainty. Therefore, the impact of each parameter is analysed and summarized in Table 2-11. First, the scenario with maximum uncertainty is analysed, hence none of the parameters is certain. This yields in a uncertainty range of about 60 000 in the Nyangores sub-catchment. If all uncertainties in the conceptual parameter β would be removed, hence this parameter would be fixed to a certain value then this difference would be reduced to 17.44. This is also the largest uncertainty reduction possible as shown in Table 2-11 and Figure 2-14. This is also the parameter with the largest sensitivity as shown in the previous section.

To reduce the mode uncertainty as much as possible, it is advised to first estimate the conceptual parameters α and β using turbidity and water level data. With this data, the sediment concentration can be estimated and compared to the modelling results. Then, it is advised to study the peak runoff more accurately.

Table 2-11: Impact of each parameter on the model uncertainty

	Uncertainty range Nyangores	Uncertainty range Mines
Nothing fixed	$3.92 \cdot 10^{4}$	$1.26 \cdot 10^{6}$
Nothring fixed, β range reduced	35.25	$5.26 \cdot 10^{1}$
Parameter β fixed	17.44	19.76
Parameters β, α fixed	3.15	3.57
Parameters β, α, q_p fixed	1.65	1.89
Parameters β, α, q_p, P fixed	0.61	0.91
Parameters β, α, q_p, P, K fixed	0.1	0.28

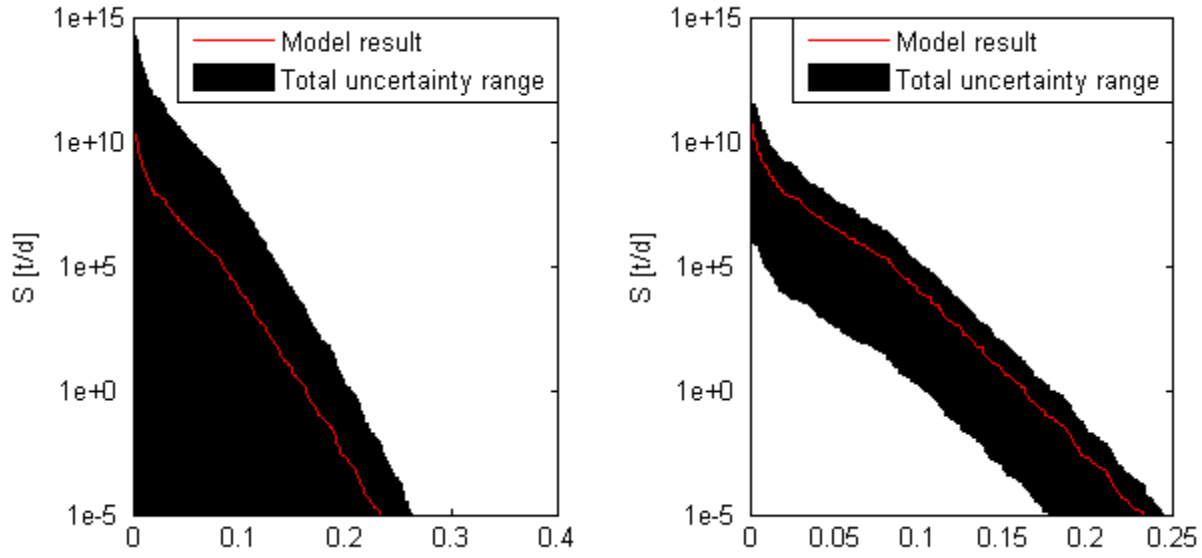

Figure 2-14: Reduction of the model uncertainty for the entire catchment: Maximum model uncertainty (left); reduced uncertainty by fixing the conceptual parameter α and β (right)

Appendix G: Excerpts of the model script

Table of Contents

1. Calculation of the outflow of a sub-catchment

```
function [Qm, Qo] = SubMod(Par,ExtraPar,sub, indices)

%% Binding
% calibration parameters
ImaxF = Par(1);
ImaxA = Par(2);
ImaxG = Par(3);
ImaxS = Par(4);
beta  = Par(5);
TlagH = Par(6);
KfH   = Par(7);
Kf    = Par(8);
Fmin  = Par(9);
a     = Par(10);
Ssmax = Par(11);
SH     = Par(12);
ST     = Par(13);
% fixed parameters
Ks      = ExtraPar.Fixed(1);
k       = ExtraPar.Fixed(2);
Ce      = ExtraPar.Fixed(3);
SumaxF  = ExtraPar.Fixed(4);
SumaxA  = ExtraPar.Fixed(5);
SumaxG  = ExtraPar.Fixed(6);
SumaxS  = ExtraPar.Fixed(7);
Smax    = ExtraPar.Fixed(7+sub);
% forcing data
P=ExtraPar.forcing(:,indices);
d=ExtraPar.forcing(:,4);
A=d.*(43.81+0.5*(3.524899+1.182903)*d);
R=A./(43.81+d.*(sqrt(1+3.524899^2)+sqrt(1+1.182903^2)));
Qo=a*A.*R.^(2/3);
tmax=length(Qo);
% storage
SuS=zeros(tmax,1);
SuA=zeros(tmax,1);
SuF=zeros(tmax,1);
SuG=zeros(tmax,1);
SfS=zeros(tmax,1);
SfF=zeros(tmax,1);
SfA=zeros(tmax,1);
SfG=zeros(tmax,1);
SfA1=zeros(tmax,1);
SfG1=zeros(tmax,1);
SfA2=zeros(tmax,1);
SfG2=zeros(tmax,1);
SoA=zeros(tmax,1);
SoG=zeros(tmax,1);
Ss=zeros(tmax,1);
% internal fluxes
RfF=zeros(tmax,1);
RfS=zeros(tmax,1);
RfA=zeros(tmax,1);
RfG=zeros(tmax,1);
RuF=zeros(tmax,1);
```

```
RuS=zeros(tmax,1);
RuA=zeros(tmax,1);
RuG=zeros(tmax,1);
RflF=zeros(tmax,1);
RflS=zeros(tmax,1);
RflA=zeros(tmax,1);
RflG=zeros(tmax,1);
PercS=zeros(tmax,1);
PercF=zeros(tmax,1);
PercA=zeros(tmax,1);
PercG=zeros(tmax,1);
FA=zeros(tmax,1);
FG=zeros(tmax,1);
HOFA=zeros(tmax,1);
HOFG=zeros(tmax,1);
Qfinf=zeros(tmax,1);
Qf_tot=zeros(tmax,1);
% Output fluxes
PeF=zeros(tmax,1);
PeS=zeros(tmax,1);
PeA=zeros(tmax,1);
PeG=zeros(tmax,1);
EF=zeros(tmax,1);
ES=zeros(tmax,1);
EA=zeros(tmax,1);
EG=zeros(tmax,1);
EoA=zeros(tmax,1);
EoG=zeros(tmax,1);
QfF=zeros(tmax,1);
QfS=zeros(tmax,1);
QfA=zeros(tmax,1);
QfG=zeros(tmax,1);
QfA1=zeros(tmax,1);
QfG1=zeros(tmax,1);
QfA2=zeros(tmax,1);
QfG2=zeros(tmax,1);
Qs=zeros(tmax,1);
Qm=zeros(tmax,1);
% proportion
PropF=ExtraPar.Topo{sub}(1,1);
PropS=ExtraPar.Topo{sub}(1,4);
PropA=ExtraPar.Topo{sub}(1,2);
PropG=ExtraPar.Topo{sub}(1,3);
% Potential Evaporation
ETh.y=ExtraPar.forcing(:,1);
ETh.m=ExtraPar.forcing(:,2);
ETh.d=ExtraPar.forcing(:,3);
ETh.Temp=ExtraPar.forcing(:,indices+1);
ETh.Tmax=ExtraPar.forcing(:,indices+2);
ETh.Tmin=ExtraPar.forcing(:,indices+3);
Ep=Hargreave(ETh);
% Interception
EiF=min(Ep,min(P,ImaxF));
EiS=min(Ep,min(P,ImaxS));
EiA=min(Ep,min(P,ImaxA));
EiG=min(Ep,min(P,ImaxG));
PeF=max(P-EiF,0);
```

```
PeS=max(P-EiS,0);
PeA=max(P-EiA,0);
PeG=max(P-EiG,0);

%% Forest
% Unsaturated reservoir
for t=1:tmax;
    C=1-(1-SuF(t)/SumaxF)^beta;
    RuF(t)=(1-C)*PeF(t);
    SuF(t)=SuF(t)+RuF(t);
    EF(t)=min((Ep(t)-EiF(t)),min(SuF(t),(Ep(t)-EiF(t))*SuF(t)/SumaxF/Ce));
    SuF(t)=SuF(t)-EF(t);
    PercF(t)=min(SH*C*PeF(t));
    RfF(t)=C*PeF(t)-PercF(t);
    if t<tmax
        SuF(t+1)=SuF(t);
    end
end
% Lag time for hillslope
PeakH=Tlag(TlagH);
RflF=conv(RfF,PeakH);
% Fast response reservoir
for t=1:tmax;
    SfF(t)=SfF(t)+RflF(t);
    QfF(t)=SfF(t)/KfH;
    SfF(t)=SfF(t)-QfF(t);
    if t<tmax;
        SfF(t+1)=SfF(t);
    end
end

%% Shrubs
% Unsaturated reservoir
for t=1:tmax;
    C=1-(1-SuS(t)/SumaxS)^beta;
    RuS(t)=(1-C)*PeS(t);
    SuS(t)=SuS(t)+RuS(t);
    ES(t)=min((Ep(t)-EiS(t)),min(SuS(t),(Ep(t)-EiS(t))*SuS(t)/SumaxS/Ce));
    SuS(t)=SuS(t)-ES(t);
    PercS(t)=min(SH*C*PeS(t));
    RfS(t)=C*PeS(t)-PercS(t);
    if t<tmax
        SuS(t+1)=SuS(t);
    end
end
% Lag time for hill slope
PeakH=Tlag(TlagH);
RflS=conv(RfS,PeakH);
% Fast response reservoir
for t=1:tmax;
    SfS(t)=SfS(t)+RflS(t);
    QfS(t)=SfS(t)/KfH;
    SfS(t)=SfS(t)-QfS(t);
    if t<tmax;
        SfS(t+1)=SfS(t);
    end
end
```

```
%% Grass
for t=1:tmax
    % Terrace: split HOF
    SoG(t)=SoG(t)+PeG(t);
    FG(t)=min(SoG(t),Fmin);
    SoG(t)=SoG(t)-FG(t);
    HOFG(t)=max(0,SoG(t)-Smax);
    SoG(t)=SoG(t)-HOFG(t);
    EoG(t)=max(0,min((Ep(t)-EiG(t)),SoG(t)));
    SoG(t)=SoG(t)-EoG(t);
    % Terrace: unsaturated zone
    C=1-(1-SuG(t)/SumaxG)^beta;
    RuG(t)=(1-C)*FG(t);
    SuG(t)=SuG(t)+RuG(t);
    EG(t)=min((Ep(t)-EiG(t)-EoG(t)),min(SuG(t),(Ep(t)-EiG(t)-
EoG(t))*SuG(t)/SumaxG/Ce));
    SuG(t)=SuG(t)-EG(t);
    PercG(t)=min(ST*C*FG(t));
    RfG(t)=C*FG(t)-PercG(t);
    % Terrace: fast reservoir
    SfG1(t)=SfG1(t)+RfG(t);
    QfG1(t)=SfG1(t)/Kf;
    SfG1(t)=SfG1(t)-QfG1(t);
    SfG2(t)=SfG2(t)+HOFG(t);
    QfG2(t)=SfG2(t)/Kf;
    SfG2(t)=SfG2(t)-QfG2(t);
    QfG(t)=QfG1(t)+QfG2(t);
    if t<tmax
        SoG(t+1)=SoG(t);
        SuG(t+1)=SuG(t);
        SfG1(t+1)=SfG1(t);
        SfG2(t+1)=SfG2(t);
    end
end

%% Agriculture
for t=1:tmax
    % Terrace: split HOF
    SoA(t)=SoA(t)+PeA(t);
    FA(t)=min(SoA(t),Fmin);
    SoA(t)=SoA(t)-FA(t);
    HOFA(t)=max(0,SoA(t)-Smax);
    SoA(t)=SoA(t)-HOFA(t);
    EoA(t)=max(0,min((Ep(t)-EiA(t)),SoA(t)));
    SoA(t)=SoA(t)-EoA(t);
    % Terrace: unsaturated zone
    C=1-(1-SuA(t)/SumaxA)^beta;
    RuA(t)=(1-C)*FA(t);
    SuA(t)=SuA(t)+RuA(t);
    EA(t)=min((Ep(t)-EiA(t)-EoA(t)),min(SuA(t),(Ep(t)-EiA(t)-
EoA(t))*SuA(t)/SumaxA/Ce));
    SuA(t)=SuA(t)-EA(t);
    PercA(t)=min(ST*C*FA(t));
    RfA(t)=C*FA(t)-PercA(t);
    % Terrace: fast reservoir
    SfA1(t)=SfA1(t)+RfA(t);
```

```
    QfA1(t)=SfA1(t)/Kf;
    SfA1(t)=SfA1(t)-QfA1(t);
    SfA2(t)=SfA2(t)+HOFA(t);
    QfA2(t)=SfA2(t)/Kf;
    SfA2(t)=SfA2(t)-QfA2(t);
    QfA(t)=QfA1(t)+QfA2(t);
    if t<tmax
        SoA(t+1)=SoA(t);
        SuA(t+1)=SuA(t);
        SfA1(t+1)=SfA1(t);
        SfA2(t+1)=SfA2(t);
    end
end

%% Groundwater
Qinf=zeros(tmax,1);
Qfinf=ones(tmax,1);
for t=1:tmax
    Ss(t)=Ss(t)+PercS(t)*PropS;
    Ss(t)=Ss(t)+PercF(t)*PropF;
    Ss(t)=Ss(t)+PercG(t)*PropG;
    Ss(t)=Ss(t)+PercA(t)*PropA;
    % Sfinf in the Sand River
    Qf_tot(t)=QfF(t)*PropF+QfS(t)*PropS+QfA(t)*PropA+QfG(t)*PropG;
    if sub==4
        if Ss(t)<Ssmax
            DD=2;
            while DD==2
                Qfinf(t)=k*Qf_tot(t);
                Qf_tot(t)=Qf_tot(t)-Qfinf(t);
                Ss(t)=Ss(t)+Qfinf(t);
                Qinf(t)=Qinf(t)+Qfinf(t);
                if Ss(t)>Ssmax|| Qfinf(t)<0.0001
                    DD=1;
                else
                    DD=2;
                end
            end
        end
    end
    Qs(t)=Ss(t)/Ks;
    Ss(t)=Ss(t)-Qs(t);
    if t<tmax
        Qfinf(t+1)=Qfinf(t);
        Qf_tot(t+1)=Qf_tot(t);
        Ss(t+1)=Ss(t);
    end
end

%% Total fluxes
Qm=Qs+Qf_tot;
E =(EF+EiF)*PropF+(EA+EiA+EoA)*PropA+(EG+EiG+EoG)*PropG+(ES+EiS)*PropS;

%% Process constraint parameter
% Runoff factor using Bodyko
years=floor(tmax/365);
Ep_tot=sum(Ep(1:365*years));
```

```
P_tot=sum(P(1:365*years));
Em_tot=sum(E(1:365*years));
Q_tot=sum(Qm(1:365*years));
R_tot=P_tot*exp(-Ep_tot/P_tot);
E_tot=P_tot*(1-exp(-Ep_tot/P_tot));
% total evaporation and runoff based on Budyko
years=floor(tmax/365);
Year=ExtraPar.forcing(:,1);
Month=ExtraPar.forcing(:,2);
Day=ExtraPar.forcing(:,3);
date_vec=[Day Month];
ind= find(date_vec(:,1)==Day(1) & date_vec(:,2)==Month(1));
for iii=1:length(ind)-1
    Ep_tot_per_year(iii,1)=sum(Ep(ind(iii):ind(iii+1)-1));
    P_tot_per_year(iii,1)=sum(P(ind(iii):ind(iii+1)-1));
    Em_tot_per_year(iii,1)=sum(E(ind(iii):ind(iii+1)-1));
    Qm_tot_per_year(iii,1)=sum(Qm(ind(iii):ind(iii+1)-1));
end
R_Budyko_per_year=P_tot_per_year.*exp(-Ep_tot_per_year./P_tot_per_year);
E_Budyko_per_year=P_tot_per_year.*(1-exp(-Ep_tot_per_year./P_tot_per_year));
C_Budyko=R_Budyko_per_year./P_tot_per_year;
Cm_mean=mean(Qm_tot_per_year./P_tot_per_year);
CC_mean=mean(C_Budyko);
CC_std=std(C_Budyko);
Em_mean=mean(Em_tot_per_year);
EE_mean=mean(E_Budyko_per_year);
EE_std=std(E_Budyko_per_year);

Ep_tot=sum(Ep(1:365*years));
P_tot=sum(P(1:365*years));
Em_tot=sum(E(1:365*years));
Q_tot=sum(Qm(1:365*years));
R_tot=P_tot*exp(-Ep_tot/P_tot);
E_tot=P_tot*(1-exp(-Ep_tot/P_tot));
ALL=[Ep_tot; P_tot; E_tot; Q_tot];

E_ref=E_tot;
Em=Em_tot;
C_ref=R_tot/P_tot; % reference runoff coefficient
C=Q_tot/P_tot; % runogg coefficient
CC=(C-C_ref)/C_ref;
EE=(Em-E_ref)/E_ref;

% max GW level based on observation: flow of peaks merely twice a year
if sub==4
    Qpeak=2;
    Q=Qf_tot;
    ind=find(Q>=Qpeak);
    ind2=find(Q<Qpeak);
    Q(ind)=1;
    Q(ind2)=0;

    for i=2:length(Q)
        if Q(i)==1
            if Q(i-1)==1
                Q(i-1)=0;
```

```
            end
        end
    end
    nr=length(find(Q==1));
    QQ=nr/years;
else
    QQ=0;
end

% evaporation ratio based on NDVI ratio
mu=  [1.26263808781096  1.50862611159655  0.916269132526600  1.09002266032592
1.38321981721236 1.19393467054500];
sigma=[0.0899609021684182         0.171850204765324         0.0600598308226034
0.0636988941903488 0.128637530754653 0.0941043535576455];
dsigma=5;

% Preferential recharge constraint
FF=sum(PercF);
SS=sum(PercS);
AA=sum(PercA);
GG=sum(PercG);

% Application of the constraints
if Cm_mean > CC_mean - dsigma*CC_std & Cm_mean < CC_mean + dsigma*CC_std
% Budyko: Runoff constraint
        if Em_mean > EE_mean - dsigma*EE_std & Em_mean < EE_mean +
dsigma*EE_std              % Budyko: Evaporation constraint
            if QQ < 5                  % Runoff constraint for the Sand River:
only twice a year there is a flow
                if           sum(EF)/sum(EA)>mu(1)-dsigma*sigma(1)           &
sum(EF)/sum(EA)<mu(1)+dsigma*sigma(1)... %% transpiration constraint
                    &          sum(EF)/sum(EG)>mu(2)-dsigma*sigma(2)          &
sum(EF)/sum(EA)<mu(2)+dsigma*sigma(2)... %% transpiration constraint
                    &          sum(ES)/sum(EA)>mu(3)-dsigma*sigma(3)          &
sum(EF)/sum(EA)<mu(3)+dsigma*sigma(3)... %% transpiration constraint
                    &          sum(ES)/sum(EG)>mu(4)-dsigma*sigma(4)          &
sum(EF)/sum(EA)<mu(4)+dsigma*sigma(4)... %% transpiration constraint
                    &          sum(EF)/sum(ES)>mu(5)-dsigma*sigma(5)          &
sum(EF)/sum(EA)<mu(5)+dsigma*sigma(5)... %% transpiration constraint
                    &          sum(EA)/sum(EG)>mu(6)-dsigma*sigma(6)          &
sum(EF)/sum(EA)<mu(6)+dsigma*sigma(6) %% transpiration constraint
                    if FF>AA & FF>GG & SS>AA & SS>GG % preferential recharge
constraint
                        PC=0; % all correct
                        count=0;
                    else
                        PC=1; % one of the processes wrong
                        count=5;
                    end
                else
                    PC=1; % one of the processes wrong
                    count=4;
                end
            else
                PC=1; % one of the processes wrong
                count=3;
```

```
            end
        else
            PC=1; % one of the processes wrong
            count=2;
        end
else
    PC=1; % one of the processes wrong
    count=1;
end
```

2. Calculation of the total outflow and objective functions

```
function [Obj, PC] = FLEXTopo(Par,ExtraPar)

%% Subcatchments
subs=5;
u=0.5;          % estimated average flow velocity
d=ExtraPar.forcing(:,4);
tmax=length(d);
for sub=1:subs;
    indices=4*sub+1;
    Prop{sub}=ExtraPar.subbasins{1}(1,sub);
    [Qm, Qo]=SubMod(Par,ExtraPar,sub, indices);
    Qmsub(:,sub)=Qm*Prop{sub};
    Distance=ExtraPar.subbasins{2}(1,sub);
    Tsub=round((Distance/u)/(24*3600));
    Qmsub(:,sub)=[zeros(Tsub,1); Qmsub(1:tmax-Tsub,sub)];
end

%% total runoff at outlet
for t = 1:tmax;
    Qm(t,1) = sum(Qmsub(t,:));
end

%% Objective function
Qm=real(Qm);
Qo=real(Qo);
SpinUp=300;
Qo_cal=Qo(SpinUp+1:end);
Qm_cal=Qm(SpinUp+1:end);
ind=find(Qo_cal>0 & Qm_cal>0);
Qo_unsorted=Qo_cal(ind);
Qm_unsorted=Qm_cal(ind);
% Flow duration curve
Qo_sorted=sort(Qo_unsorted,'descend');
Qm_sorted=sort(Qm_unsorted,'descend');
QoAv2=mean(Qo_sorted);
ErrUp3=sum((Qm_sorted-Qo_sorted).^2);
ErrDo3=sum((Qo_sorted-QoAv2).^2);
Obj(2)=ErrUp3/ErrDo3;
% Log of flow duration curve
Qolog_sorted=sort(Qolog_unsorted,'descend');
Qmlog_sorted=sort(Qmlog_unsorted,'descend');
QoAvlog2=mean(Qolog_sorted);
ErrUp4=sum((Qmlog_sorted-Qolog_sorted).^2);
ErrDo4=sum((Qolog_sorted-QoAvlog2).^2);
Obj(1)=ErrUp4/ErrDo4;
```

3. Calculation of the soil loss per sub-catchment

```
% Grassland
index=4;
[SSyield_totG]=RUSLE(index, ExtraPar, QfG2, sub, Qm, PropG, QfG2,1);
Area   =ExtraPar.RUSLEPar_AKLS(sub,1);

% Cropland
index=2;
[SSyield_totA]=RUSLE(index, ExtraPar, QfA2, sub, Qm, PropA, QfA2,2);

for t=1:length(SSyield_totG)
    SSyield_tot(t,1)=nansum([SSyield_totG(t,1),SSyield_totA(t,1)]);
    SSyield_tot(t,2)=nansum([SSyield_totG(t,2),SSyield_totA(t,2)]);
end
```

4. Calculation of the soil loss per HRU

```
function [SSyield_tot]=RUSLE(index, ExtraPar, HOF, sub, Qm, Prop, QfA2,nr)

Year=ExtraPar.forcing(:,1);
Month=ExtraPar.forcing(:,2);
Day=ExtraPar.forcing(:,3);
tmax=length(Day);

Area   =ExtraPar.RUSLEPar_AKLS(sub,1); %[ha]
K =ExtraPar.RUSLEPar_AKLS(sub,2); %[t/(MJ mm)
LS=ExtraPar.RUSLEPar_AKLS(sub,2+nr);
a =ExtraPar.RUSLEPar_abPq(1);
b =ExtraPar.RUSLEPar_abPq(2);
P =ExtraPar.RUSLEPar_abPq(3);
C =ExtraPar.RUSLEPar_C(index);
hr =ExtraPar.RUSLEPar_abPq(4);
for rnd=0:1
%     qpeak=qp(ExtraPar, sub, rnd, HOF, Qm, Area,nr); % [m3/s]
    qpeak=HOF*Area*1e4/1e3/3600/hr;
    R=a*(HOF.*qpeak*Area).^b;
    SSyield_A=R.*K*LS*C*P; %[t/day/ha]

    SSyield=SSyield_A*Prop; % [t/ha/day]
    SSyield_tot(:,rnd+1)=SSyield;
end
```

5. Calculation of the peak runoff according to the SWAT manual

```
function [qpeak]=qp(Extra, sub, rnd1, HOF, Qm, Area,nr)
%% Input data
A= Area/100;      % [km2]
i=Extra.qp(sub,nr); % average sub-catchment slope
i_c=Extra.qp(sub,3); % channel slope
L=Extra.qp(sub,4); % channel length [km]
n_ov=0.1; % friction overland flow (Manning)
n_c=1/35; % channel friction (Manning)
L_slp=90; % slope length [m] (cell size taken)
P=Extra.forcing(:,4);
Q_surf=Extra.forcing(:,5);
Q_surf(find(Q_surf<0))=nan;
years=Extra.forcing(:,1);
month=Extra.forcing(:,2);
yrs= years(end)-years(1); % nr of yrs of the used dataset
[days_wet, mu_mon]=rain_analysis(Extra, sub);
alfa_05L=0.02083;
adj_05alfa=1; % no adjustment

%% concentration time t_c [hr]
% overland flow
v_ov=n_ov^(-0.6)*(mean(HOF).*1e-3*A*(1e3)^2/3600/24).^0.4*i^0.3; % [m/s]
t_ov=L_slp/v_ov; %[s]
% channel
L_ch=sqrt(0.5)*L*1e3; %[m]
v_ch=0.489*(mean(Qm).*1e-3*A*(1e3)^2/3600/24).^0.25*i_c^0.375/n_c^0.75; %
[m/s]
t_ch=L_ch/v_ch; %[s]
% total
t_c= (t_ov+t_ch)/3600; % [hr]

%% fraction of daily rainfall during t_c
for ii=1:length(rnd1); % random nr between 0 and 1
    for i=1:length(P)
        month_nr=month(i);
        R_05smmon=P(i)/24/2; % underestimation!
        alfa_05mon=adj_05alfa*(1-
exp(R_05smmon/mu_mon(month_nr)*log(0.5/yrs/days_wet(month_nr))));
        alfa_05U=1-exp(-125/(P(i)+5));
        alfa_05mean=mean([alfa_05L, alfa_05mon, alfa_05U]);
         if rnd1(ii)<=(alfa_05mon-alfa_05L)/(alfa_05U-alfa_05L)
            alfa_05=alfa_05mon*(alfa_05L+(rnd1(ii)*(alfa_05U-
alfa_05L)*(alfa_05mon-alfa_05L))^0.5)/alfa_05mean;
        elseif rnd1(ii)>(alfa_05mon-alfa_05L)/(alfa_05U-alfa_05L)
            alfa_05=alfa_05mon*(alfa_05U-(alfa_05U-alfa_05mon)*((alfa_05U*(1-
rnd1(ii))-alfa_05L*(1-rnd1(ii)))/(alfa_05U-alfa_05mon))^0.5)/alfa_05mean;
        end
        % fraction of daily rainfall falling in the half-hour highest
intensity rainfall
        alfa_tc= 1-exp(2*t_c*log(1-alfa_05));
           %% peak runoff rate
        qpeak(i,ii)=real(alfa_tc*Q_surf(i)*A/3.6/t_c);
```

```
    end
end
```

Appendix H: Field trip activities

Table of Contents

1. Visited locations

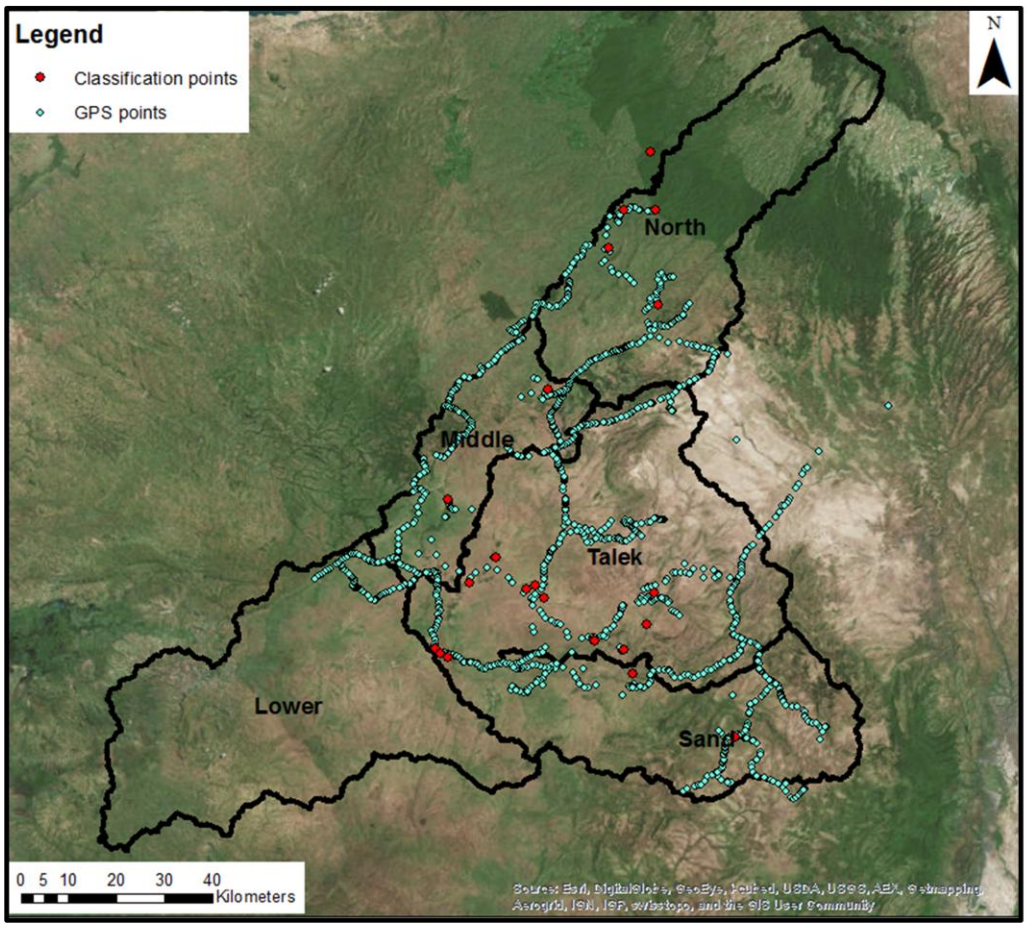

Figure 1-1: Locations visited. At the Classification points (red dots), an extensive classification analysis is done based on a checklist (see next section). At all locations, landscape pictures are taken to confirm land cover maps and landscape maps used for the classification into HRUs.

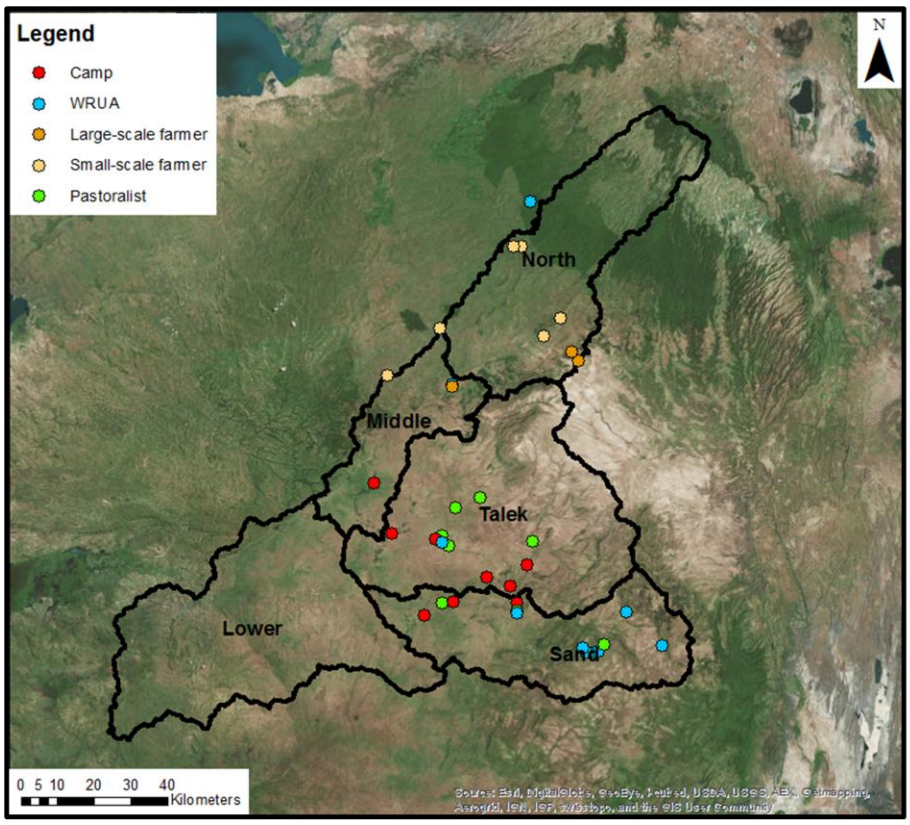

Figure 1-2: Locations where interviews are conducted

2. Field observation checklist

Goals

- Refine model structure
  - Determine dominant flow mechanisms
  - Identify and where possible lump classes
- Improve parameter ranges and establish constraints

Start

1. Location and time
   a. Date
   b. Time
   c. GPS coordinates
   d. Closest village
   e. Special features

Part A: Describe

Detailed description

2. Vegetation => I_{max}, S_{umax}, wetland, classes, dominant flow mechanism
   a. Type
   b. Density
   c. Layers
   d. Height
   e. Leaves
   f. Trunk (colour, roughness, swollen)
   g. Roots (above / below surface)
   h. Fruits / flowers
   i. Smell
   j. Rooting depth
   k. Specific wetland plants visible?
   l. Natural/exotic vegetation? => influences evaporation in dry seasons (increased evaporation through exotic plants)

3. Soil type => infiltration, percolation, dominant flow mechanisms, erosion, delay time
   a. Sand / clay / peat
   b. Rocks
   c. Crusts
   d. Trampling by animals
   e. Cracks
   f. Bare / covered

g. Profile
h. Macropores => at roads or steep river banks cutting through hillslope
i. Root channels => at roads or steep river banks cutting through hillslope
j. Animals burrows => at roads or steep river banks cutting through hillslope
k. Dark stains (rub through fingers: stains?) => wetland
l. Decomposing plant material (thickness layer) => wetland
m. Does the soil smell like rotten eggs? => wetland
n. Colour just below the surface => wetland

4. Erosion / sedimentation evidence => erosion, overland flow
    a. Dust clouds in the air
    b. Gullies / rills (estimate dimensions)
    c. Stones on top of land surface
    d. Pedestals of soil supporting stones and plants
    e. Exposed tree roots
    f. Soil accumulation along boundaries
    g. Sediment deposited on pavements
    h. Sediments deposited at the base of slopes and at depressions, upper layer
    i. Exposure of lighter coloured subsoil at the surface
    j. Different elevation fields compared to paths
    k. River bank: cracks in the soil, overhanging top park, collapsed
    l. Clumps of grass in the river

5. Flow of water
    a. Rainfall: current, day(s) before, intensity, duration
    b. Current overland flow
    c. Water marks on trees/objects => wetland, overland flow
    d. Debris or sediments lodged on trees/objects/ground => wetland, overland flow
    e. Stream dimensions => feeling for area
        a. Maximum before bank overflow
        b. Maximum wet area
        c. Current wet area
    f. Colour of the water => erosion, overland flow
    g. Diver measurement => flow mechanisms
    h. Depressions => delay, thresholds
    i. Puddles (depth) => infiltration

6. Wetland
    a. Groundwater level
    b. Road (not expected)
    c. Scoop holes (depth)

Conclusions

7. Parameter estimation
    a. Interception
    b. Unsaturated zone
    c. Lag times

8. Landscape
    a. Flat / sloped
    b. Wetland
    c. Plateau / terrace

9. Land use/cover
    a. Land use
    b. Land cover
        i. Forest
        ii. Bush
        iii. Grass
        iv. Bare

10. Flow mechanisms:
    a. Hortonian overland flow
    b. Saturation overland flow
    c. Rapid subsurface flow
    d. Deep percolation
        a. Kan bij hill slope, maar ook op plateaus; infiltratie in depressies

Part B: Questions

11. *River/stream*

    If there is a river or stream:
    a. Does the river ever become completely dry?
    b. What are the highest and lowest water levels you have ever seen in the river?
    c. What are the water levels in the river in the dry and in the wet season? How does it vary during the year (on monthly timescale)?
    d. Does the water level in the river vary fast? Does it ever rise or decline within one day/week or even less (if yes: how much)? During which months does this happen? After every rainfall event or only (very) heavy or prolonged rainfall? Does this happen immediately after rainfall or with a delay (of how long)?
    e. Does the river become difficult to cross during some months of the year, for you or for animals/vehicles? During which months is it difficult to cross?
    f. Do you have pictures of that? (Possibly ask for pictures after other questions as well)

12. *Overland flow*

    Have you ever seen water flowing over the land? If yes:

    a. During which months does this happen?
    b. After every rainfall event or only (very) heavy or prolonged rainfall?
    c. Immediately after the rainfall or with a delay (of how long)?
    d. How deep is the water that flows over the land?
    e. Is the water concentrated in streams?
    f. Does the water flow rapidly/slowly or not at all?
    g. Can you walk through the water (can animals/vehicles cross it)?

13. *Infiltration & saturation*

    Do you ever see puddles on the land? If yes:

    a. How deep are the puddles approximately?
    b. After every rainfall event or only (very) heavy or prolonged rainfall?
    c. How fast do they disappear? At the same day? Within hours/minutes?

14. *Wetland*

    a. Does the soil get swampy during times of the year (difficult to walk or drive on)?
    b. Do you ever see standing water on the area along the river(s)/stream(s)?
    c. Does the width of the river(s) change during the year?

    => If yes on any of these questions: What are the boundaries? How do the boundaries change during the year (on monthly timescale)?

15. *Suspended sediment*

    Does the water in the streams ever become turbid? If yes:

    a. After every rainfall event or only (very) heavy or prolonged rainfall?
    b. Immediately after the rainfall or with a delay (of how long)?
    c. During which months?
    d. What is the colour? How dark is the colour?
    e. Is it turbid everywhere in the stream or only at a few locations (e.g. stream outlets)?

16. *Gullies*

    Have you ever seen gullies or rills in your land that you can plough so they disappear? If yes:

    a. In which month do these develop?
    b. When do you plough?
    c. How deep and how wide are the rills/gullies?

    If there are gullies/rills in the land:

    d. When did these develop (years/months)?
    e. Can you plough them so they disappear?
    f. Do they increase in size every year? How much?

17. *Vegetation*

a. Do you know the names of the most common plants here?
b. After how many years do they produce seeds (if unknown: how old do they get)?
c. Does the vegetation shed its leaves? During which months does it become/is it bare?
d. Does the density of the vegetation change during the year? Can you describe the variation over the year (on monthly timescale)?
e. Does the vegetation get different colours during the year? What are the colours over the year (on monthly timescale)?
f. Does the vegetation become dry in any other ways during the year? How and when does this happen?

18. *Land use change*

Has the land use always been the same here? If not:

a. What was the land use before?
b. When did the land use change?
c. Why did the land use change?
d. How fast did it change?
e. What were the consequences of this change?
f. Did you notice any increase in erosion after the changes?
g. Did you notice any increase in overland flow after the changes?

Do you think the land use will change in the future? How? When? Why? How much? How fast? What do you think that the consequences will be?

19. *Groundwater.*

Do you use wells? If yes:

a. Are they ever dry?
b. How fast do they refill if you empty them?

Look at conclusions again and adjust them.

Part C: Measurements

- Water level?
- EC?
- Temperature?

3. Interview questions

Target group: Members of the Water Resources Users Associations (WRUA).

Similar questions are asked to other local people such as pastoralists, farmers or camp owners focusing on their observation in their near environment to confirm personal observations.

Problem identification

1. **Have you experienced any effects related to soil loss/ deposition/sediments in river water? If yes, what exactly have you noticed?**
2. **Where do the sediments originate from?**
3. **Are there any differences throughout the year? If yes, what is the most extreme time of the year?**
4. **Is the sediment transport causing any difficulties or problems?**
5. **Have there been any long term changes in the past (e.g. past 30 years)?**
   5.1. What was the original location of the river? When was that?
   5.2. Did the river banks erode? Did the river width change?
   5.3. Have gullies developed or increased?
   5.4. When were these effects noticed for the first time?
   5.5. Have there been any trends or striking/outstanding events?

Problem solving

1. **How are you currently coping with the situation?**
2. **Do you have any plans/ideas on how to minimize possible problems?**
3. **What would be an ideal solution? What is your goal?**
   3.1. What time span?

Future expectations

1. **Do you expect any changes in the future? Potential problems?**